

UNCLASSIFIED

AD NUMBER

AD827530

LIMITATION CHANGES

TO:

Approved for public release; distribution is unlimited.

FROM:

Distribution authorized to U.S. Gov't. agencies and their contractors;
Administrative/Operational Use; JAN 1968. Other requests shall be referred to Air Force Weapons Lab., Kirtland AFB, NM 87117.

AUTHORITY

AFWL ltr 30 Nov 1971

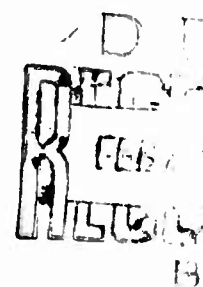
THIS PAGE IS UNCLASSIFIED

AFWL-TR-67-134

AFWL-TR
67-134

**FLIGHT DYNAMICS OF THE
BLUE GOOSE VEHICLE TRAVERSING A
HIGH ALTITUDE NUCLEAR EXPLOSION**

Urban H. D. Lynch
Captain USAF



TECHNICAL REPORT NO. AFWL-TR-67-134

January 1968

AIR FORCE WEAPONS LABORATORY
Air Force Systems Command
Kirtland Air Force Base
New Mexico

This document is subject to special export controls and each transmittal to foreign governments or foreign nationals may be made only with prior approval of AFWL (WLRT) , Kirtland AFB, NM, 87117.

AD827530



AFWL-TR-67-134

ACCESSION for	
CPSTI	WHITE SECTION <input type="checkbox"/>
DDC	DIFF SECTION <input checked="" type="checkbox"/>
UNANNOUNCED	<input type="checkbox"/>
JUSTIFICATION	
BY	
DISTRIBUTION/AVAILABILITY CODES	
DIST.	AVAIL. md/yr SPECIAL
2	

AIR FORCE WEAPONS LABORATORY
Air Force Systems Command
Kirtland Air Force Base
New Mexico

When U. S. Government drawings, specifications, or other data are used for any purpose other than a definitely related Government procurement operation, the Government thereby incurs no responsibility nor any obligation whatsoever, and the fact that the Government may have formulated, furnished, or in any way supplied the said drawings, specifications, or other data, is not to be regarded by implication or otherwise, as in any manner licensing the holder or any other person or corporation, or conveying any rights or permission to manufacture, use, or sell any patented invention that may in any way be related thereto.

This report is made available for study with the understanding that proprietary interests in and relating thereto will not be impaired. In case of apparent conflict or any other questions between the Government's rights and those of others, notify the Judge Advocate, Air Force Systems Command, Andrews Air Force Base, Washington, D. C. 20331.

DO NOT RETURN THIS COPY. RETAIN OR DESTROY.

AFWL-TR-67-134

FLIGHT DYNAMICS OF THE BLUE GOOSE VEHICLE TRAVERSING
A HIGH ALTITUDE NUCLEAR EXPLOSION

Urban H. D. Lynch
Captain USAF

TECHNICAL REPORT NO. AFWL-TR-67-134

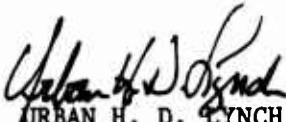
This document is subject to special export controls and each transmittal to foreign governments or foreign nationals may be made only with prior approval of AFWL (WLRT), Kirtland AFB, NMex 87117. Distribution is limited because of the technology discussed in the report.


FOREWORD

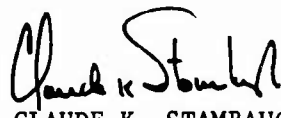
This research was performed under Program Element 7.60.08.01.D, Project 5710, Subtask 7.505T, and was funded by the Defense Atomic Support Agency (DASA).

Inclusive dates of research were January 1967 to November 1967. The report was submitted 15 December 1967 by the Air Force Weapons Laboratory Project Officer, Captain Urban H. D. Lynch (WLRT).

This report has been reviewed and is approved.


URBAN H. D. LYNCH
Captain, USAF
Project Officer


TRUMAN L. FRANKLIN
Colonel, USAF
Chief, Theoretical Branch


CLAUDE K. STAMBAUGH
Colonel, USAF
Chief, Research Division

ABSTRACT

(Distribution Statement No. 2)

This report investigates the flight dynamics of the Blue Goose vehicle traversing a high altitude nuclear explosion. The problem is analyzed for a detonation of 200 kilotons at an altitude of 30 kilometers. The vehicle is launched such that it intercepts the fireball edge at approximately 1 second after detonation. Calculation of vehicle trajectory is done by incorporating the output of a detailed one-dimensional hydrodynamic calculation of the explosion environment, with a six-degree-of-freedom computer program for the vehicle. The report analyzes the attitude and position time histories of the vehicle, time history of environment as seen by the vehicle, vehicle dynamic loads, trajectory dispersion, and worst flight path through the environment.

(This page intentionally left blank)

CONTENTS

<u>Section</u>		<u>Page</u>
I	INTRODUCTION	1
II	PROBLEM FORMULATION	2
III	HIGH ALTITUDE NUCLEAR EXPLOSION ENVIRONMENT	10
IV	FORTTRAN MODIFICATIONS	70
V	COMPUTER RESULTS	82
VI	CONCLUSIONS	206
	Appendix I UNGUIDED BLUE GOOSE VEHICLE	209
	Appendix II GUIDED BLUE GOOSE VEHICLE	227
	Distribution	240

ILLUSTRATIONS

<u>Figure</u>		<u>Page</u>
1	Vehicle Coordinate System	5
2	Problem Definition	6
3-58	Explosion Environment Data	14-69
59	Environment Growth and Intercept	92
60-74	Graphs for Miss Distance 1000 Feet	93-107
75-89	Graphs for Miss Distance 2000 Feet	108-122
90-104	Graphs for Miss Distance 3000 Feet	123-137
105-119	Graphs for Miss Distance 4000 Feet	138-152
120-134	Graphs for Miss Distance 6000 Feet	153-167
135	Angular Acceleration at Shock Penetration	168
136	Transverse Acceleration at Shock Penetration	169
137	Maximum Yaw Angle After Shock Penetration	170
138	Maximum Pitch Angle After Shock Penetration	171
139	Position Change in Horizontal Plane at 49 Seconds	172
140	Position Change in Vertical Plane at 49 Seconds	173
141	Change in Velocity at 49 Seconds	174
142	Angular Perturbation of Velocity at 49 Seconds	175
143-157	Graphs for No Spin	176-190
158-172	Graphs for Guided Vehicle	191-205

SECTION I

INTRODUCTION

This report investigates the flight dynamics of the Blue Goose vehicle traversing a high altitude nuclear explosion. The problem is analyzed for a detonation of 200 kilotons (KT) at an altitude of 30 kilometers (km). The vehicle is launched such that it intercepts the fireball edge at approximately 1 second after detonation. Calculations of the vehicle trajectory are made by incorporating the output of a detailed one-dimensional hydrodynamic calculation of the explosion environment, with a six-degree-of-freedom computer program for the vehicle. Basic information on the Blue Goose Vehicle is given in Appendix I and II.

SECTION II

PROBLEM FORMULATION

The dynamic interaction of a vehicle with a nuclear explosion is mainly hydrodynamic. One is also naturally concerned with the structural effects of nuclear and thermal radiation, but from the standpoint of wanting to know the position-time history of the vehicle, the hydrodynamic interaction predominantly defines this problem. The solution to the position-time history problem lies in an accurate, simultaneous simulation of vehicle dynamics, explosion environment, and the interaction of the two.

1. Vehicle Dynamics

A six-degree-of-freedom digital computer program was used to simulate the vehicle dynamics. The formulation of the program is documented in AFWL-TR-66-156. Rigid body equations of motion are used with no linear assumptions. The earth model is oblate, spheroidal, and rotating. The equations of motion are general in that they apply to most axially symmetric vehicles. The existing program is specific in that the equations of motion have been applied to a specific vehicle.

2. Explosion Environment

The essential environment properties needed as a function of time and position are velocity, density, and temperature. An accurate simulation of these properties was obtained from the output of a detailed one-dimensional, hydrodynamic computer program called SPATTER. Section III briefly explains SPATTER and shows in detail the output of the program.

3. Vehicle Hydrodynamic Interaction

The problem of accurately calculating the aerodynamic force and moment acting on the vehicle in the explosion environment is a formidable one. The relative fluid flow over the vehicle can easily have a high angle of attack and be non-steady. In hopes of making some simplifying assumptions about the relationship between the aerodynamic force and moment and the fluid flow, the following observations were noted:

a. Vehicle length (30 ft) and vehicle maximum velocity times the integration interval ($4000 \text{ ft/sec} \times .01 \text{ sec} = 40 \text{ ft}$) are small in comparison to the spatial distances in the environment over which the predominant changes in environmental properties occur.

b. Because of very high temperature, the flow is below Mach 1.0 for a good portion of the time the vehicle is in the environment.

c. The time it takes a fluid particle to pass the length of the vehicle ($30 \text{ ft}/3000 \text{ ft/sec} = .01 \text{ sec}$) is small in comparison to the time it takes the vehicle to see an appreciable change in the environment properties.

Observation "a" suggests that in the ambient flow, the fluid properties over the length of the vehicle can be considered uniform. Observation "b" suggests that subsonic aerodynamics would be valid most of the time. Observation "c" suggests that the flow over the vehicle has a good chance to stabilize before the ambient flow properties change appreciably, i.e., steady flow. These observations led to the following assumptions concerning the relationship between the aerodynamic force and moment and the fluid flow:

a. Assume environment properties as seen by the vehicle are solely a function of vehicle C.G. location in the environment.

b. Assume steady flow.

c. Assume conventional wind tunnel aerodynamic coefficients as a function of Mach number for fluid flow with a small angle of attack.

d. Assume subsonic wind tunnel aerodynamics as a function of angle of attack for fluid flow with a high angle of attack.

4. Mathematical Formulation

a. Aerodynamic Formulation Change.

The aerodynamic logic of the original six-degree formulation documented in AFWL-TR-66-156 (see pages 59-65)*, assumes that although the angle of attack can be in a nonlinear range (i.e., greater than five degrees) the angle of attack is not so large that it cannot be treated as a vector with components in the pitch and yaw planes of the vehicle. Under the extreme environment of a nuclear

*"Blue Goose Six-Degree-of-Freedom Digital Computer Trajectory Calculation," March, 1967.

explosion, the angle of attack can become extremely large, and therefore can no longer be treated as a vector with components. The following formulation corrects this problem.

Examine figure 1. The assumption is made that the vehicle is symmetric in roll. As such the aerodynamic force on the vehicle will lie in the plane formed by the relative velocity vector, \bar{V}_R , and the vehicle longitudinal axis \bar{k}_3 . The direction of the aerodynamic force, \bar{l}_f , in the transverse plane of the vehicle can therefore be written as

$$\bar{l}_f = \frac{-V_{RX3}}{V_{XY}} \bar{i}_3 - \frac{V_{RY3}}{V_{XY}} \bar{j}_3 \quad (1)$$

where

$$V_{XY} = \sqrt{V_{RX3}^2 + V_{RY3}^2} \quad (2)$$

For a stable vehicle (i.e., one for which the aerodynamic force is concentrated behind the vehicle C.G.), the direction of the aerodynamic restoring moment, \bar{l}_m can be written as

$$\bar{l}_m = \bar{l}_f \times \bar{k}_3 \quad (3)$$

Substituting Eq. 1 into Eq. 3 and expanding the vector cross products yields

$$\bar{l}_m = \frac{V_{RX3}}{V_{XY}} \bar{j}_3 - \frac{V_{RY3}}{V_{XY}} \bar{i}_3 \quad (4)$$

The total angle of attack, α_T as seen by the vehicle can be written

$$\alpha_T = \cos^{-1} \left(\frac{V_{RZ3}}{V_R} \right) \quad (5)$$

The scalar magnitudes of the aerodynamic force, F_{aero} , and aerodynamic moment, M_{aero} , are calculated in the usual fashion from total angle of attack, Mach number, dynamic pressure, etc. Once the scalar magnitudes F_{aero} and M_{aero} are known, the

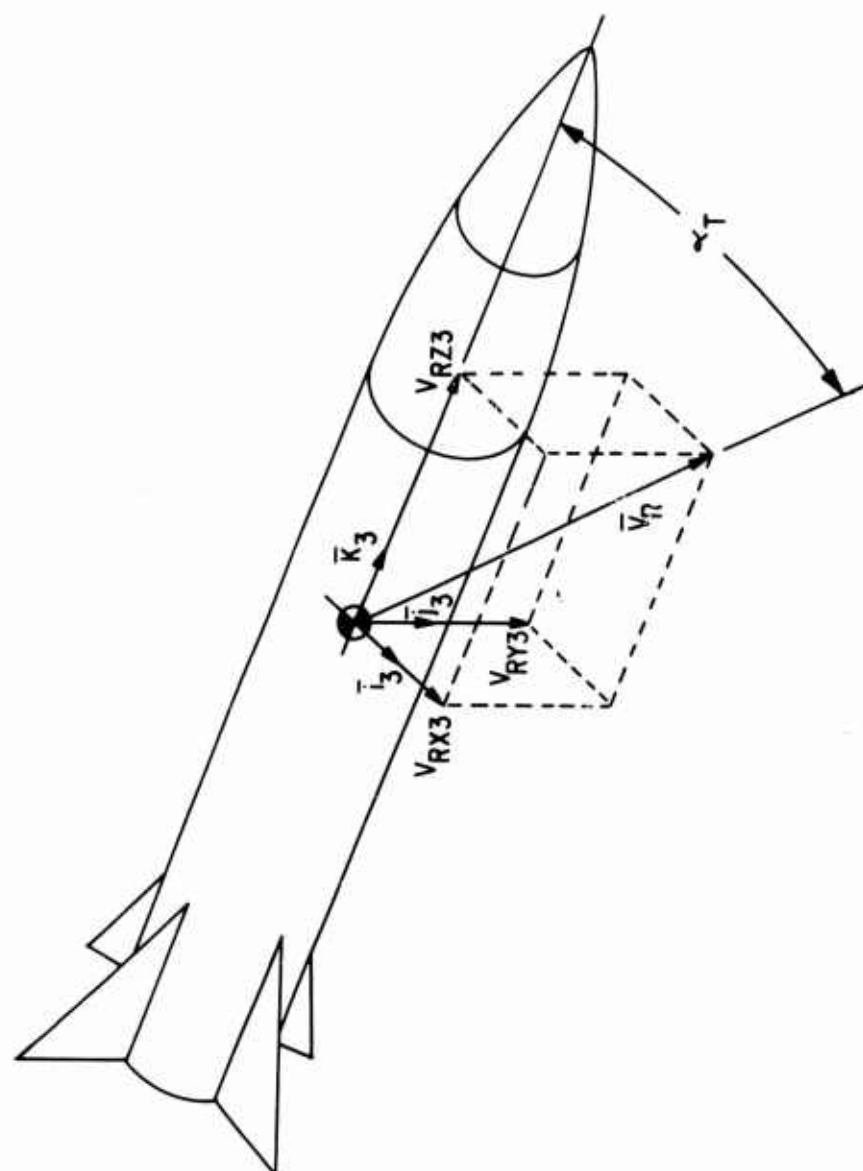


Figure 1. Vehicle Coordinate System

aerodynamic vector force, \bar{F}_{aero} , and aerodynamic vector moment, \bar{M}_{aero} can be written as

$$\bar{F}_{\text{aero}} = F_{\text{aero}} \bar{l}_f \quad (6)$$

$$\bar{M}_{\text{aero}} = M_{\text{aero}} \bar{l}_m \quad (7)$$

The FORTRAN modifications to incorporate these changes into the existing six-degree-of-freedom program are outlined in Section IV.

b. Formulation Concepts for Explosion Environment.

Examine figure 2. The vehicle flight can be divided into two portions: flight through the normal atmosphere and flight through the blast environment. So far as the vehicle is concerned, the only difference between the atmosphere and the blast environment is the change in fluid properties, i.e., density, wind velocity, and velocity of sound.

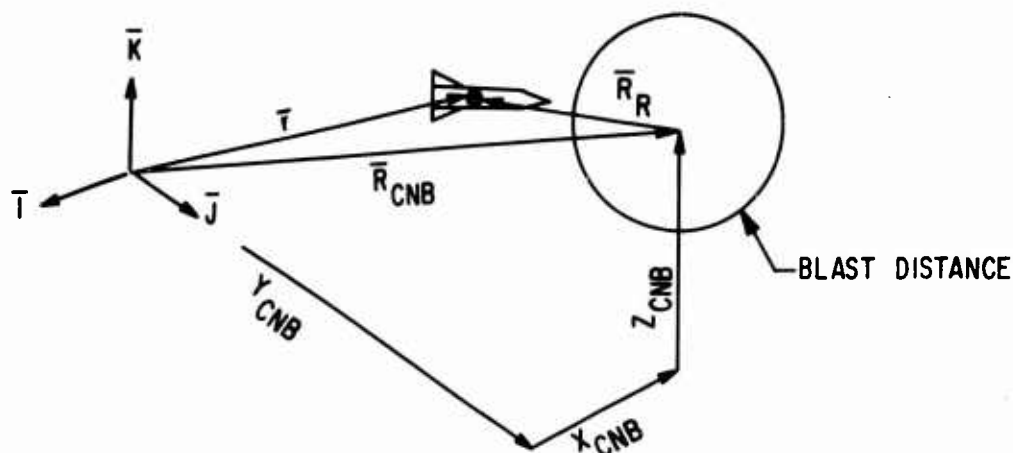


Figure 2. Problem Definition

The first thing that must be known is whether or not the vehicle is in the blast environment at any given time, t . The whole problem is formulated on the assumption that the ideal flight of the vehicle will go through the center of the detonation and be timed such that the vehicle intercepts the edge of the fireball 1 second after detonation. The time of flight when the nominal trajectory intercepts the fireball at 1 second after detonation, T_p , was determined from a six-degree calculation to be approximately 43.36 seconds. The coordinate transformation from vehicle time of flight, t , to time after detonation, T_{fb} is therefore

$$T_{fb} = t - T_p + 1 \quad (8)$$

The program is set up so that flight through the atmosphere is calculated until a time T_e (called "time examine", T_e is slightly less than T_p) is reached, after which a test is performed to see if the vehicle has entered the blast area. This test is formulated as follows:

The center of the detonation relative to the launch coordinate system \bar{I} , \bar{J} , \bar{K} is written in vector form as

$$\bar{R}_{CNB} = X_{CNB} \bar{I} + Y_{CNB} \bar{J} + Z_{CNB} \bar{K} \quad (9)$$

The vector to the vehicle C.G. is written

$$\bar{r} = X \bar{I} + Y \bar{J} + Z \bar{K} \quad (10)$$

The vector from the center of detonation to the vehicle C.G is written as

$$\bar{R}_R = \bar{r} - \bar{R}_{CNB} \quad (11)$$

Once time has exceeded T_e , T_{fb} is calculated and the outermost radius of the blast disturbance is determined from the environment data. This outer blast radius is then compared with the scalar magnitude of \bar{R}_R to see if the vehicle has reached the environment. If the vehicle has not reached the environment, the program uses the properties of the normal atmosphere. As soon as the environment is reached, the program then uses T_{fb} and \bar{R}_R to arrive at the ambient flow properties from the environmental data.

The environmental data are one-dimensional. The environment fluid flow is therefore radial and the properties of the fluid depend solely on distance from the detonation, \bar{R}_R , and time from detonation, T_{fb} . The stored environment data closest to T_{fb} are used and an interpolation of radius is done to get the fluid properties. An interpolation in time was not felt necessary since the end result would be an averaging effect similar to that achieved by using the stored data closest to T_{fb} . Since the fluid flow is assumed radial from the center of detonation, the vector wind, \bar{V}_W , can be written as

$$\bar{V}_W = V_W \frac{\bar{R}_R}{R_R} \quad (12)$$

where V_W is the scalar wind velocity at the radius R_R . Substituting Eqs. 9 and 10 into Eq. 12 yields

$$\bar{V}_W = V_{WX} \bar{I} + V_{WY} \bar{J} + V_{WZ} \bar{K} \quad (13)$$

where

$$V_{WX} = \frac{V_W (X - X_{CNB})}{R_R} \quad (14)$$

$$V_{WY} = \frac{V_W (Y - Y_{CNB})}{R_R} \quad (15)$$

$$V_{WZ} = \frac{V_W (Z - Z_{CNB})}{R_R} \quad (16)$$

The FORTRAN modifications to incorporate these concepts into the existing six-degree-of-freedom program are outlined in Section IV.

SECTION III

HIGH ALTITUDE NUCLEAR EXPLOSION ENVIRONMENT

The explosion environment was obtained from the Theoretical Branch of the Air Force Weapons Laboratory. The data for the environment was stored on magnetic tape and calculated by a detailed one-dimensional, hydrodynamic computer program called SPUTTER.

1. SPUTTER

The SPUTTER program is designed to solve the equations which describe the behavior of a variety of physical systems involving time-dependent, inviscid, compressible fluid flow in one spatial dimension coupled with energy transfer by radiation and thermal conduction. The equations are expressed in a Lagrangian coordinate system and are solved by finite-difference techniques. The independent thermodynamic variables of the calculation are temperature, θ , and specific volume, τ (or density, $\rho \equiv 1/\tau$). All other thermodynamic-state variables, such as specific internal energy, E , pressure, P , the radiative absorption coefficients for the material, and any other properties of the fluid needed to describe its behavior, are expressed as functions of θ and τ . Local thermodynamic equilibrium is assumed to exist at all points in space and time in the problems of interest. The CGS system of units is used in the SPUTTER program and the unit of temperature used is the electron volt (11,605.7°K).

2. Magnetic Tape

The detailed output of the SPUTTER program is stored on magnetic tape. Environment properties are stored as a function of time from detonation and radius from the center of detonation. The environment properties available are as follows: velocity, pressure, density, temperature, specific internal energy, and flux of energy.

The following FORTRAN statements are necessary in order to call the data from the magnetic tape:

```

      READ(4,101)N
101  FØRMAT(I10)
      DØ 109 J=1,N
      DØ 109 I=1,50
      READ(4,104)(IJA(K),K=1,120)
109  CØNTINUE
- 104  FØRMAT(120A1)

This part of the program need be read only once.
      8  CØNTINUE
      READ(4,102)CØUNT,TH,IA,IB,MAXL,(HEAD(I),I=1,12)
102  FØRMAT(1X,F7.1,E13.6,3I9,12A6)
      READ(4,105)(LMDA(I),I=1,MAXL)
105  FØRMAT(1X,13I9)
      MAXLM = MAXL-1
110  FØRMAT(1X,7E17.9)
      READ(4,110)(ØKLM(I),I=1,MAXLM)
      READ(4,110)(CHRNØ(I),I=1,MAXLM)
      READ(4,110)(AMASNØ(I),I=1,MAXLM)
      READ(4,111)(ITEMP(I),I=1,16)
111  FØRMAT(1X,16I7)
      IBM1=IB-1
      READ(4,110)(R(I),I=1,IB)
      READ(4,110)(RD(I),I=1,IB)
      READ(4,110)(P1(I),I=1,IBM1)
      READ(4,110)(THETA(I),I=1,IBM1)
      READ(4,110)(DENS(I),I=1,IBM1)
      READ(4,110)(E(I),I=1,IBM1)
      READ(4,110)(RDD(I),I=1,IB)
      READ(4,110)(SMLQ(I),I=1,IB)
      READ(4,110)(SMLR(I),I=1,IB)

```

The variable TH is the time in seconds after detonation. The variable IBM1 (its value is always less than 150) is an index that represents the outermost zone of the mesh to which the environment has propagated. The variable R(I) is an arbitrary radius in the environment in centimeters. R(0) is zero and R(IBM1) is the last radius to which the environment has propagated. The variable RD(I) is the velocity of the medium in cm/sec at radius R(I). The variable P1(I)

is the pressure of the medium in dynes/cm² at radius R(I). The variable THETA(I) is the temperature of the medium in electronvolts at the radius R(I). The variable DENS(I) is the density of the medium in grams/cm³ at the radius R(I). The variable E(I) is the internal energy of the medium in ergs/gram at the radius R(I). The variable RDD(I) is the energy flux in watts/cm² outward across an area oriented normal to the radius at radius R(I). The variable SMLQ(I) is the energy flux in watts/cm² inward across an area oriented normal to the radius at radius R(I). The variable SMLR(I) is the energy flux in watts/cm² across an area oriented normal to a tangent to the spherical mesh at radius R(I).

When the last statement has been executed, the complete environment has been received off the tape for the first time TH. To read the environment for the next consecutive TH, the program must go back to statement 8. An end of file follows the last stored data.

3. Environment Data

An environment calculation of 200 KT at 30 km of sufficient time span (~7 seconds) was not available. However, a 200-KT calculation at 40 km was available with a time span of 8.5 seconds. For expediency, it was decided to use the 40-km data and scale it to the desired 30 km. The scaling laws used were as follows:

$$t_2 = \left(\frac{W_2}{W_1} \right)^{1/3} \left(\frac{P_{01}}{P_{02}} \right)^{1/3} \left(\frac{C_{01}}{C_{02}} \right) t_1$$

$$R_2 = \left(\frac{P_{01}}{P_{02}} \right)^{1/3} \left(\frac{W_2}{W_1} \right)^{1/3} R_1$$

$$P_2 = \left(\frac{P_{02}}{P_{01}} \right) P_1$$

$$\rho_2 = \left(\frac{\rho_{02}}{\rho_{01}} \right) \rho_1$$

where

t = time
 C_0 = velocity of sound
 P_0 = ambient pressure
 W = yield
 R = radius
 P = pressure
 ρ = density

The values at 40 km were as follows:

$W_1 = 200 \text{ KT}$
 $P_{01} = 4.712 \times 10^{-2} \text{ psi}$
 $C_{01} = 1064 \text{ ft/sec}$
 $\rho_{01} = .752 \times 10^{-5} \text{ slug/ft}^3$

The values at 30 km were as follows:

$W_2 = 200 \text{ KT}$
 $P_{02} = 11.32 \times 10^{-2} \text{ psi}$
 $C_{02} = 1003 \text{ ft/sec}$
 $\rho_{02} = 3.311 \times 10^{-5} \text{ slug/ft}^3$

The scaling laws are therefore as follows:

$t_{30} = .7929 t_{40}$
 $R_{30} = .7475 R_{40}$
 $P_{30} = 2.402 P_{40}$
 $\rho_{30} = 4.402 \rho_{40}$

where the subscript 30 refers to 30 km.

The values available on the tape for t_{40} ranged from 1×10^{-5} seconds to 8.5 seconds. In the time interval of major concern to this problem (i.e., 0.5 second to 8.5 seconds), there were approximately 45 time increments stored on the tape. Figures 3 through 58 show the explosion environment approximately every 0.5 second from detonation as scaled to 30 km.

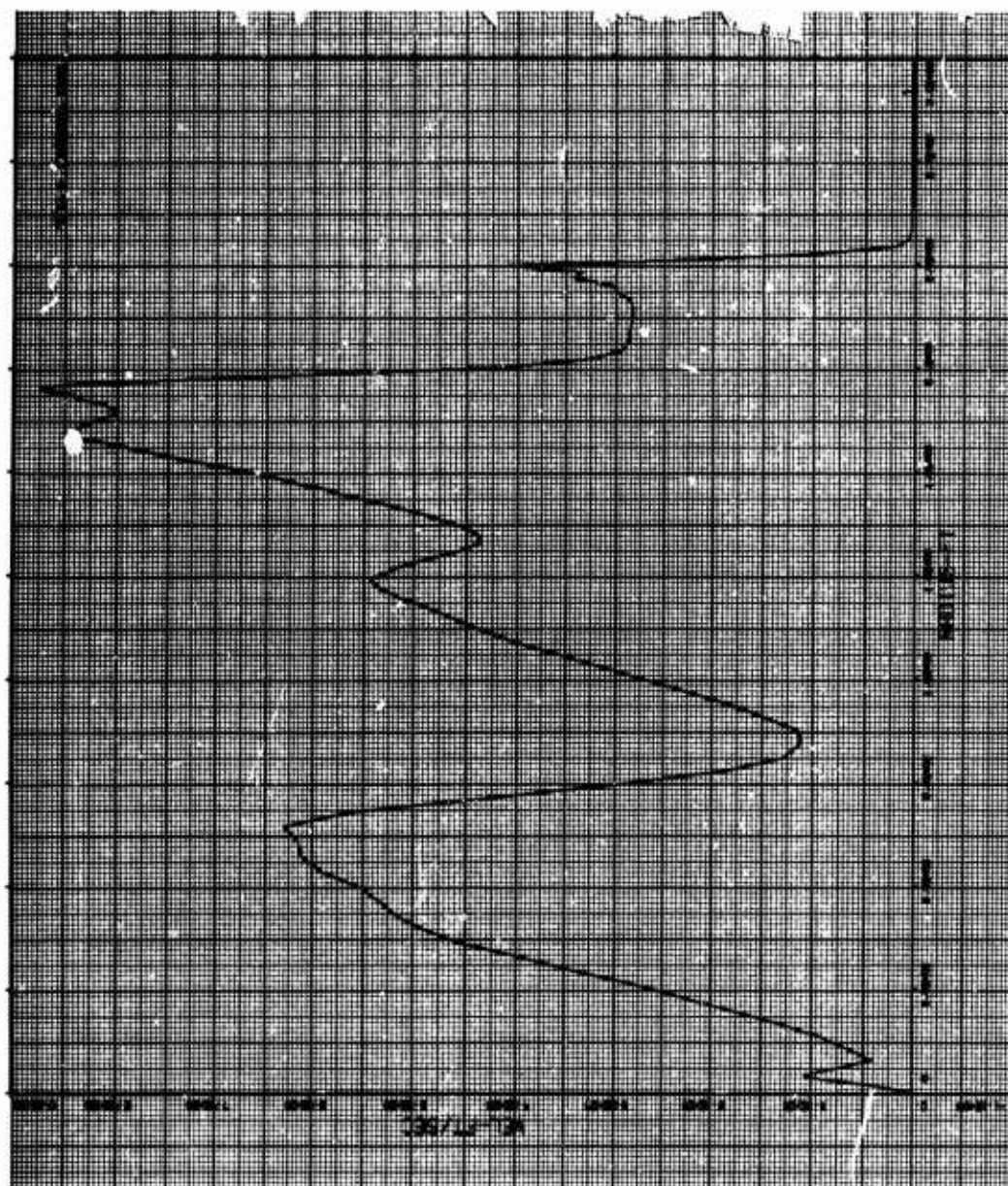


Figure 3. Explosion Environment Data

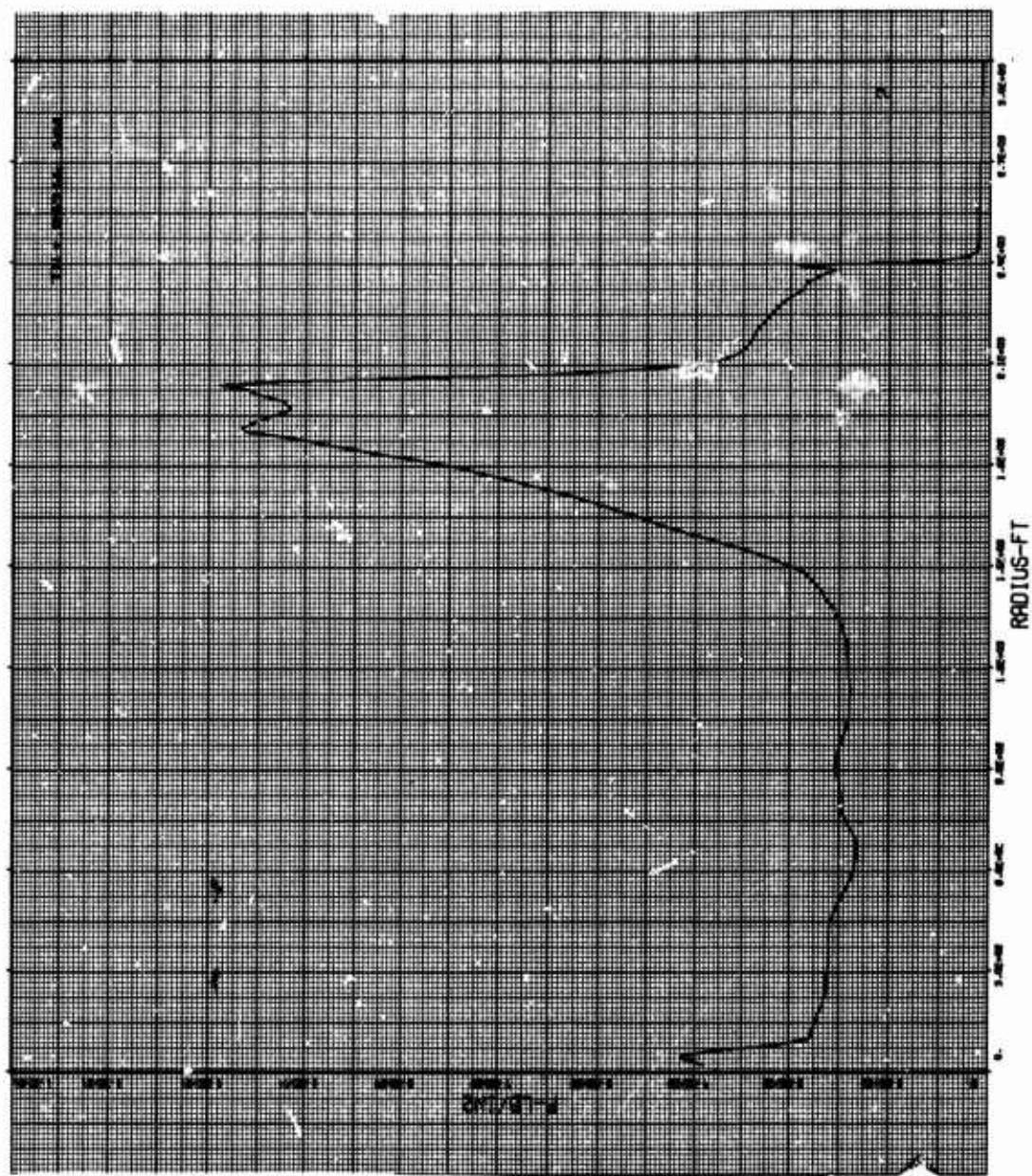


Figure 4. Explosion Environment Data

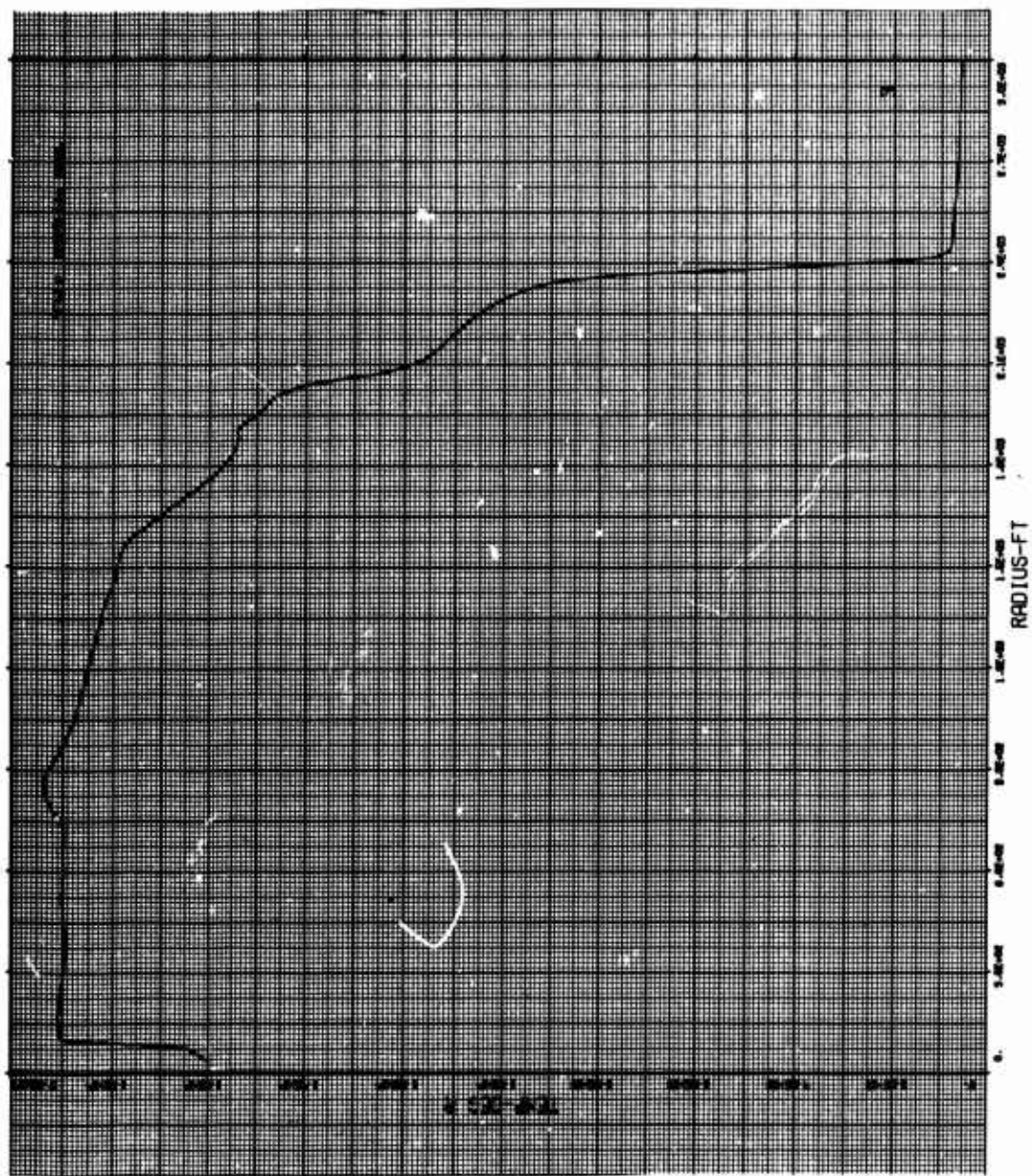


Figure 5. Explosion Environment Data

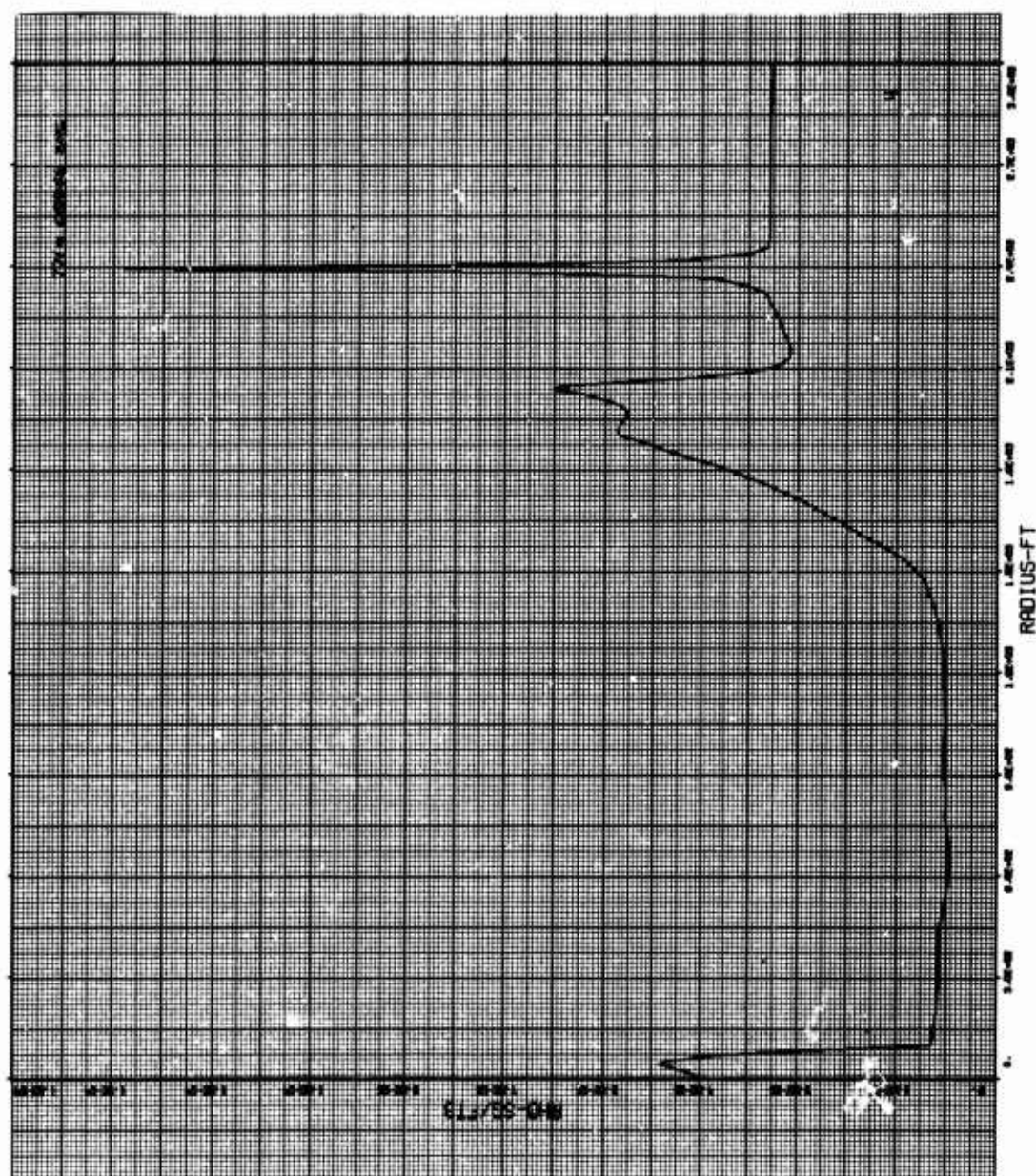


Figure 6. Explosion Environment Data

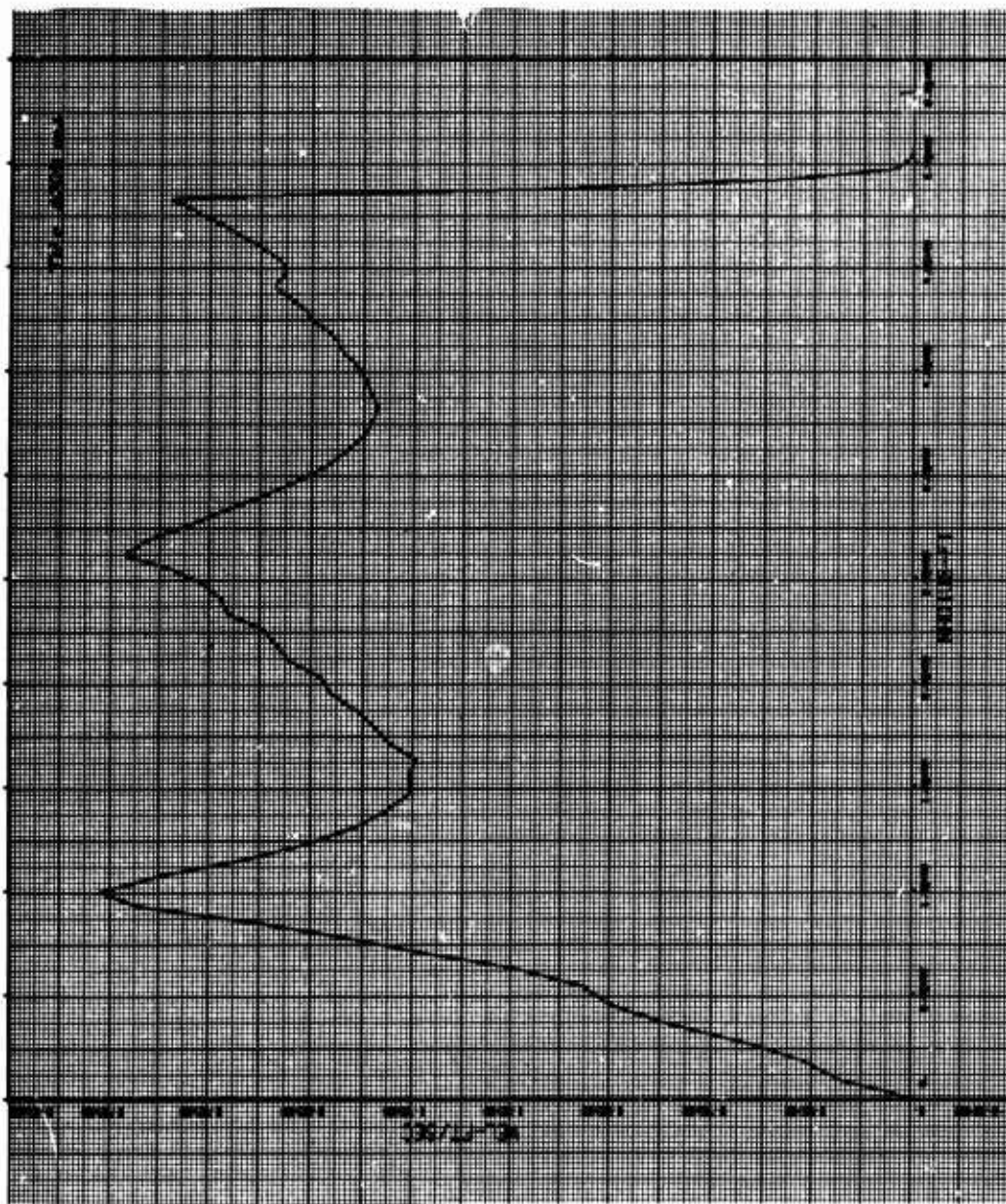


Figure 7. Explosion Environment Data

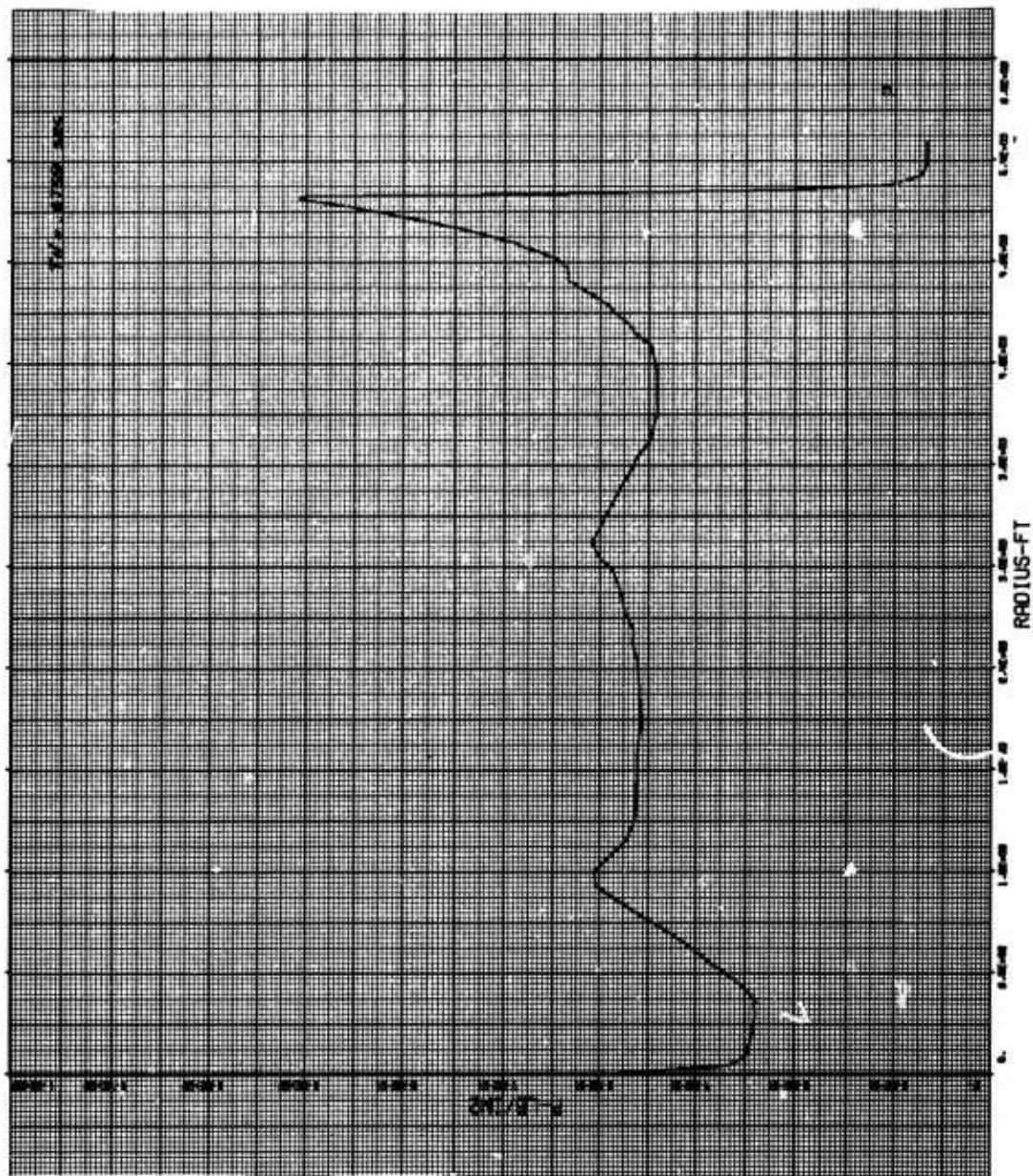


Figure 8. Explosion Environment Data

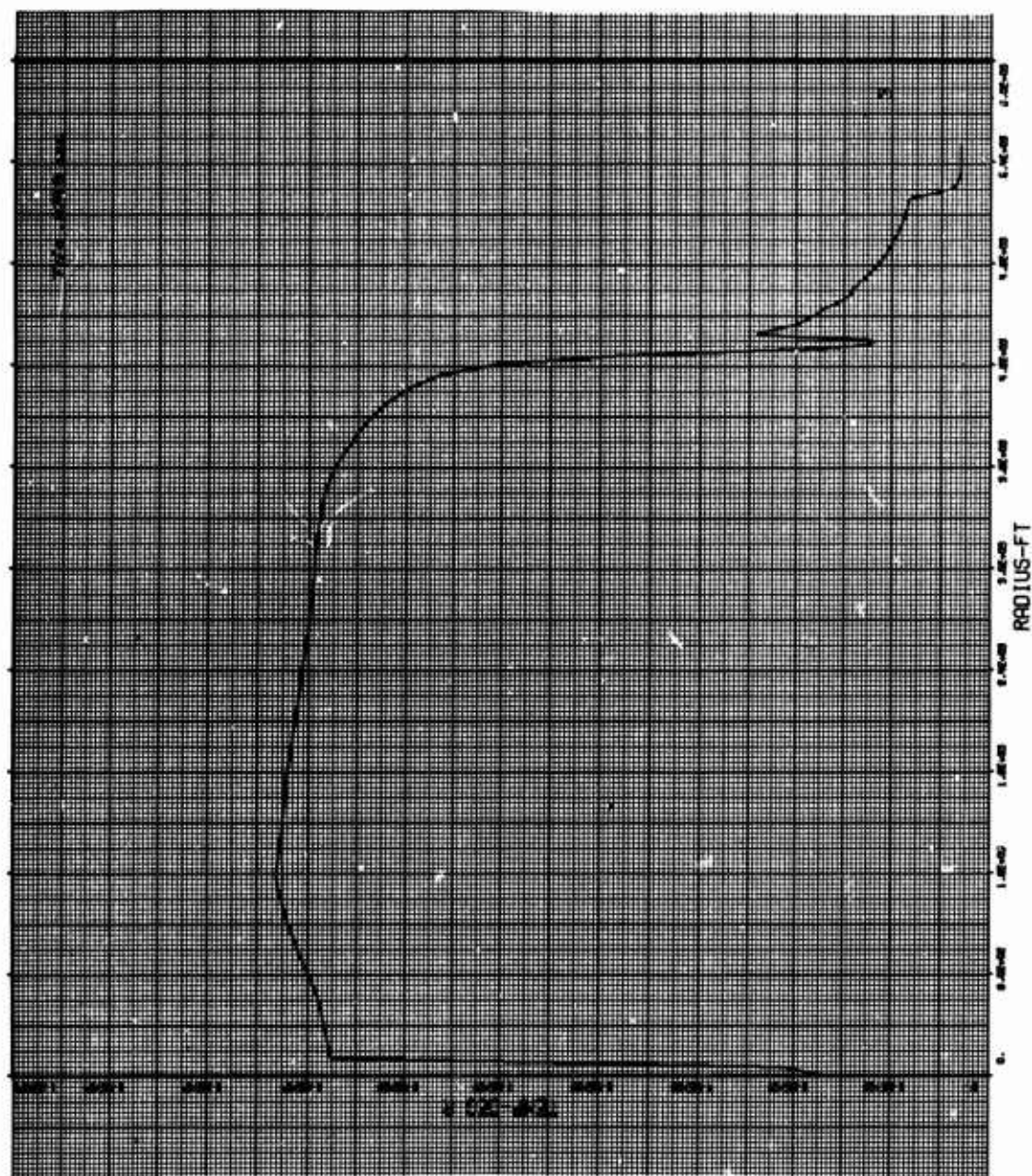


Figure 9. Explosion Environment Data

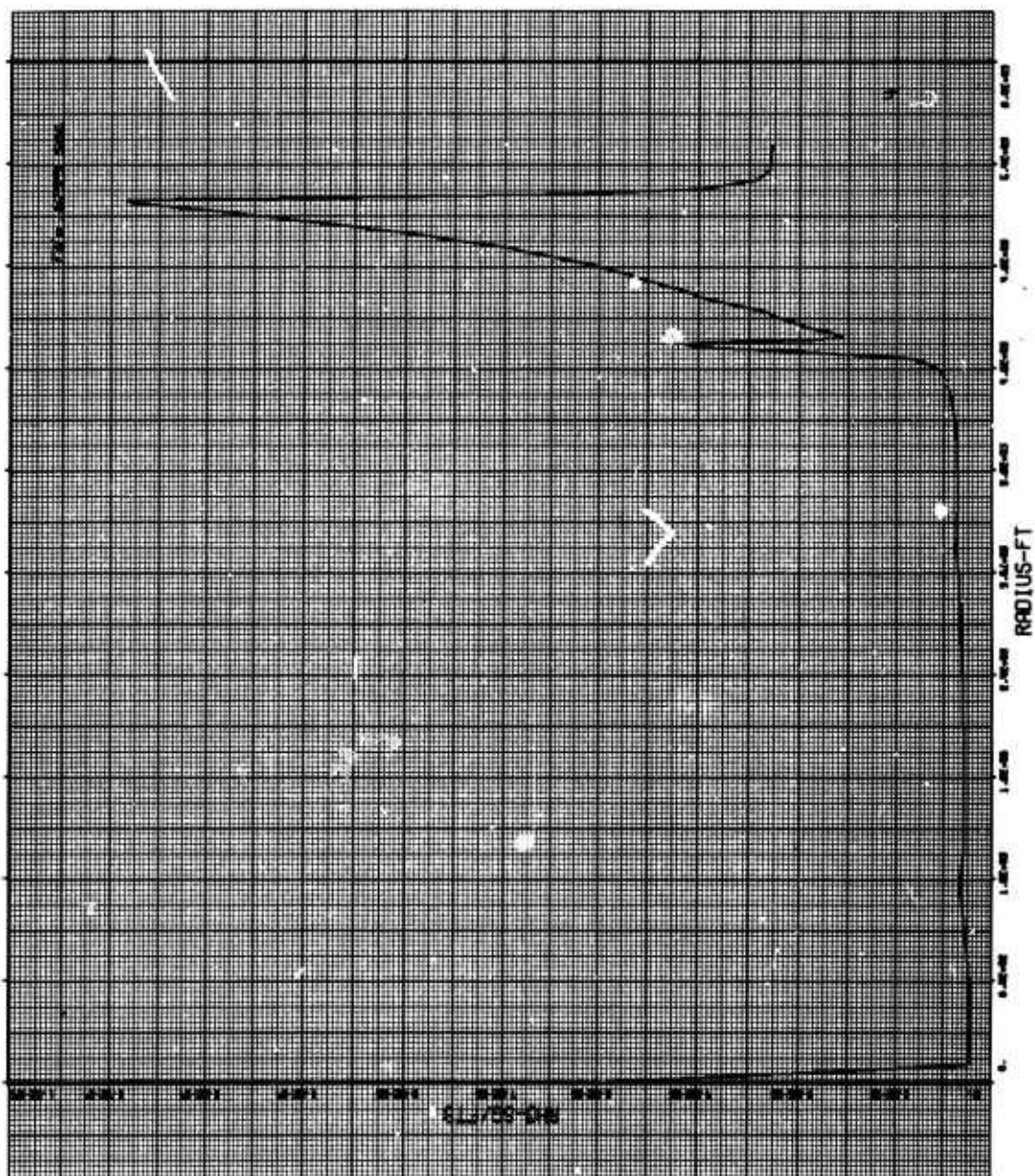


Figure 10. Explosion Environment Data

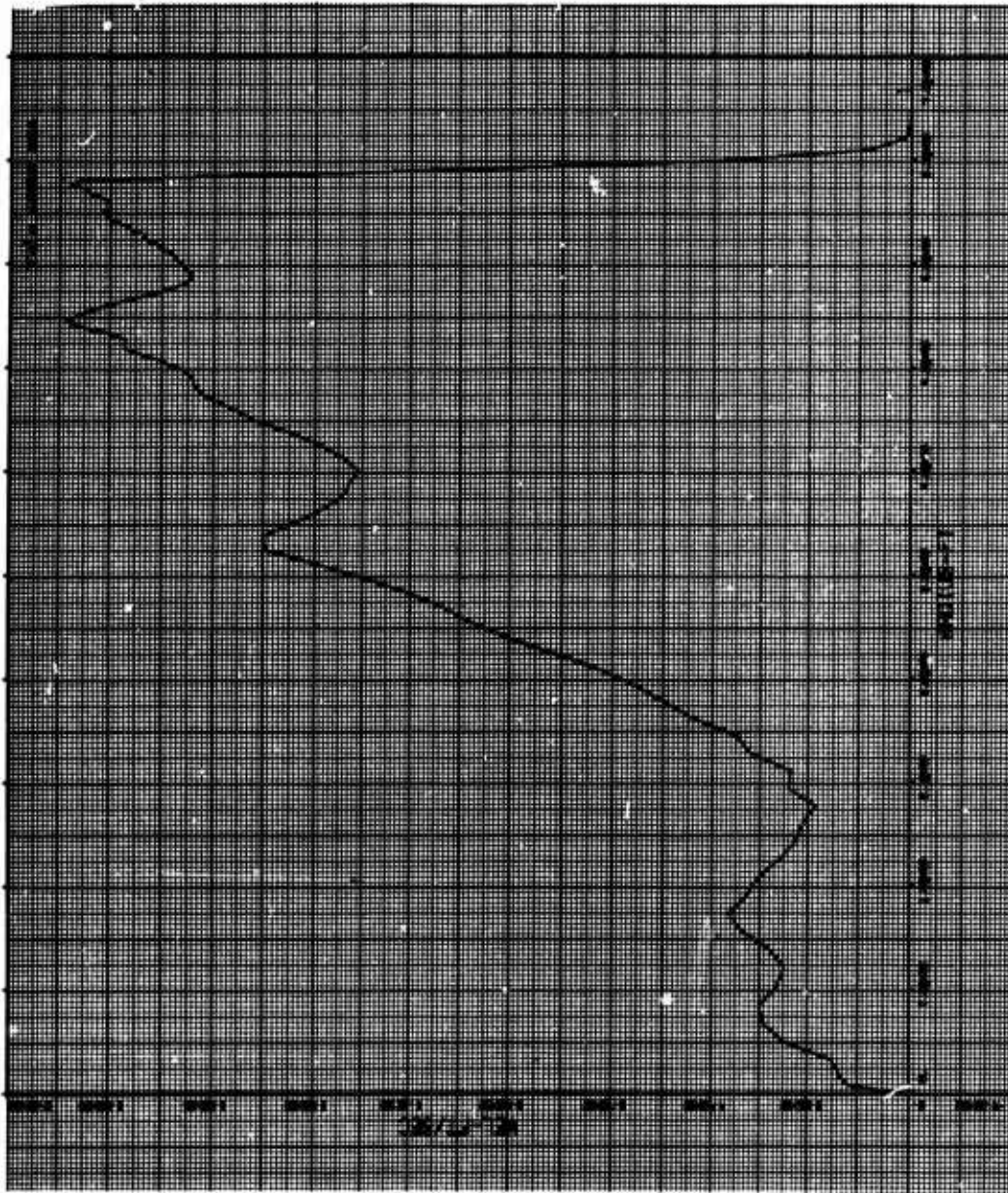


Figure 11. Explosion Environment Data

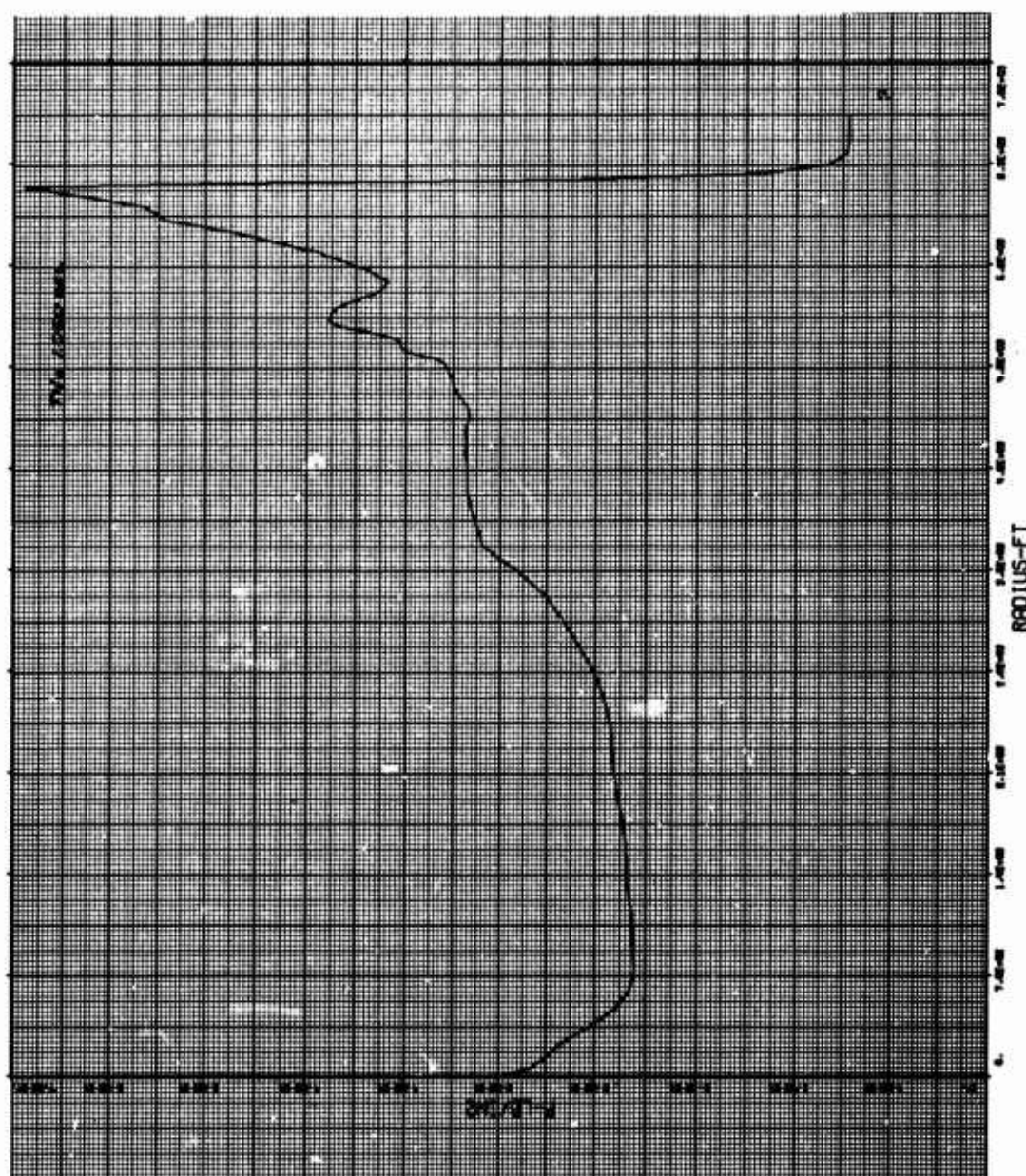


Figure 12. Explosion Environment Data

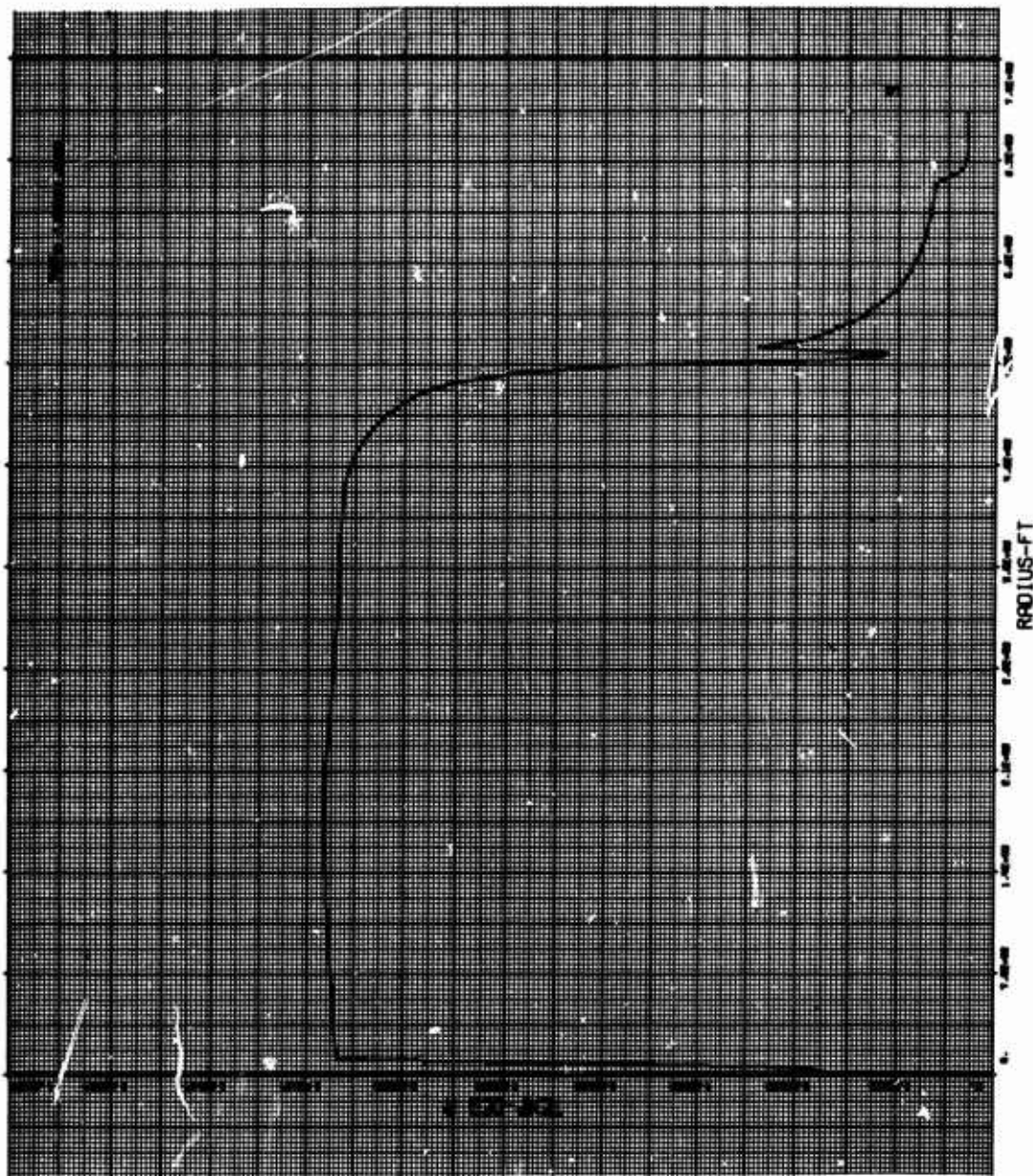


Figure 13. Explosion Environment Data

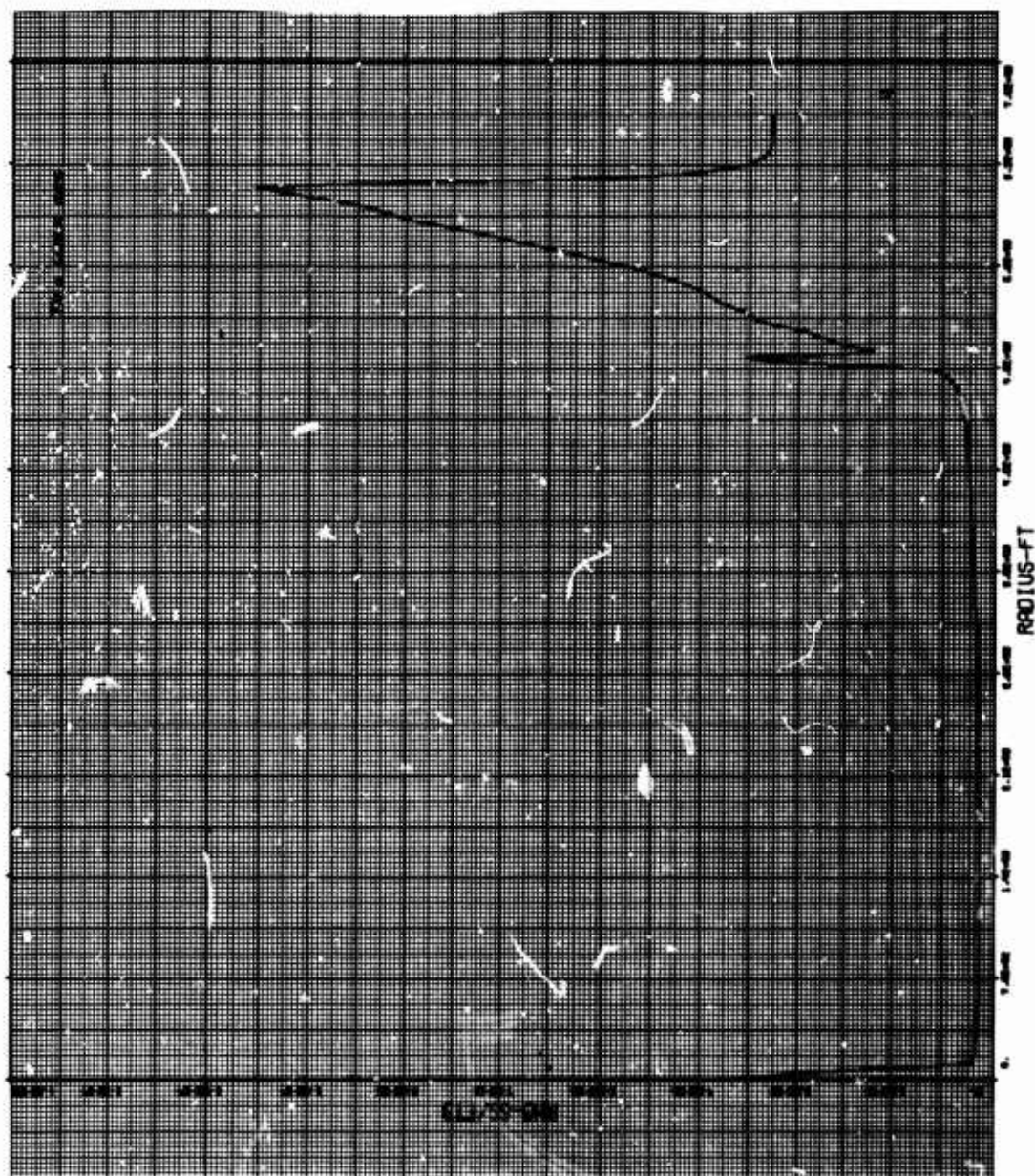


Figure 14. Explosion Environment Data

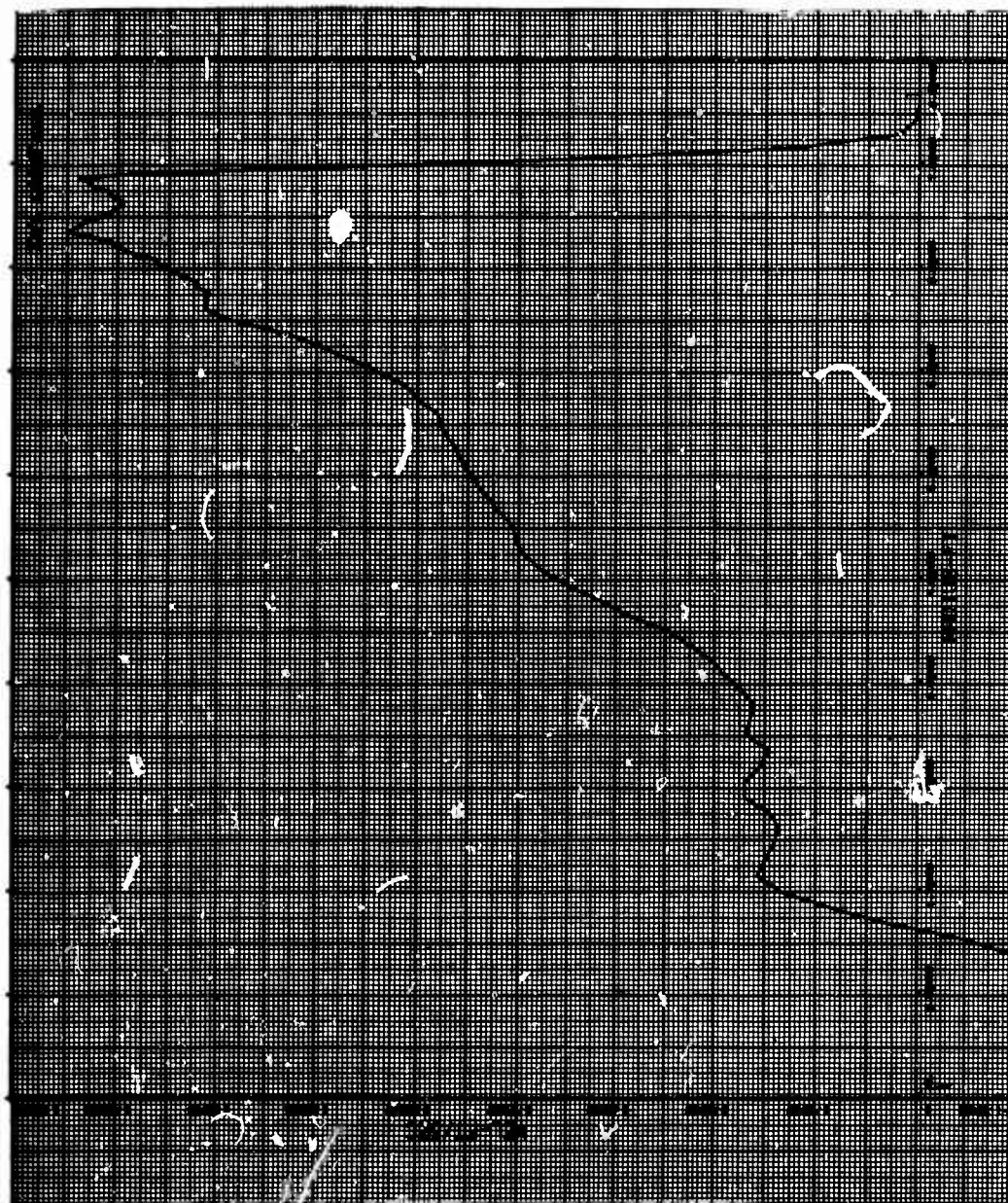


Figure 15. Explosion Environment Data

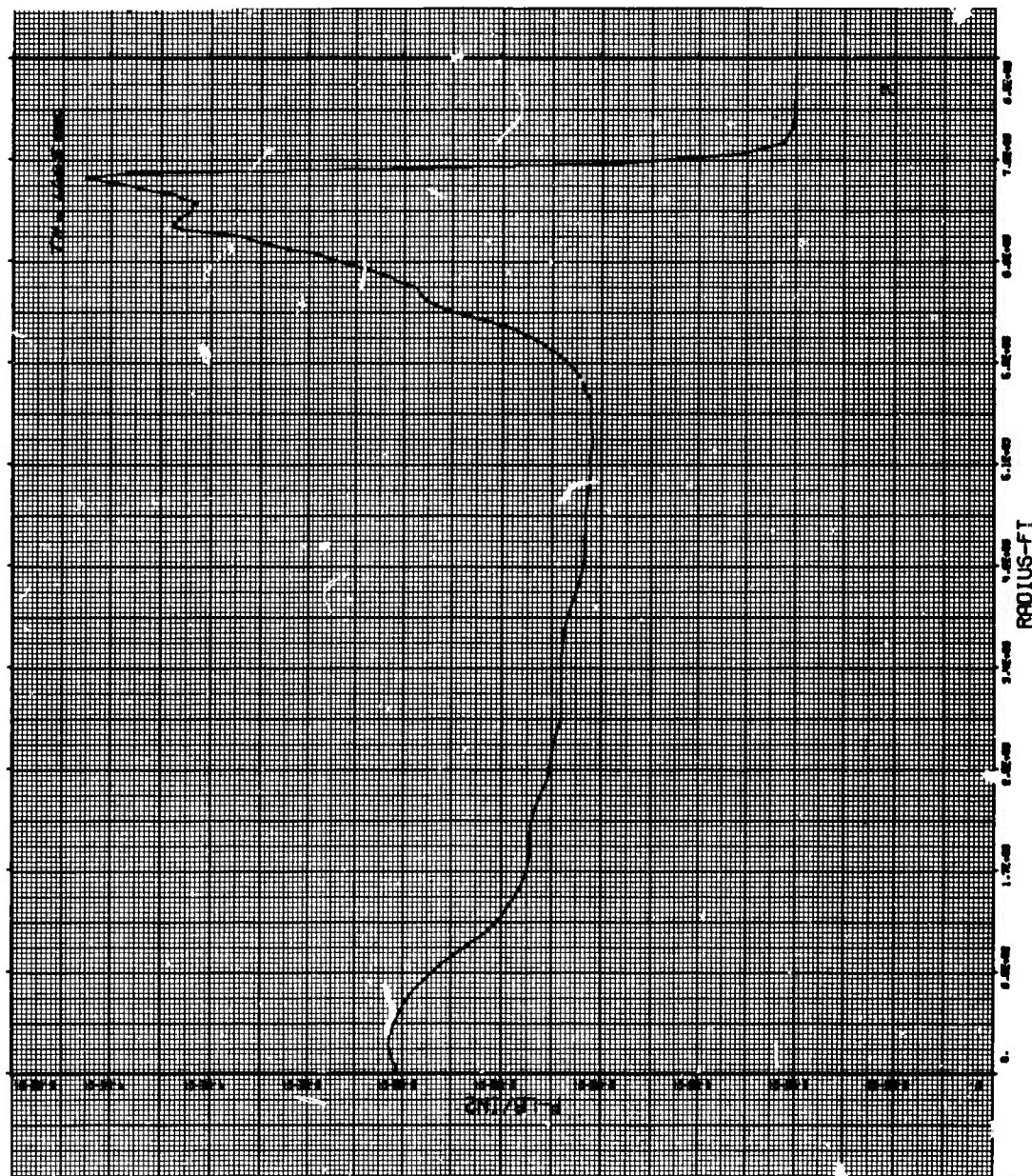


Figure 16. Explosion Environment Data

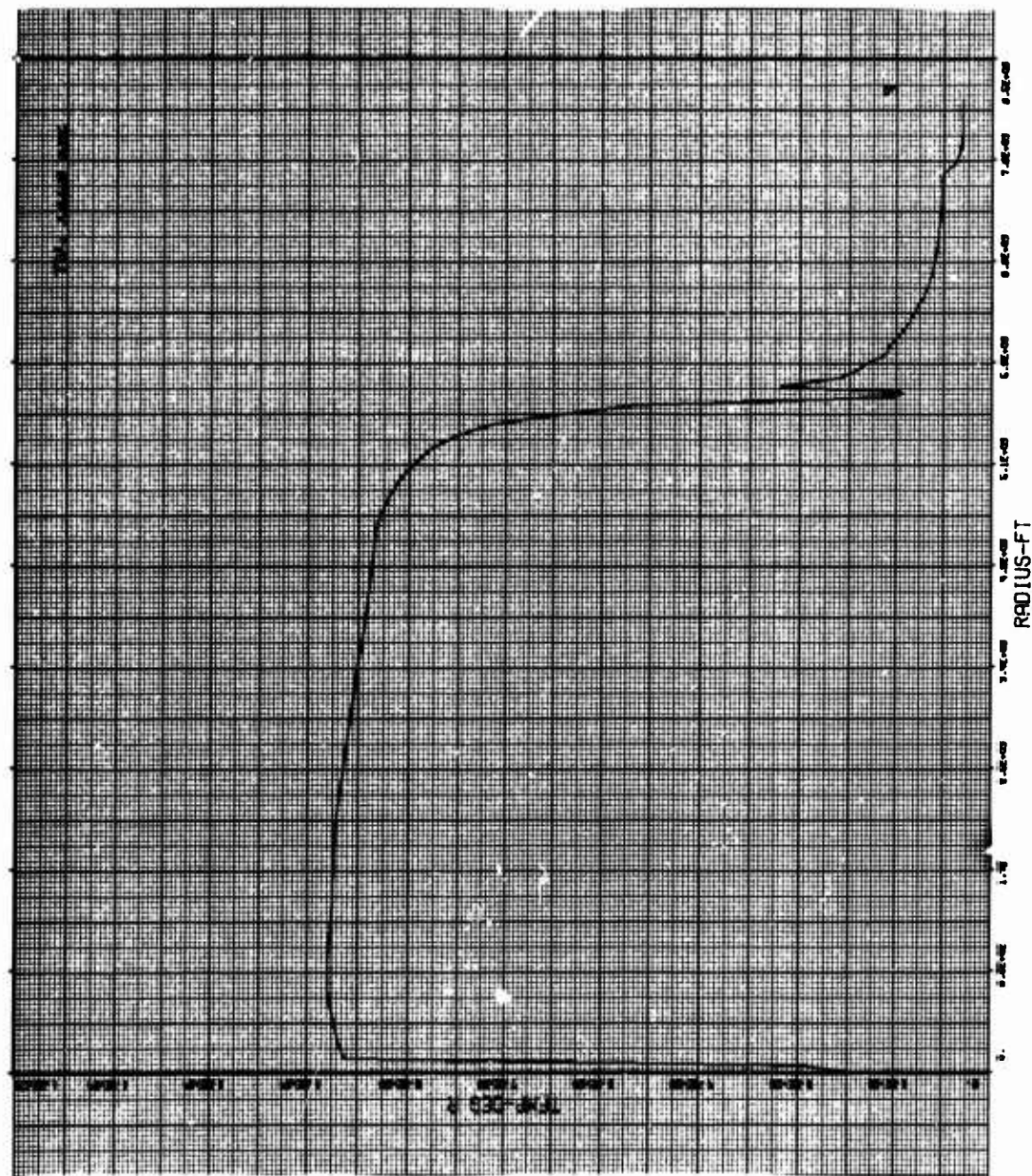


Figure 17. Explosion Environment Data

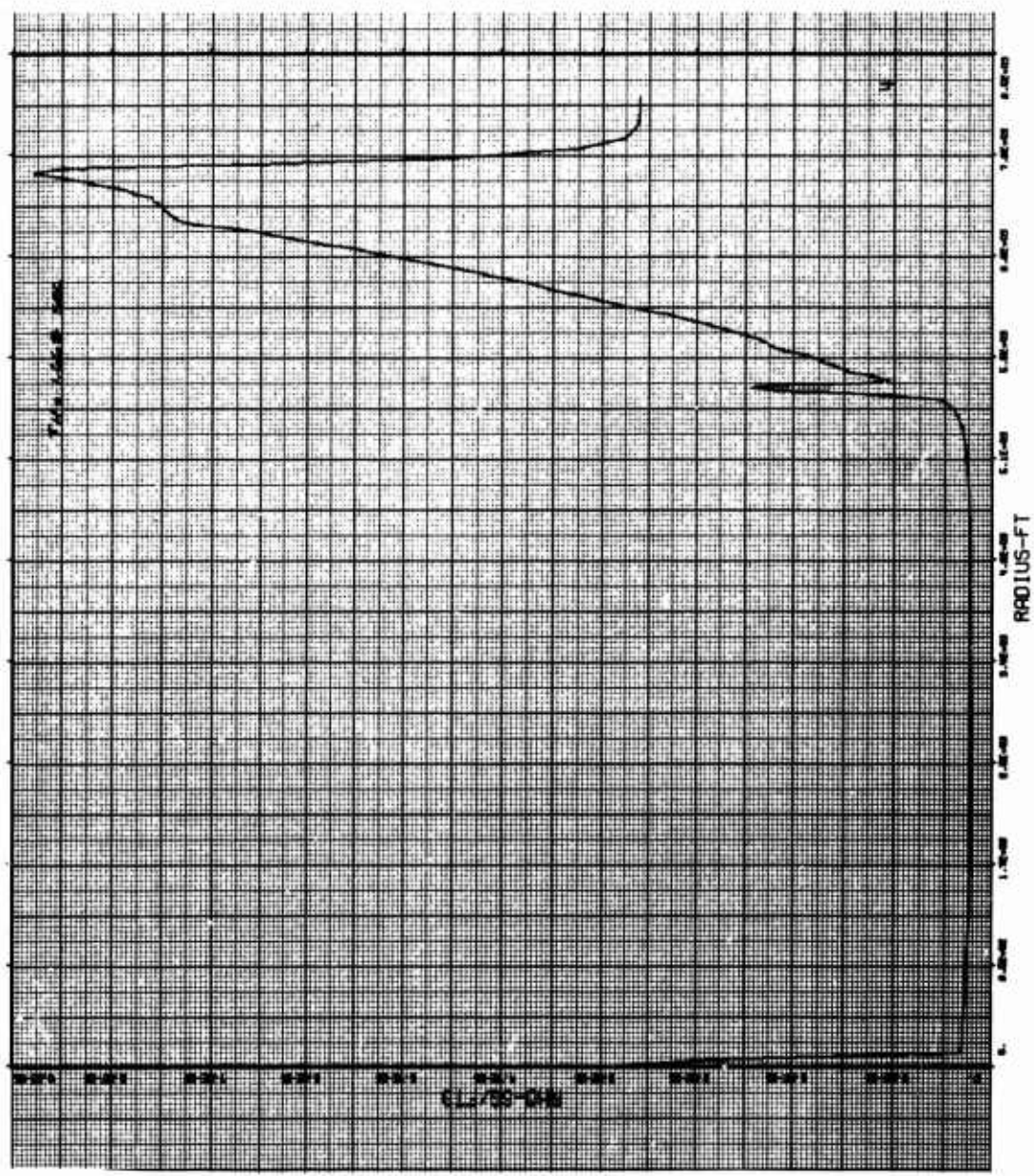


Figure 18. Explosion Environment Data

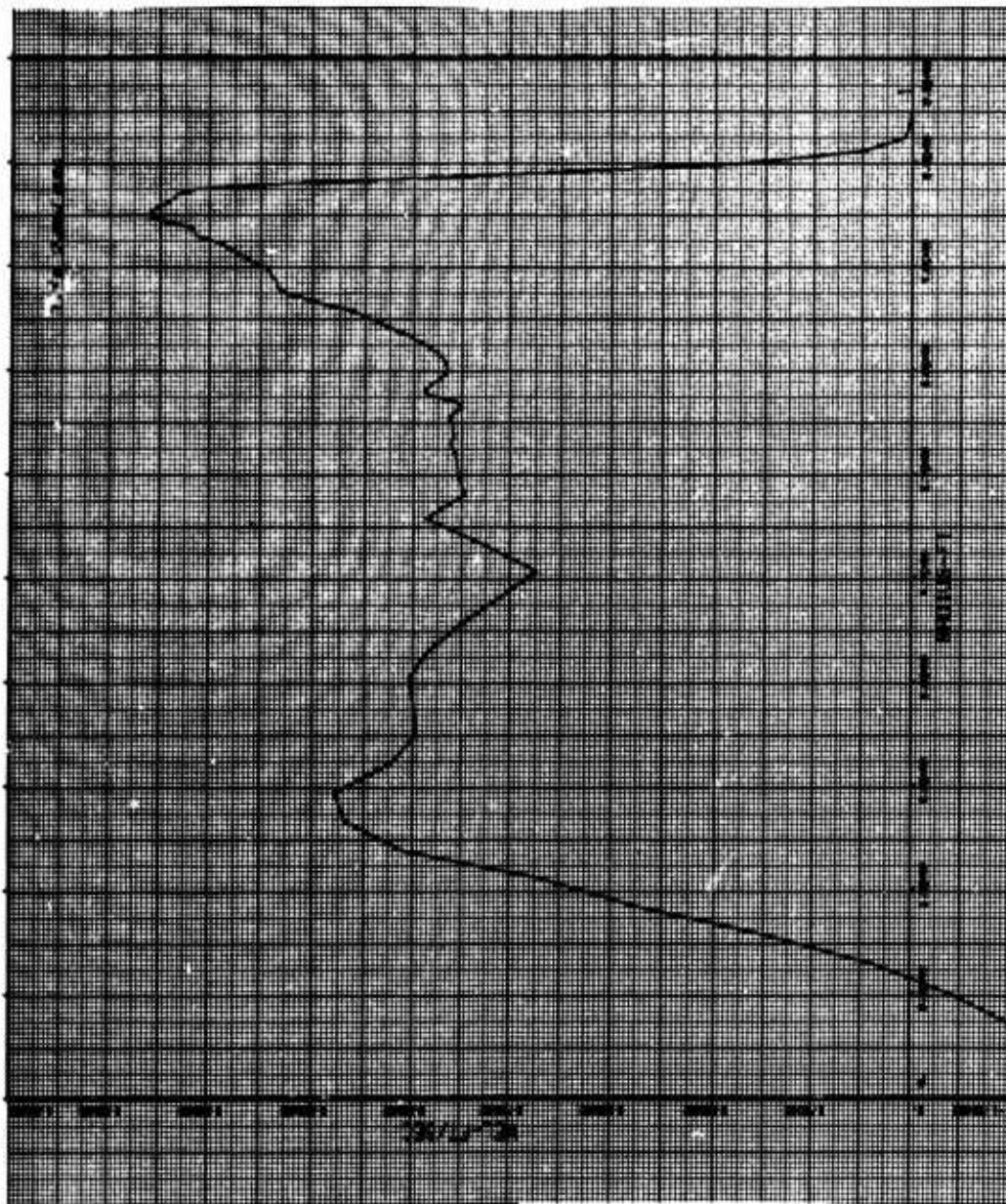


Figure 19. Explosion Environment Data

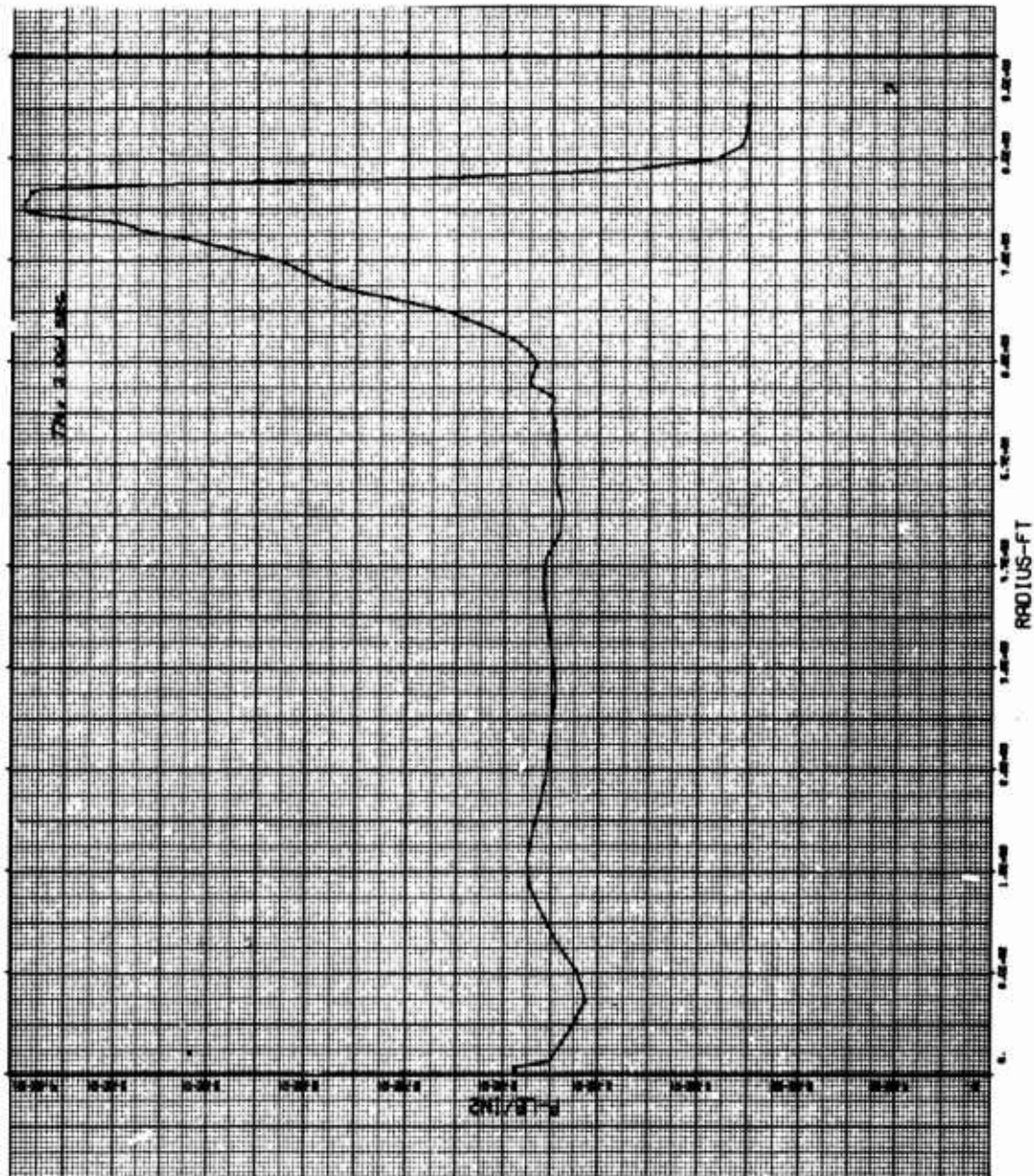


Figure 20. Explosion Environment Data

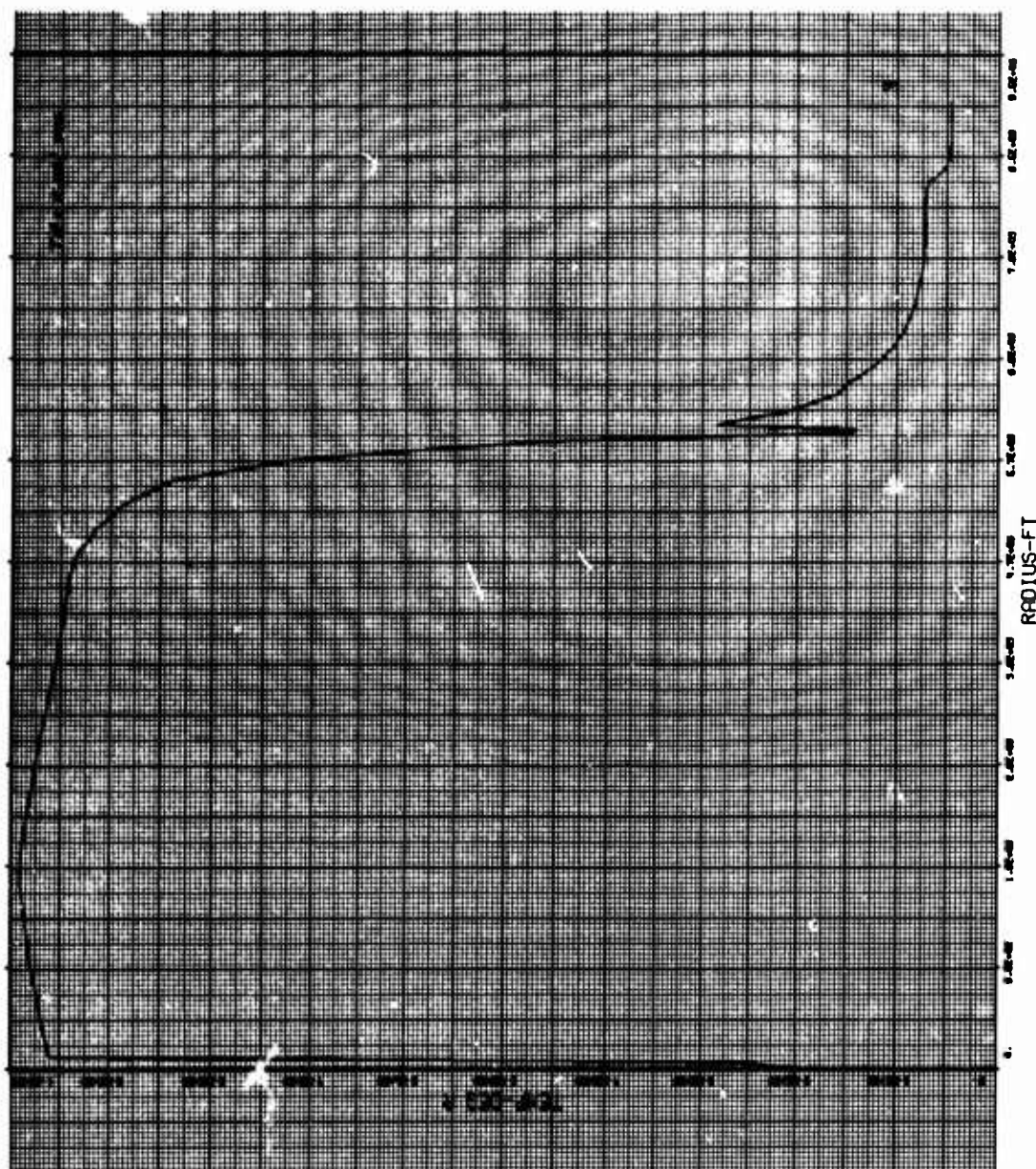


Figure 21. Explosion Environment Data

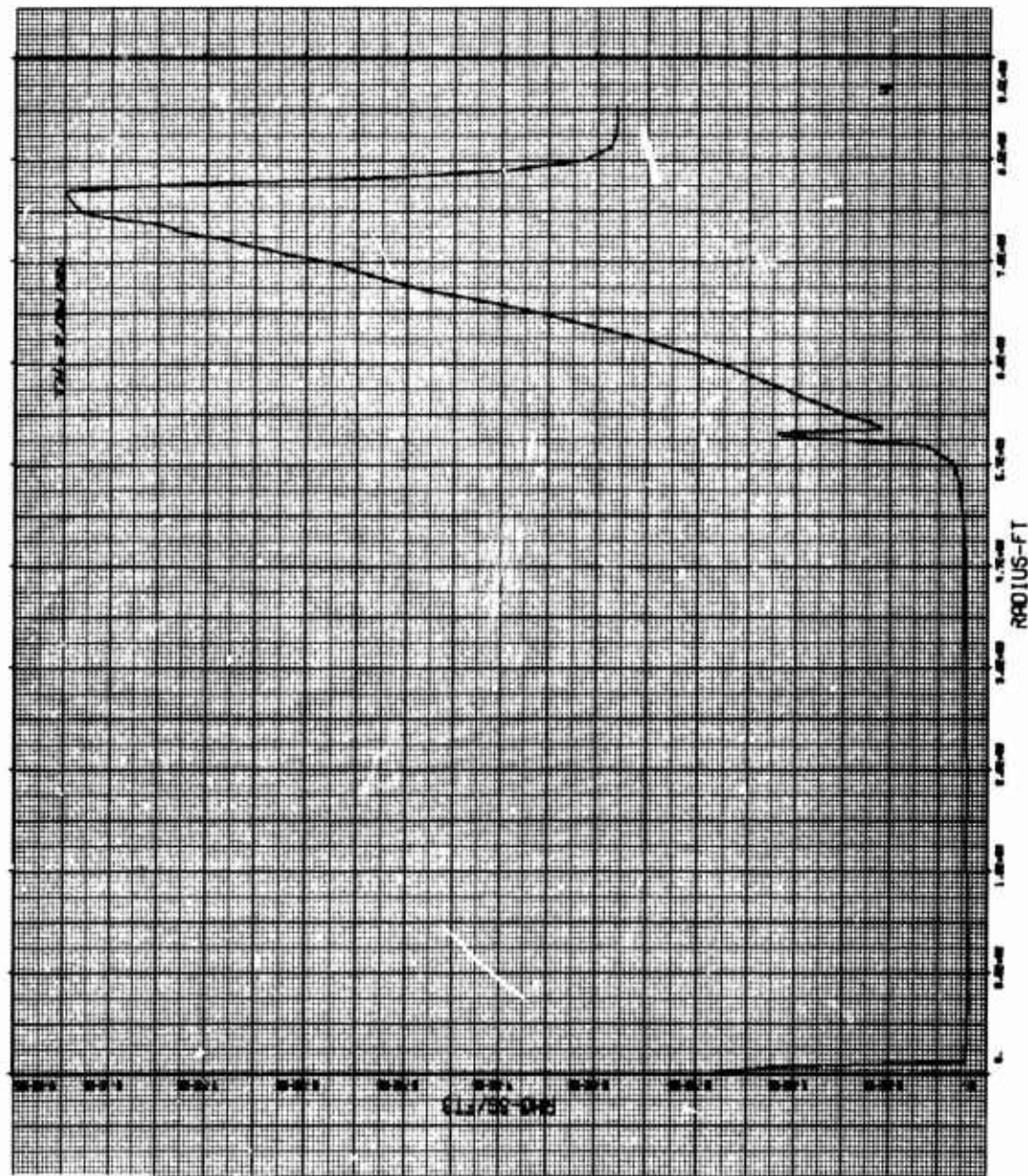


Figure 22. Explosion Environment Data

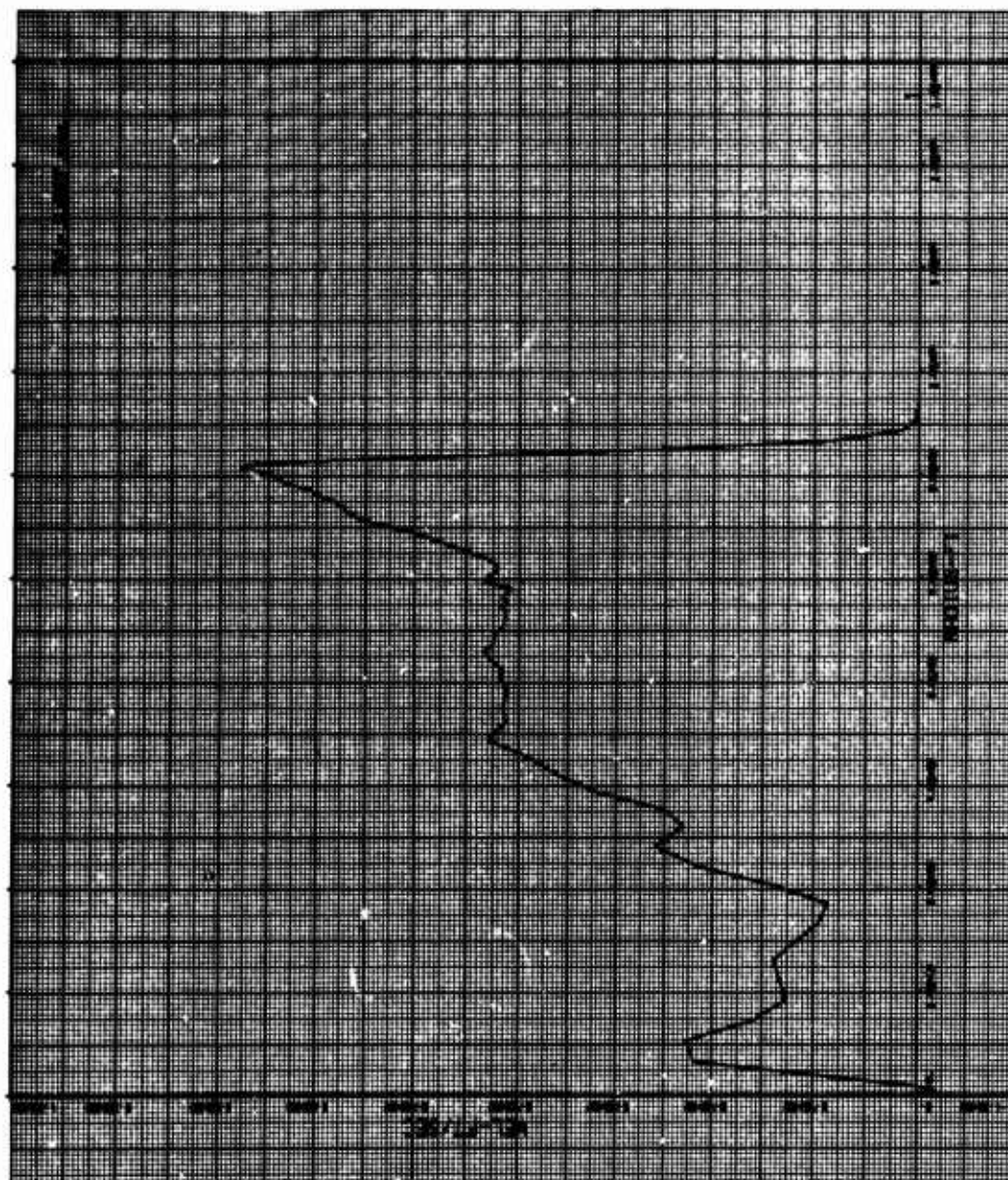


Figure 23. Explosion Environment Data

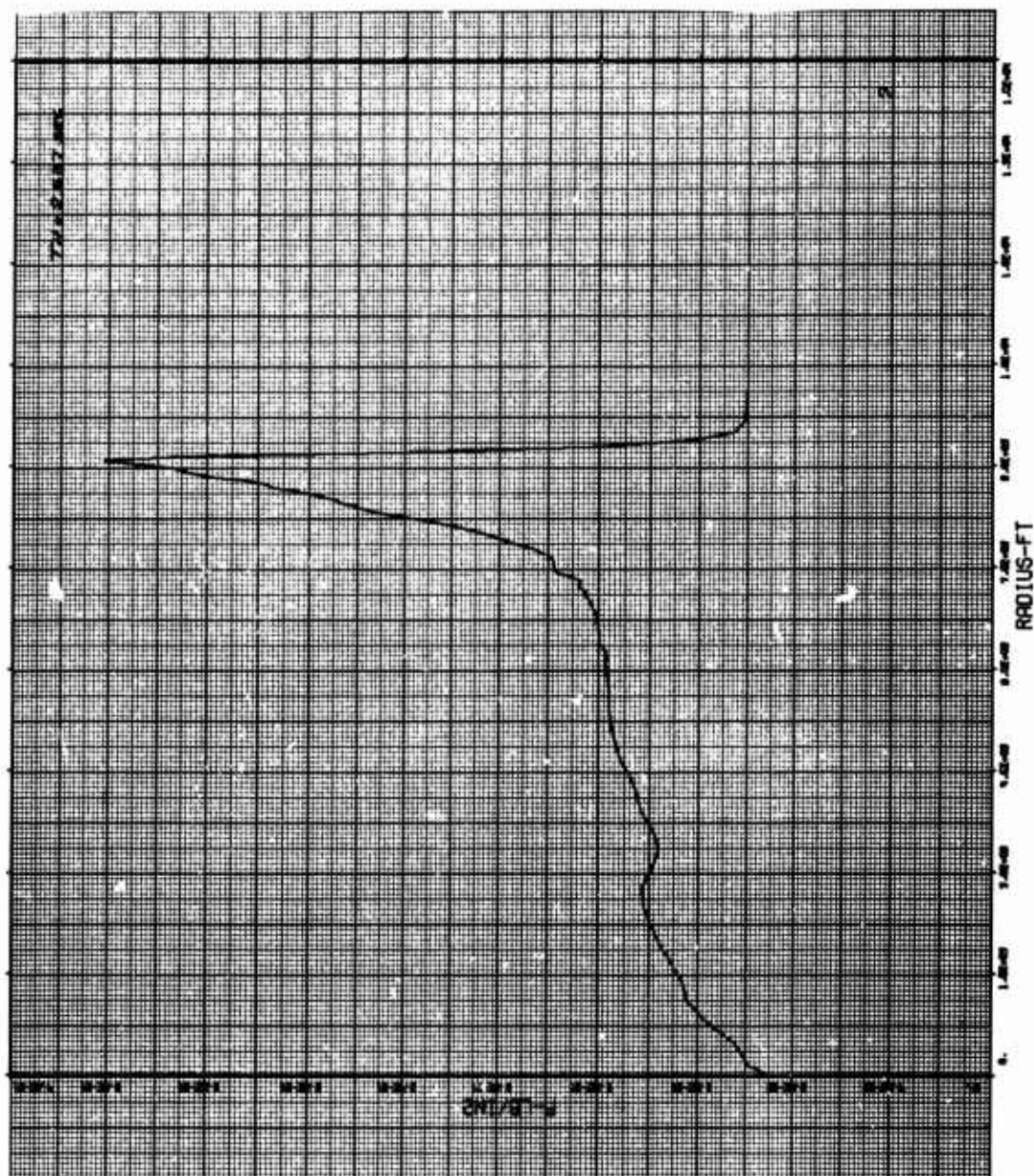


Figure 24. Explosion Environment Data

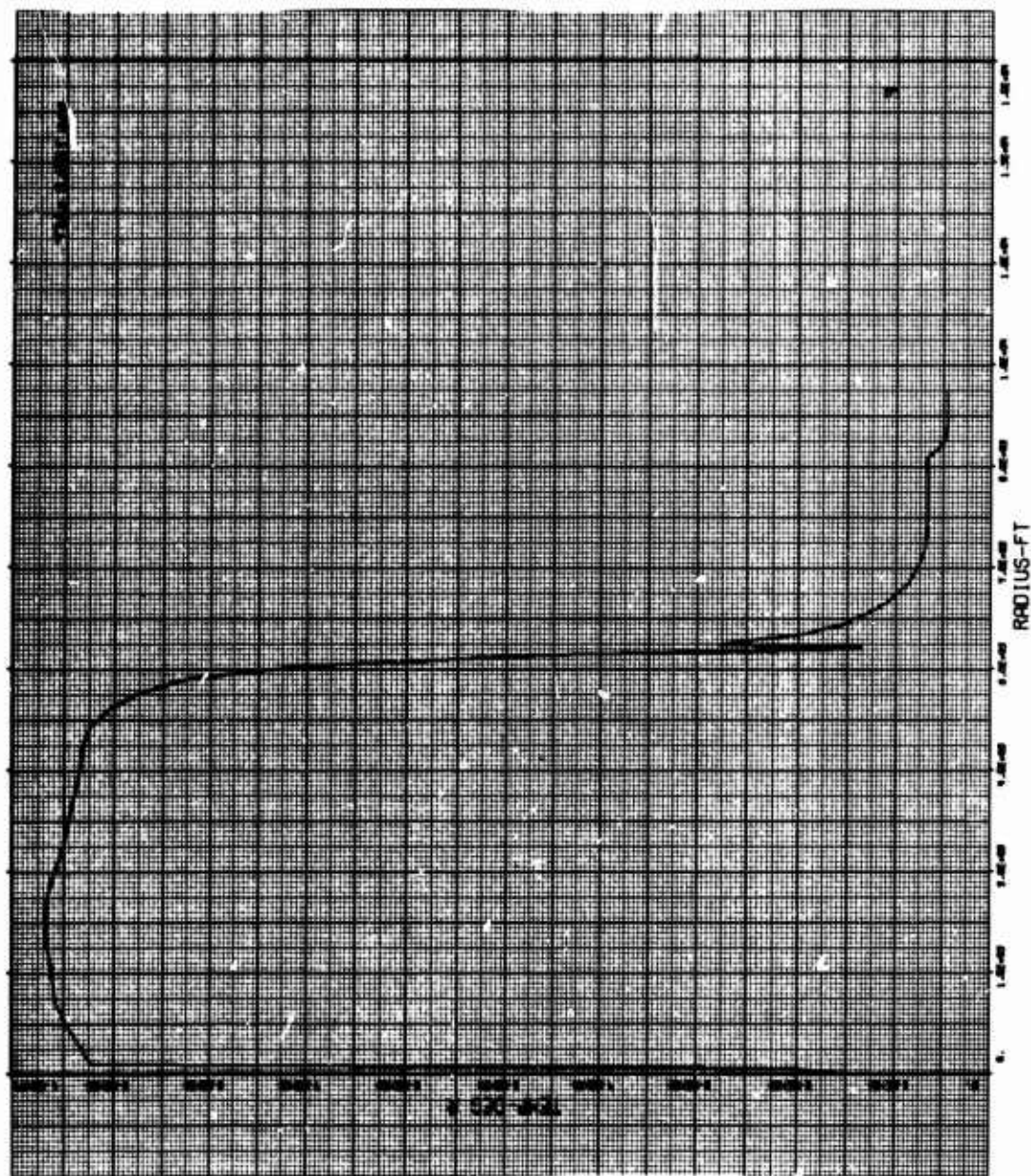


Figure 25. Explosion Environment Data

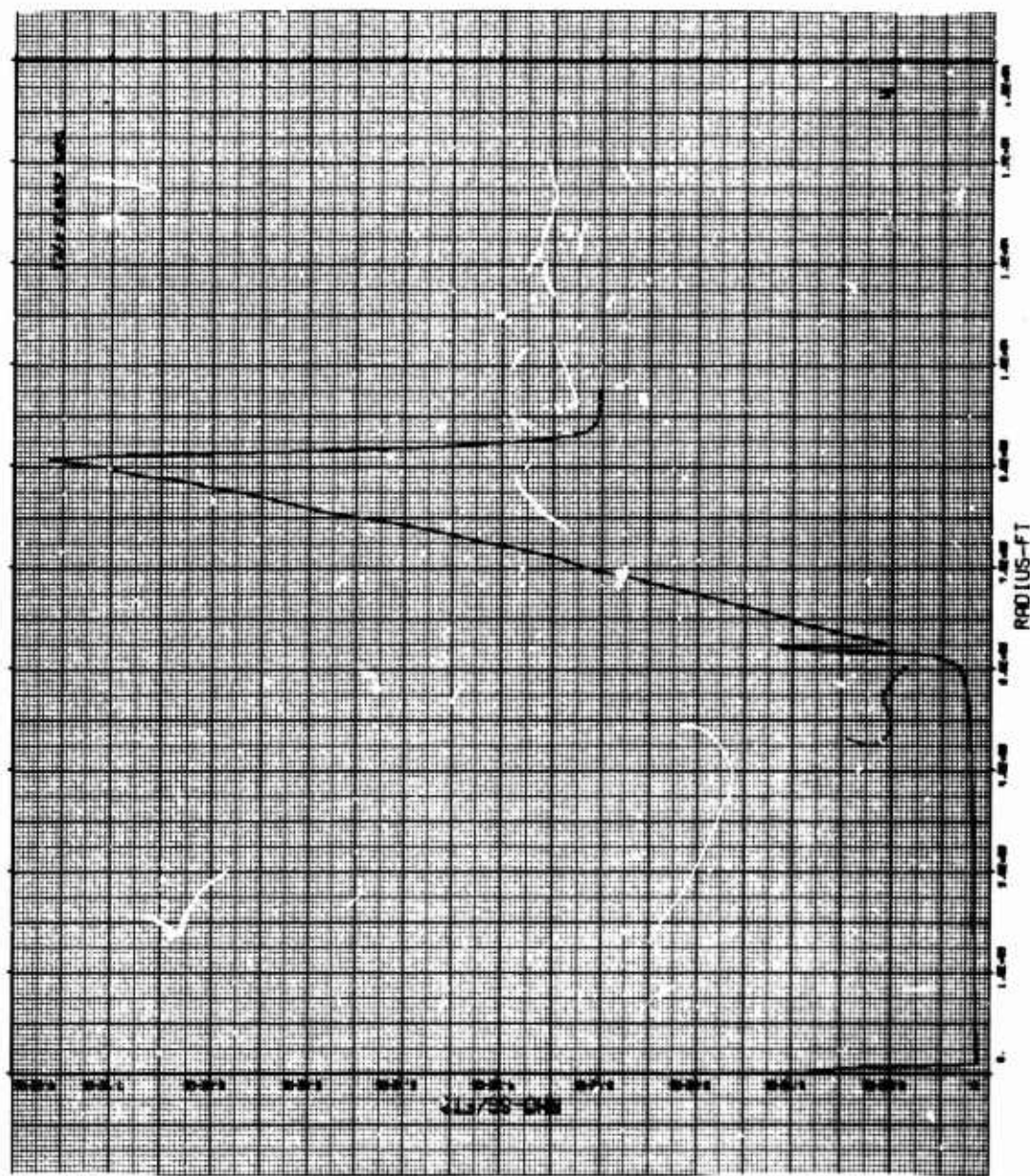


Figure 26. Explosion Environment Data

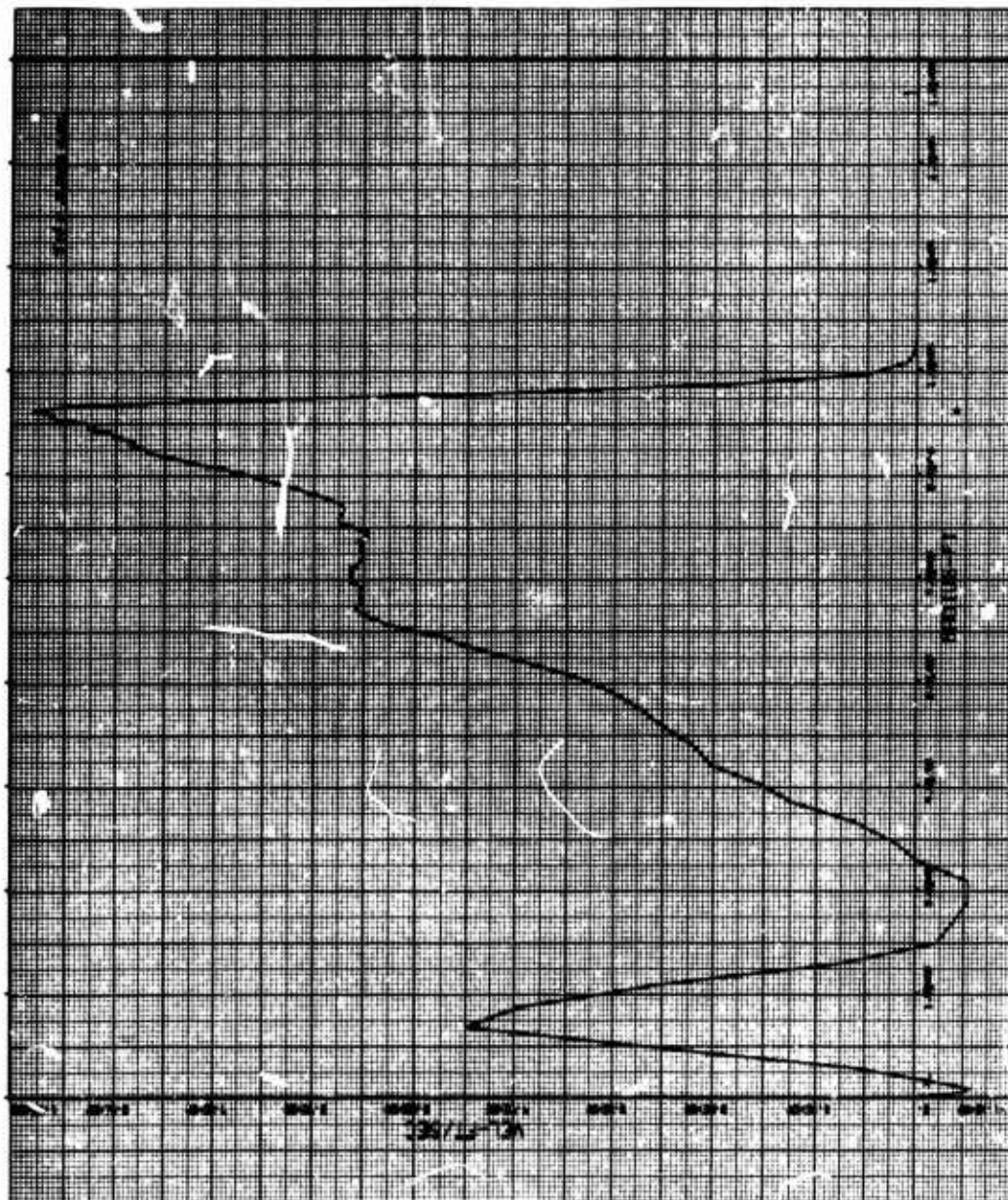


Figure 27. Explosion Environment Data

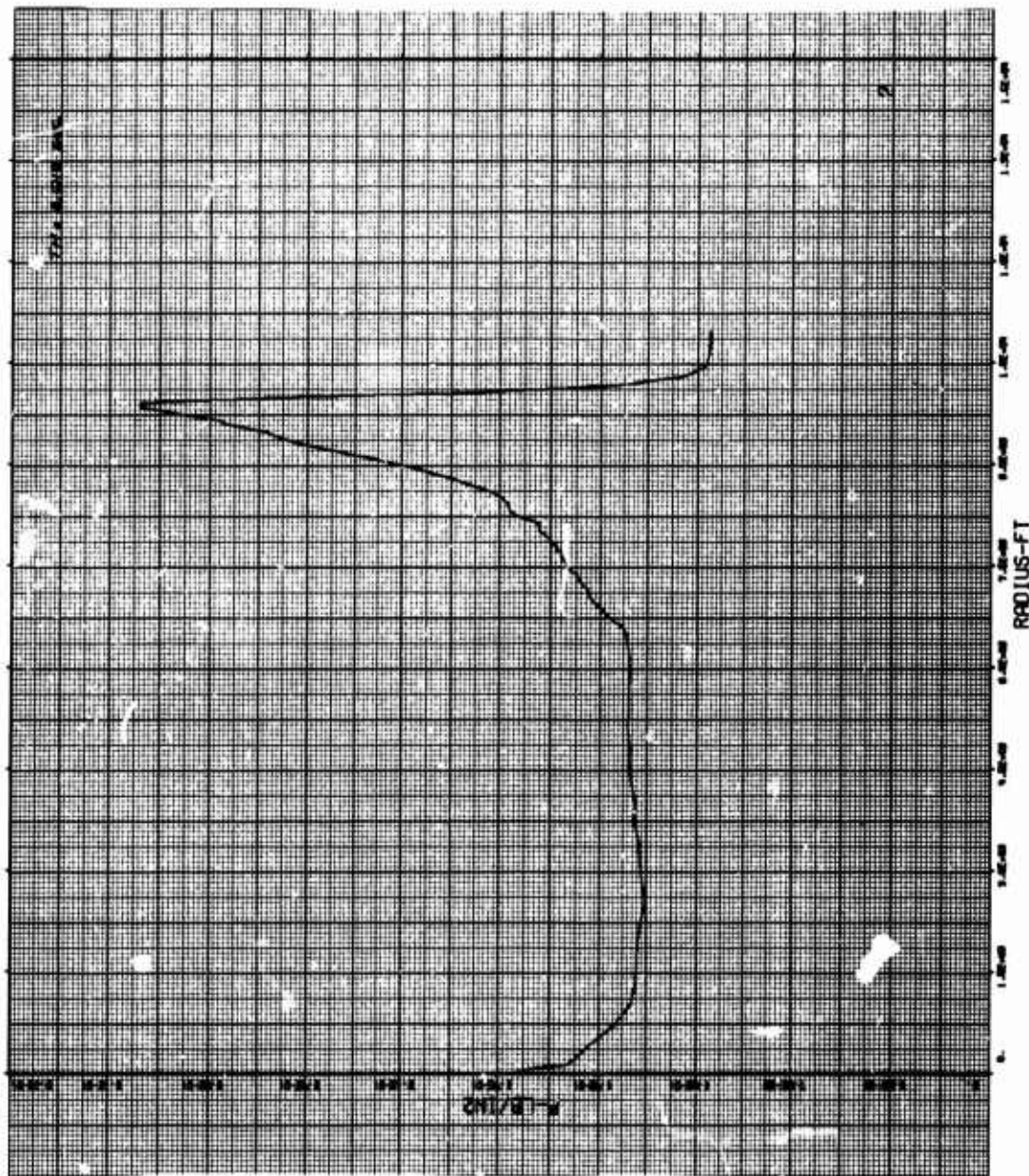


Figure 28. Explosion Environment Data

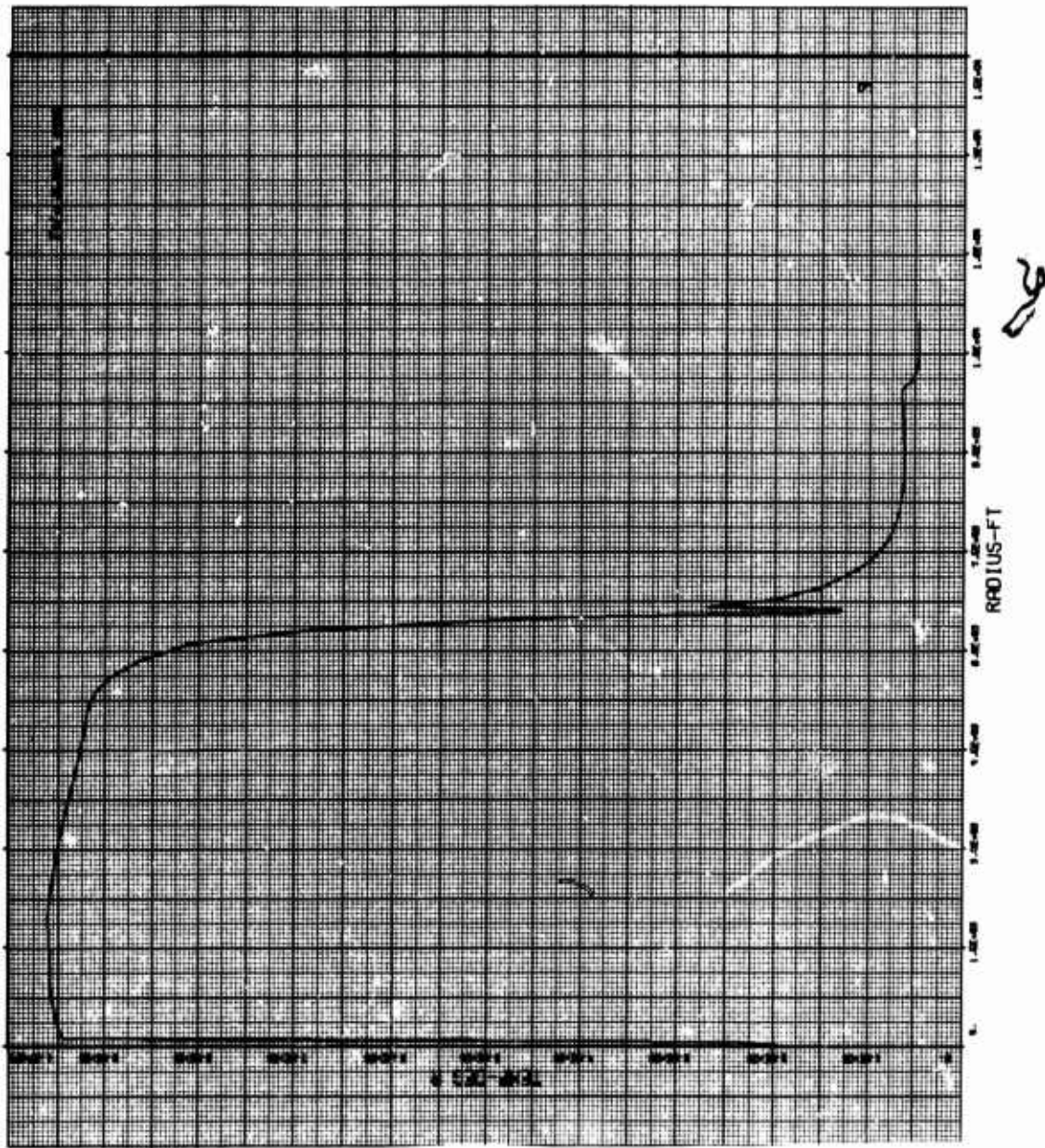


Figure 29. Explosion Environment Data

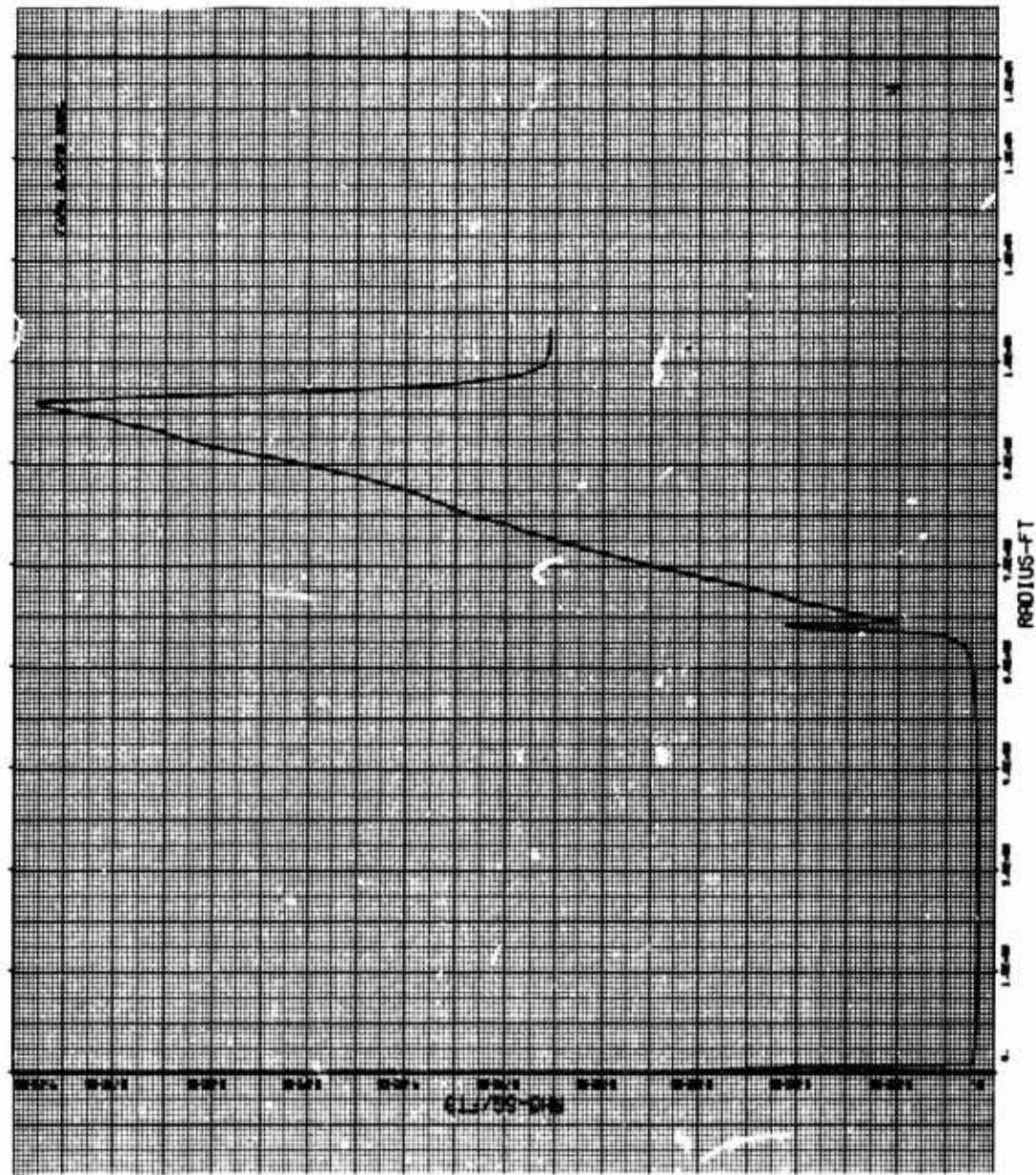


Figure 30. Explosion Environment Data

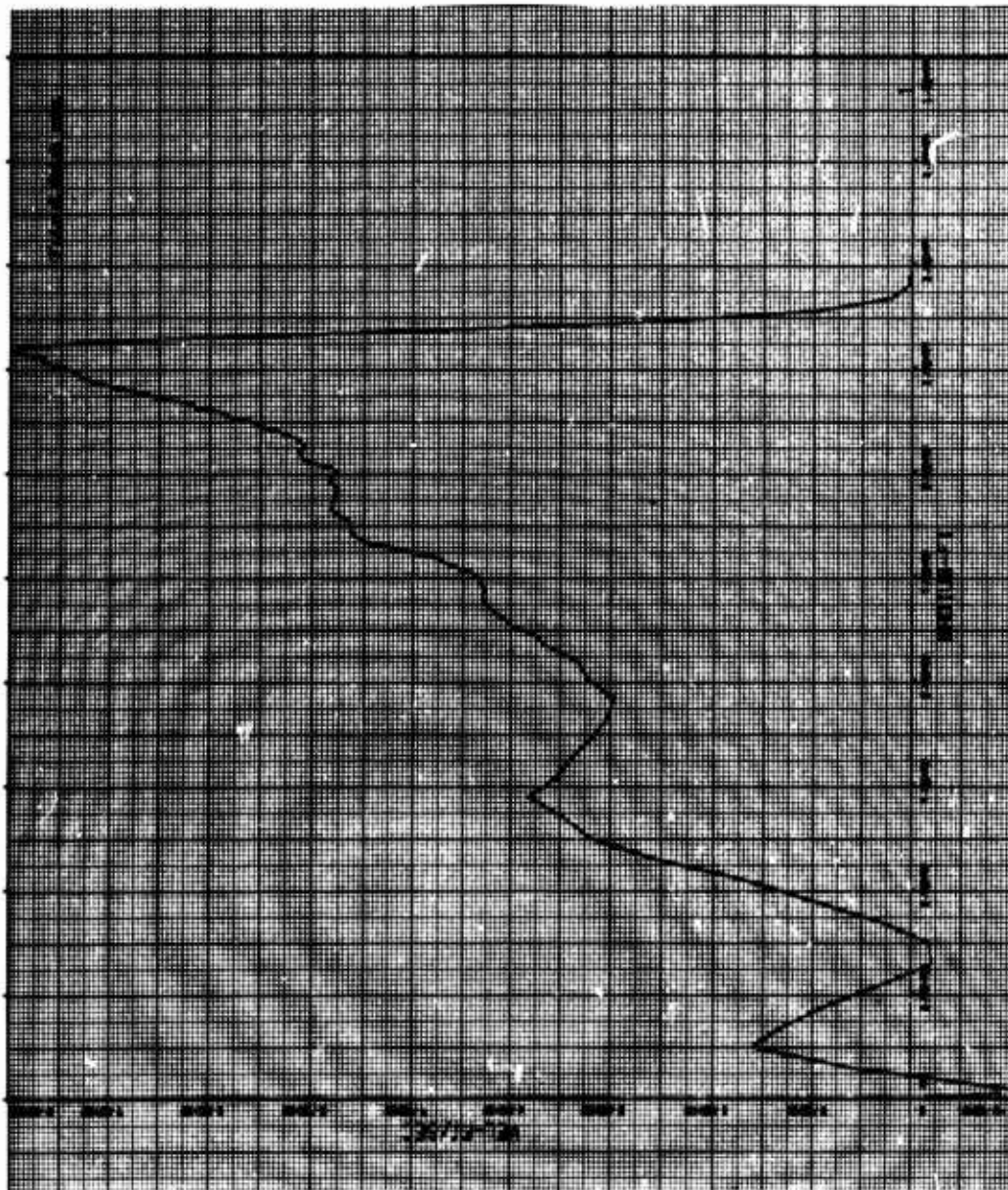


Figure 31. Explosion Environment Data

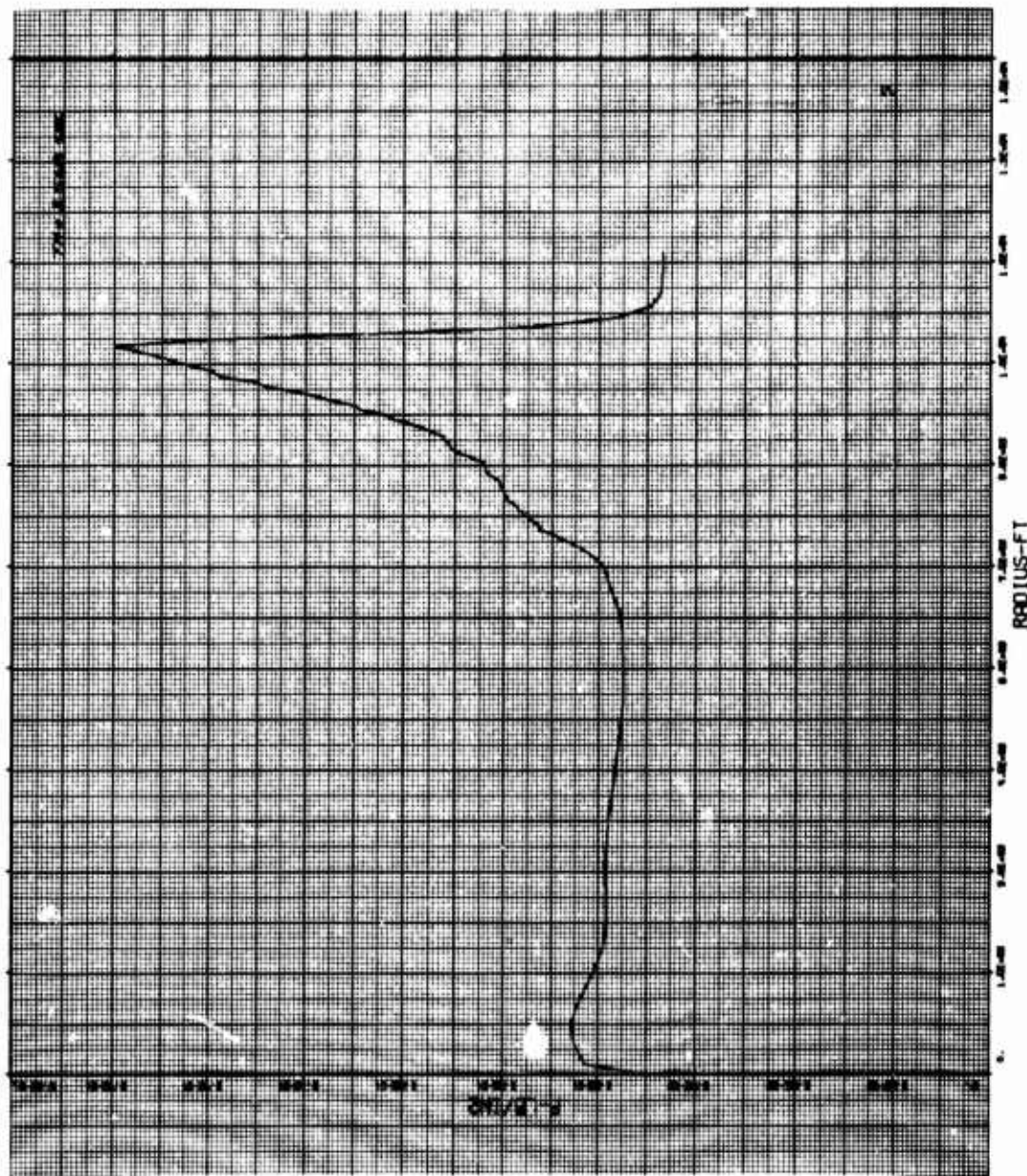


Figure 32. Explosion Environment Data

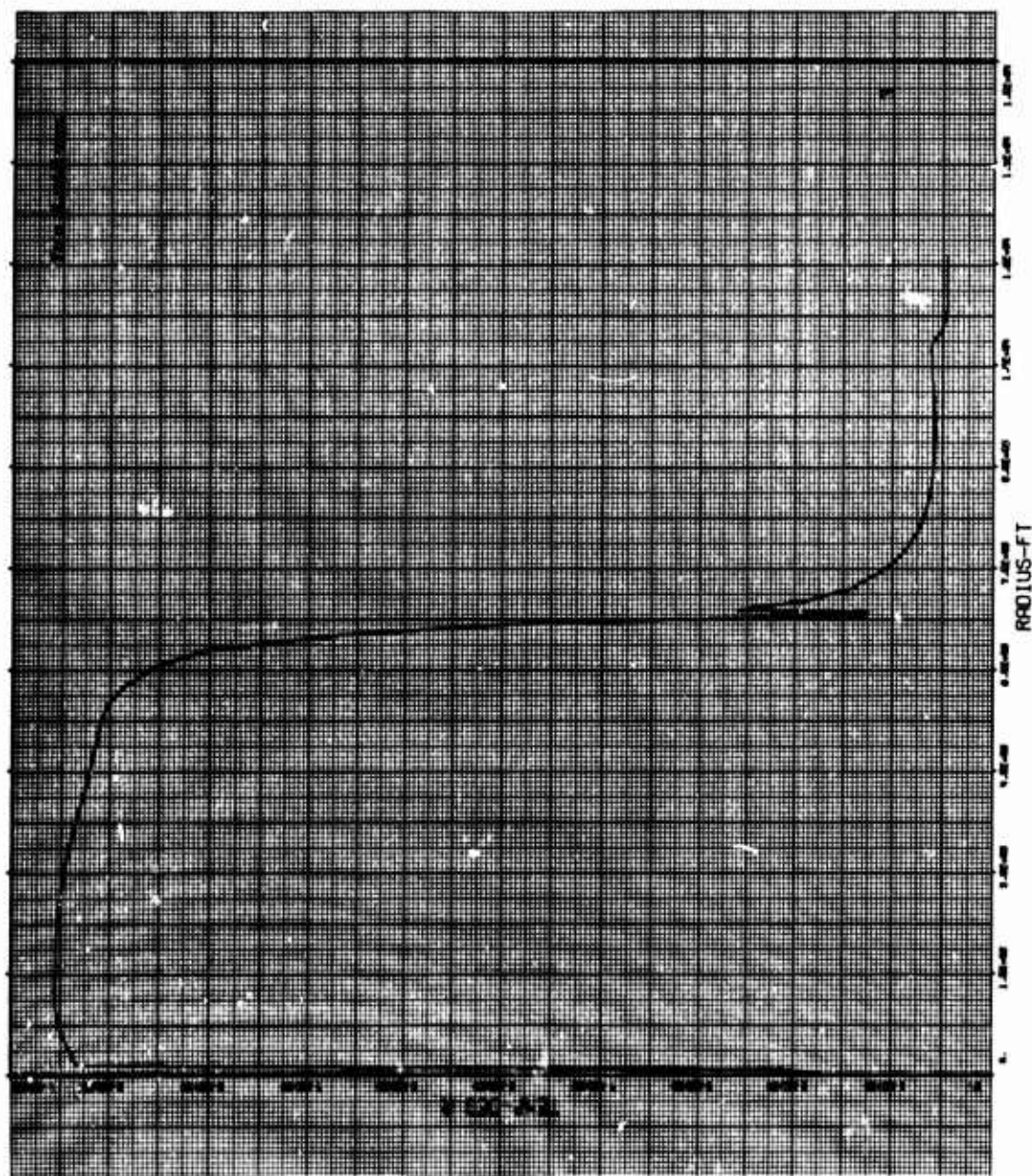


Figure 33. Explosion Environment Data

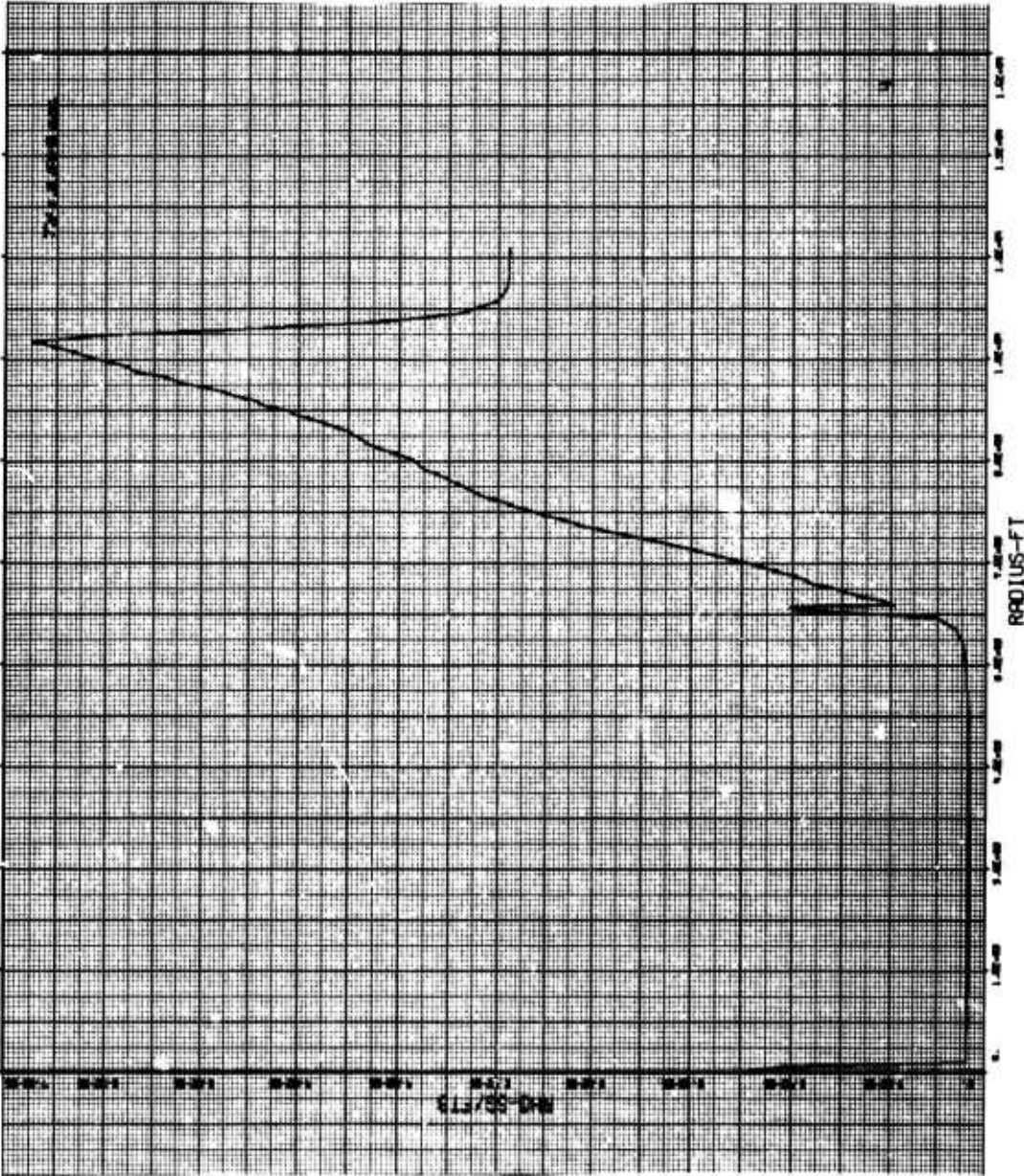


Figure 34. Explosion Environment Data

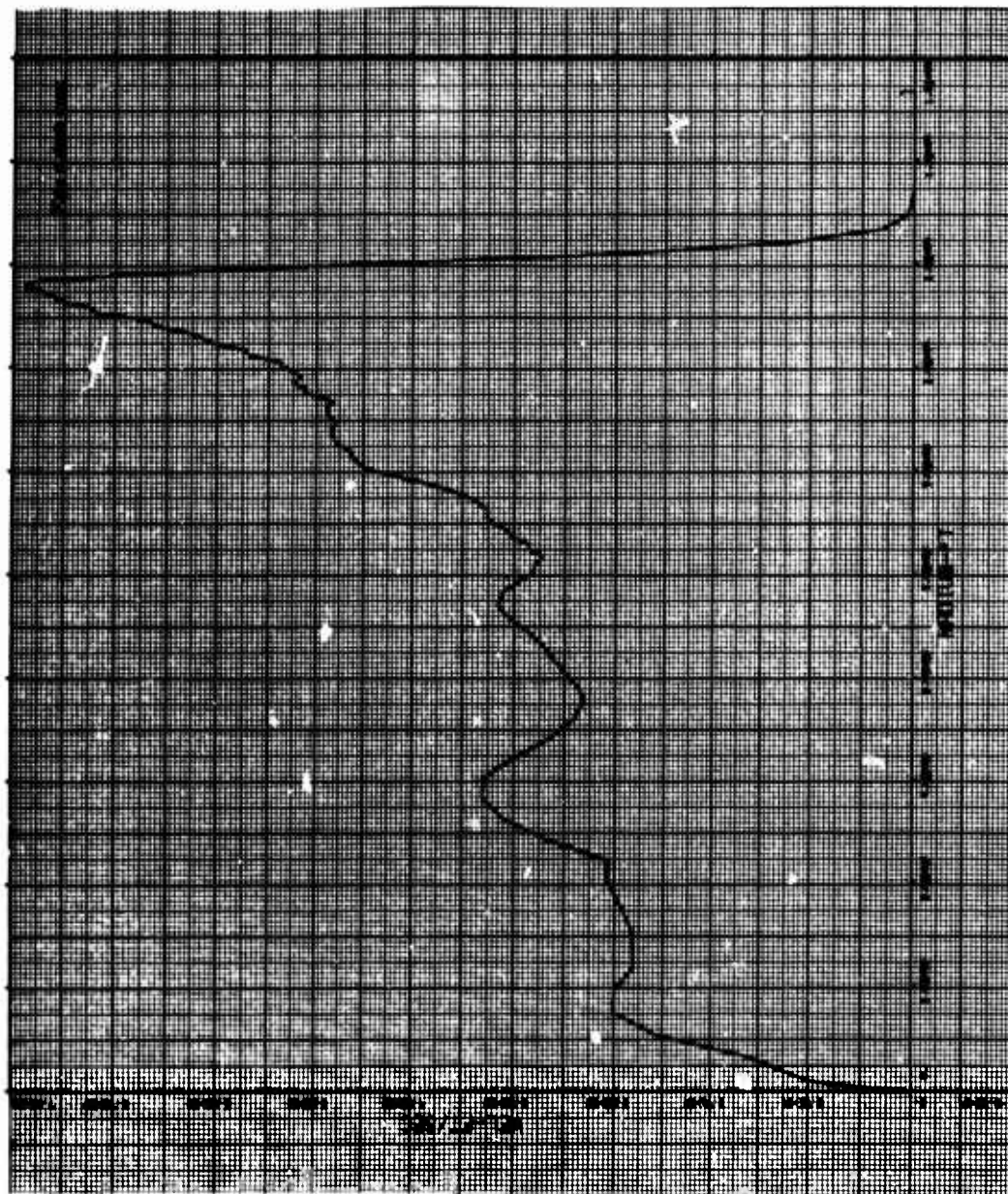


Figure 35. Explosion Environment Data

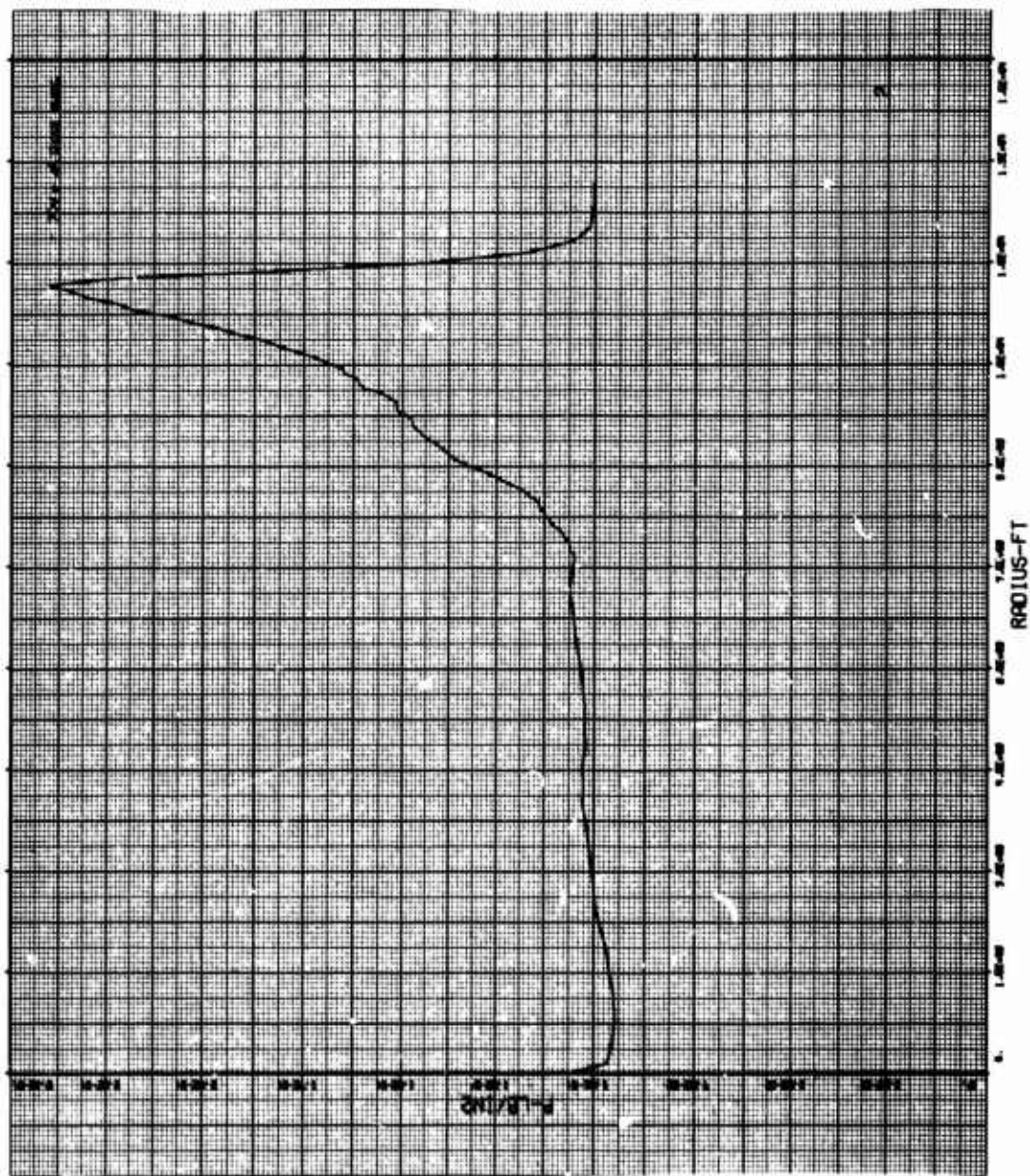


Figure 36. Explosion Environment Data

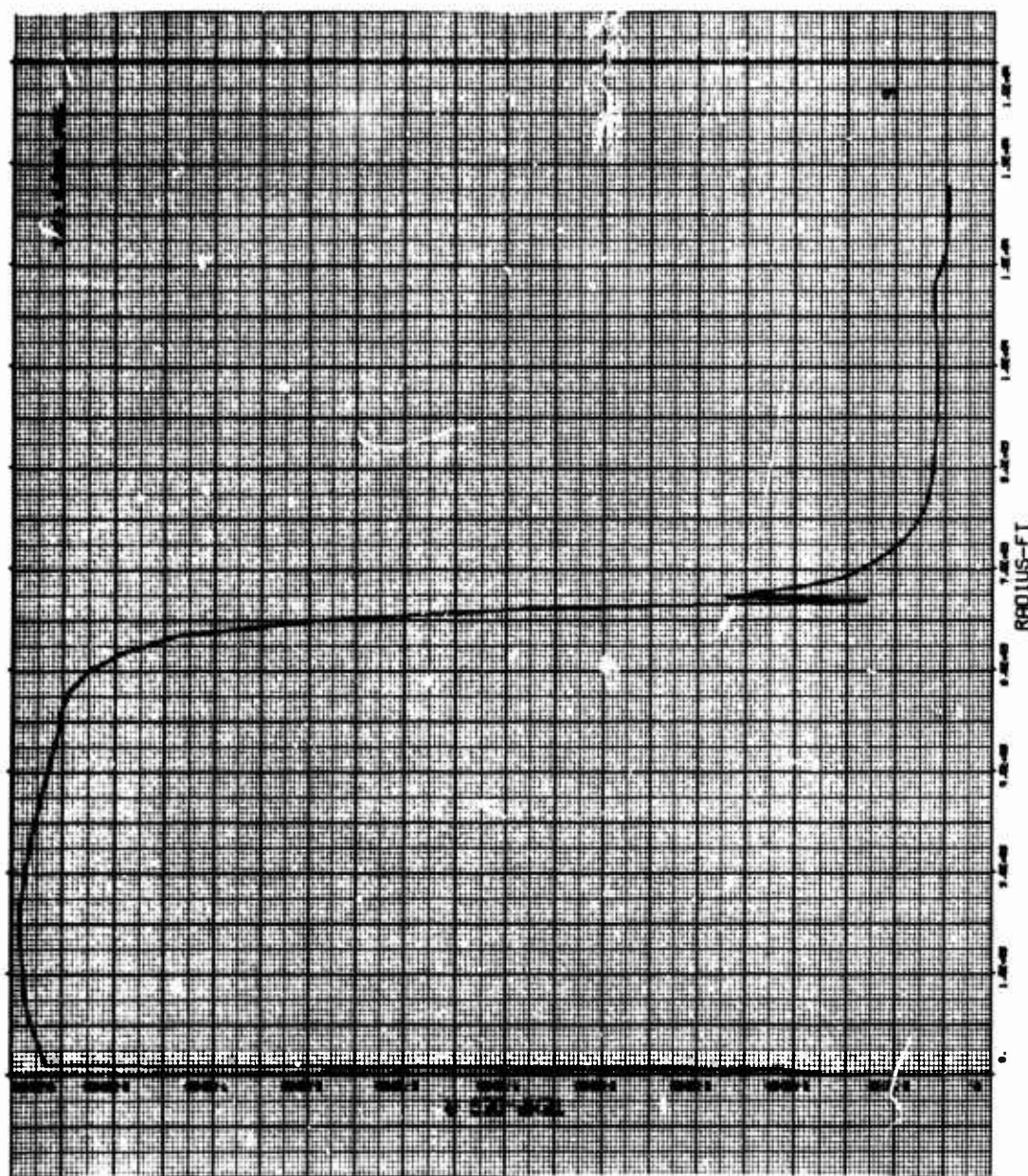


Figure 37. Explosion Environment Data

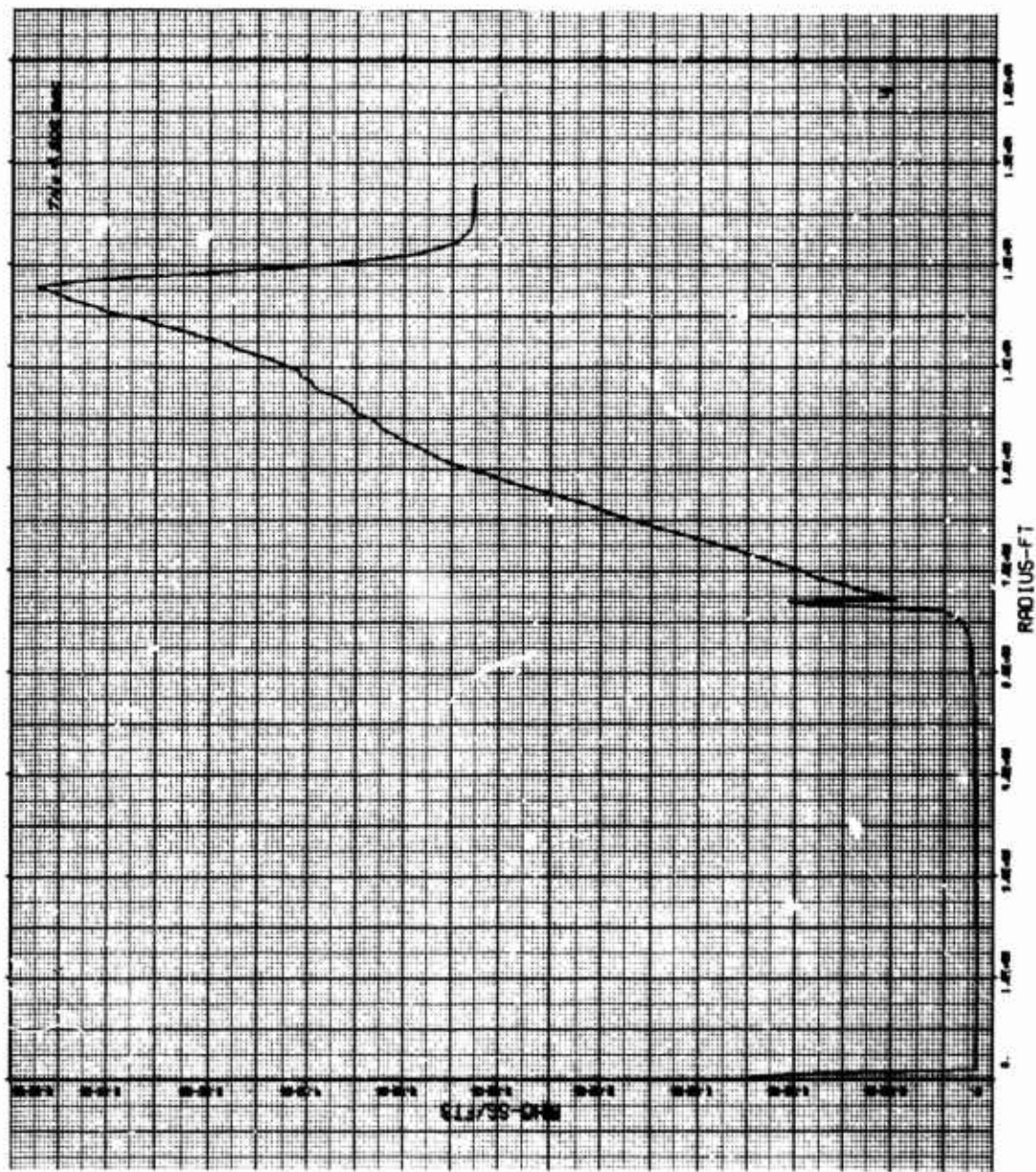


Figure 38. Explosion Environment Data

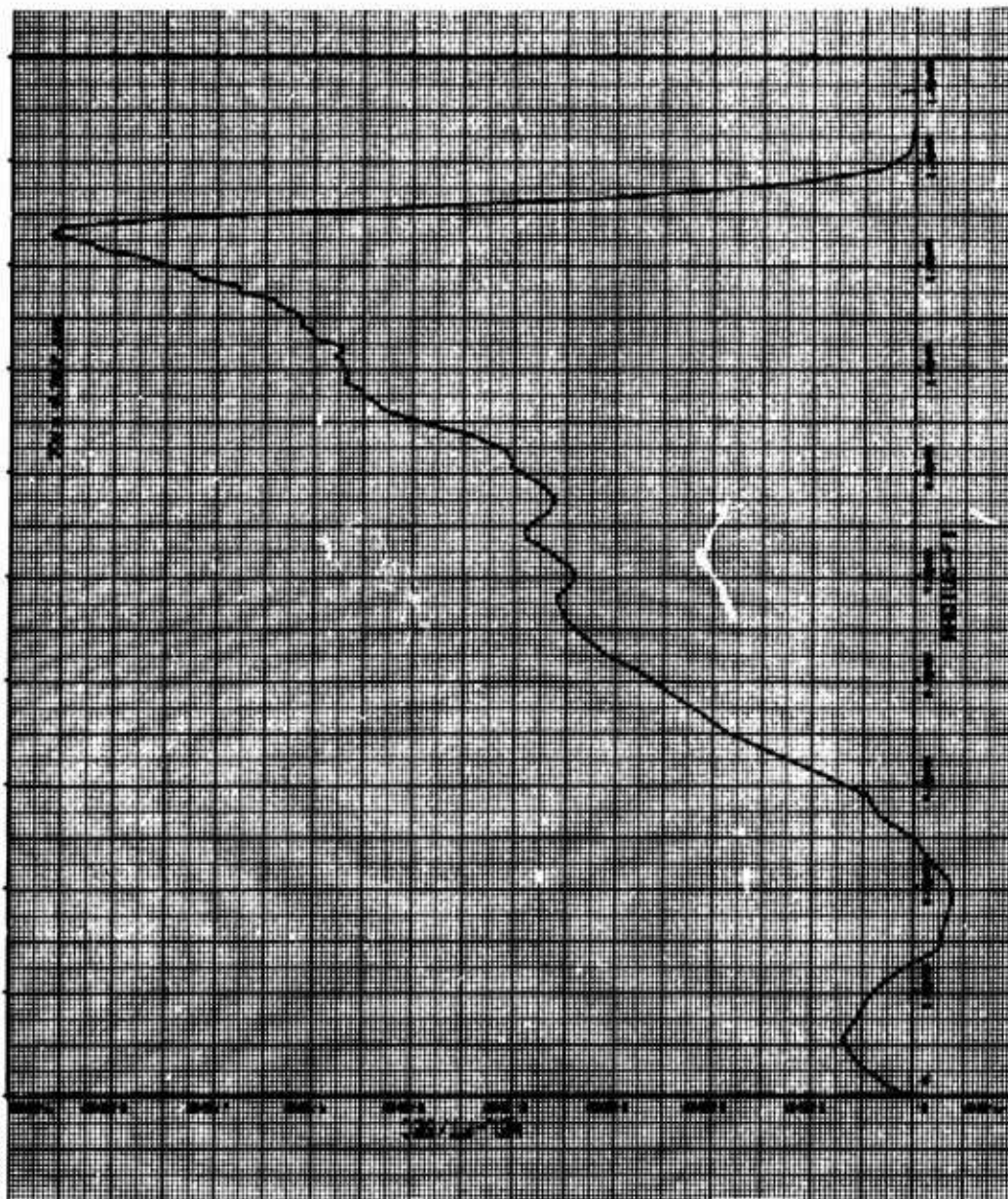


Figure 39. Explosion Environment Data

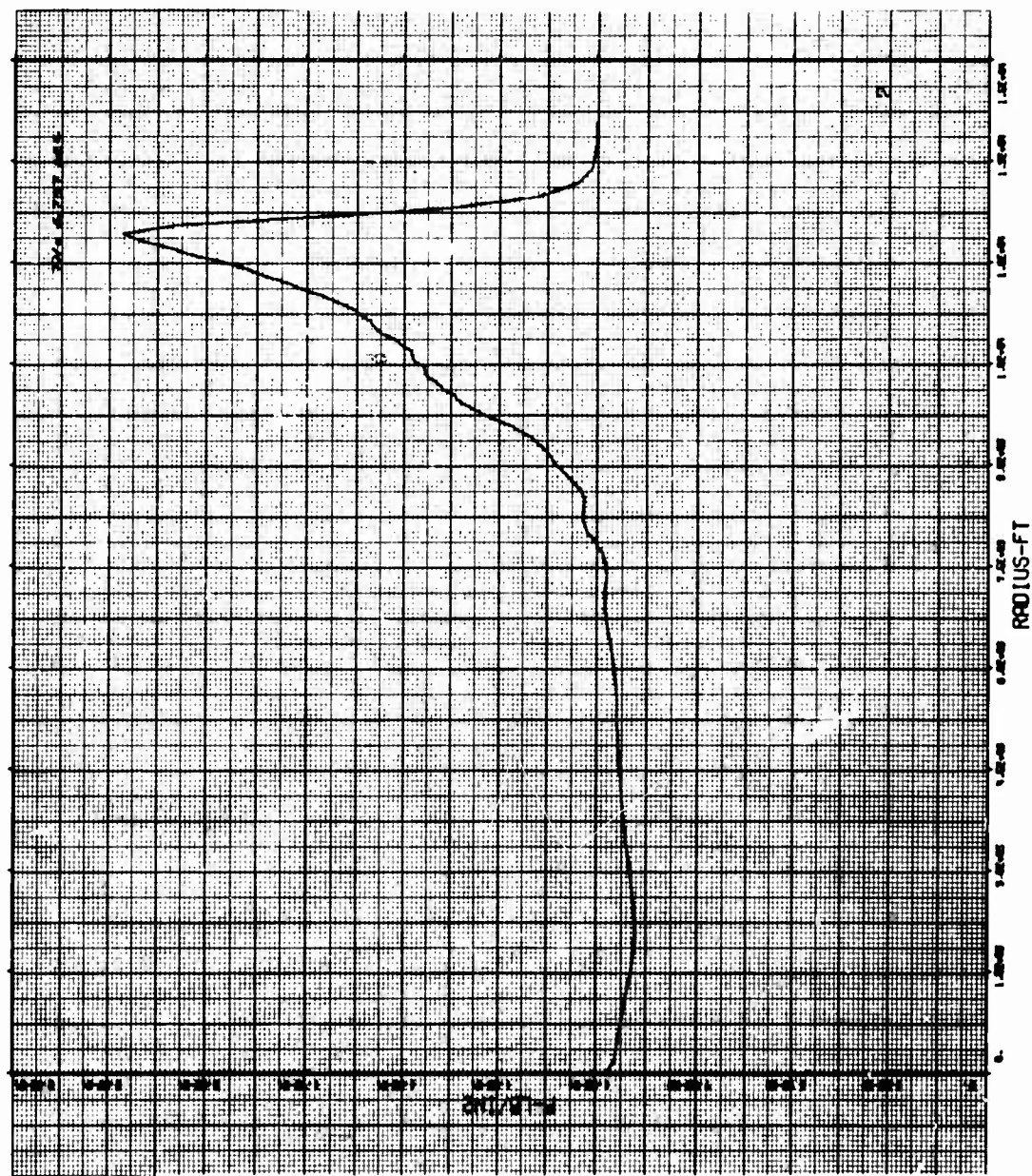


Figure 40. Explosion Environment Data

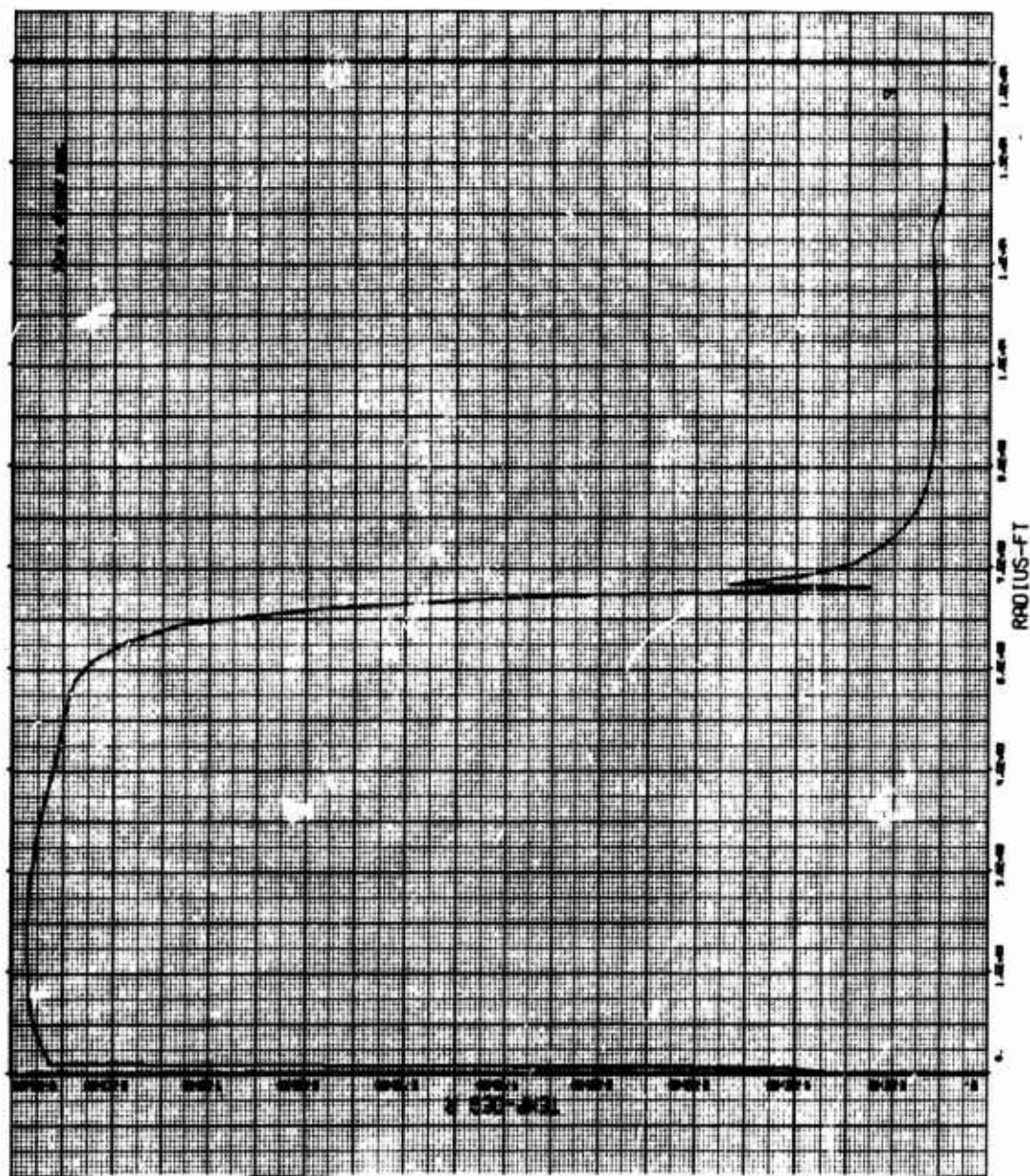


Figure 41. Explosion Environment Data

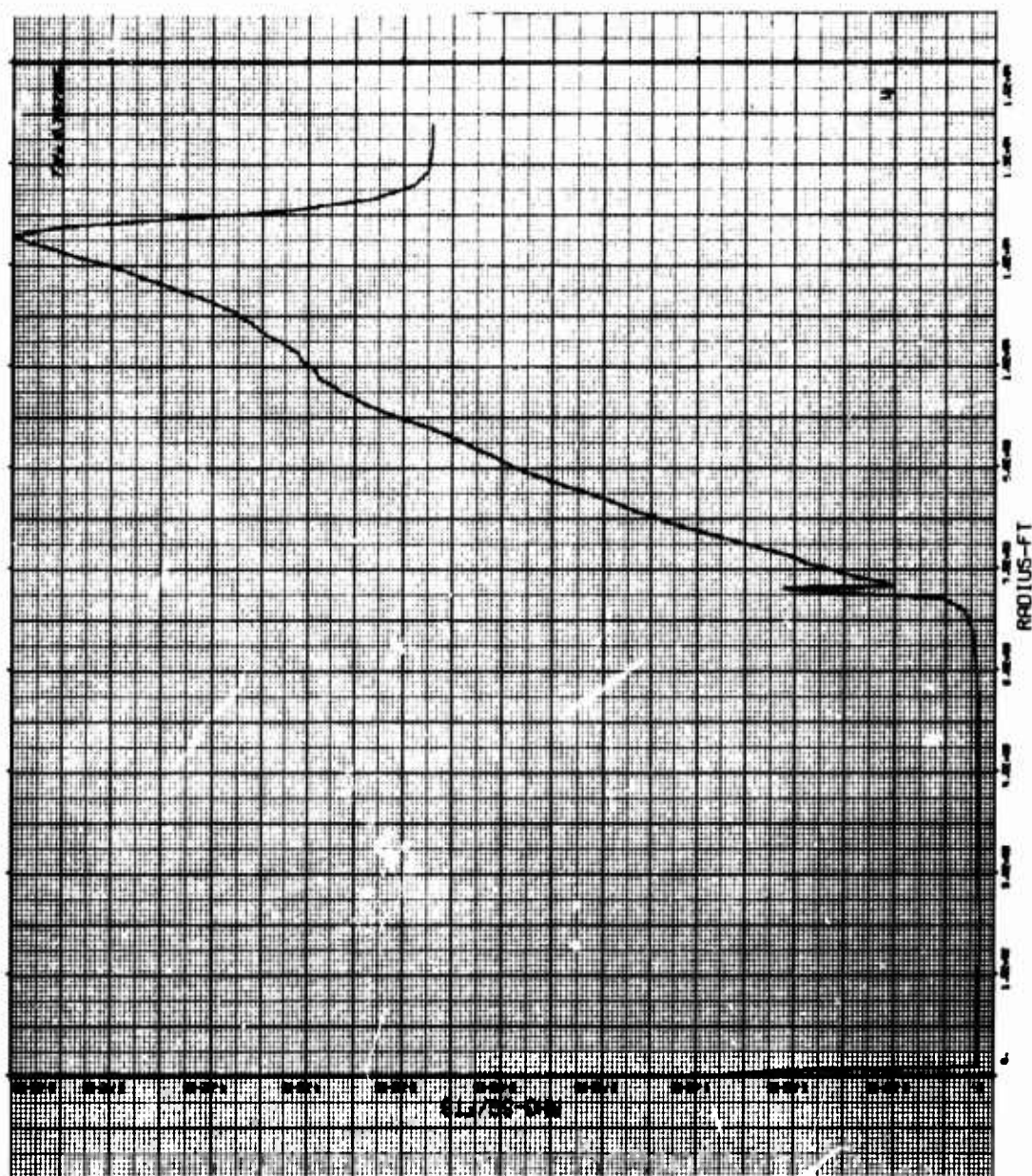


Figure 42. Explosion Environment Data

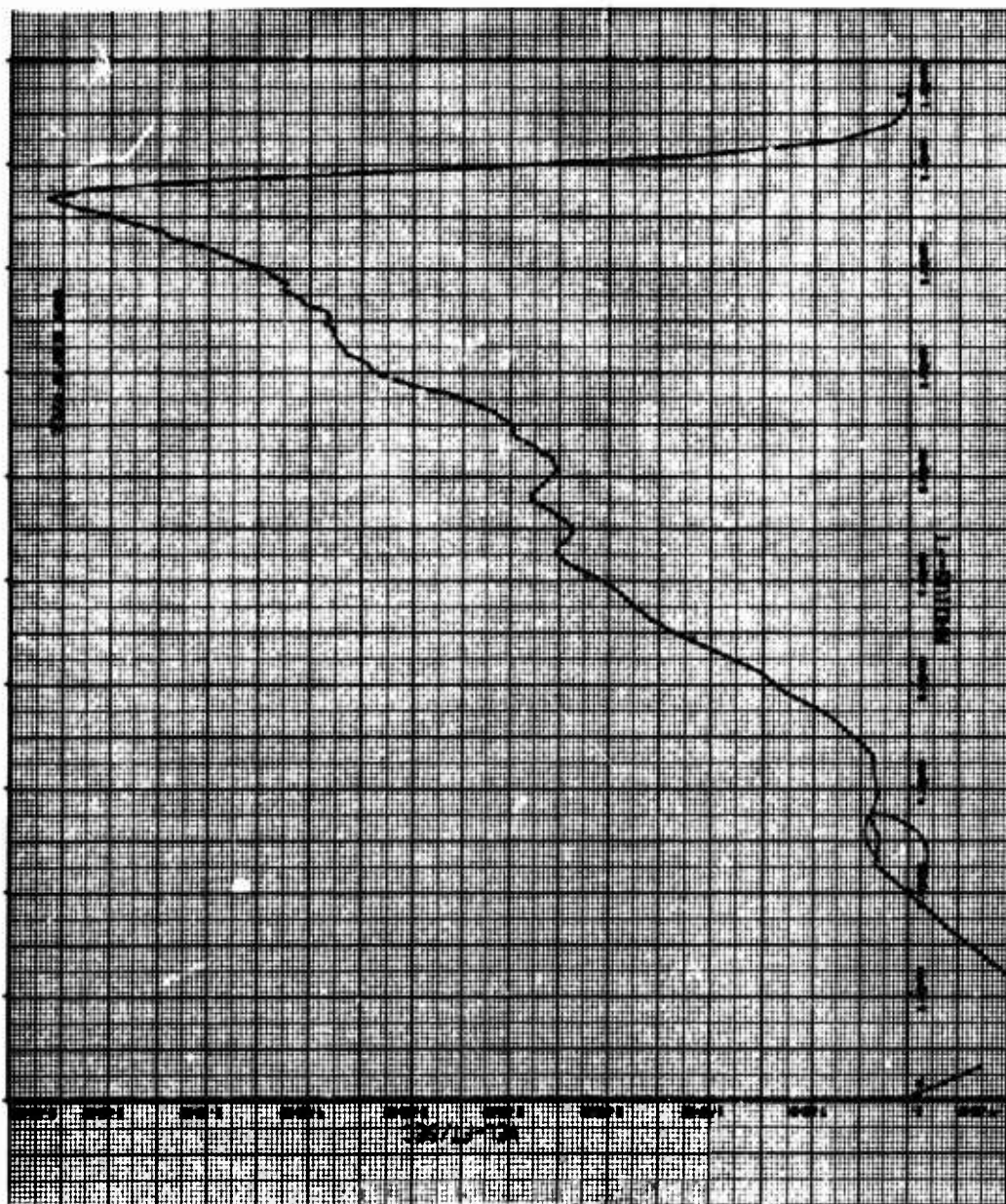


Figure 43. Explosion Environment Data

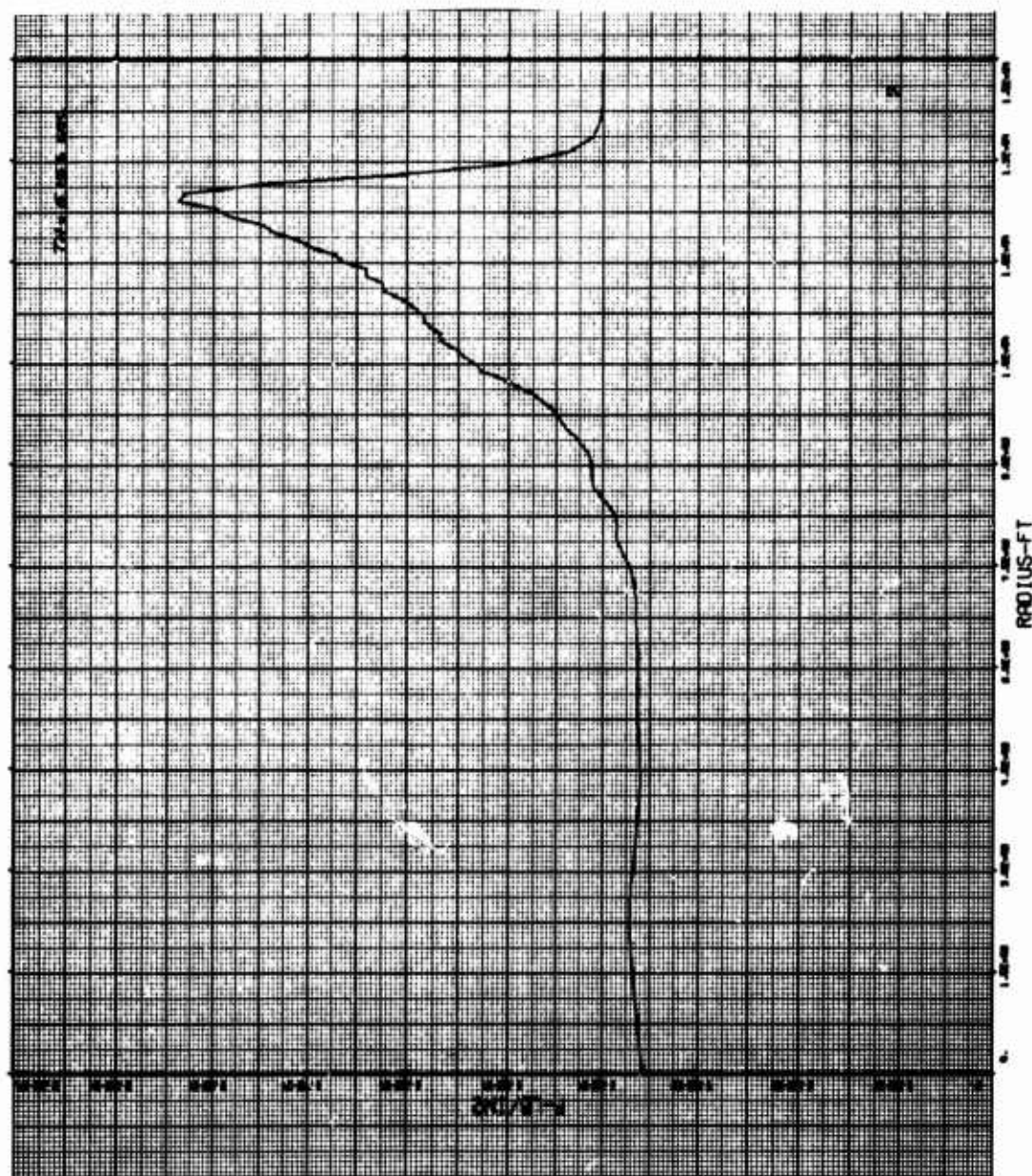


Figure 44. Explosion Environment Data

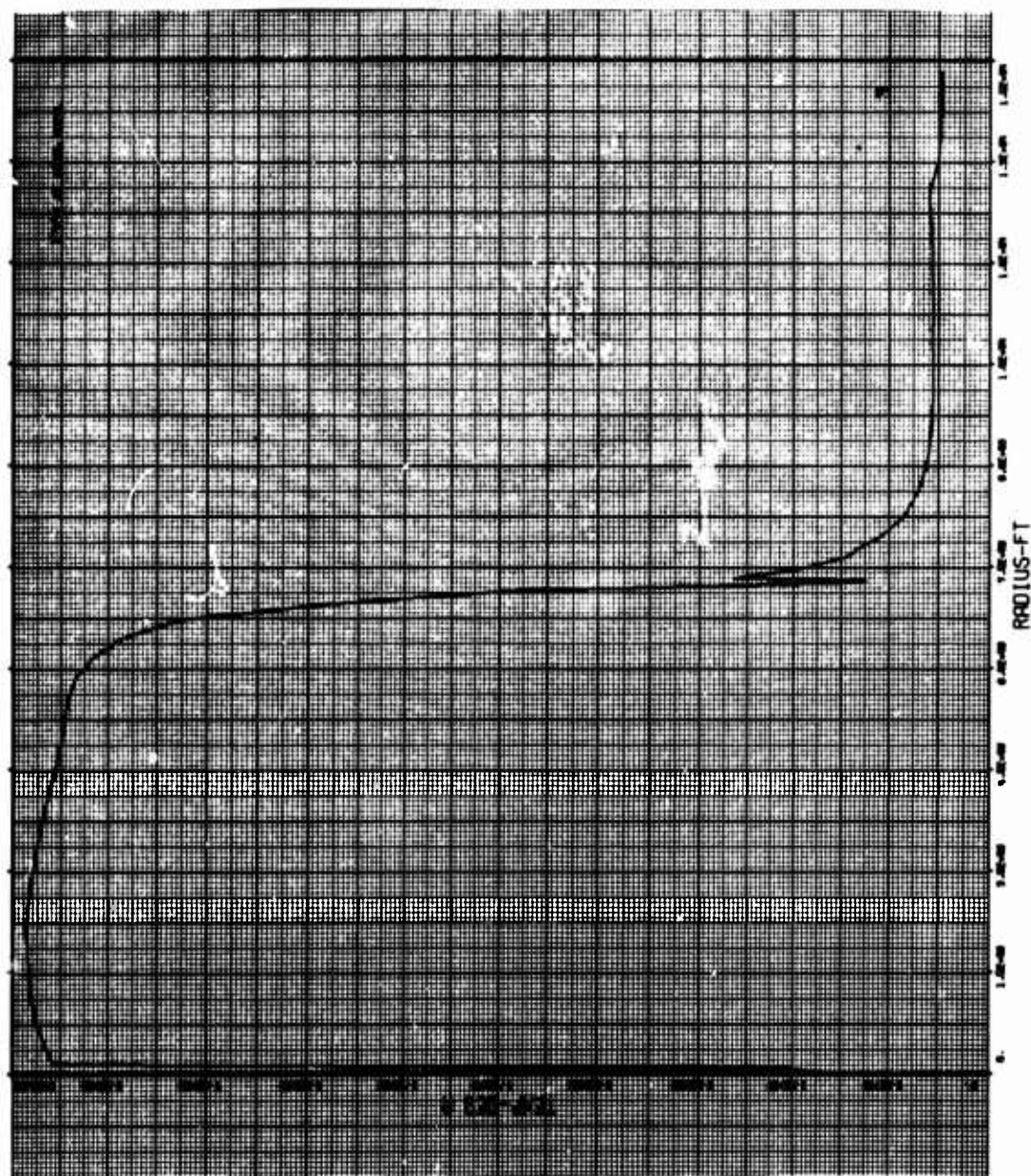


Figure 45. Explosion Environment Data

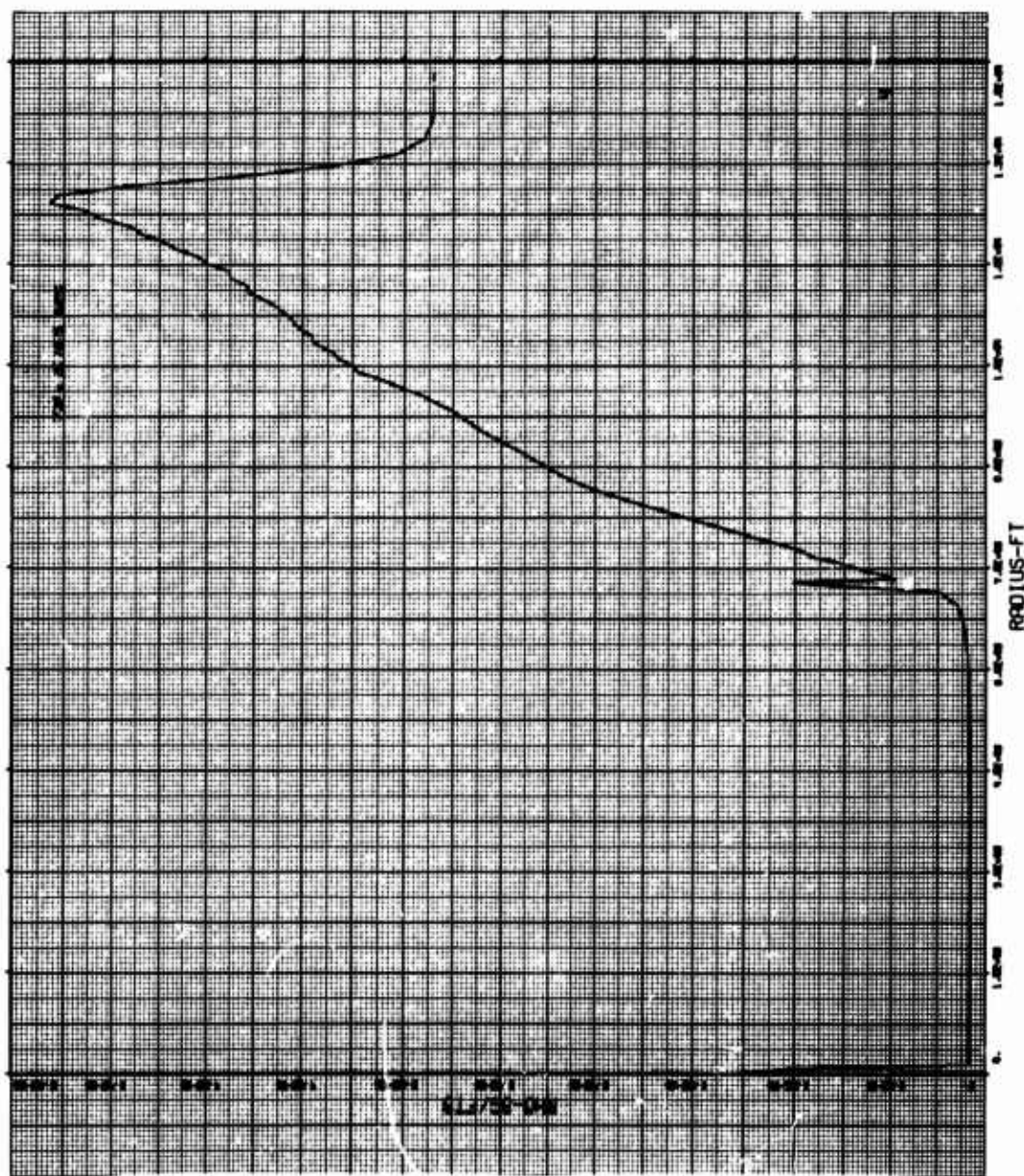


Figure 46. Explosion Environment Data

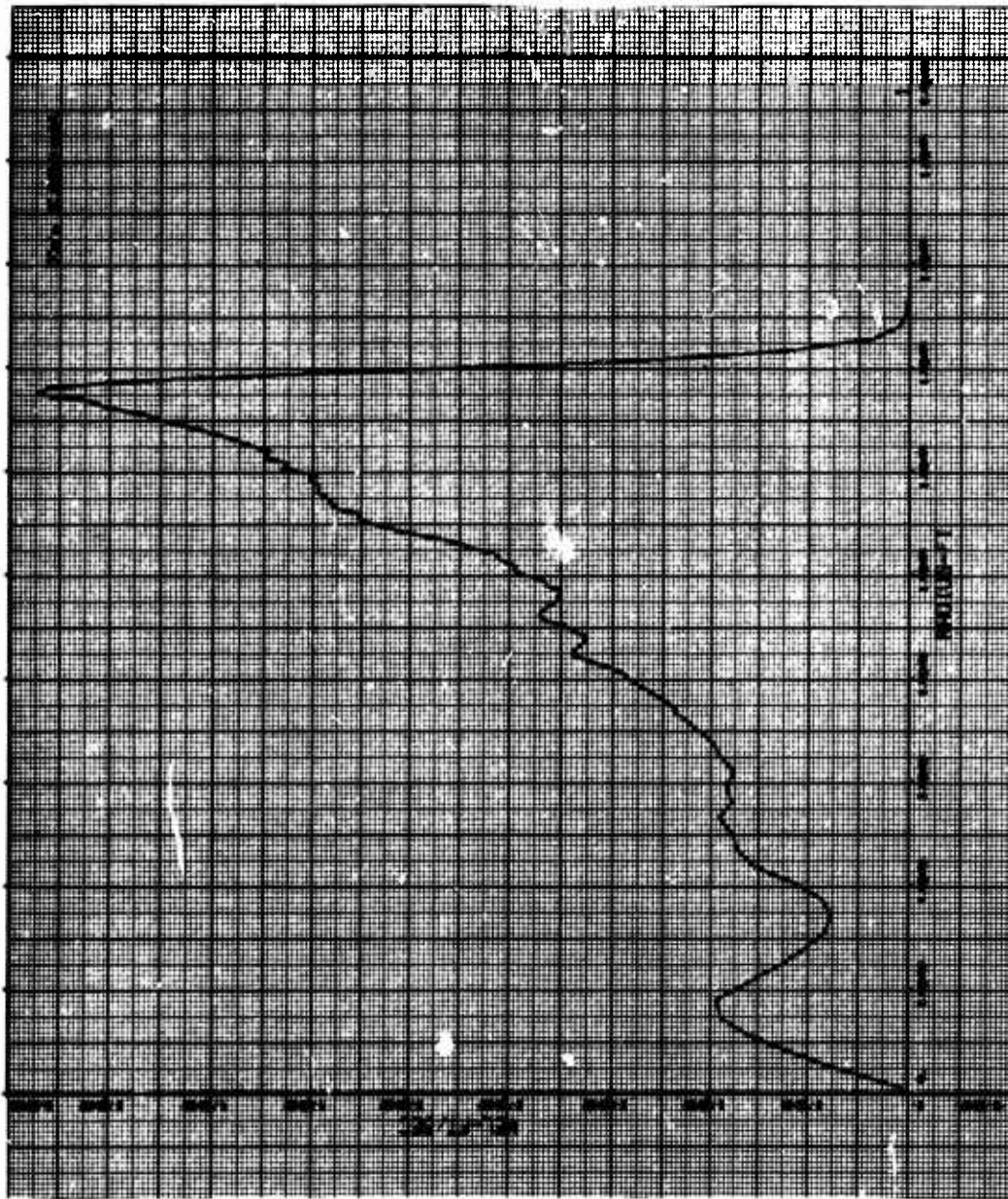


Figure 47. Explosion Environment Data

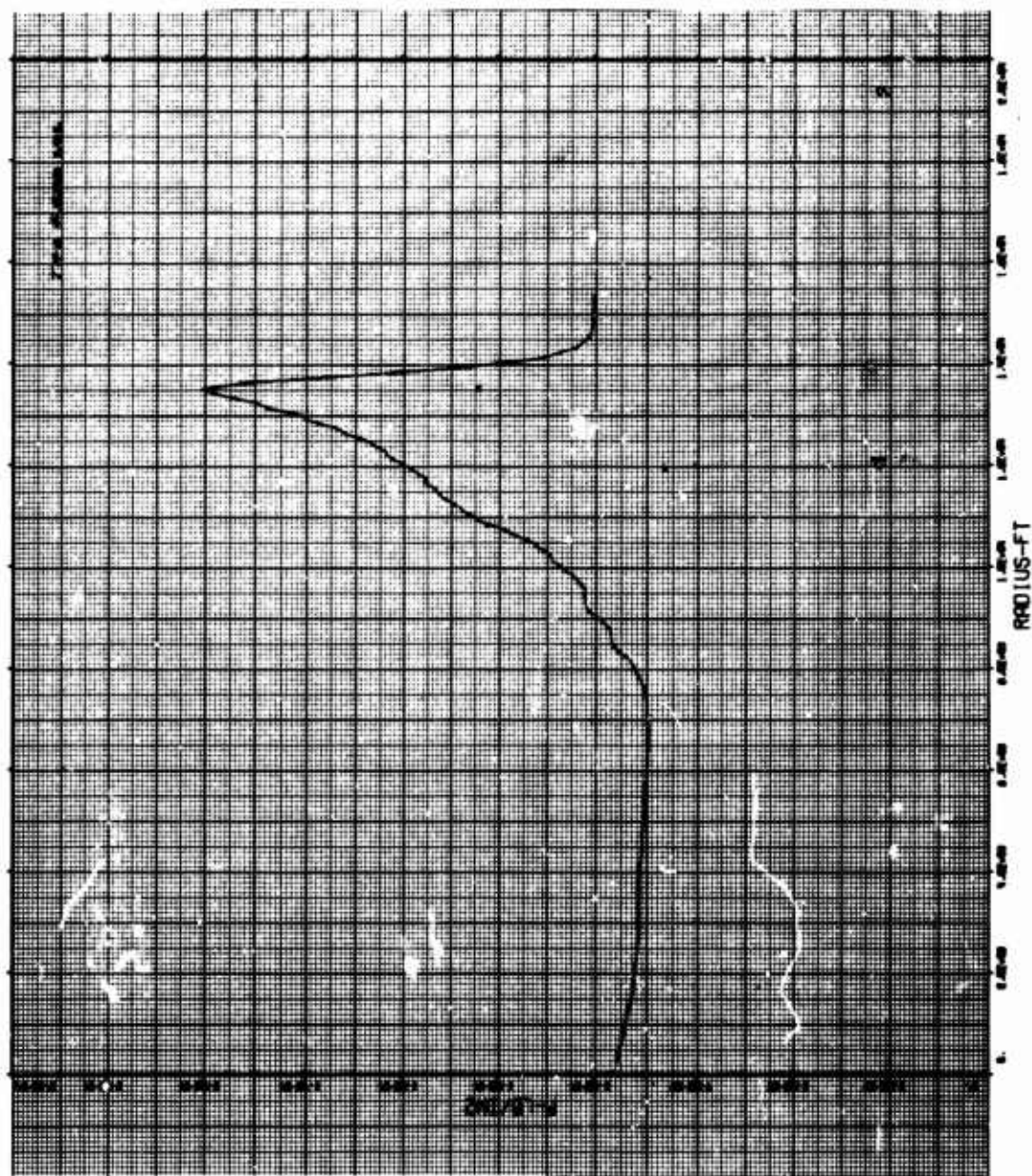


Figure 48. Explosion Environment Data

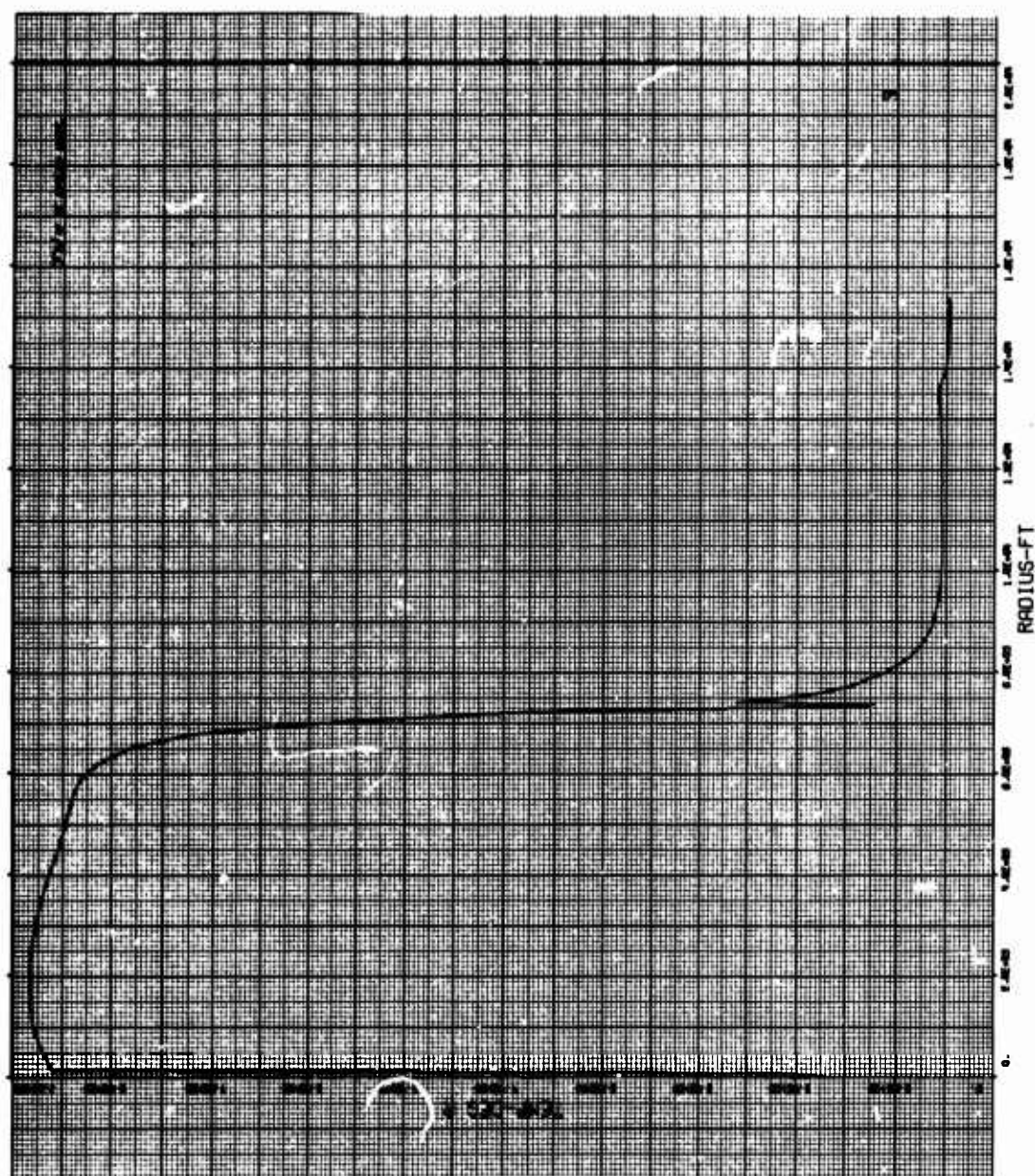


Figure 49. Explosion Environment Data

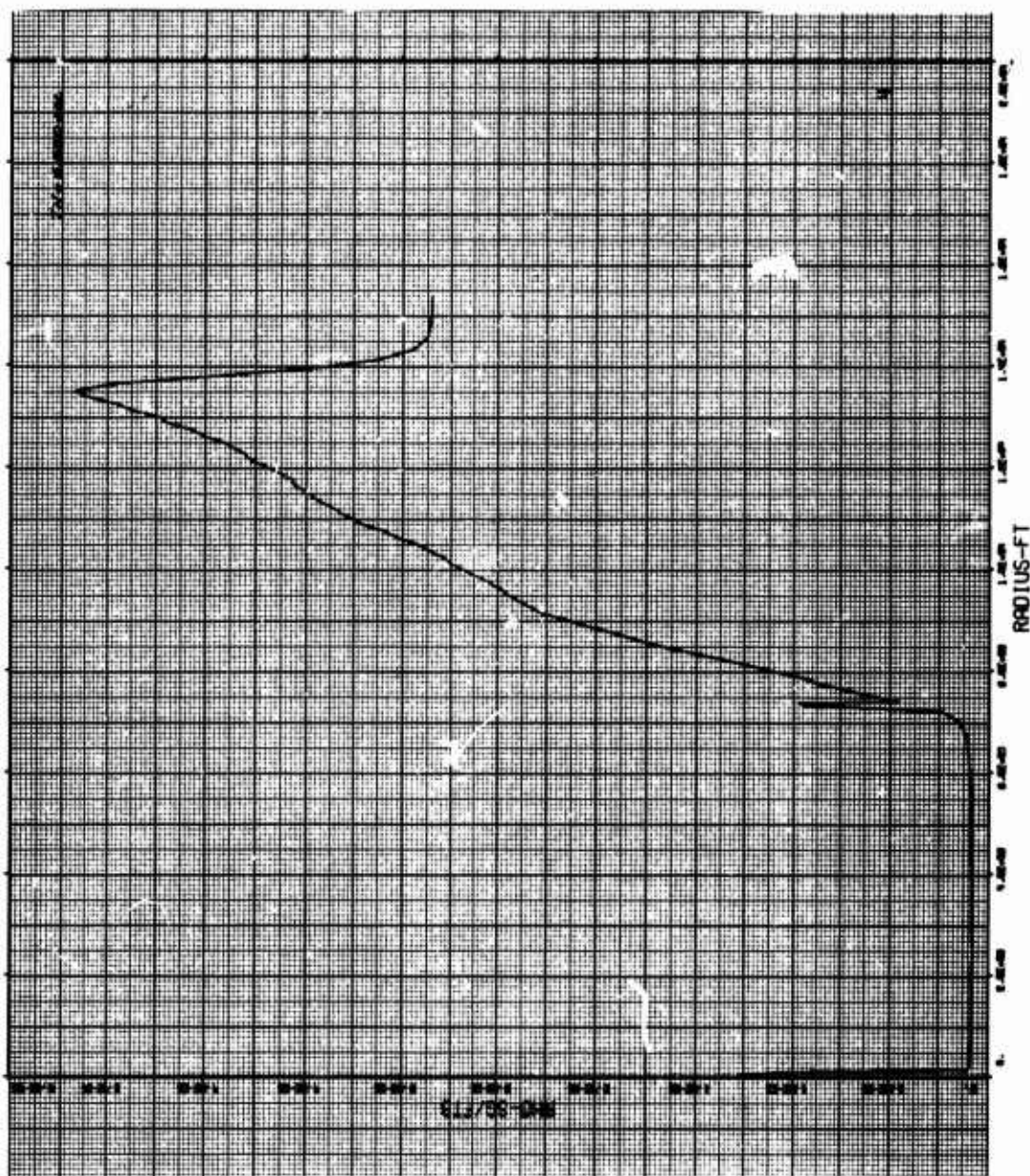


Figure 50. Explosion Environment Data

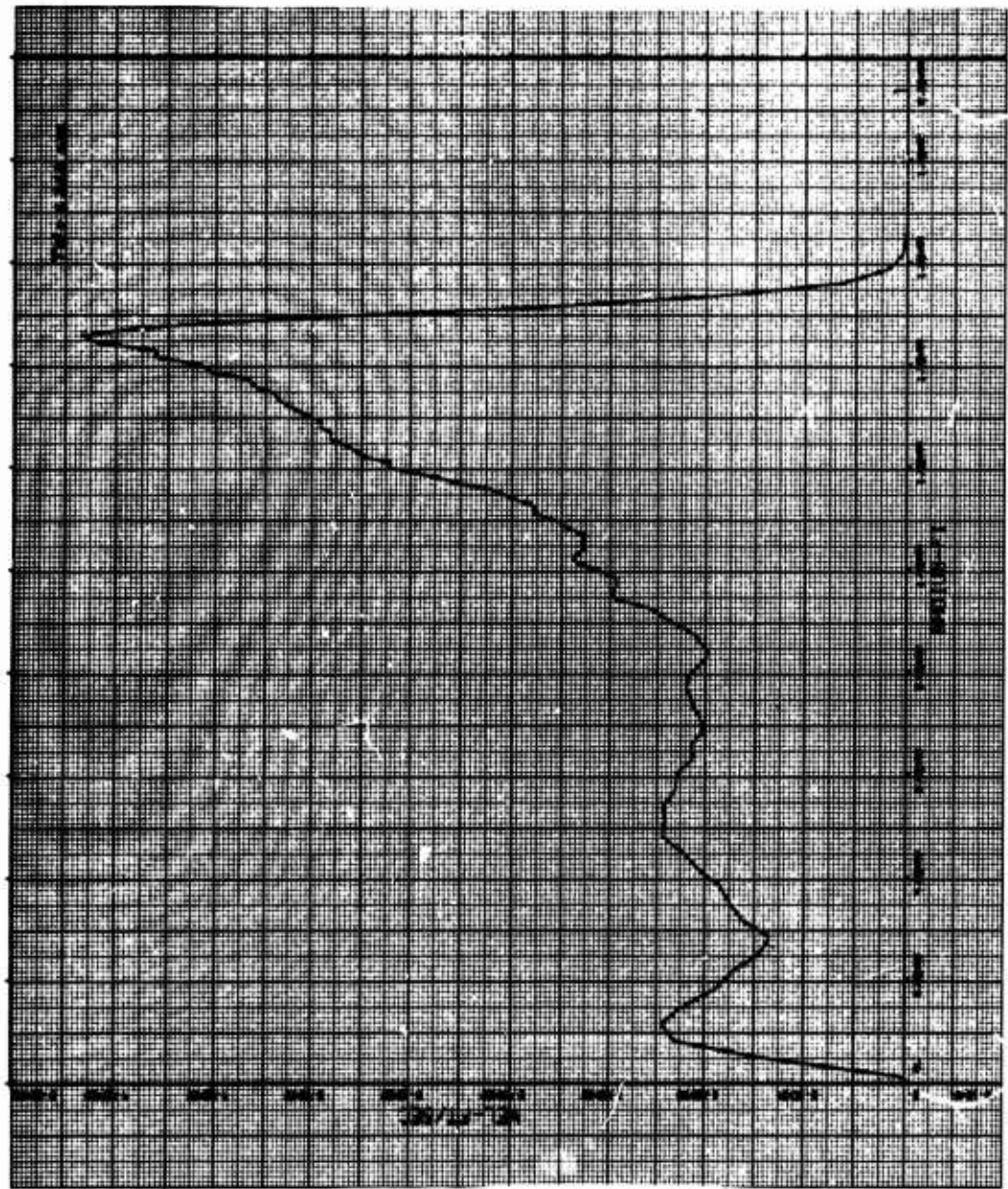


Figure 51. Explosion Environment Data

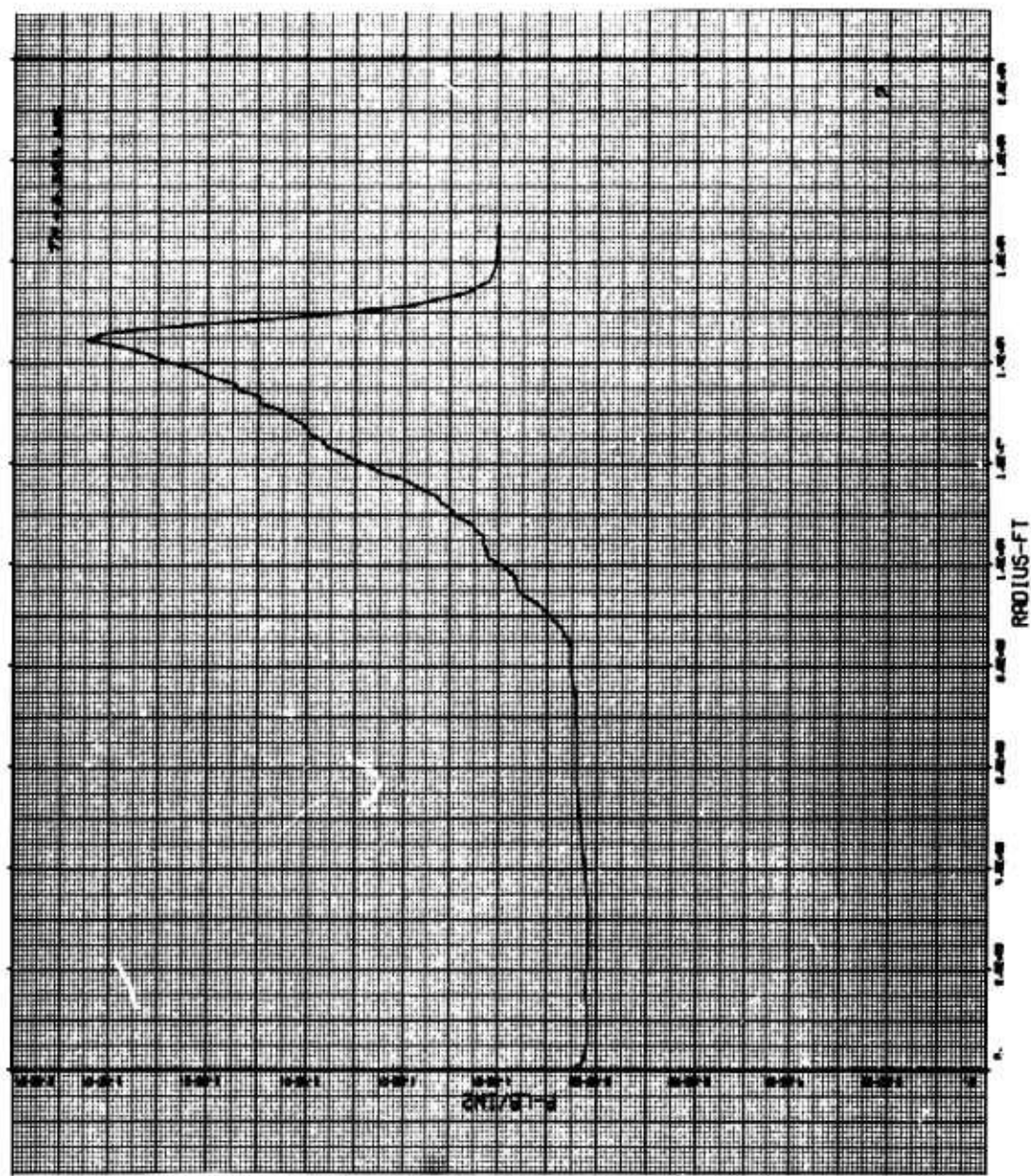


Figure 52. Explosion Environment Data

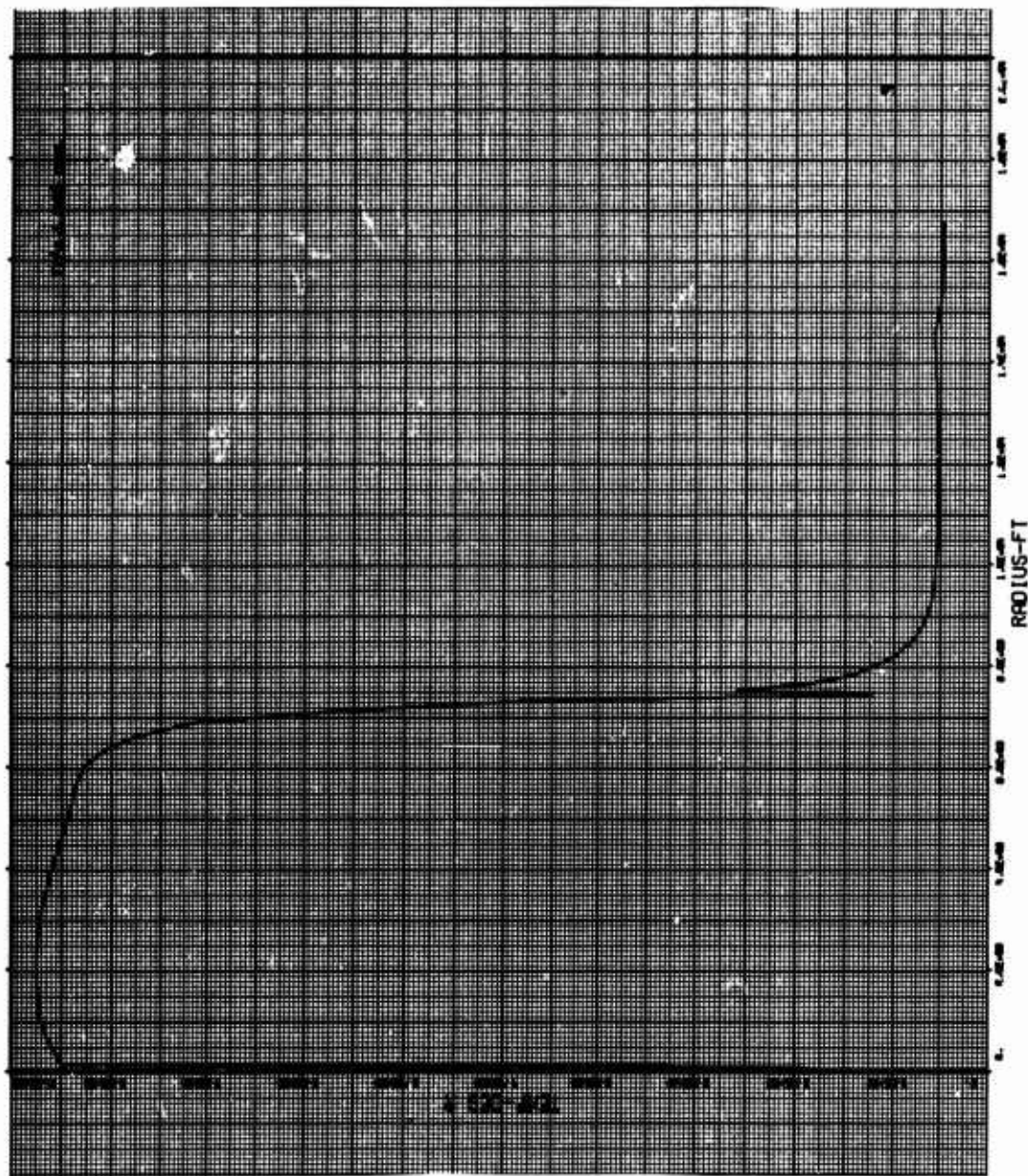


Figure 53. Explosion Environment Data

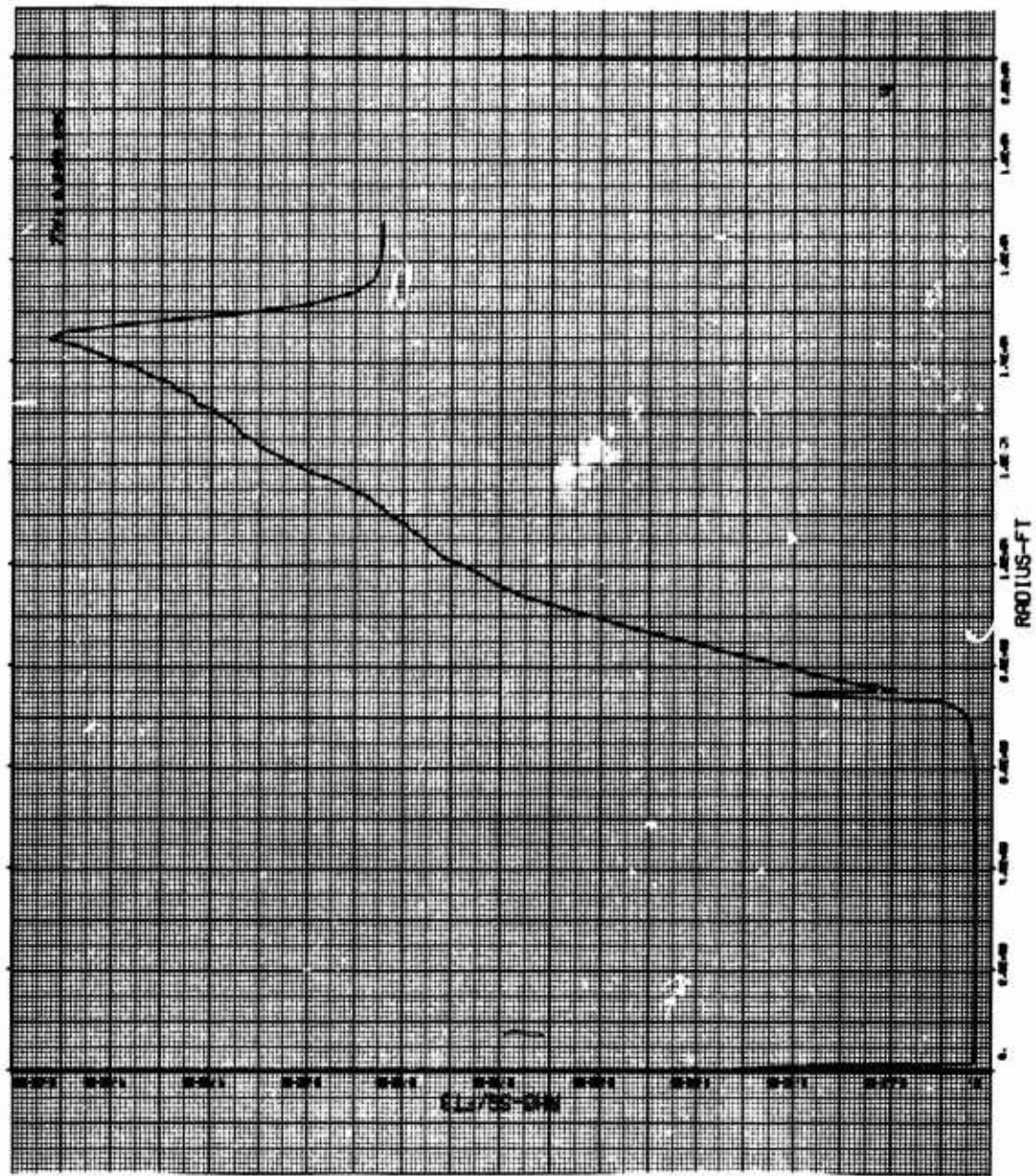


Figure 54. Explosion Environment Data

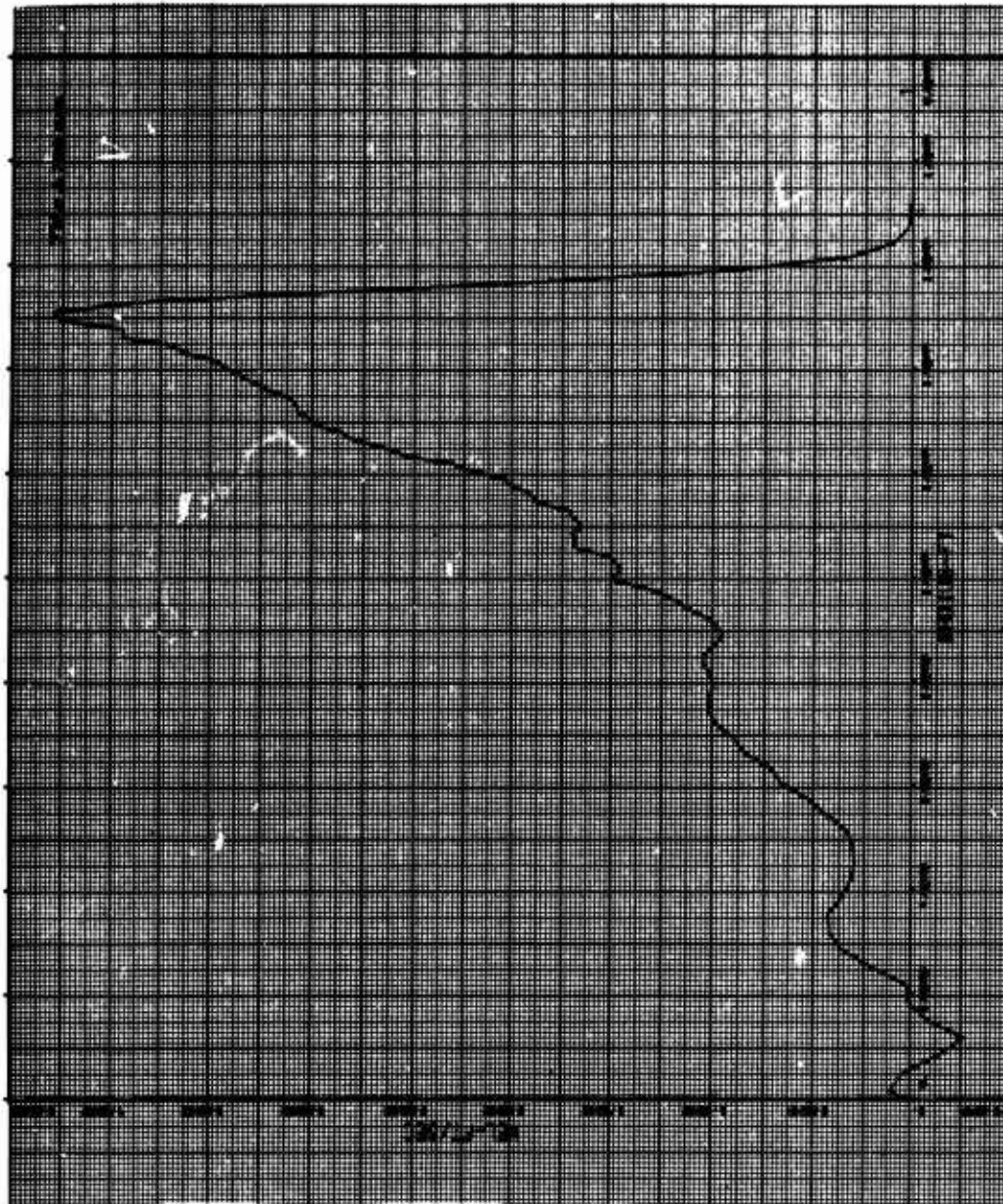


Figure 55. Explosion Environment Data

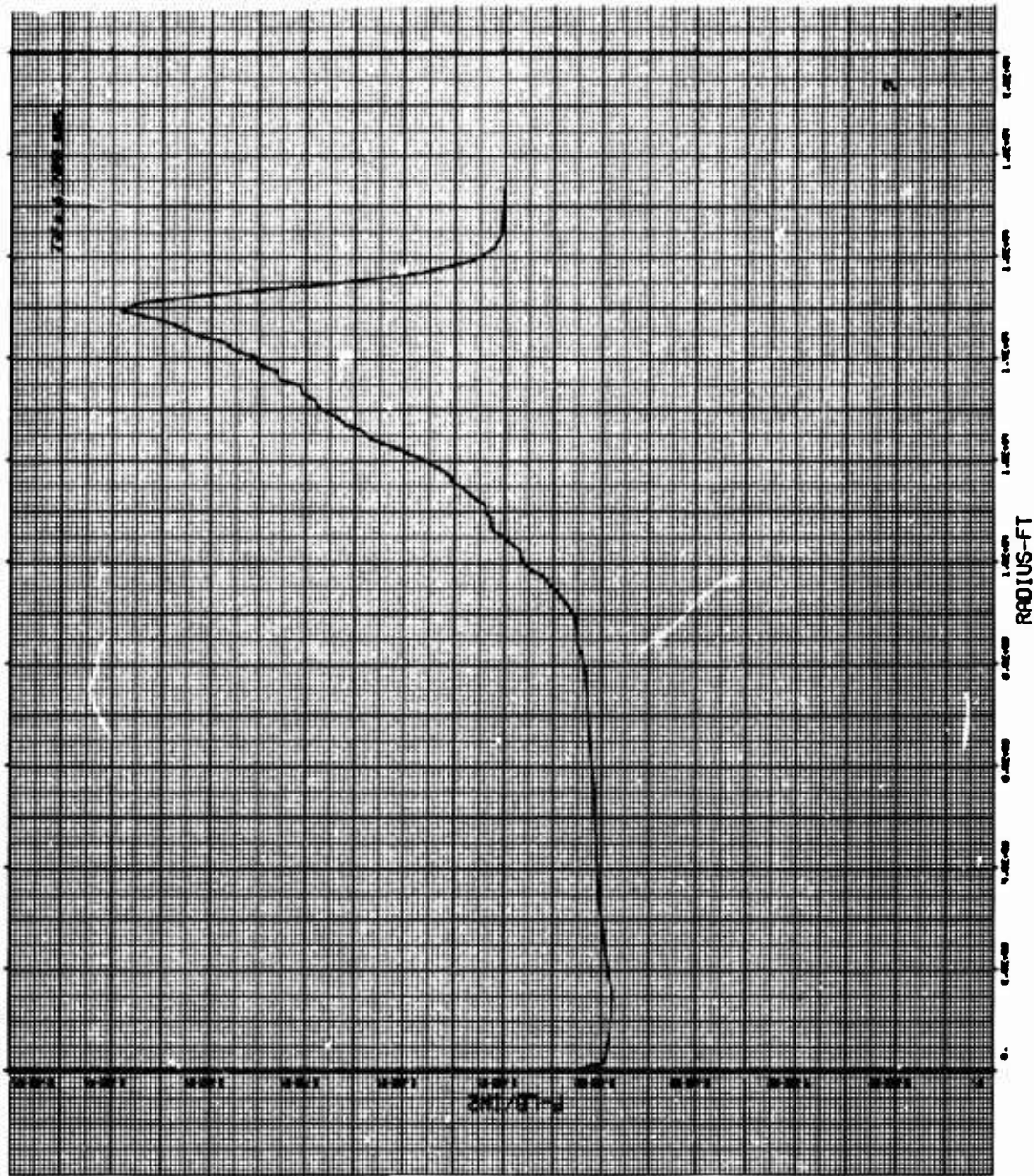


Figure 56. Explosion Environment Data

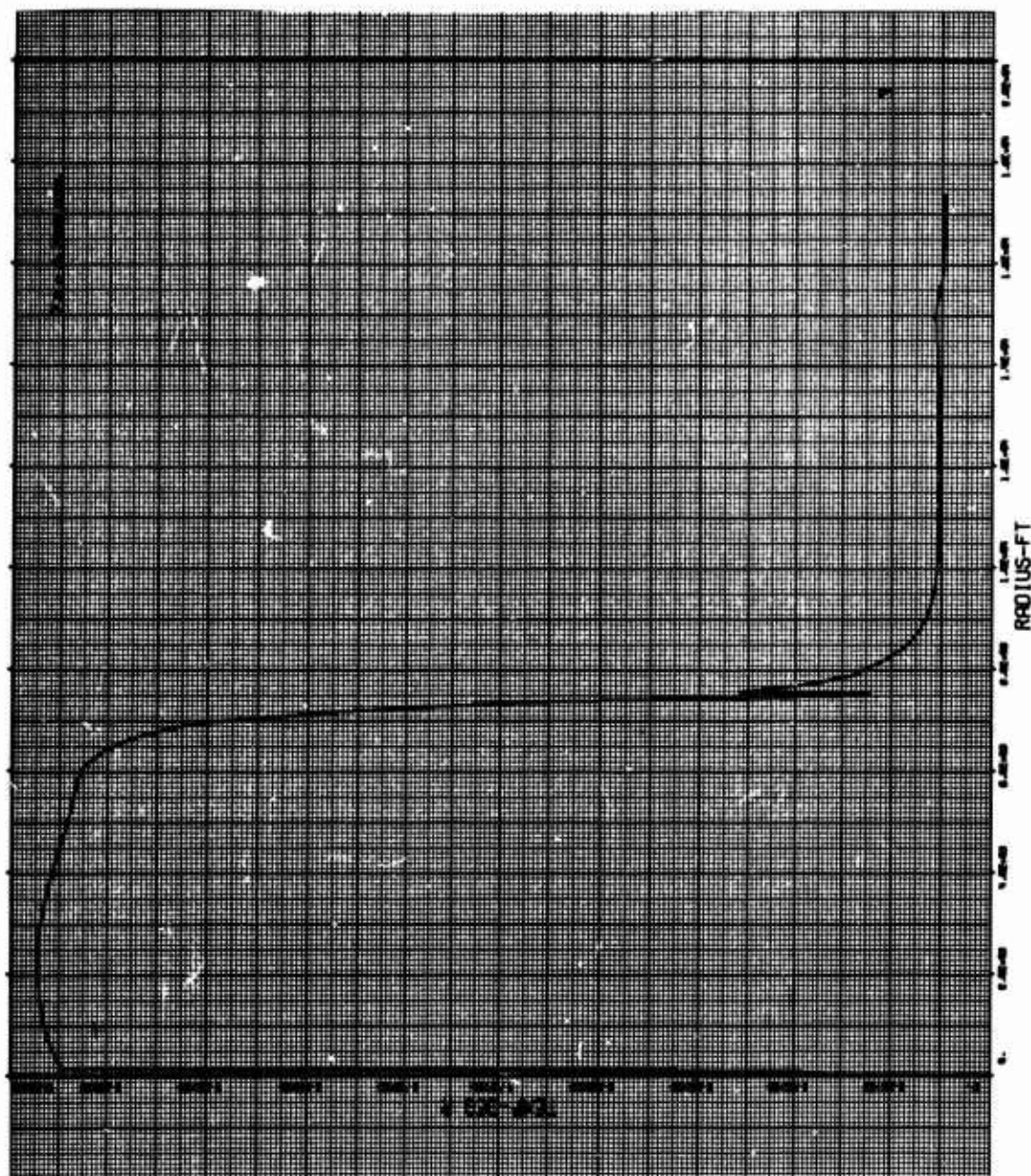


Figure 57. Explosion Environment Data

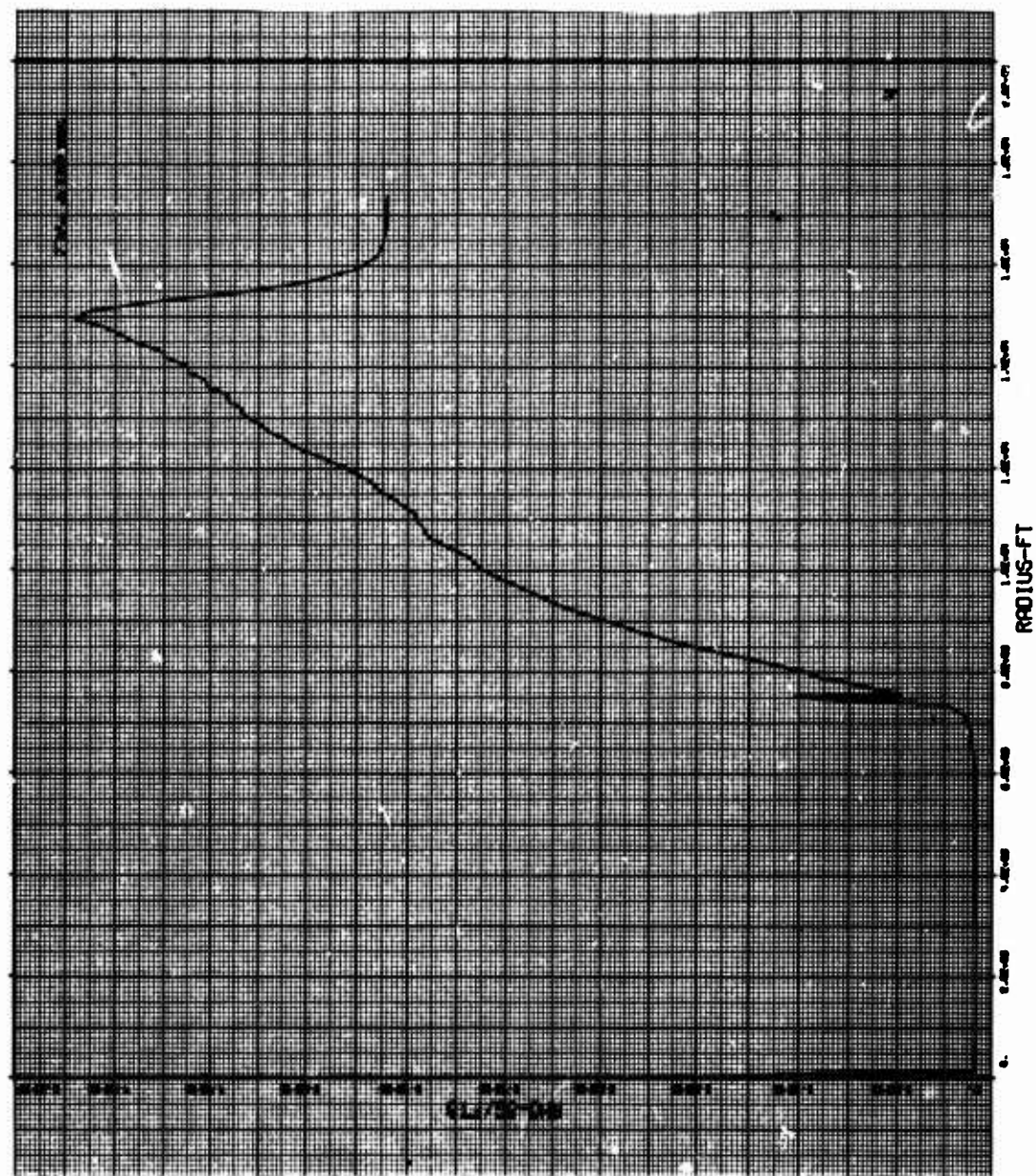


Figure 58. Explosion Environment Data

SECTION IV

FORTTRAN MODIFICATIONS

The FORTRAN modifications to the existing six-degree-of-freedom trajectory program documented in TR-66-156 are discussed in the order which the card deck appears.

1. Input Modifications

```
DIMENSION IJA(125),HEAD(12),LMDA(20),ØKLM(20),CHRNØ(20),AMASNØ(20)
1,ITEMP(16),R(152),RD(152),P1(152),THETA(152),DENS(152),E(152),RDD(
2152),SMLQ(152),SMLR(152),VSØ(152),R1(152),RD1(152),P11(152),THETA1
3(152),DENS1(152),E1(152),RDD1(152),SMLQ1(152),SMLR1(152),VSØ1(152)
4,R2(152),RD2(152),P12(152),THETA2(152),DENS2(152),E2(152),RDD2(152
5),SMLQ2(152),SMLR2(152),VSØ2(152)
```

This statement provides for the necessary added storage. The meaning of each added array is explained later.

XCNB = -1100.	} These are the scalar magnitudes of Eq. 9 in feet.
YCNB = 65600.	
ZCNB = 98900.	

TE = 41.90 -- This is the variable T_e in seconds.

TP = 43.36 -- This is the variable T_p in seconds.

THA = 0.0 -- This is a dummy variable used to control printing of the environment data.

KX = 0 -- This is a dummy variable used in Subroutine BLAST to ensure that a section of statements is executed only once.

KY = 0 -- This is a dummy variable used in Subroutine BLAST to indicate when an end of file is reached on the environment magnetic tape.

STA = 249.2 -- This is the first input statement of the existing six-degree-of-freedom program documented on page 71 of TR-66-156.


```

.
.
.
PRINT 900
900  FORMAT (2X,...same
      14HMACH,...same
      2HTC,...same
      3Z,13X,...3HEXD,10X,3HVXY,9X,...same
      4Q,11X,...same
      5H,10X,...same
      61X,2HA2,...same
      7X,2HTL,12X,2HFD,11X,4HVRX4,8X,4HVR4,8X,4HVRZ4,/,2X,2HDX,10X,2HDY,
      811X,2HDZ)

```

This is the Hollerith statement for the six-degree program printout. The variables BET, TANG, PØL are eliminated because of the aerodynamic changes discussed in Section II, paragraph 4a. The variables VRX4, VRY4, VRZ4, DX, DY, DZ, which are already part of the six-degree program, are added to the printout for convenience.

GØTØ997 -- This is the next card following the Hollerith statement.

This concludes the input FORTRAN modifications.

2. Main Program Modifications

OZ1 = WEZ - DPH5*SINF(TH5) -- This is the last card in the main program before a modification is made. See TR-66-156, page 86.

```

IF(T-TE)400,401,401
401  XR = X5-XCNB
      ZR=Z5-ZCNB
      ZR+25-ZCNB
      RR=SQRTF(XR**2+YR**2+ZR**2)
      CALL BLAST(T,RR,XR,YR,ZR,TP,TFB,KX,L2,TH2,R2,RD2,P12,THETA2,DENS2,
1E2,RRD2,SMLQ2,SMLR2,VSØ2,RFB,FAC,VW,PRES,TEMP,RHØ,VS,VWX,VWY,VWZ,KY)
      IF(R2(L2)-RR)400,400,402
400  CALL WIND(ALT,THW,VW)
      VW=(VW+EVW)*6080./3600.
      THW=THW*PI/180.0

```

```

CALL VWNE (THW, VW, VWN, VWE, PI)
VWX = -VWN * SINF (AZ) + VWE * COSF (AZ)
VWY = VWE * SINF (AZ) + VWN * COSF (AZ)
VWZ = 0.
CALL DENS (ALT, RH0, E3)
CALL VSD (ALT, VS)
402 VRX = DX5 - VWX
    VRY = DY5 - VWY
    VRZ = DZ5 - VWZ

```

The first statement of this group allows the calculation to skip the blast environment calculation until the time of flight, T , exceeds or equals TE . When the environment calculation is skipped, program control is given to statement 400. Statements 400 down to and including `CALL VSD(ALT,VS)` are the atmospheric property calculations for density, wind velocity, and velocity of sound all gathered together into a group. The card `VWZ = 0.` was added for the atmosphere (one usually does not consider vertical wind currents in a normal six-degree calculation). The last statement in this group `VRZ = DZ5 - VWZ` was changed to `0` to include the vertical wind component, VWZ ; although VWZ is zero for the assumed atmosphere it is not zero in the blast environment.

When time, T , exceeds or equals TE , program control is given to statement 401. The variables XR , YR , ZR are the scalar components of Eq. 11. The variable RR is the scalar magnitude of the vector \bar{R}_R . Subroutine BLAST examines to see whether the vehicle has reached the blast environment; if so it then reads environment data off the magnetic tape, identifies the data closest to T_{fb} , and finally interpolates radial position to get density, wind velocity, and velocity of sound along with other environmental data. The statement following `CALL BLAST (T,...)` reexamines to see if the vehicle is in the blast area (this is necessary since the vehicle may not be in the blast area for all times after TE) and gives appropriate control to either statement 400 or statement 402. Subroutine BLAST will be discussed in detail in paragraph 3 of this section.

The main program statements following `VRZ = DZ5 - VWZ` are the same as shown in TR-66-156, page 87 (except that `CALL DENS(ALT,RH0,E3)` and `CALL VSD(ALT,VS)` were regrouped as previously mentioned) down to and including `P = 14.70 * E3 * TAU4`. The next statement `CALL ATTK(VRZ4,VRY4,ALP,PI)` and all statements down to and including `FY1 = CYB * QD * SW * BET` are removed. These statements are the original

six-degree aerodynamic calculations that need to be changed for the large angle of attack mentioned in Section II, paragraph 4a. The following statements are inserted in their place.

```

VXY=SQRTF(VRX4**2+VRY4**2)
ALP=180./PI*ACØSF(VRZ4/VR)
CALL ACMQ(T,AMACH,CMQ,PI,E3)
IF(ALP-5.00)197,197,198
198 CALL CMN1(ALP,CM1,CN1)
CM=-CM1-CN1*(G-STA)/(12.*D1)
CN=CN1
GØTØ255
197 CALL ACMA(AMACH,CMA,PI,E3)
CALL ACNA(AMACH,CNA,PI,E3)
CM=-CMA*ALP-CNA*(G-STA)*ALP/(12.*D1)
CN=CNA*ALP
255 TMN=CM*QD*SW*D1
FYN=CN*QD*SW
T=-TMN*VRY4/VXY+CMQ*WX4*D1/(2.*VR)*QD*SW*D1
TN=TMN*VRX4/VXY+CMQ*WY4*D1/(2.*VR)*QD*SW*D1
FY1=-FYN*VRX4/VXY
FN=-FYN*VRY4/VXY

```

The variable VXY is V_{XY} in Eq. 2. The variable ALP is the total angle of attack α_T in Eq. 5. The variable CMQ is the pitch damping coefficient. The variable CM is the positive pitch moment coefficient. The variable CN is the positive normal force coefficient. The variable TMN is M_{aero} (see Eq. 7) and the variable FYN is F_{aero} (see Eq. 6). The variable TM is the positive aerodynamic restoring moment in pitch. The variable TN is the positive aerodynamic restoring moment in yaw. The variable FY1 is the aerodynamic force in the positive yaw direction. The variable FN is the aerodynamic force in the positive pitch direction.

```

390 CALL ACLD(AMACH,CLD,PI,E3) -- This is the next card in the main program
                                following the aerodynamic calculations (see
                                TR-66-156, page 90).

```

FY4=FN+THT*ET+FJY4 -- The negative sign in front of FN (see TR-66-156, page 91) is removed because FN is now in the positive pitch direction due to the aerodynamic change described above.

The statements for TANG and PØL are removed (see TR-66-156, page 95) because of the aerodynamic change. The remainder of the main program is the same except for the following changes in the output instructions (see TR-66-156, page 95).

```

PRINT 800,T,AL1,...same
1Y4,DPH...EXD,VXY,WZ4,...same
2S,P,...same...,FD,VRX4,VR4,VRZ4,DX,
3DY,DZ
800 FØRMAT(2X,...same
1E11.4,...same
212.5,1X,...same
3E13.6,...same
4E12.5,...same...,3
5(E11.4,1X),/,2X,E11.4,1X,2(E11.4,2X),/)

```

These are the program print and format changes for excluding BET, TANG, PØL, and including VXY, VRX4, VR4, VRZ4, DX, DY, and DZ.

IF(T.LT.TE)GØTØ600 -- This avoids printing data on environment position until time T_e is reached.

IF(R2(L2) - RR)605,605,601 -- This avoids printing environment data until vehicle gets into blast area.

```

601 PRINT602,FAC,VW,VWX,VWY,VWZ,PRES,TEMP,VS,RHØ
602 FØRMAT(2X,3HFAC,8X,2HVW,11X,3HVWX,10X,3HVWY,10X,3HVWZ,10X,4HPRES,8
1X,4HTEMP,10X,2HVS,11X,3HRHØ,/,2X,E10.3,1X,4(E12.5,1X),E11.4,1X,E13
2.6,1X,E12.5,1X,E11.4,/)

```

These are the print and format statements for the environment as seen by the vehicle.

```

605 PRINT606,TFB,TH2,XR,YR,ZR,RR,RFB
606 FØRMAT(2X,3HTFB,9X,3HTH2,9X,2HXR,11X,2HYR,11X,2HZR,11X,2HRR,11X,3H
1RFB,/,2X,2(E11.4,1X),5(E12.5,1X),/)

```


These are the print and format statements for the environment position data.

```

      IF (TH2-THA) 600, 600, 607 -- Controls printing of raw environment data.
607  PRINT 608
608  FORMAT (2X, 1HR, 12X, 2HRD, 10X, 2HP1, 10X, 5HTHETA, 9X, 4HDENS, 8X, 1HE, 12X, 3
      1HRDD, 10X, 4HSMLQ, 9X, 4HSMLR, 11)
      DØ610 I=1, L2
      PRINT 609, R2(I), RD2(I), P12(I), THETA2(I), DENS2(I), E2(I), RDD2(I), SML
      1Q2(I), SMLR2(I)
609  FORMAT (2X, E12.5, 1X, 2(E11.4, 1X), E13.6, 1X, E11.4, 1X, 4(E12.5, 1X))
610  CONTINUE
      THA=TH2 -- This prevents raw environment data from being printed more than
              once.

```

The above statements are for the raw environment data print-out.

```

600  THO=ABSF (THO)
      IF (T.GE.80..ØR.THØ.GE.80.) GØTØ801
      GØTØ999
801  PRINT 1050
1050  FORMAT (2X, 4HSTØP)
      STØP
      END

```

These cards stop the program if time exceeds 80 seconds or if the yaw angle exceeds 80 degrees. This completes the main program modifications.

3. Subroutine Modifications

a. Aerodynamic Subroutines.

The Subroutine ATTK can be eliminated because of the aerodynamic changes discussed in Section II, paragraph 4a (see TR-66-156, page 105).

b. Subroutine BLAST.

```

SUBROUTINE BLAST (T, RR, XR, YR, ZR, TP, TFB, KX, L2, TH2, R2, RD2, P12, THETA2,
1DENS2, E2, RDD2, SMLQ2, SMLR2, VSØ2, RFB, FAC, VW, PRES, TEMP, RHØ, VS, VWX, VWY
2, VWZ, KY)

```

```

DIMENSION IJA(125),HEAD(12),LMDA(20),ØKLM(20),CHRNØ(20),AMASNØ(20)
1,ITEMP(16),R(152),RD(152),P1(152),THETA(152),DENS(152),E(152),RDD(
2152),SMLQ(152),SMLR(152),VSØ(152),R1(152),RD1(152),P11(152),THETA1
3(152),DENS1(152),E1(152),RDD1(152),SMLQ1(152),SMLR1(152),VSØ1(152)
4,R2(152),RD2(152),P12(152),THETA2(152),DENS2(152),E2(152),RDD2(152
5),SMLQ2(152),SMLR2(152),VSØ2(152),AAKPV(30)

```

These statements are the heading and dimension cards for the subroutine. Each variable and array is explained in the discussion that follows.

TFB=T-TP-1.00 -- This is Eq. 8 where TFB is T_{fb} .

IF(KY)625,415,625 -- KY is a dummy variable that is zero until the last data are read from the magnetic tape and the end of file (EØF) is reached. When the EØF is reached, KY is set to 1 and the above statement then prevents the tape from reading past the EØF and stopping the program.

```

415 IF(KX)500,400,500
400 READ650,AAKPV
650 FØRMAT(F5.0)
    CØN1=.7929
    CØN2=.7475
    CØN3=2.402
    CØN4=4.402
    READ(4,101)N
101 FØRMAT(I10)
    DØ 109 J=1,N
    DØ 109 I=1,50
    READ(4,104)(IJA(K),K=1,120)
109 CØNTINUE
104 FØRMAT(120A1)
8    CØNTINUE
    READ(4,102)CØUNT,TH,IA,IB,MAXL,(HEAD(I),I=1,12)
    TH=CØN1*TH
    IF(EØF,4)409,410
409 KY=1
    GØTØ625
102 FØRMAT(1X,F7.1,E13.6,3I9,12A6)

```

```

410 READ(4,105)(LMDA(I),I=1,MAXL)
105 FØRMAT(1X,13I9)
    MAXLM=MAXL-1
110 FØRMAT(1X,7E17.9)
    READ(4,110)(ØKLM(I),I=1,MAXLM)
    READ(4,110)(CHRNØ(I),I=1,MAXLM)
    READ(4,110)(AMASNØ(I),I=1,MAXLM)
    READ(4,111)(ITEMP(I),I=1,16)
111 FØRMAT(1X,16I7)
    IBM1=IB-1
    READ(4,110)(R(I),I=1,IB)
    READ(4,110)(RD(I),I=1,IB)
    READ(4,110)(P1(I),I=1,IBM1)
    READ(4,110)(THETA(I),I=1,IBM1)
    READ(4,110)(DENS(I),I=1,IBM1)
    READ(4,110)(E(I),I=1,IBM1)
    READ(4,110)(RDD(I),I=1,IB)
    READ(4,110)(SMLQ(I),I=1,IB)
    READ(4,110)(SMLR(I),I=1,IB)
    DØ 406,I=1,IBM1
    R(I)=CØN2*R(I)
    P1(I)=CØN3*P1(I)
406 DENS(I)=CØN4*DENS(I)
    KX=1

```

Through the variable KX in statement 415, statements 400 down to and including statement 104 are executed only once (see Section III, paragraph 2). Array AAKPV stores 30 data points for the ratio of specific heat at constant pressure to specific heat at constant volume for air from 500 degrees K every 500-degree increment to 15000 degrees K. This array is necessary in order to calculate velocity of sound in the environment from temperature. The variables CØN1, CØN2, CØN3, and CØN4 are the constants for scaling the environment from 40 kilometers to 30 kilometers (see Section III, paragraph 3). The statements from READ(4,101)N down to and including READ(4,110)(SMLR(I),I=1,IB) are the instructions for reading the raw environment data off the magnetic tape. The statement TH=CØN1*TH scales time, TH, for the lower altitude. The EØF check follows this statement. The final "do loop" in this group of statements scales the radius

R(I), the pressure P1(I), and the density DENS(I) to the 30-kilometer altitude. The variable KX is then made 1, and program control is given to statement 500.

500 IF(TH-TFB)270,250,250

270 L1=IBM1

DØ 271 I=1,L1

TH1=TH

R1(I)=R(I)

RD1(I)=RD(I)

P11(I)=P1(I)

THETA1(I)=THETA(I)

DENS1(I)=DENS(I)

E1(I)=E(I)

RDD1(I)=RDD(I)

SMLQ1(I)=SMLQ(I)

271 SMLR1(I)=SMLR(I)

GØTØ8

These statements cause the magnetic tape to be read progressively in time and to store the data in the arrays signified by the number 1 until the time, TH, read on the magnetic tape just exceeds the actual time from detonation, TFB. As such, the arrays signified by the number 1 always contain the raw environmental data available on the tape just prior to the actual time TFB. When a TH that is equal to or larger than TFB is read off the tape, program control is given to statement 250.

250 IF((TFB-TH1).LT.(TH-TFB))GØTØ290

L2=IBM1

DØ 300 I=1,L2

TH2=TH

R2(I)=3.28E-02*R(I)

RD2(I)=3.28E-02*RD(I)

P12(I)=1.45E-05*P1(I)

THETA2(I)=1.16057E+04*THETA(I)

CALL CPCV (THETA2(I),AKPV,AAKPV)

THETA2(I)=1.8*1.16057E+04*THETA(I)

DENS2(I)=1.94*DENS(I)

E2(I)=E(I)


```

      RDD2(I)=RDD(I)
      SMLQ2(I)=SMLQ(I)
      SMLR2(I)=SMLR(I)
300 VSØ2(I)=1068.*SQRTF(AKPV*THETA2(I)/(1.387*481.))
      GØTØ600
290 L2=L1
      DØ 272 I=1,L2
      TH2=TH1
      R2(I)=3.28E-02R1(I)
      RD2(I)=3.28E-02*RD1(I)
      P12(I)=1.45E-05*P11(I)
      THETA2(I)=1.16057E+04*THETA1(I)
      CALL CPCV (THETA2(I),AKPV,AAKPV)
      THETA2(I)=1.8*1.16057E+04*THETA1(I)
      DENS2(I)=1.94*DENS1(I)
      E2(I)=E1(I)
      RDD2(I)=RDD1(I)
      SMLQ2(I)=SMLQ1(I)
      SMLR2(I)=SMLR1(I)
272 VSØ2(I)=1068.*SQRTF(AKPV*THETA2(I)/(1.387*481.))

```

Statement 250 examines the two stored environmental times TH1 and TH (which bracket the time TFB) and determines which time is closer to TFB. The environmental data closer to TFB are then stored in the arrays signified by the number 2. When TFB progresses past the last read value for TH, statement 500 causes that environmental data associated with TH to be stored in the arrays signified by the number 1 and the tape to be read again until TFB is equaled or exceeded by a new TH. In this manner, the arrays signified by the number 1 always contain the data available on the tape just prior to TFB, and the arrays signified by the number 2 always contain the data closest to TFB. Note that in the arrays signified by the number 2 the data have been converted from the CGS system of units to the following:

```

R2(I) -- feet
RD2(I) -- feet/sec
P12(I) -- lb/in2
THETA2(I) -- degrees Kelvin first, later to degrees Rankine after calling
              Subroutine CPCV

```

DENS2(I) -- slugs/ft³

VSØ2(I) -- ft/sec

Control is finally given to statement 600.

600 DØ 260 I=2,L2

IF(SMLQ2(I)-.1)261,261,260

261 L=I

GØTØ262

260 CØNTINUE

262 RFB=R2(L)

This "do loop" determines the radius of the fireball, RFB, indirectly through the behavior of the inward flux of energy, SMLQ. Program control is then given to statement 625.

625 IF(R2(L2)-RR)253,253,254

253 RETURN

These statements return program control to the main program if the vehicle is outside the blast area. If not, program control is given to statement 254.

254 DØ 256 I=1,L2

IF(R2(I)-RR)256,257,257

257 K=I

GØTØ258

256 CØNTINUE

258 FAC=(RR-R2(K-1))/(R2(K)-R2(K-1))

VW=RD2(K-1)+(RD2(K)-RD2(K-1))*FAC

PRES=P12(K-1)+(P12(K)-P12(K-1))*FAC

TEMP=THETA2(K-1)+(THETA2(K)-THETA2(K-1))*FAC

RHØ=DENS2(K-1)+(DENS2(K)-DENS2(K-1))*FAC

VS=VSØ2(K-1)+(VSØ2(K)-VSØ2(K-1))*FAC

VWX=VW*XR/RR

VW1=VW*YR/RR

VWZ=VW*ZR/RR

RETURN

END

These statements interpolate the arrays signified by the number 2 along the radius R2(I) to find the values of wind velocity VW, pressure PRES, temperature, TEMP,

density $RH\emptyset$, and velocity of sound VS at the vehicle radial position RR . The variables VWX , VWY , VWZ are equations 14, 15, and 16 respectively. This concludes Subroutine BLAST.

c. Subroutine CPCV.

```

SUBROUTINE CPCV (THETA2,AKPV,AAKPV)
DIMENSION AAKPV(30)
IF(THETA2-500.)1,1,2
1 AKPV=1.387
  RETURN
2 DØ 3 J=1,31
  IF(J-31)7,8,8
8 AKPV=1.293
  GØTØ6
7 A=J*500
  IF(A-THETA2)3,3,5
5 K=J
  AKPV=AAKPV(K-1)+(AAKPV(K)-AAKPV(K-1))/500.*(THETA2-A+500.)
  GØTØ6
3 CØNTINUE
6 RETURN
END

```

This subroutine interpolates the array AAKPV to get AKPV which is the ratio of specific heat at constant pressure to specific heat at constant volume for air. At the time CPCV is called, the temperature THETA2 is in degrees Kelvin which is commensurate with the units stored in AAKPV. The variable AKPV is then used to calculate the velocity of sound, $VS\emptyset2(I)$, in subroutine BLAST. The formula for $VS\emptyset2(I)$ takes the form:

$$VS\emptyset2 = VS_{\text{reference}} \frac{\sqrt{KT}}{\sqrt{KT_{\text{reference}}}}$$

where

K-CPCV

T-THETA2(I)

SECTION V

COMPUTER RESULTS

1. Explosion Environment

Figures 3 through 58 in Section III show the explosion environment in considerable detail. An attempt to explain the detail of the environment and why the environment behaves as it does is not attempted in this report. It is, however, worthwhile to note that the SPUTTER program output is very complex and is by no means a simple simulation. Some general comments about the properties of the environment are worthwhile to note: the velocities are very high (around 2000 ft/sec); the overpressures past 1 second are less than 1 psi; the high temperatures are associated with the fireball; inside the environment the air is rarefied. The general expansion of the fireball and shock versus time is shown in figure 59.

2. Vehicle Response to Environment

Many questions come to mind when flight through a nuclear explosion is considered. Consider the following:

- What happens to the attitude and position of the vehicle?
- What is the time history of the environment as seen by the vehicle?
- What are the dynamic loads and does the vehicle stay together?
- How badly is the trajectory dispersed after the vehicle leaves the environment?
- How does vehicle response change with trajectory miss distance from the center of detonation?

These are just some of the questions that can be conveniently answered by the six-degree trajectory simulation.

a. Data Presentation

Much data is generated in the six-degree program. The main part of the data is presented with a series of plotted graphs. For each six-degree calculation, 15 graphs were plotted by a CDC Cal-Comp plotter. The horizontal axis of the first 13 plots is the time of flight, t , beginning at $t = 42.0$ seconds (this

is just prior to the vehicle's entering the environment). Each of the graphs is explained in the following paragraphs.

(1) Wind, VW - FT/SEC

This graph shows the wind velocity in ft/sec as seen by the vehicle as it traverses the environment.

(2) Density, RHO - SG/FT³

This graph shows the density of the fluid in slug/ft³ as seen by the vehicle as it traverses the environment.

(3) Velocity of Sound, VS - FT/SEC

This graph shows the velocity of sound in ft/sec as seen by the vehicle as it traverses the environment.

(4) Relative Velocity, VR - FT/SEC

This graph shows the total relative velocity in ft/sec as seen by the vehicle as it traverses the environment.

(5) Dynamic Pressure, QD - LB/FT²

This graph shows the dynamic pressure in lb/ft² as seen by the vehicle as it traverses the environment.

(6) Mach Number, AMACH

This graph shows the Mach number as seen by the vehicle as it traverses the environment.

(7) Total Angle of Attack, ALP -DEG

This graph shows the total angle of attack in degrees as seen by the vehicle as it traverses the environment.

(8) Aerodynamic Moment, TMN - LB-FT

This graph shows the total aerodynamic moment about the vehicle C.G. in lb-ft as the vehicle traverses the environment.

(9) Aerodynamic Force, FNY - LB

This graph shows the total aerodynamic force in lb as seen by the vehicle as it traverses the environment.

(10) Euler Pitch Angle, PH - DEG

This graph shows the Euler pitch angle measured from the zenith in degrees as the vehicle traverses the environment.

(11) Euler Yaw Angle, TH - DEG

This graph shows the Euler yaw angle measured from the vertical plane in degrees as the vehicle traverses the environment.

(12) Static Pressure, P - LB/IN²

This graph shows the static pressure in lb/in² as seen by the vehicle as it traverses the environment.

(13) Temperature, TEMP - DEG - R

This graph shows the temperature of the environment in degrees Rankine as seen by the vehicle as it traverses the environment.

(14) Trajectory in Vertical Plane, ZR - FT vs YR - FT

This graph shows the trajectory in the vertical plane as seen from the center of detonation.

(15) Trajectory in Horizontal Plane, XR - FT vs YR - FT

This graph shows the trajectory in the horizontal plane as seen from the center of detonation.

b. Unguided Blue Goose Vehicle

The unguided Blue Goose vehicle (see Appendix I for basic properties) is flying at approximately 4000 ft/sec and spinning at 3 cycles per second when it reaches the explosion environment. To try to determine the trajectory path through the environment that gives the worst vehicle response, five six-degree calculations were made where the vehicle missed the center of detonation in the horizontal plane by 1000, 2000, 3000, 4000, and 6000 feet.

(1) Miss Distance 1000 Feet

Figures 60 to 74 are the 15 graphs discussed in paragraph 2a for the six-degree calculation where the vehicle missed the center of detonation to the right by 1000 feet in the horizontal plane. Each graph is discussed in turn.

(a) Wind, Figure 60

This graph shows that the expanding shock of the environment is intercepted at approximately 43.12 seconds time of flight. Figure 59 shows the intercept takes place at .77 seconds after detonation which when transformed to time of flight through Eq. 8 yields $t = 42.36 + .77 = 43.13$ seconds. A very large wind velocity (2000 ft/sec) is experienced as the vehicle penetrates the expanding shock. Inside the environment the wind velocities reduce (see environment graphs in Section III) and increase again as the vehicle catches up and passes through the expanding shock on leaving the environment. Figure 59 shows that the environment is exited around 6.80 seconds after detonation (i.e., $t = 42.36 + 6.8 = 49.16$ seconds). Figure 60 also shows that the environment is exited somewhere around 49.1 seconds.

(b) Density, Figure 61

This graph shows the decay of atmosphere density as the vehicle rises to meet the environment. When the shock is penetrated (the atmospheric model and environment model were matched at this point as closely as possible) a large increase of density is experienced followed by a larger decrease of density. Inside the environment the air is rarefied (mainly due to the high temperatures, see figure 72). The density again increases as the environment is exited at which time (around 49.1 seconds) the normal atmospheric decay continues (note that the one-dimensional environment model does not account for density variations with altitude).

(c) Velocity of Sound, Figure 62

The large increase in velocity of sound is mainly due to the high temperatures in the environment (see figure 72). It is for this reason that the fluid flow is below Mach 1 for most of the flight through the environment.

(d) Relative Velocity, Figure 63

This graph shows the normal decrease of vehicle relative velocity (due to gravity) until the vehicle reaches the environment head on and relative velocity increases. As the vehicle passes through the environment the winds progress from head to side, and finally to tail winds as the vehicle exits the environment. The tail winds during exit cause the relative velocity to be lower than that which would be experienced in the no-wind atmosphere.

(e) Dynamic Pressure, Figure 64

This graph shows the combined effects of density and relative velocity squared. This variable has a linear influence on the aerodynamic force and moment exerted on the vehicle. Note the large increase of dynamic pressure as the shock is penetrated. Note also the very low dynamic pressures associated with the rarefied atmosphere inside the environment.

(f) Mach Number, Figure 65

Note that the Mach number is below 1.0 for a good portion of the flight as was expected for this vehicle.

(g) Total Angle of Attack, Figure 66

In this particular calculation, the vehicle experiences an immediate three-degree angle of attack at shock penetration. The aerodynamically stable vehicle begins to align itself with the relative velocity vector and reduce the angle of attack. The vehicle aligns itself at approximately 43.6 seconds but overshoots badly. The trend thereafter is a ten-degree oscillation with very little indication of damping.

(h) Aerodynamic Moment, Figure 67

The aerodynamic moment curve is predominantly shaped by the dynamic pressure curve (figure 64) and the angle-of-attack curve (figure 66). Note the large aerodynamic moment (11,000 lb-ft) experienced at shock penetration. Since the transverse moment of inertia is 21544 slug-ft^2 , the 11,000 lb-ft moment results in an angular acceleration of $.51 \text{ rad/sec}^2$. Note that the aerodynamic restoring moment is very small during the time period 43.6 to 46.3 seconds; this is due to the low dynamic pressure experienced in the rarefied atmosphere. As the dynamic pressure increases during environment exit, the aerodynamic moment increases and oscillates as does the angle of attack.

(i) Aerodynamic Force, Figure 68

This curve is shaped the same as figure 67 since the only difference is the static margin of the vehicle. Note that at shock penetration the force is approximately 4000 pounds. This results in a transverse acceleration of $.57 \text{ g}$ (vehicle weight is 7000 pounds).

(j) Angular Response, Figures 69 and 70

As was previously explained, the six-degree calculation was run such that the vehicle flew through the altitude of the detonation center, but missed the center of the detonation to the right (as viewed from launch) in the horizontal plane by 1000 feet. As such, one would expect the vehicle to turn left (negative yaw) and precess upward (due to clockwise roll). Figures 69 and 70 confirm this initial motion and show an oscillatory motion thereafter.

(k) Static Pressure, Figure 71

This curve shows the static pressure experienced by the vehicle. Note the pressures are less than 1 psi.

(l) Temperature, Figure 72

This curve shows the temperatures of the environment as seen by the vehicle. The high temperatures are associated with fireball passage. Figure 59 shows that the vehicle was in the fireball from 1.0 to 3.88 seconds after detonation. These times correspond to a time of flight range from 43.36 to 46.24 seconds. These latter times agree very closely with the high temperature pulse shown in figure 72.

(m) Trajectory in Vertical Plane, Figure 73

Since the vehicle was aimed at the detonation center, as viewed in the vertical plane, one would not expect a significant change from the nominal trajectory in this plane. Figure 73 shows the vehicle passing very close to the detonation center with little noticeable deviation.

(n) Trajectory in Horizontal Plane, Figure 74

Since this is the plane in which the vehicle misses the detonation center, one would expect to see a trajectory change in this plane. When the vehicle penetrates the shock, the aerodynamic force is one that pushes the vehicle C.G. away from the detonation center. However, figure 66 shows that several oscillations about the relative velocity vector occur before the vehicle exits the environment. These oscillations complicate the problem of intuitively predicting the net direction of trajectory displacement. Figure 74 does show, however, that the net vehicle movement is away from the detonation center.

(2) Miss Distance 2000 Feet

Figures 75 to 89 are the graphs for the six-degree calculation where the vehicle missed the center of detonation by 2000 feet in the horizontal plane. The general shapes of the curves are similar to those just discussed. Note, however, that the angular acceleration and transverse acceleration at shock penetration are 2.55 rad/sec^2 and $2.0g$ respectively. Note also the large attitude changes and that the vehicle is still moving out from the center of detonation.

(3) Miss Distance 3000 Feet

Figures 90 to 104 are the graphs for the six-degree calculation for a miss distance in the horizontal plane of 3000 feet. The general shape of the curves are still the same as those previously discussed. The angular acceleration and transverse acceleration at shock penetration are 4.26 rad/sec^2 and $2.78g$ respectively. Note that the attitude excursions are very large.

(4) Miss Distance 4000 Feet

Figures 105 to 119 are the graphs for a horizontal miss distance of 4000 feet. The general shapes of the curves are still the same, as previously discussed. The angular acceleration and transverse acceleration at shock penetration are 5.05 rad/sec^2 and $3.08g$ respectively. Note the extreme attitude excursions.

(5) Miss Distance 6000 Feet

Figures 120 to 134 show the curves for a horizontal miss distance of 6000 feet. Figure 59 shows that in this case the vehicle just touches the edge of the fireball. The general shapes of the curves are the same as previously discussed except that velocity of sound, Mach number, and temperature are changed because the fireball is missed and the associated high temperatures are not experienced. The angular acceleration and transverse acceleration at shock penetration are 3.85 rad/sec^2 and $2.36g$ respectively. Note that the angular excursions are now beginning to reduce.

c. Discussion of Unguided Vehicle Results

(1) General Observation about Vehicle Response

Any one of the groups of graphs discussed in paragraphs b(1), b(2), b(3) or b(4) will suffice for the following general discussion since all the groups are similar. Figures 60 to 74 of paragraph b(1) will be used as a typical representation.

The vehicle is flying along in the normal atmosphere when abruptly it experiences a large increase in angle of attack and dynamic pressure at shock penetration. The large aerodynamic restoring moment begins to align the vehicle with the relative velocity vector and reduce the angle of attack. The angle of attack is reduced to a small value, around 43.6 to 43.7 seconds. The vehicle has considerable pitching and yawing angular velocity at this time and angle of attack once again begins to grow. However, the vehicle abruptly experiences a large decrease of dynamic pressure and the aerodynamic restoring moment becomes very small (see figure 67). As such, the vehicle continues to drift in attitude until at approximately 46.3 seconds it leaves the fireball and begins to experience increased dynamic pressure on exit from the environment. The vehicle once again begins to align itself with the relative velocity vector and begins a large coning motion. The vehicle leaves the environment at approximately 49 seconds and the coning motion continues, aided by the loss in dynamic pressure brought on by the exponentially decaying atmosphere density.

(2) Effects of Miss Distance Magnitude

Figures 60 to 134 indicate a trend of increased vehicle response with trajectory miss distance from the detonation center. The following figures help to show this trend and the trajectory that gives the worst vehicle response.

Figures 135 and 136 show angular acceleration and transverse acceleration at shock penetration versus miss distance. Note that a miss distance of approximately 4000 feet gives the largest dynamic loading for this vehicle and for this particular time of environment entry (1 second after detonation). If one assumes the C.G. is approximately in the center of the vehicle, the 5 rad/sec^2 angular acceleration results in a dynamic loading at the nose and tail of the vehicle of $5 \text{ rad/sec}^2 \times 15 \text{ ft} / 32.2 \text{ ft/sec}^2 = 2.33g$. Coupled with the transverse acceleration, this means that the rear of the vehicle will experience approximately 5.4g and the nose of the vehicle will experience approximately .8g.

Figure 137 shows the maximum yaw angle to which the vehicle drifts after the initial shock is traversed. Figure 138 shows the maximum pitch angle to which the vehicle drifts after the initial shock is traversed. Both are indications of the rotational energy imparted to the vehicle during shock traversal. Note again that maximum vehicle response occurs for a 4000-foot miss distance.

Figure 139 shows the vehicle position in the horizontal plane at environment exit (approximately 49.0 seconds). Note that the general trend is to slow the vehicle down and to push it away from the detonation center. Note also that the position deviation from the nominal trajectory is no larger than 60 feet. Figure 140 shows the vehicle position in the vertical plane at environment exit. Note that the general trend is to slow the vehicle down.

Vehicle velocity changes in magnitude and direction from the nominal were examined to estimate trajectory dispersion after environment exit. Figure 141 shows that the vehicle is slowed down no more than 100 ft/sec. Figure 142 shows that the velocity vector direction is changed no more than .71 degrees. These velocity vector changes, in conjunction with a simple point mass trajectory assumption, can be used to approximate vehicle trajectory dispersion at impact.

(3) Spin Effects

All computer results discussed so far were for the nominal vehicle which is spinning at 3 cps at environment entry. The question of whether or not the vehicle would tumble in the environment led to a computer run where the vehicle was not allowed to spin. Figures 143 to 157 show the results of the calculation. The calculation was made with the initial elevation of the vehicle 1 degree higher. As such, the vehicle intercepts the environment in the vertical plane and passes 3375 feet from the detonation center. In this case one would expect large pitch angle excursions and little yaw excursion (no coupling between pitch and yaw because of no spin). Figure 152 shows the pitch angle history and shows that the vehicle does not tumble inside the environment. Figure 153 shows the yaw angle history and confirms that it stays small (less than 1 degree) as expected. Note that the pitch change after shock traversal is approximately 60 degrees and the yaw change is very small in comparison. Figures 137 and 138, for the spinning vehicle at the same miss distance (3375 feet), show a yaw change of 55 degrees and a pitch change of 42 degrees. This seems to indicate no clear advantage, with regard to attitude excursion magnitude, in spinning the vehicle. The main reason why the vehicle does not tumble inside the environment is that the vehicle is pitching slowly enough and is traveling fast enough to intercept the shock on exit before tumbling can occur. This is not to say, however, that tumbling never occurs during the trajectory. Even though the calculation was not continued to impact, indications are that the vehicle goes into a growing pitch oscillation that progressively worsens because of the loss in dynamic pressure brought on by the exponentially decaying atmospheric density. The spinning vehicle behaves in a similar manner in its coning motion.

d. Guided Blue Goose Vehicle

The guided Blue Goose vehicle (see Appendix II) is almost the same in configuration and performance as the unguided Blue Goose vehicle. The main difference is that the guided vehicle is more stable (this is due to the forward shift of C.G. brought on by Recruit motor removal), is spinning 5 cps, and has less inertia (transverse moment of inertia 16627 slug-ft² and weight 6205 pounds).

A computer run was made where the vehicle intercepted the environment 4000 feet to the right in the horizontal plane. Figures 158 to 172 show the results of the calculation. The most striking difference between the unguided and guided vehicle is the quicker attitude response of the more stable, less-inertia, guided vehicle. The angular acceleration and transverse acceleration at shock penetration are 9 rad/sec² and 3.5g respectively. This results in a dynamic loading on the rear of the vehicle of 7.7g and .7g on the nose.

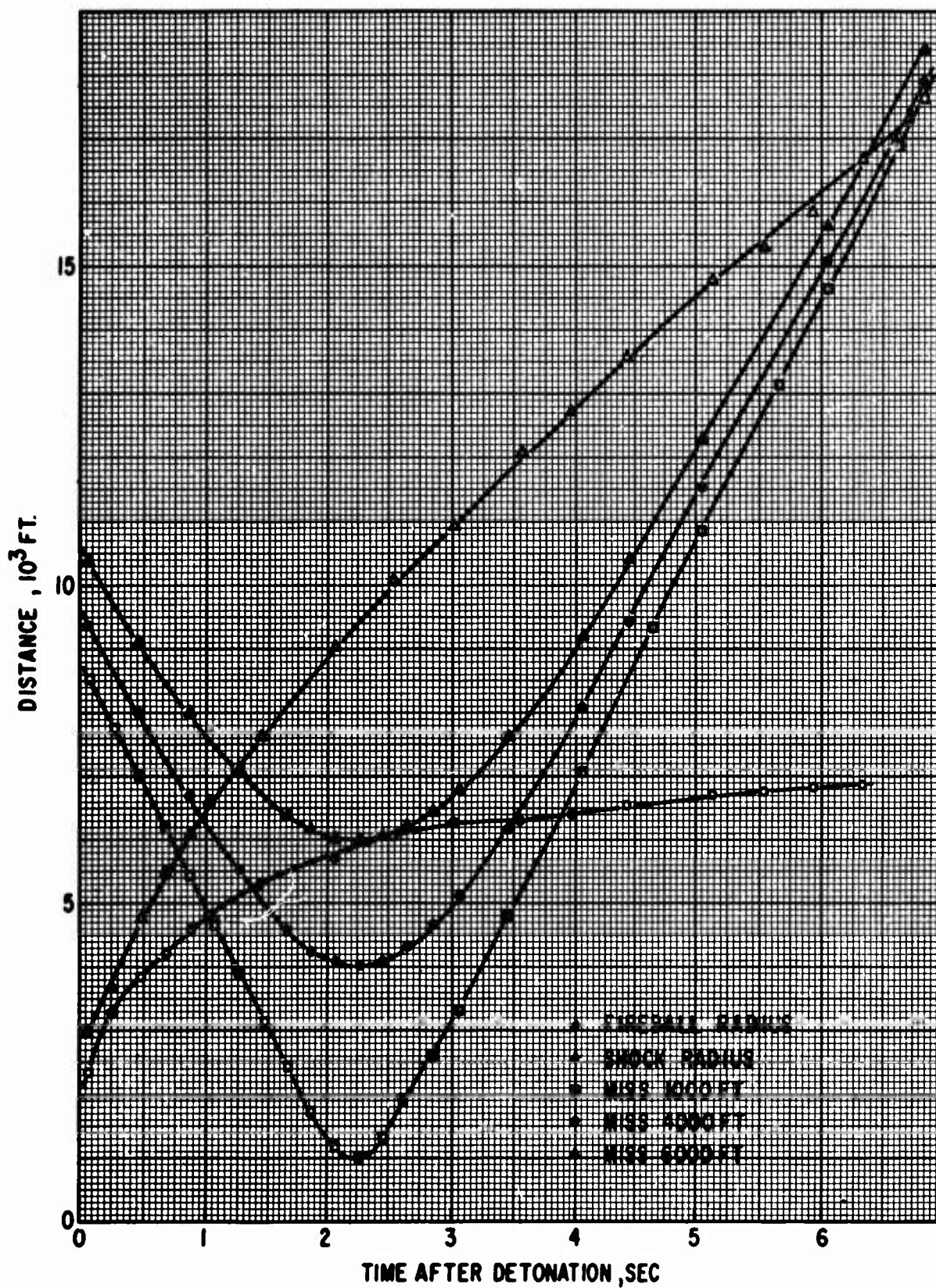


Figure 59. Environment Growth and Intercept

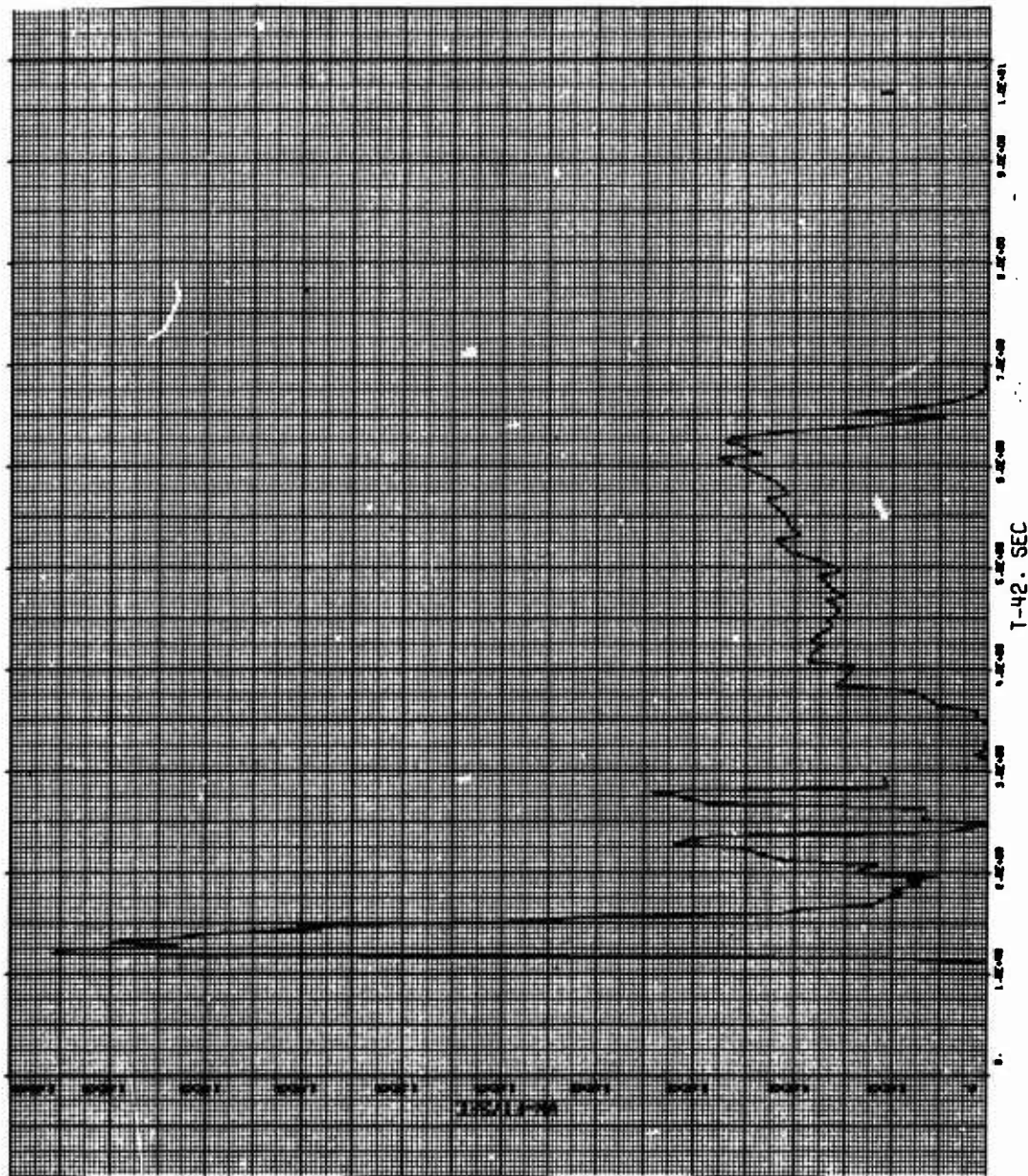


Figure 60. Graph for Miss Distance 1000 Feet

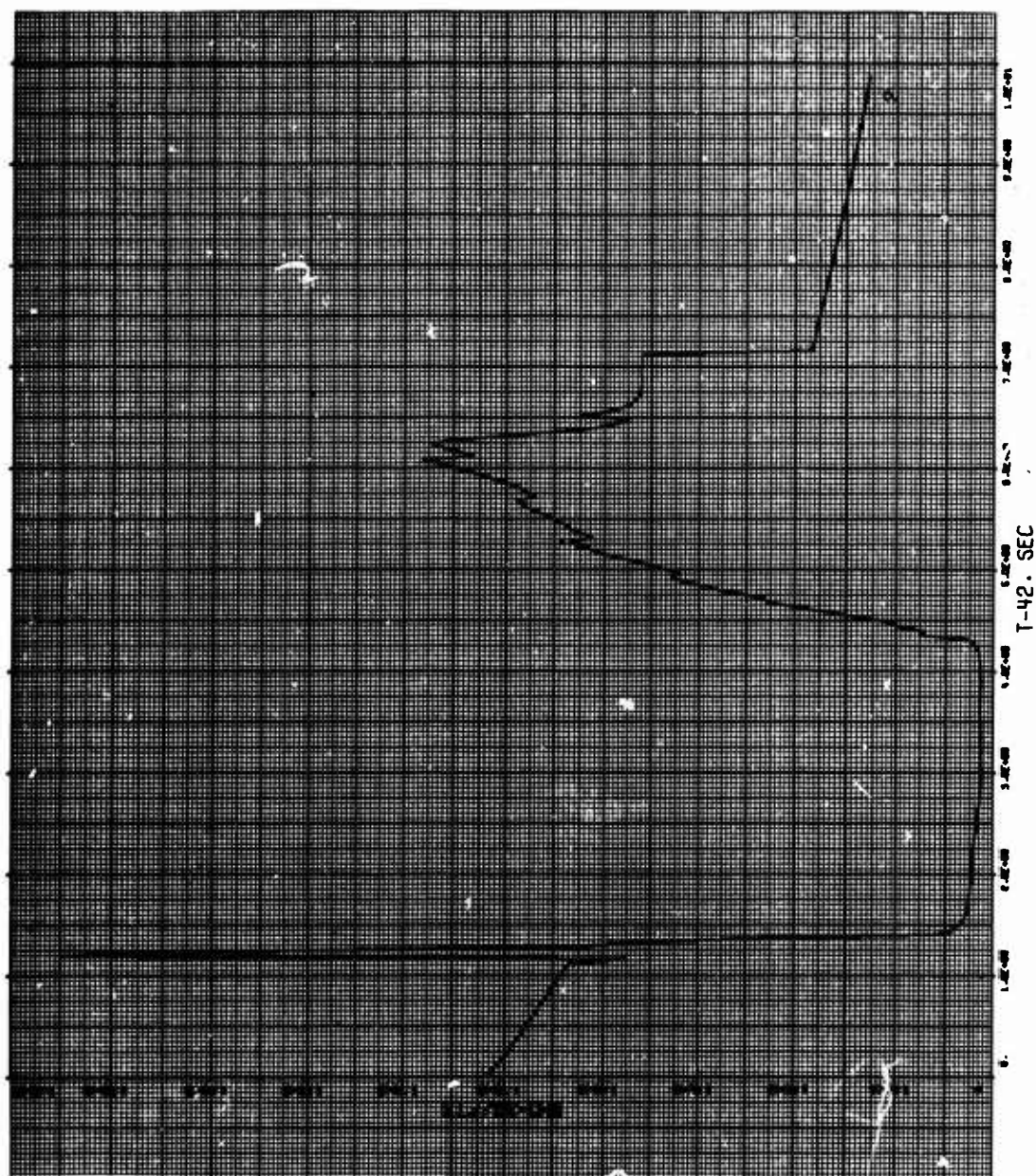


Figure 61. Graph for Miss Distance 1000 Feet

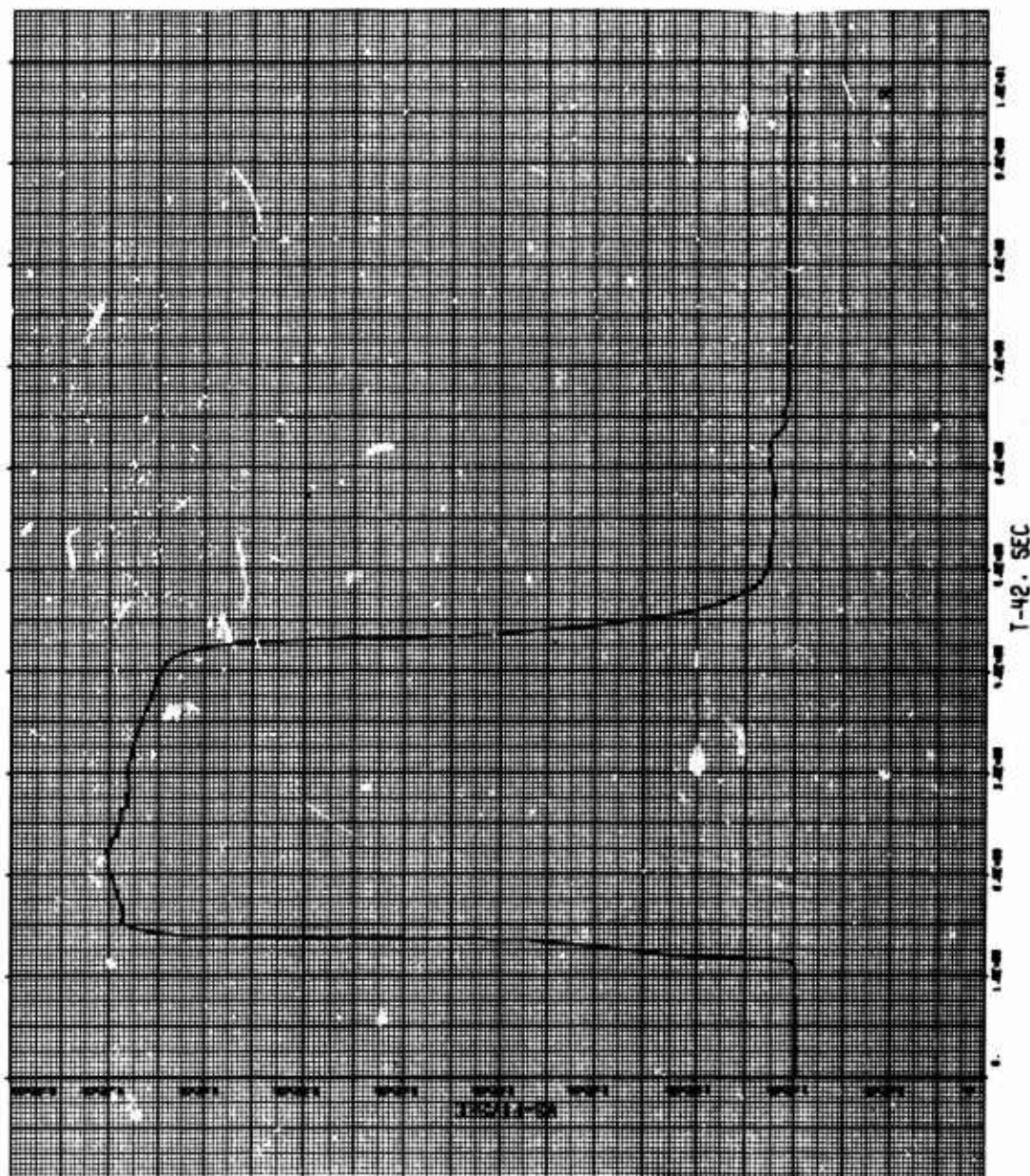


Figure 62. Graph for Miss Distance 1000 Feet

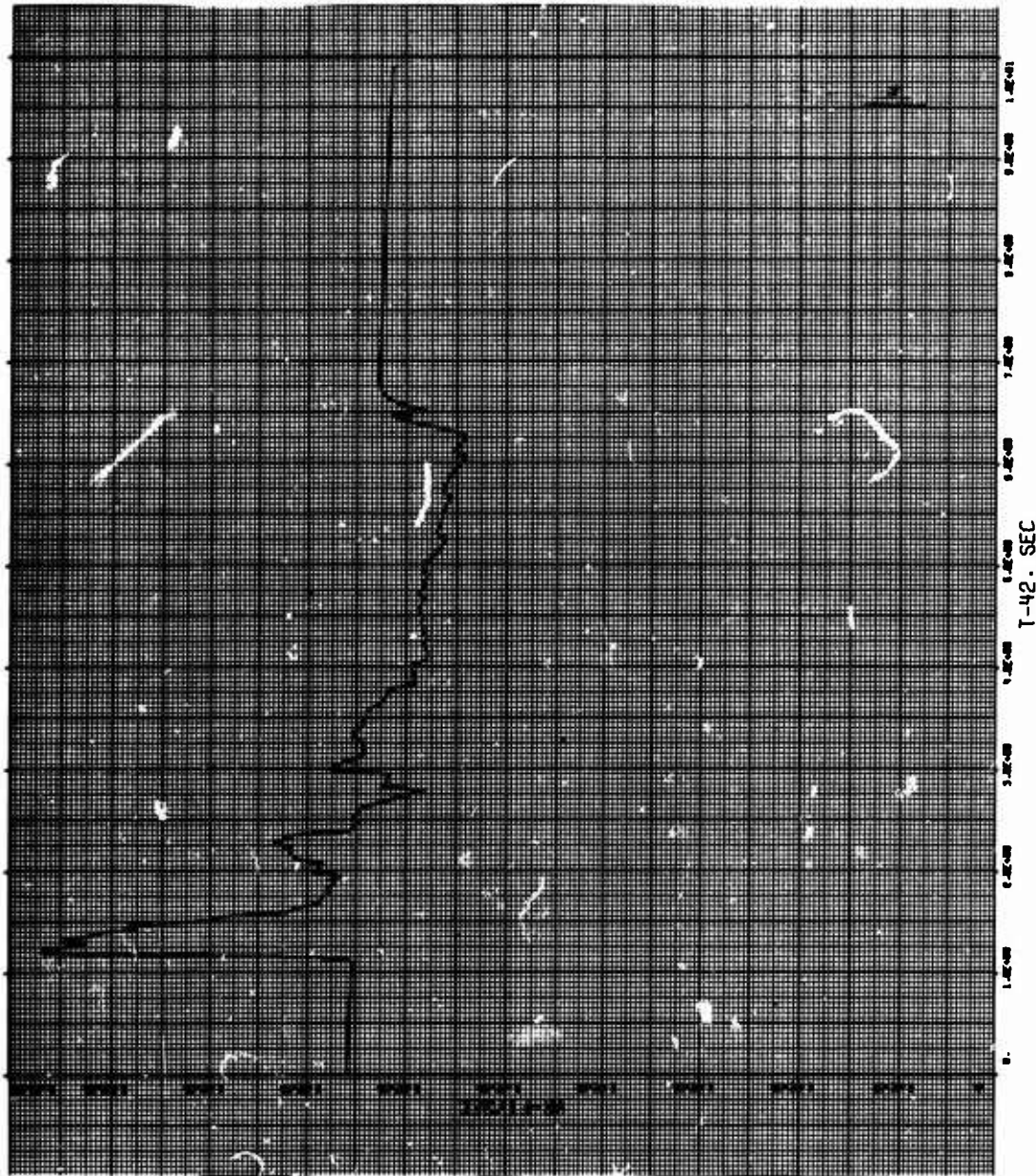


Figure 63. Graph for Miss Distance 1000 Feet

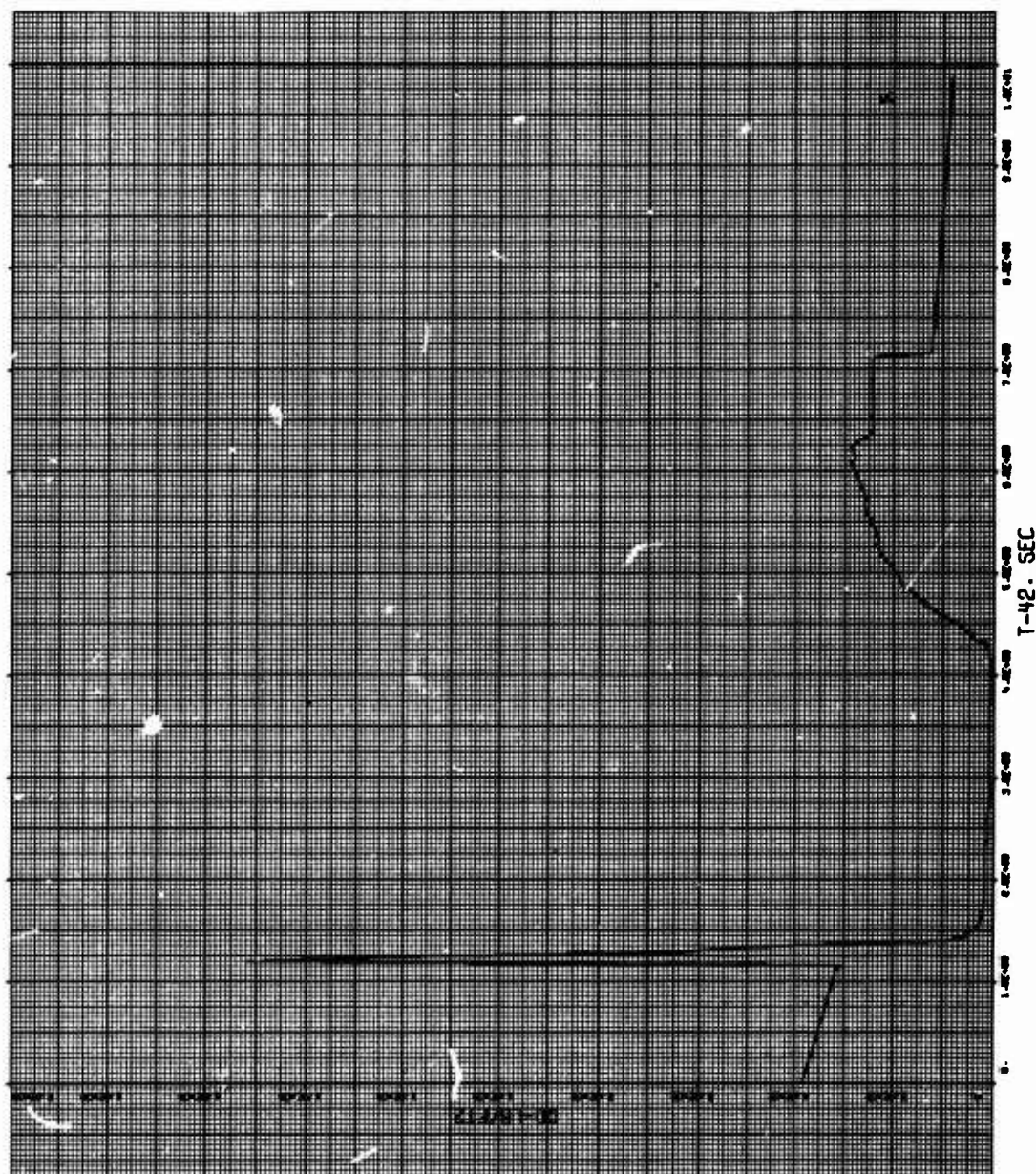


Figure 64. Graph for Miss Distance 1000 Feet

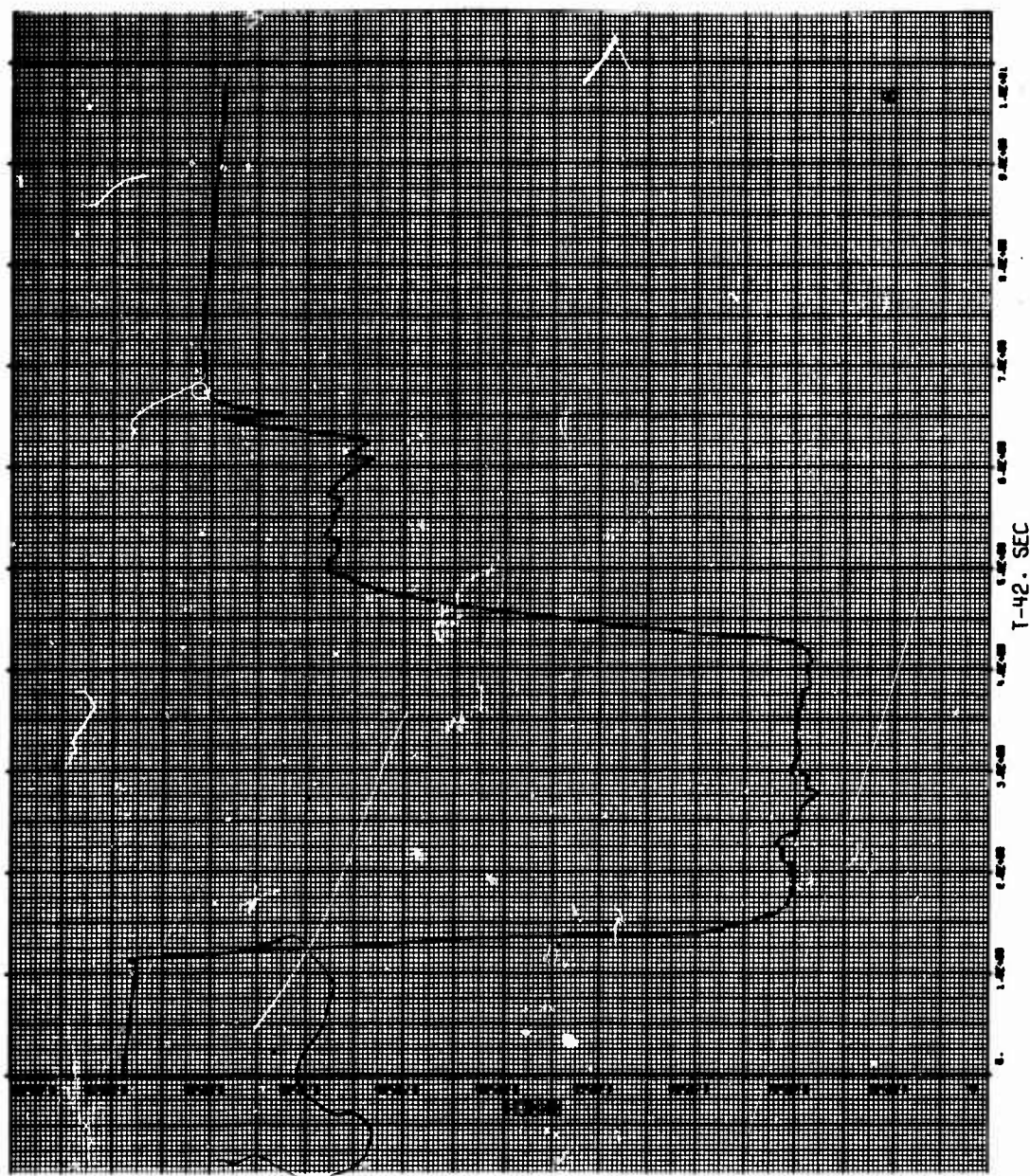


Figure 65. Graph for Miss Distance 1000 Feet

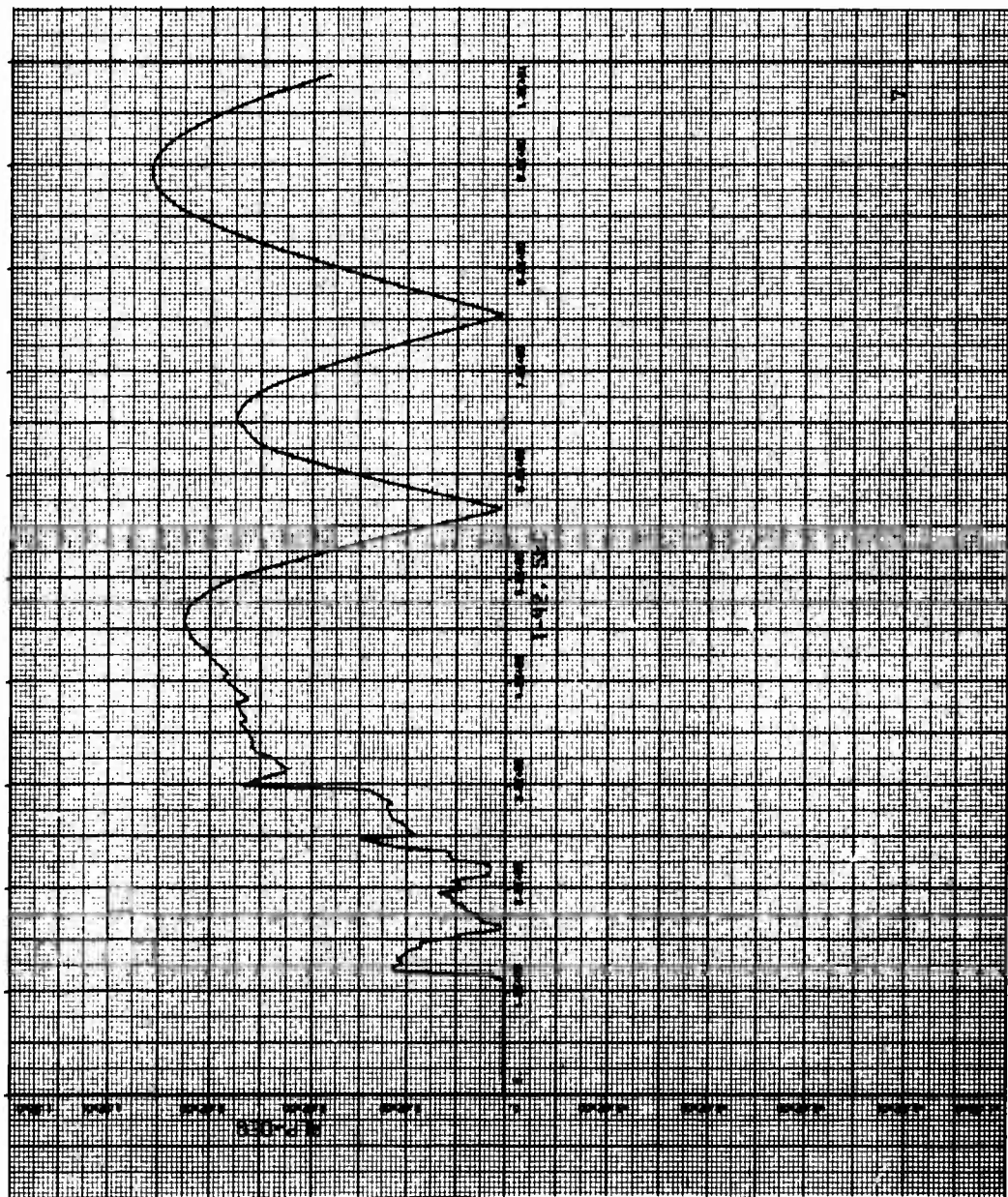


Figure 66. Graph for Miss Distance 1000 Feet

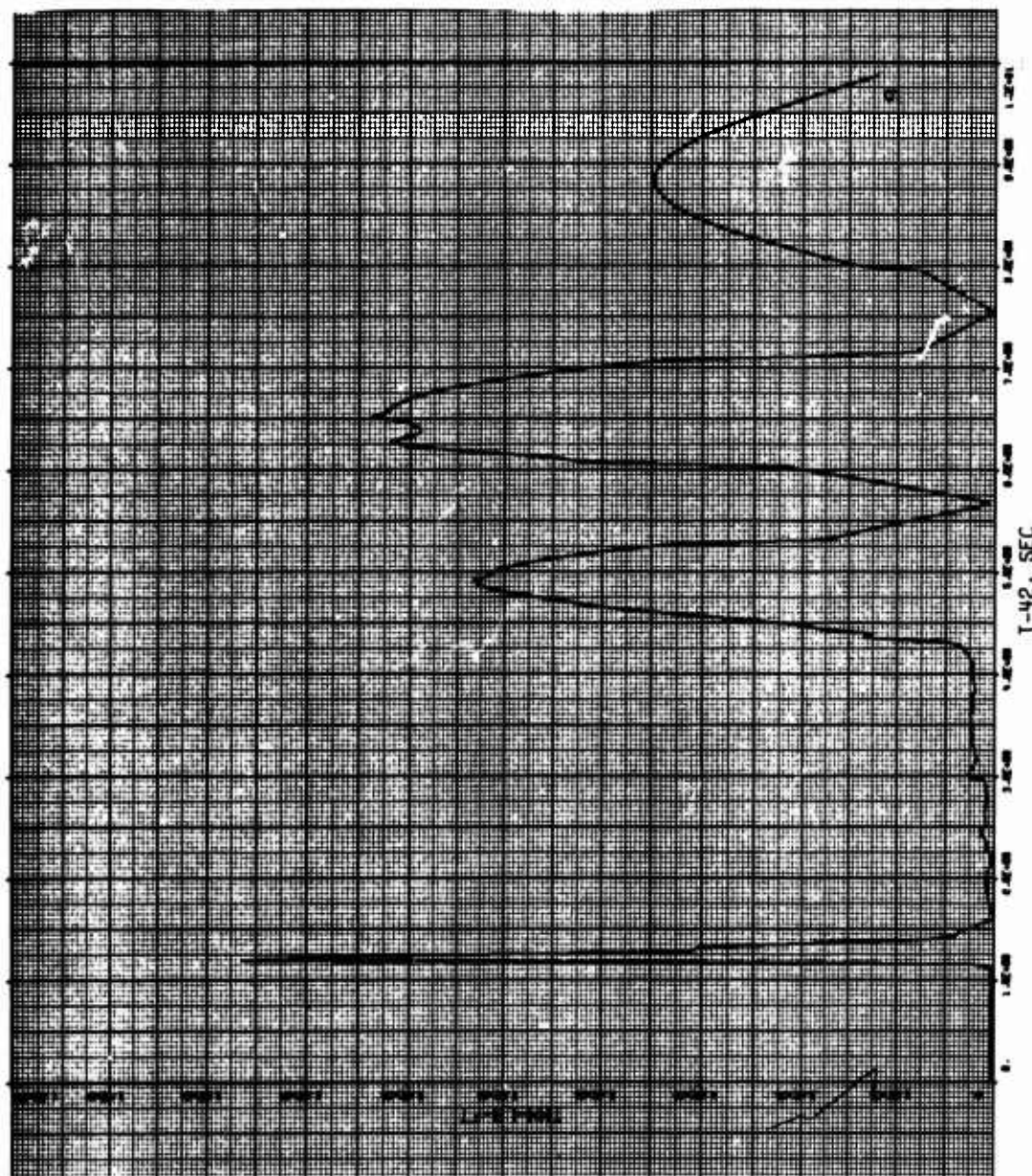


Figure 67. Graph for Miss Distance 1000 Feet

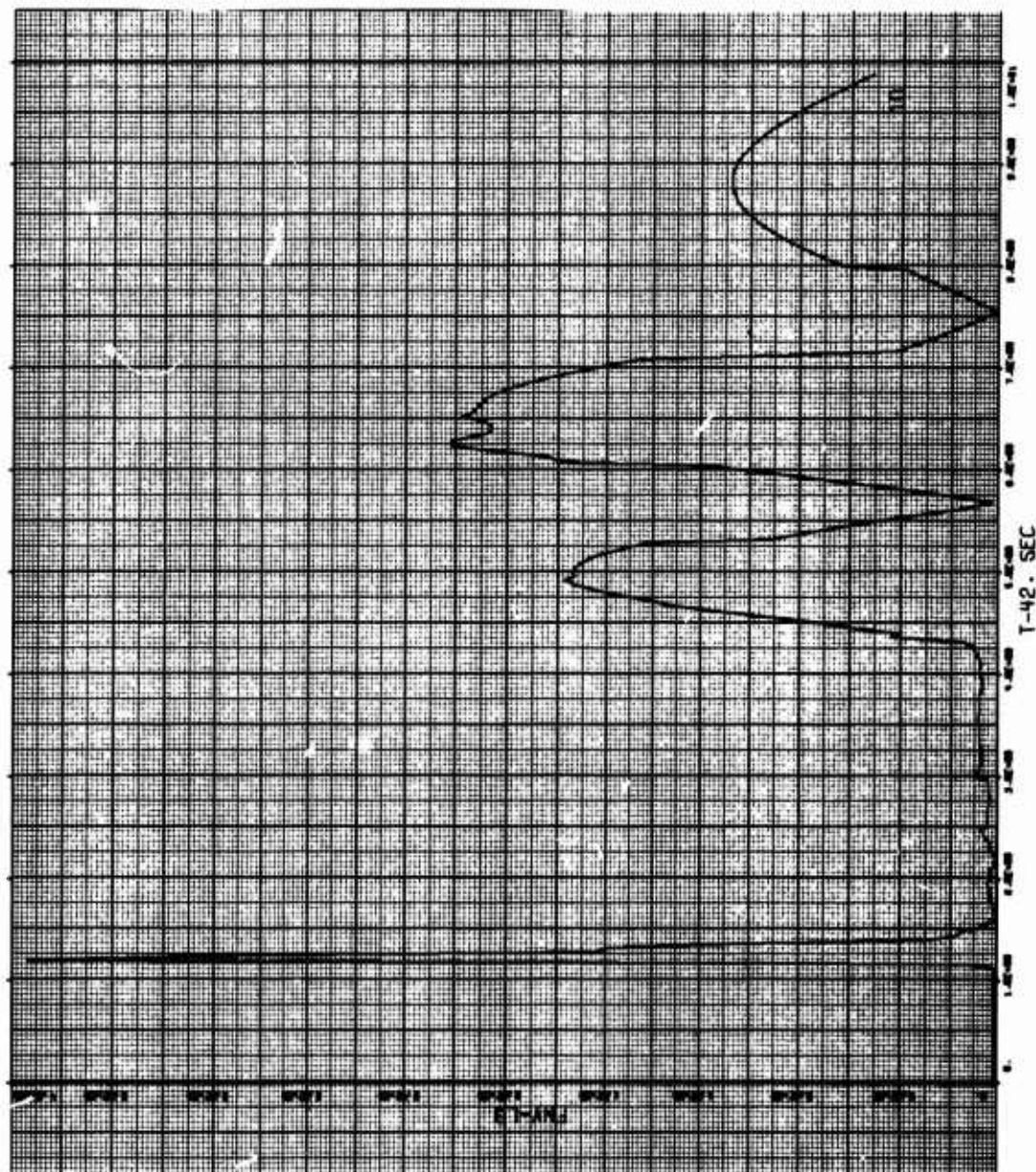


Figure 68. Graph for Miss Distance 1000 Feet

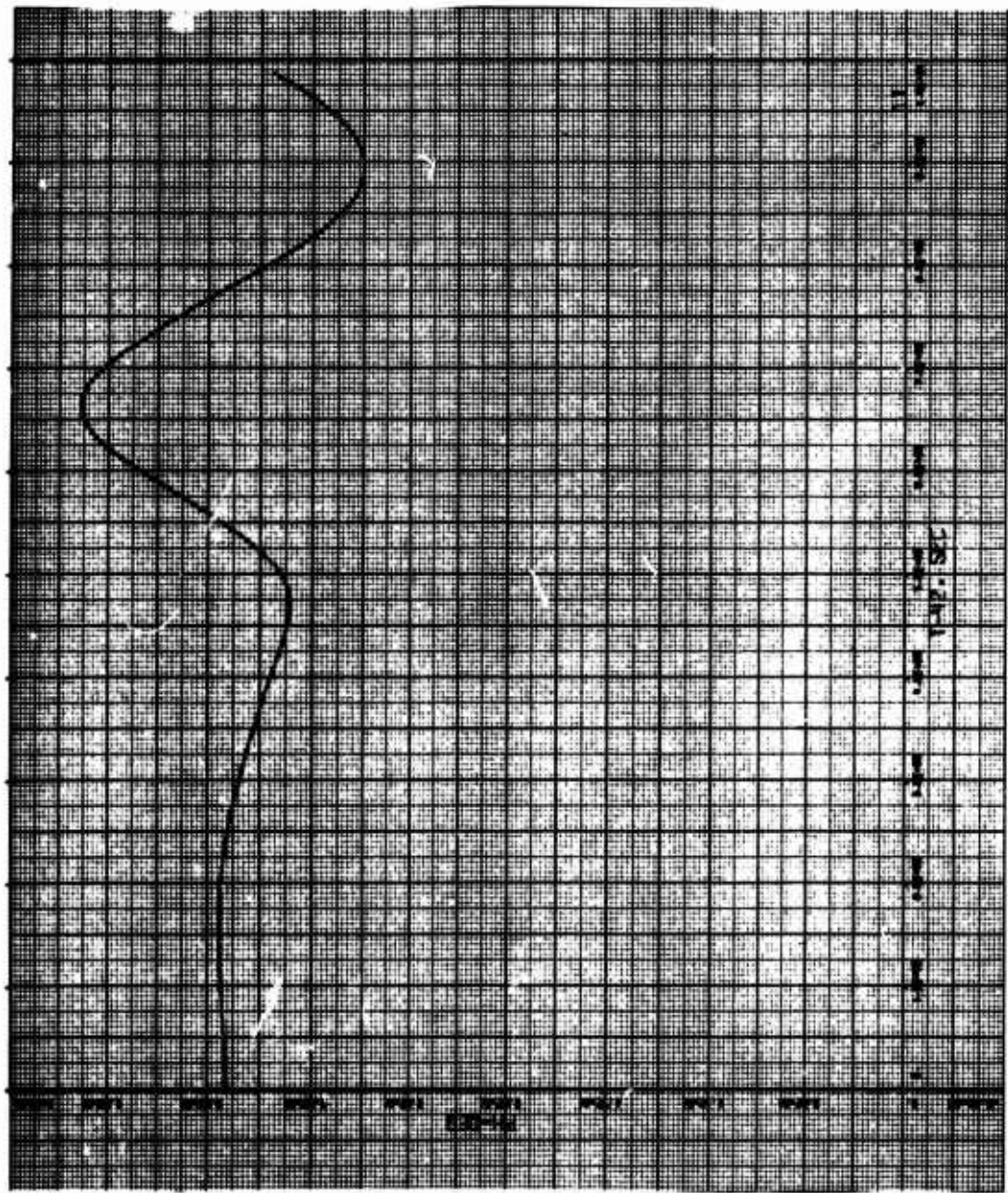


Figure 69. Graph for Miss Distance 1000 Feet

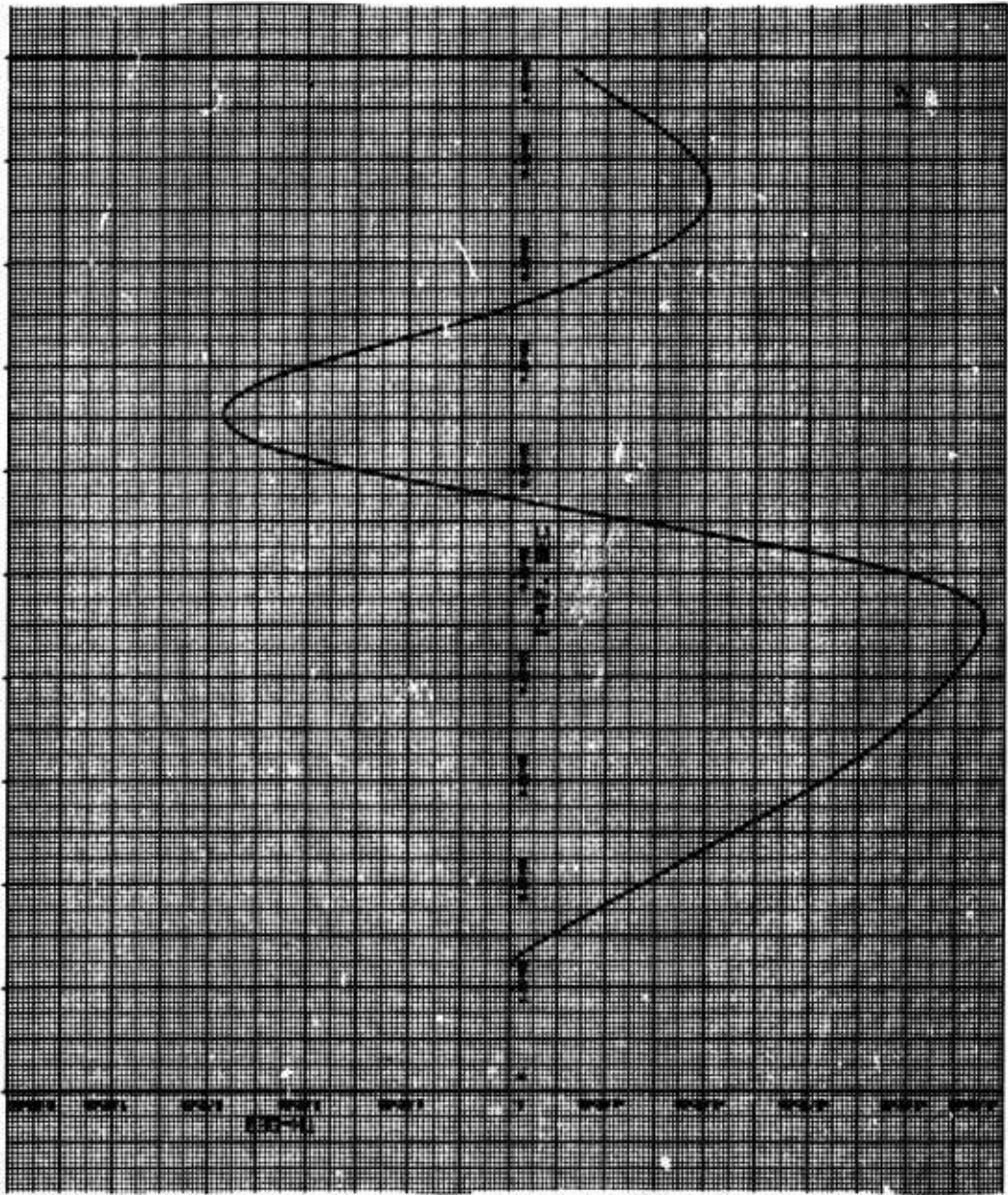


Figure 70. Graph for Miss Distance 1000 Feet

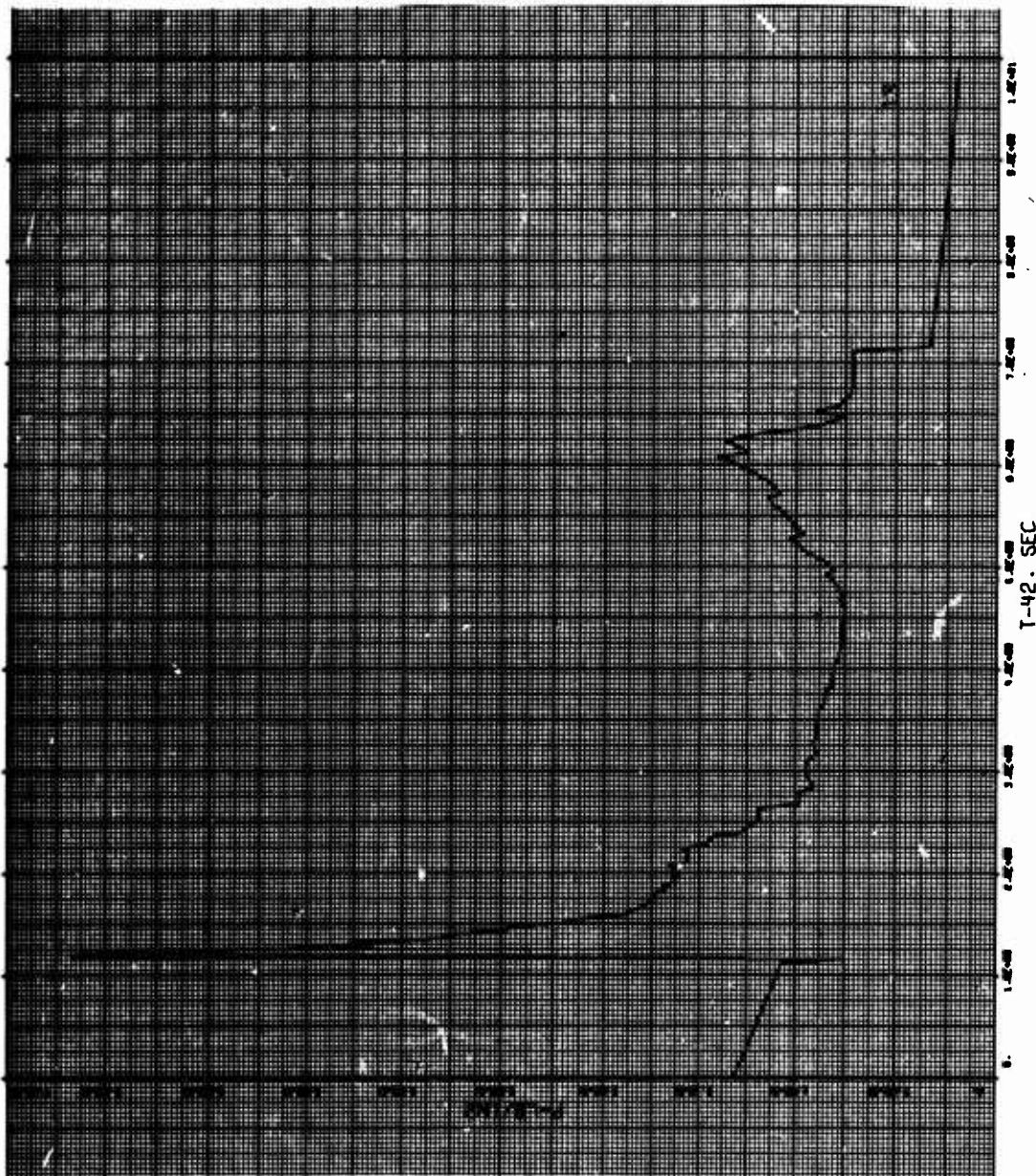


Figure 71. Graph for Miss Distance 1000 Feet

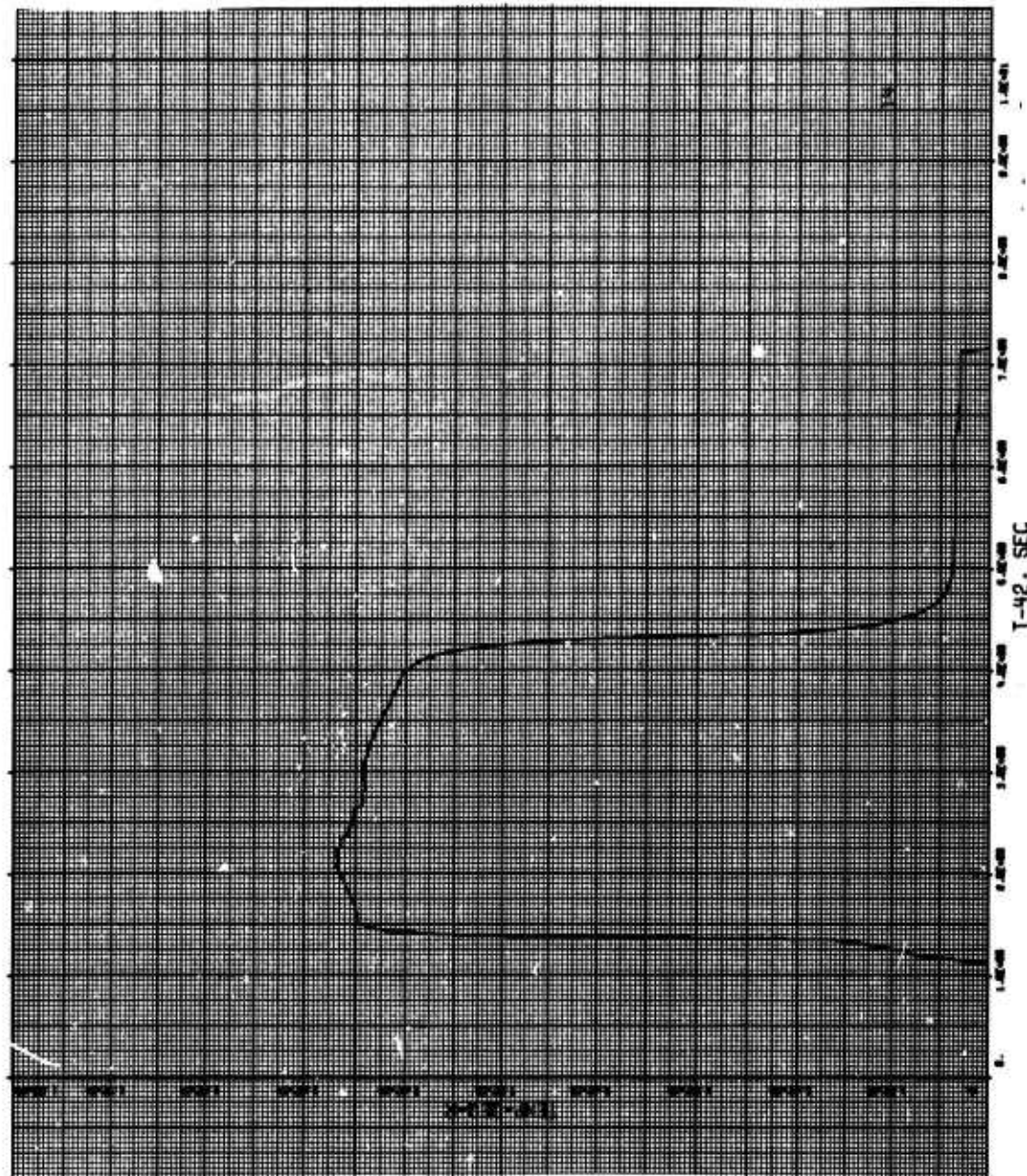


Figure 72. Graph for Miss Distance 1000 Feet

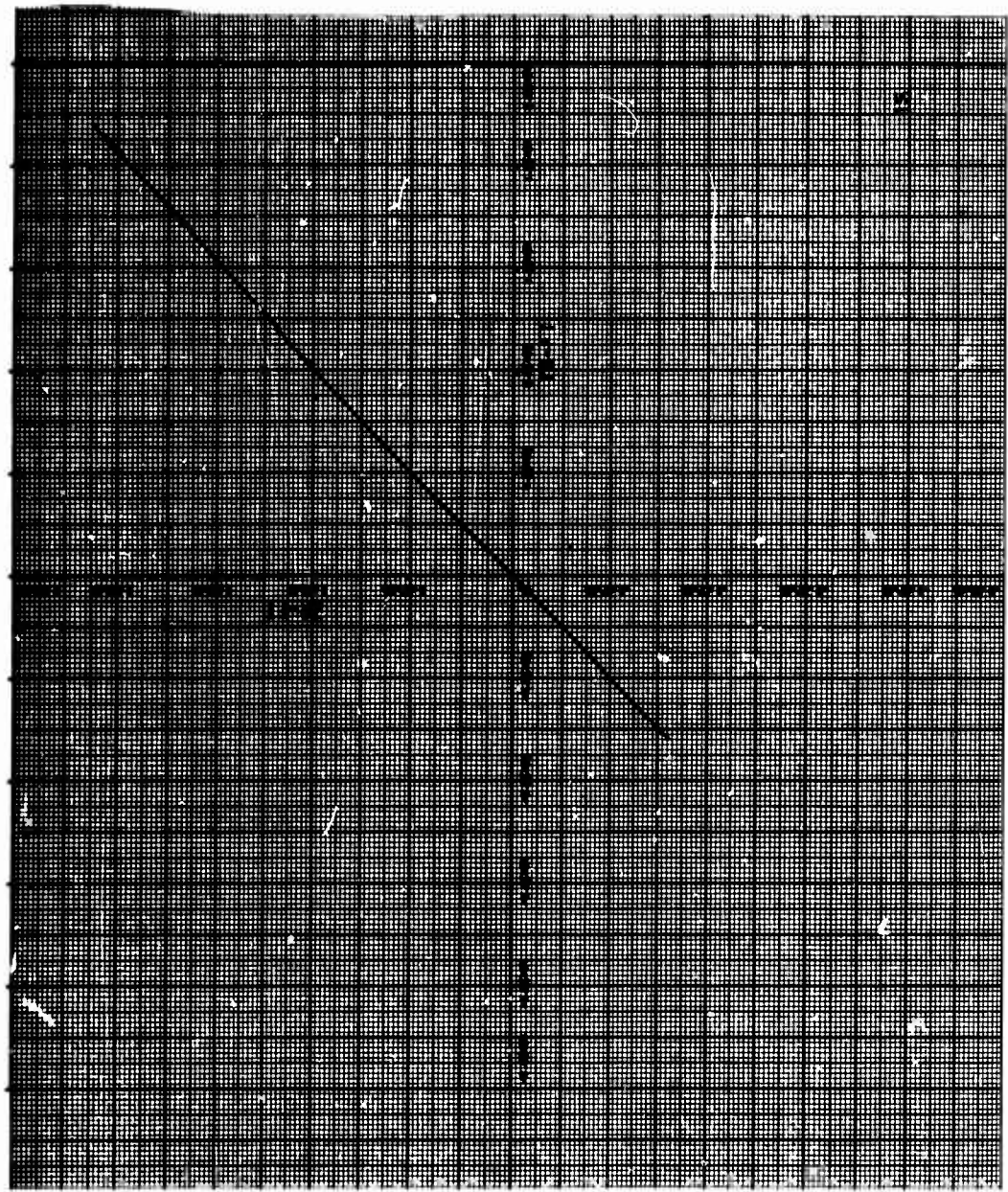


Figure 73. Graph for Miss Distance 1000 Feet

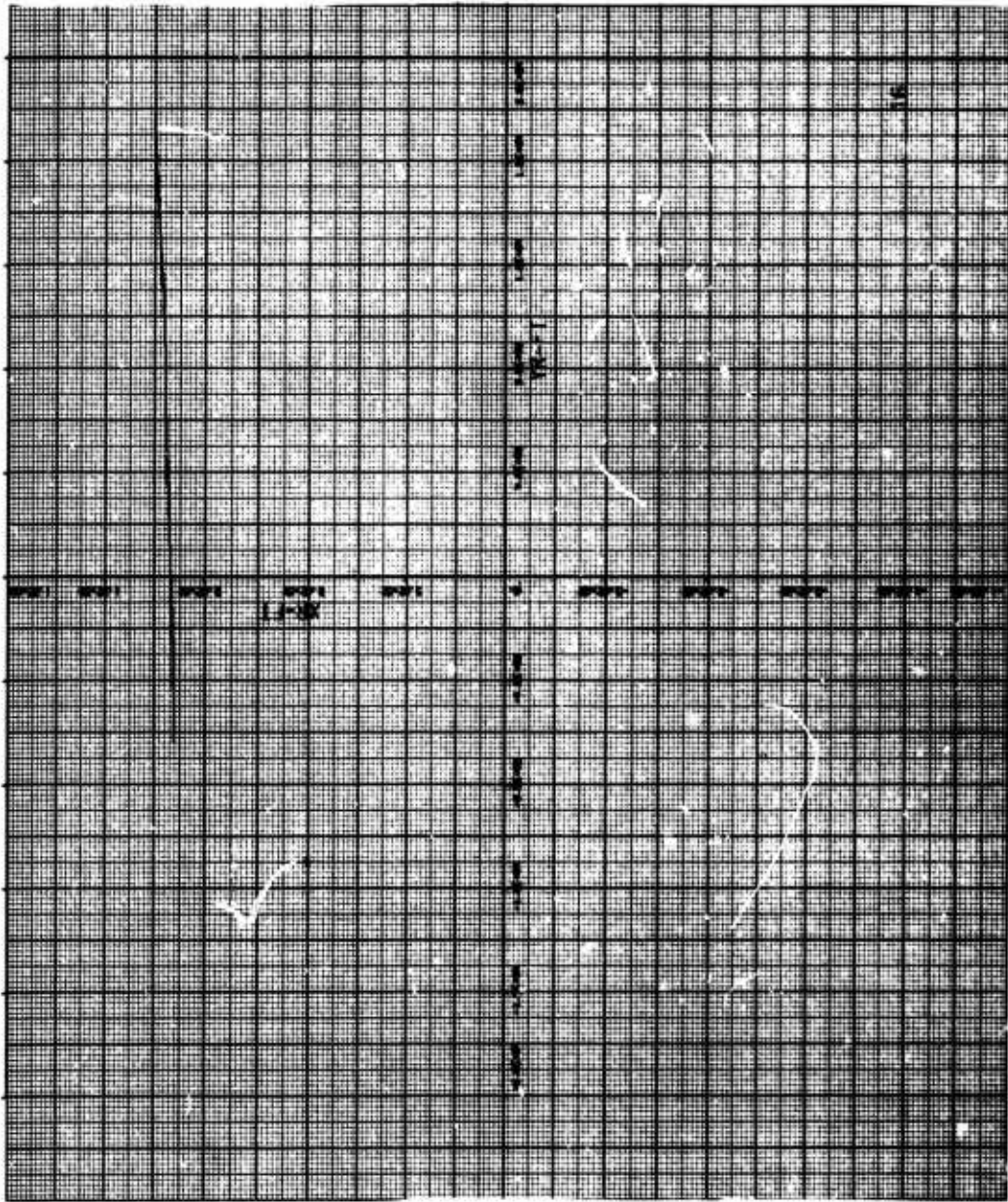


Figure 74. Graph for Miss Distance 1000 Feet

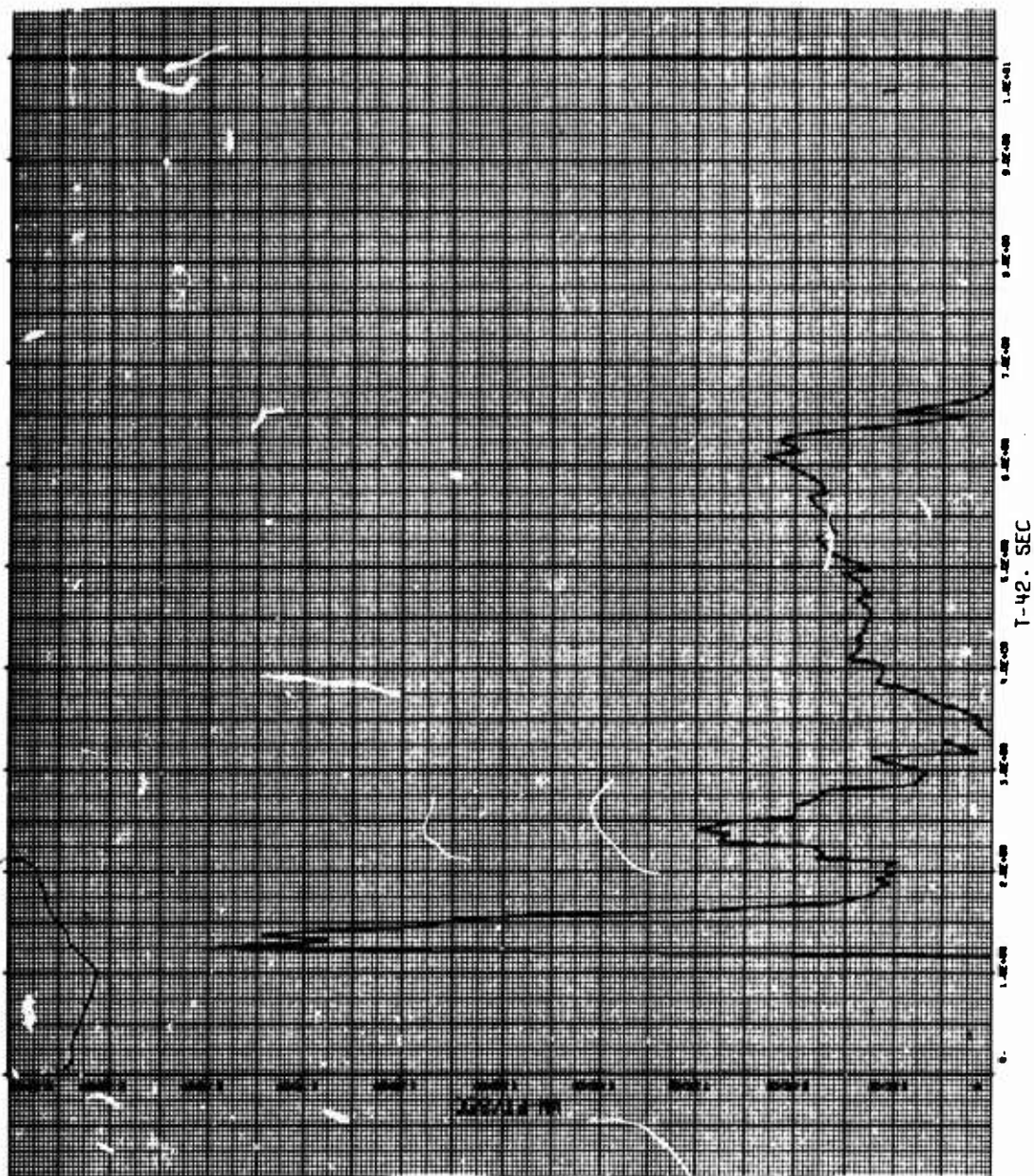


Figure 75. Graph for Miss Distance 2000 Feet

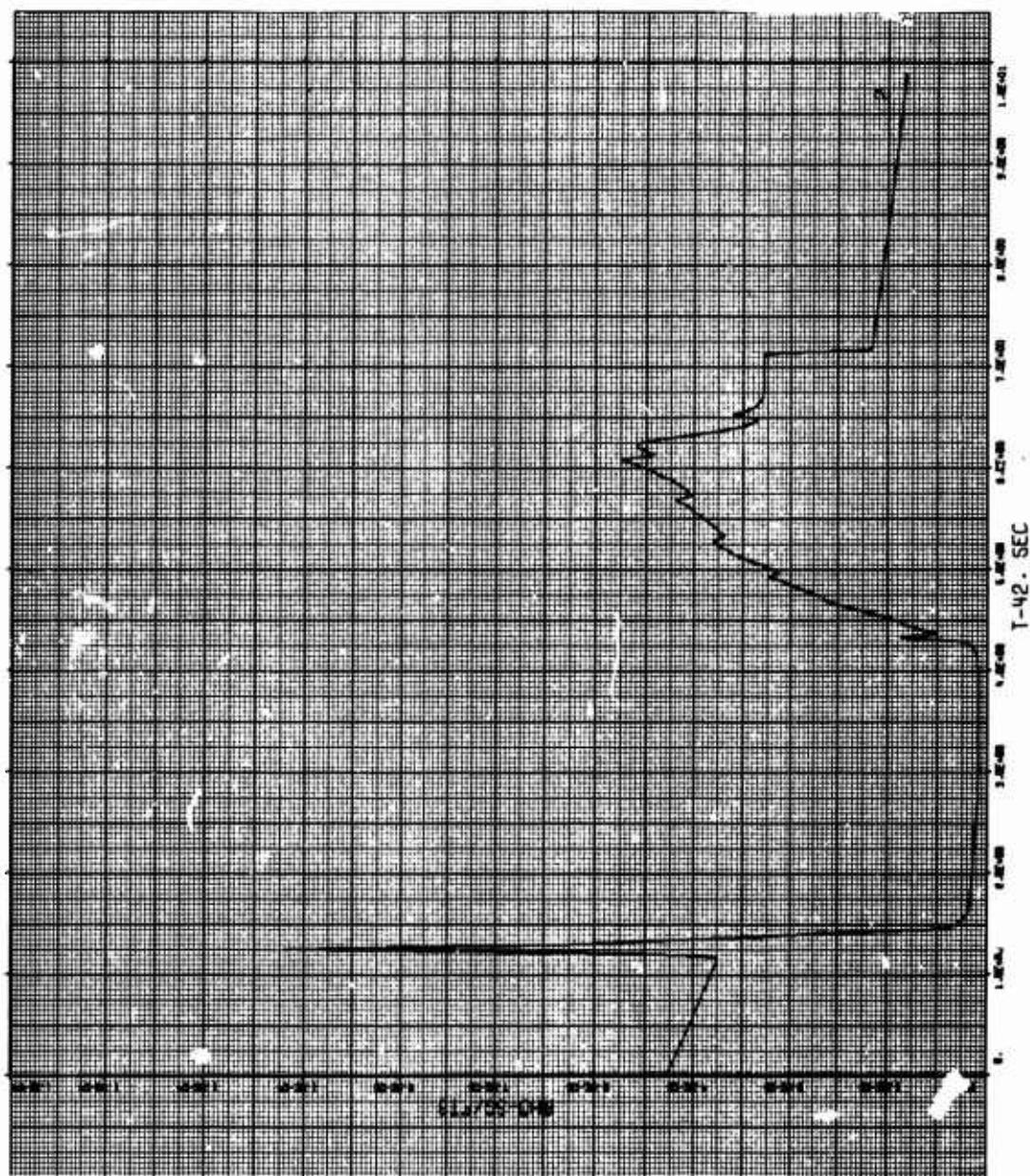


Figure 76. Graph for Miss Distance 2000 Feet

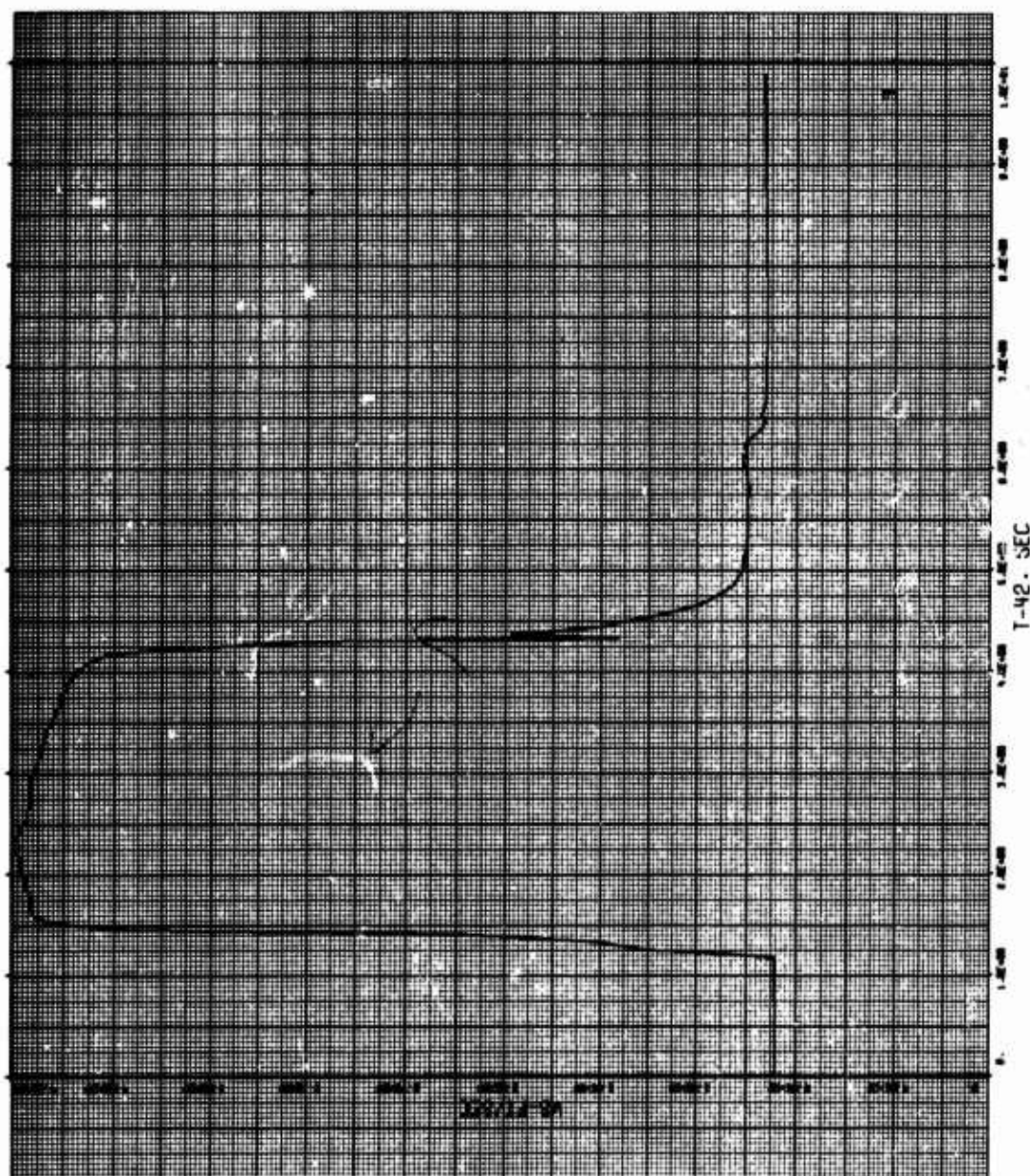


Figure 77. Graph for Miss Distance 2000 Feet

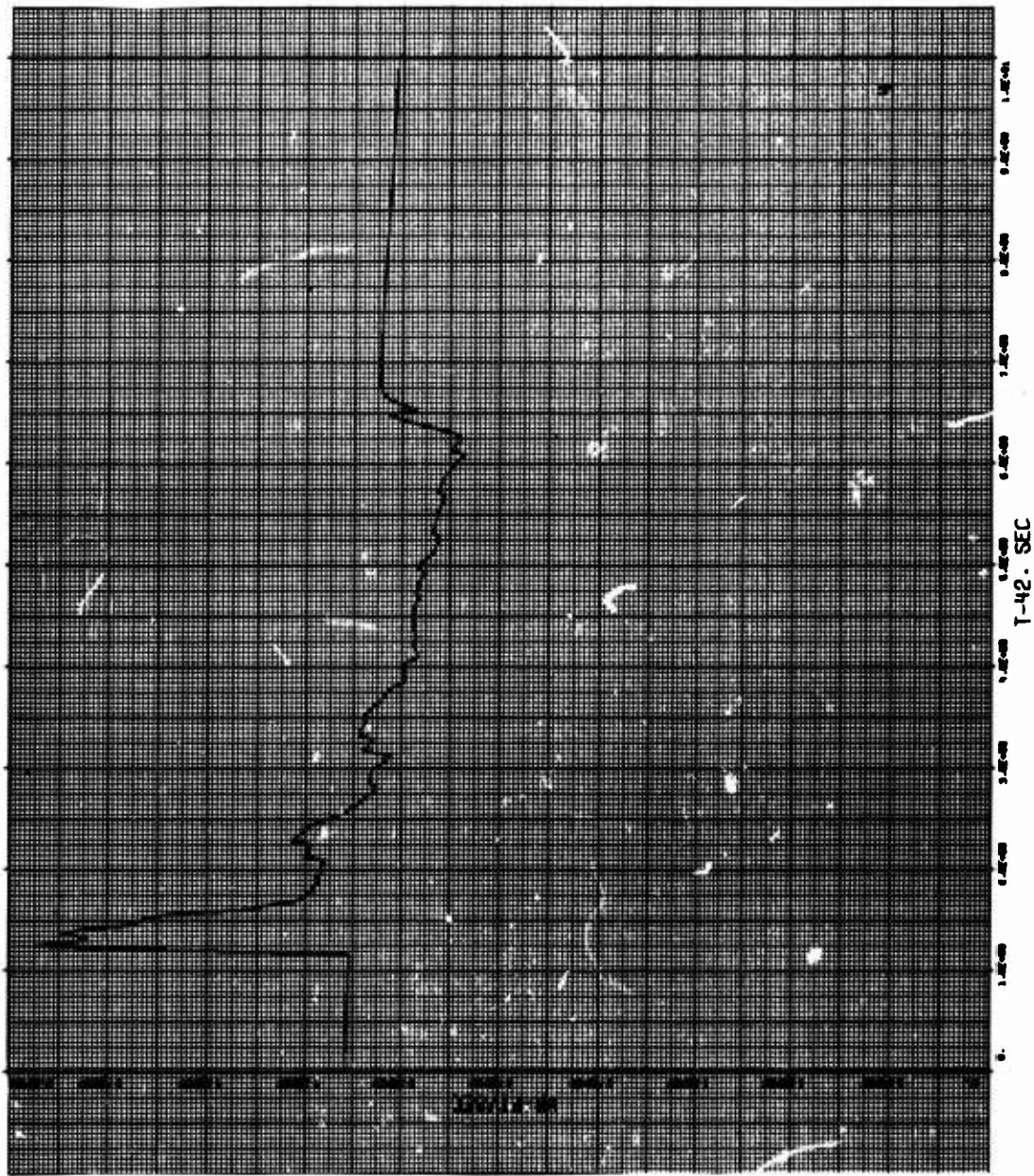


Figure 78. Graph for Miss Distance 2000 Feet

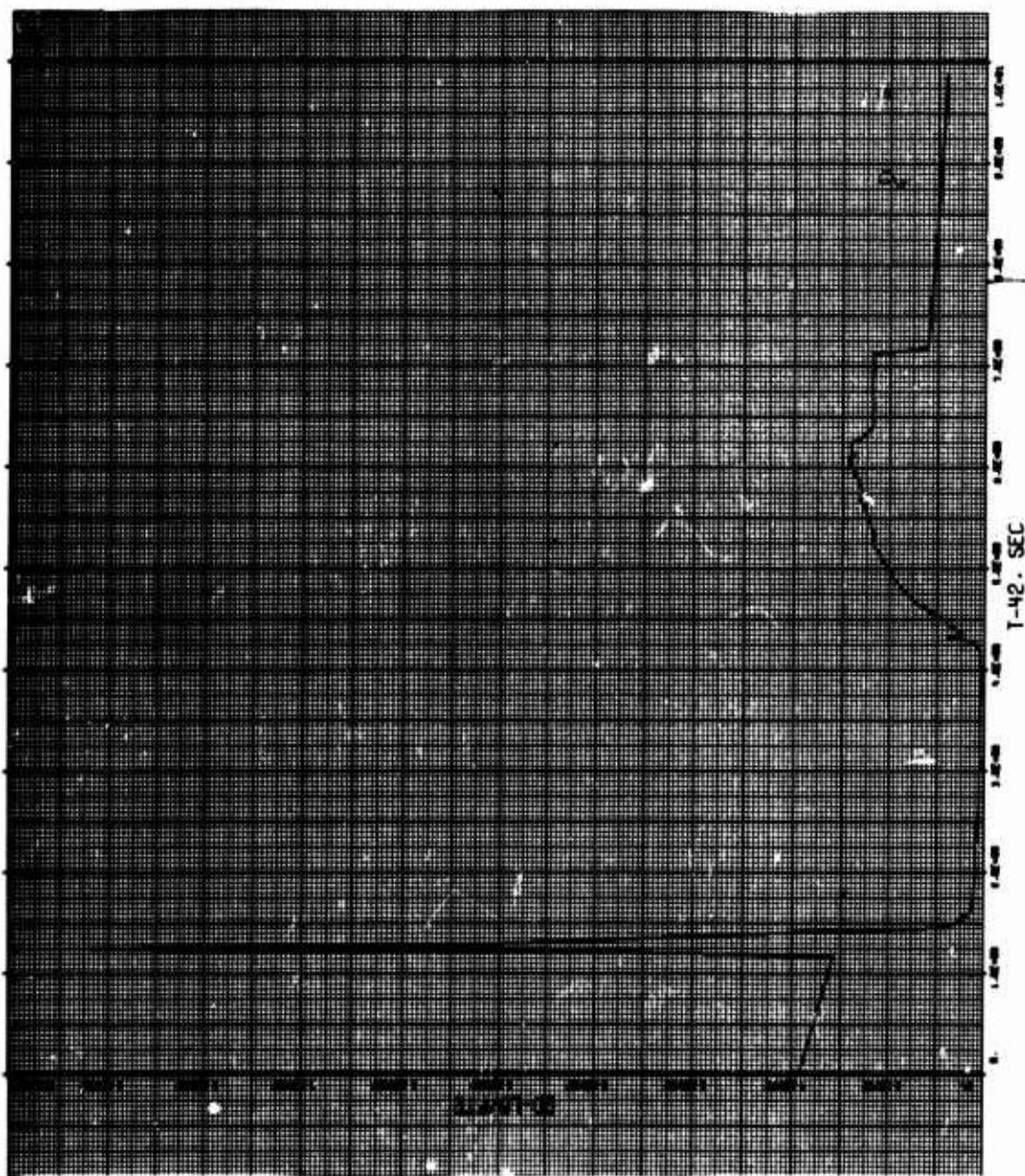


Figure 79. Graph for Miss Distance 2000 Feet

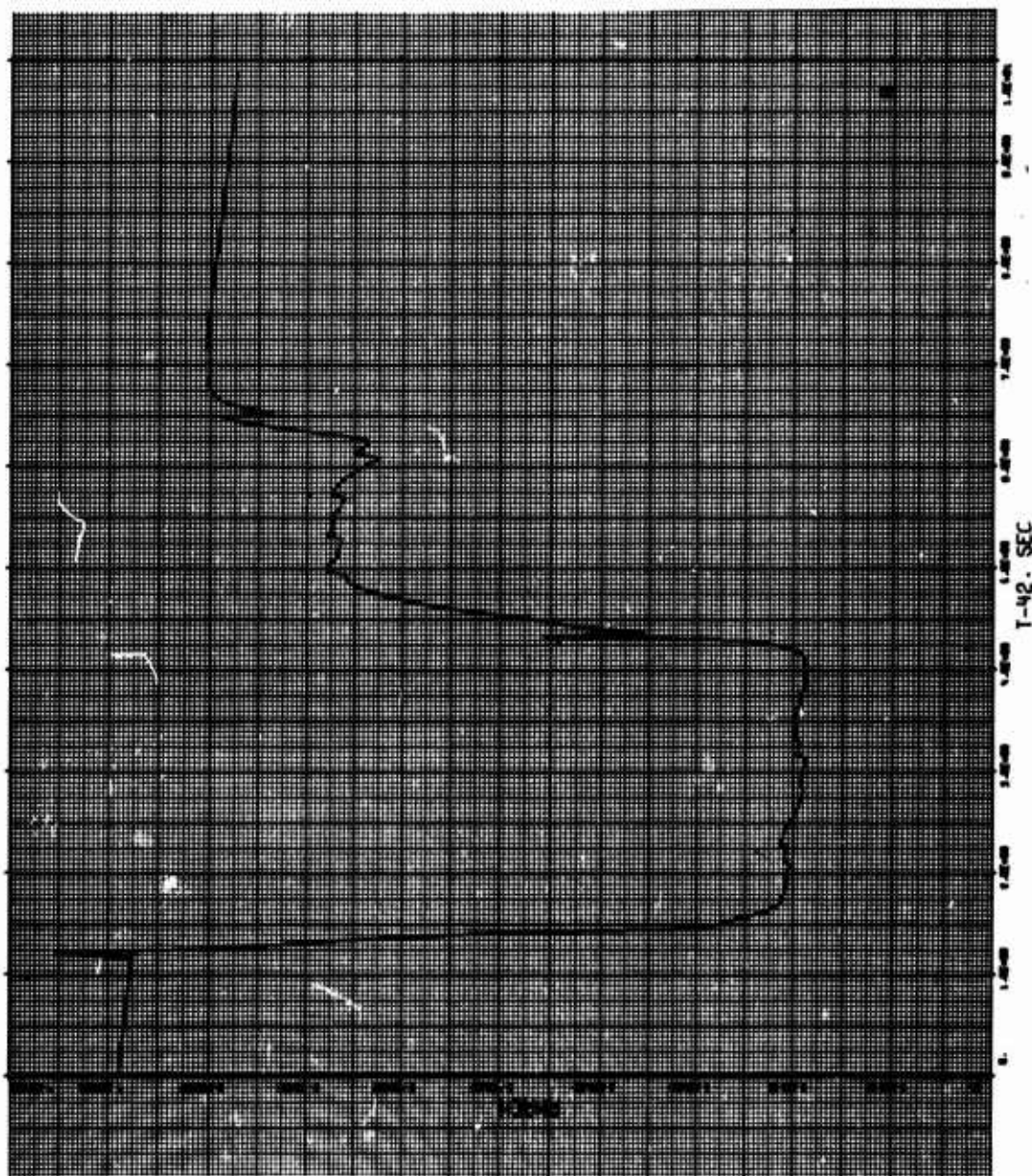


Figure 80. Graph for Miss Distance 2000 Feet

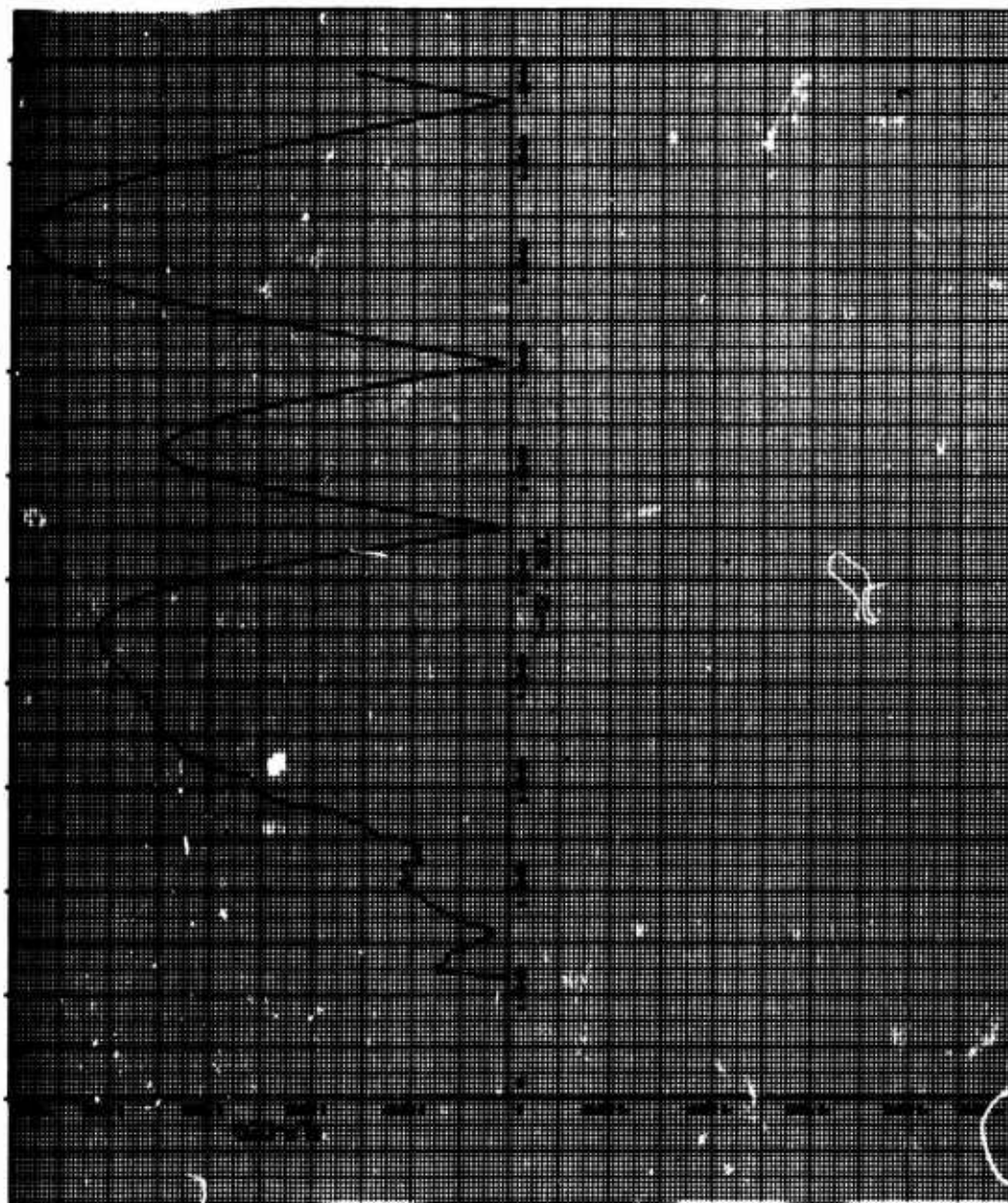


Figure 81. Graph for Miss Distance 2000 Feet

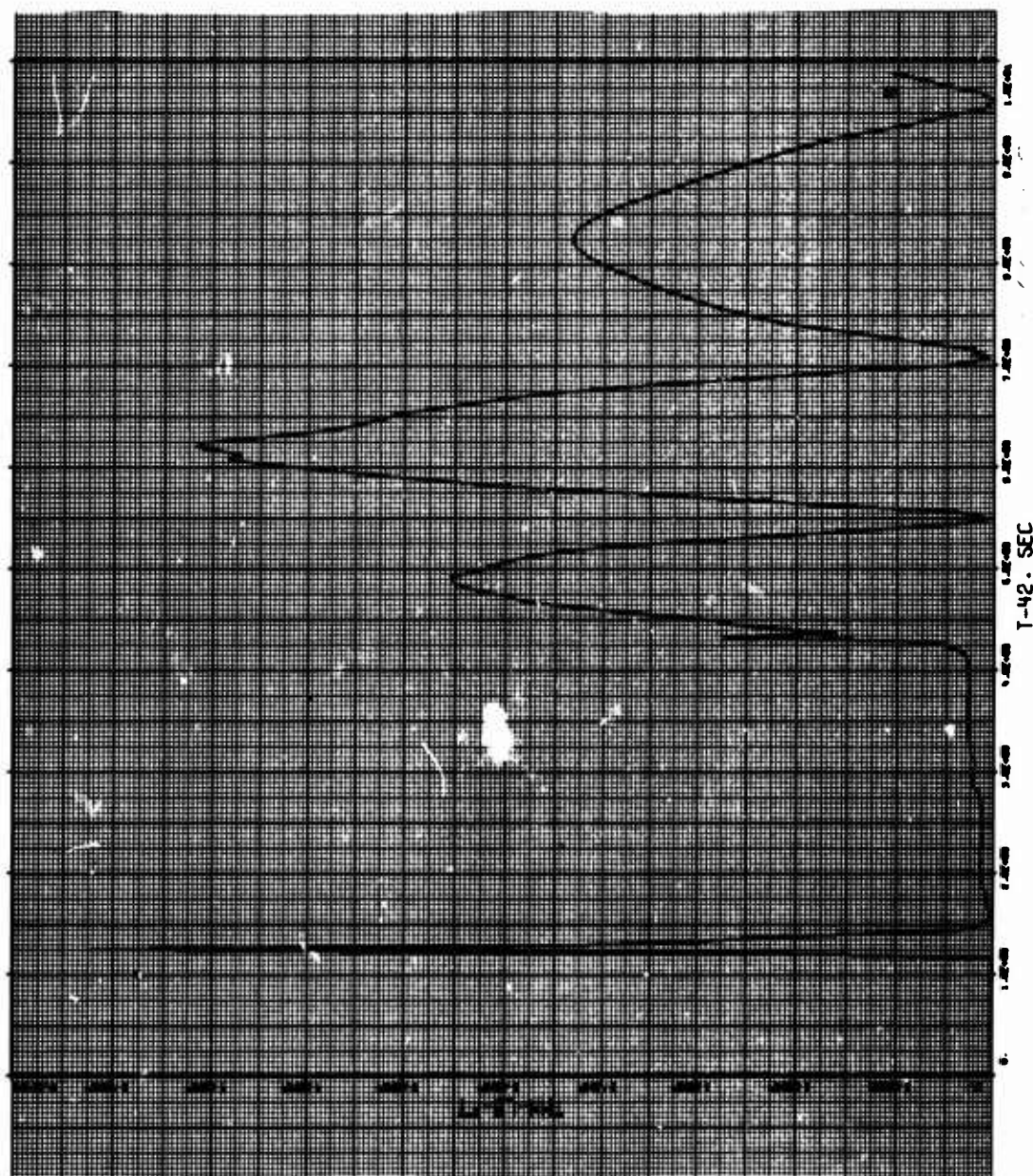


Figure 82. Graph for Miss Distance 2000 Feet

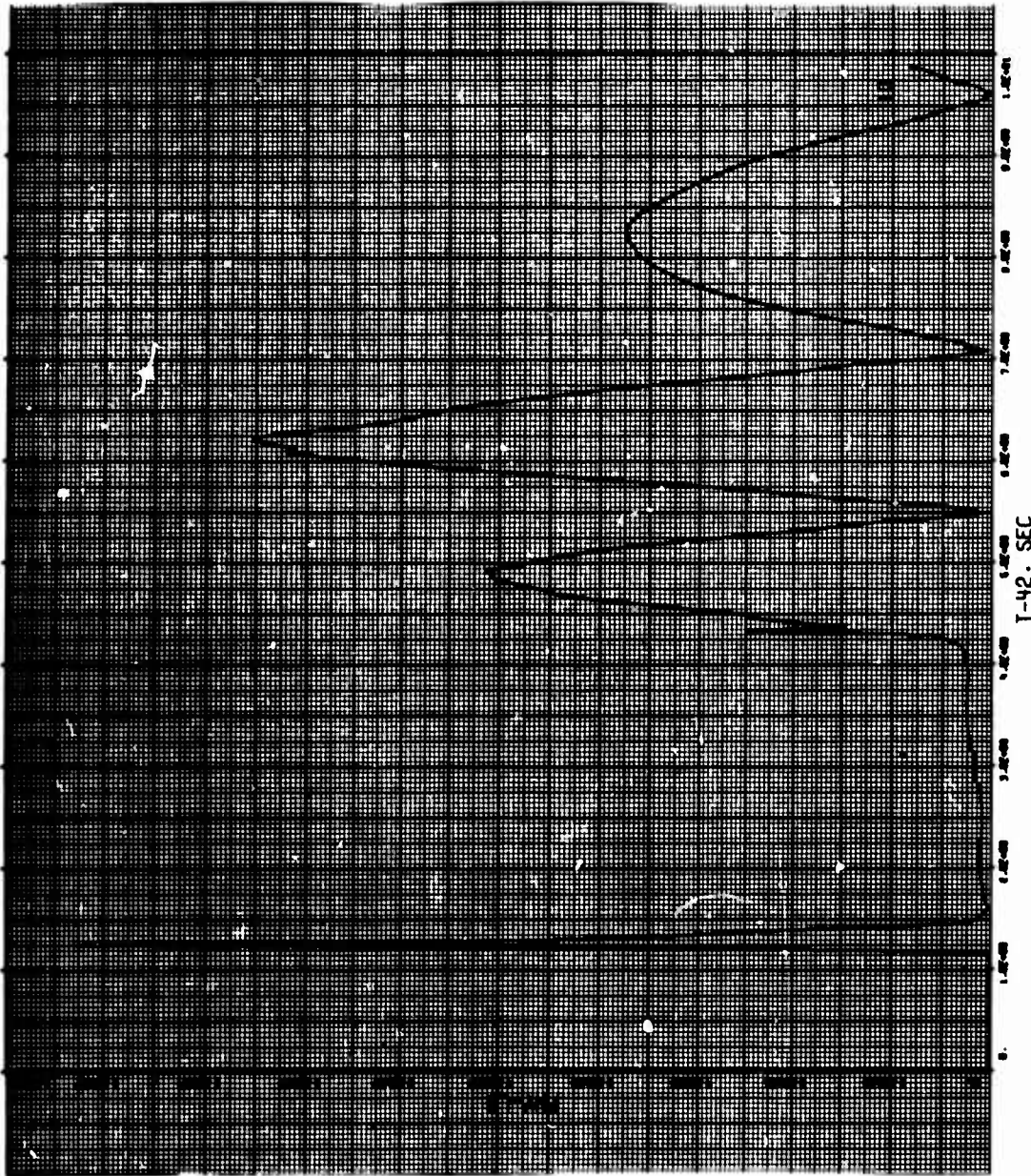


Figure 83. Graph for Miss Distance 2000 Feet

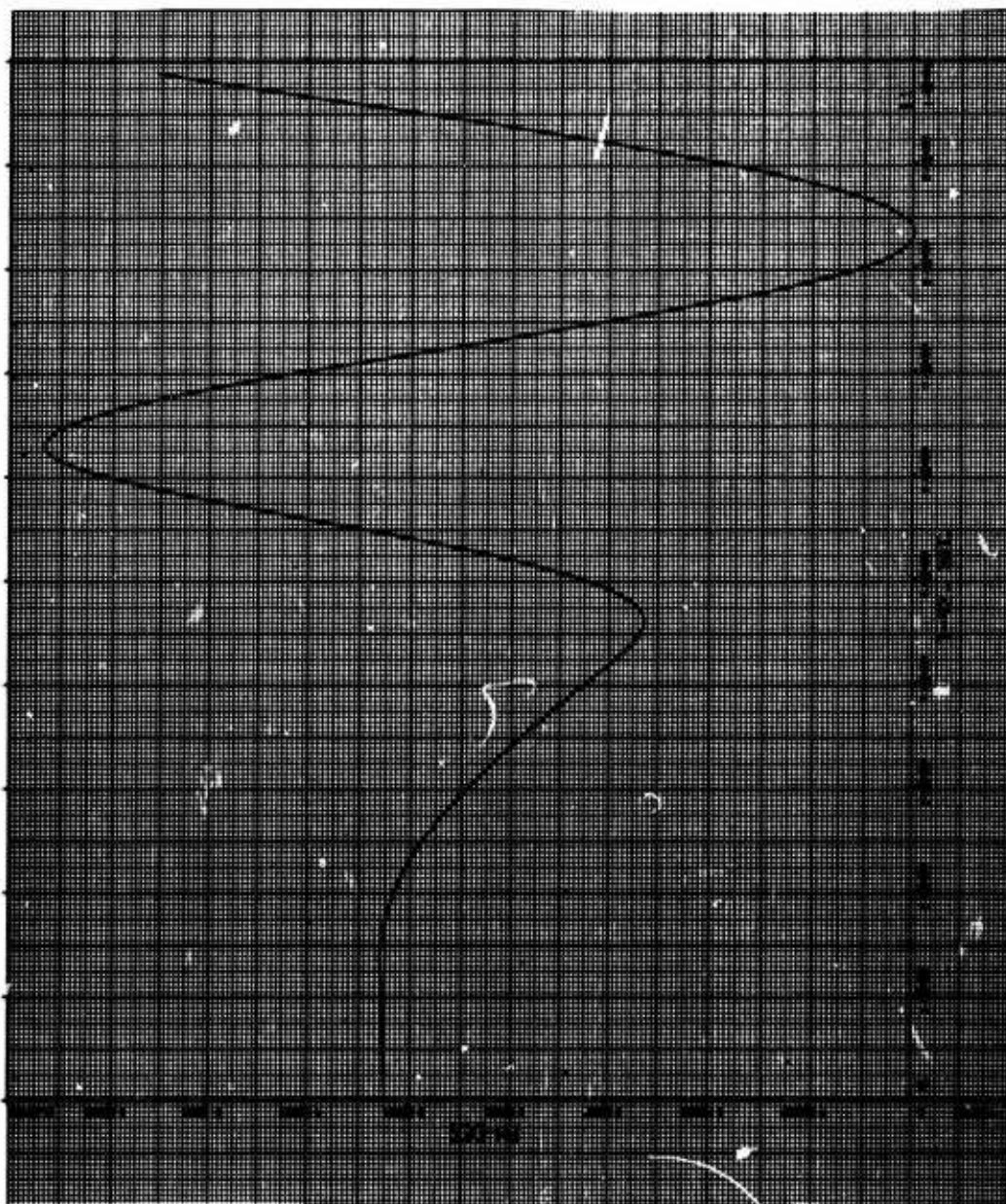


Figure 84. Graph for Miss Distance 2000 Feet

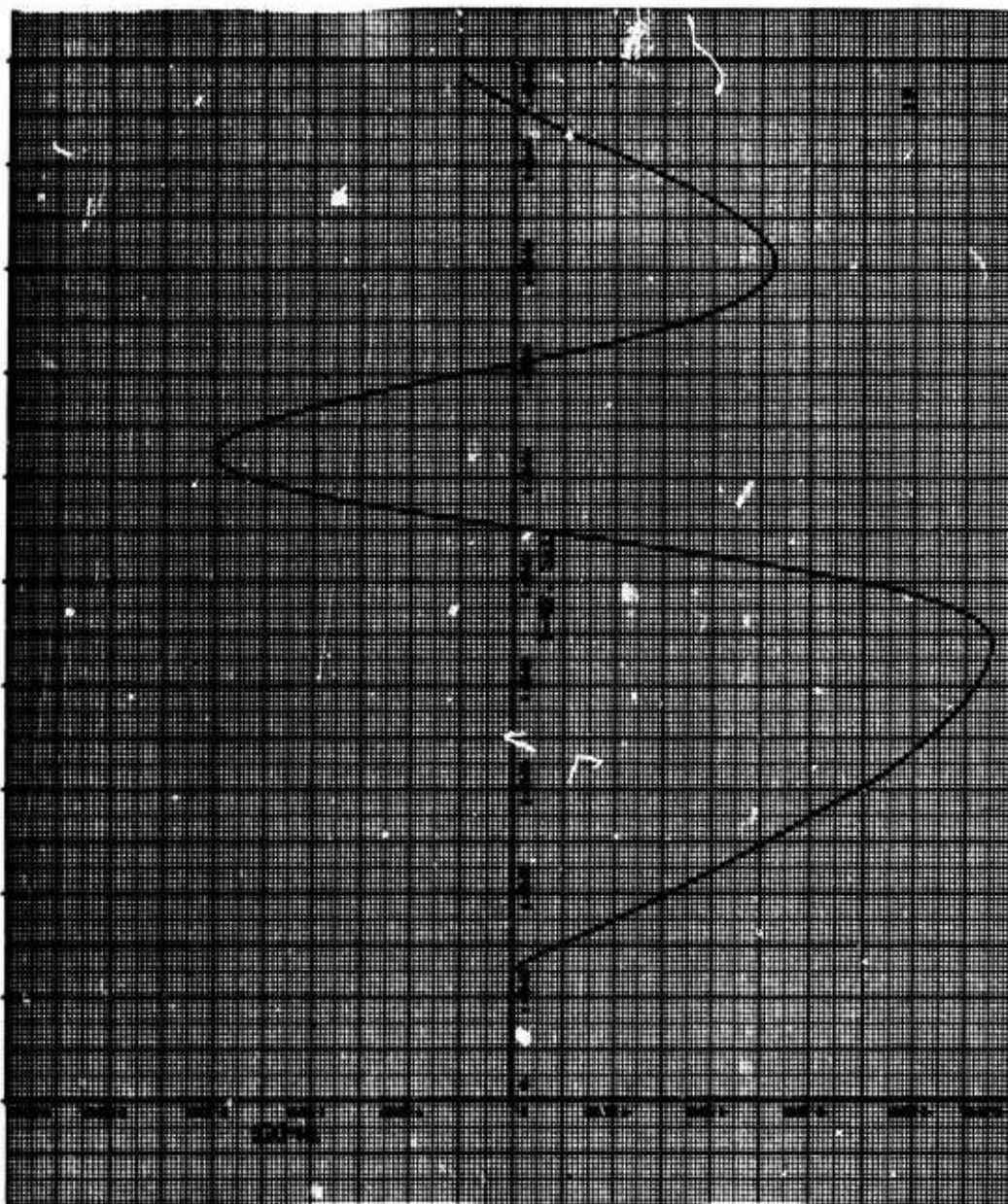


Figure 85. Graph for Miss Distance 2000 Feet

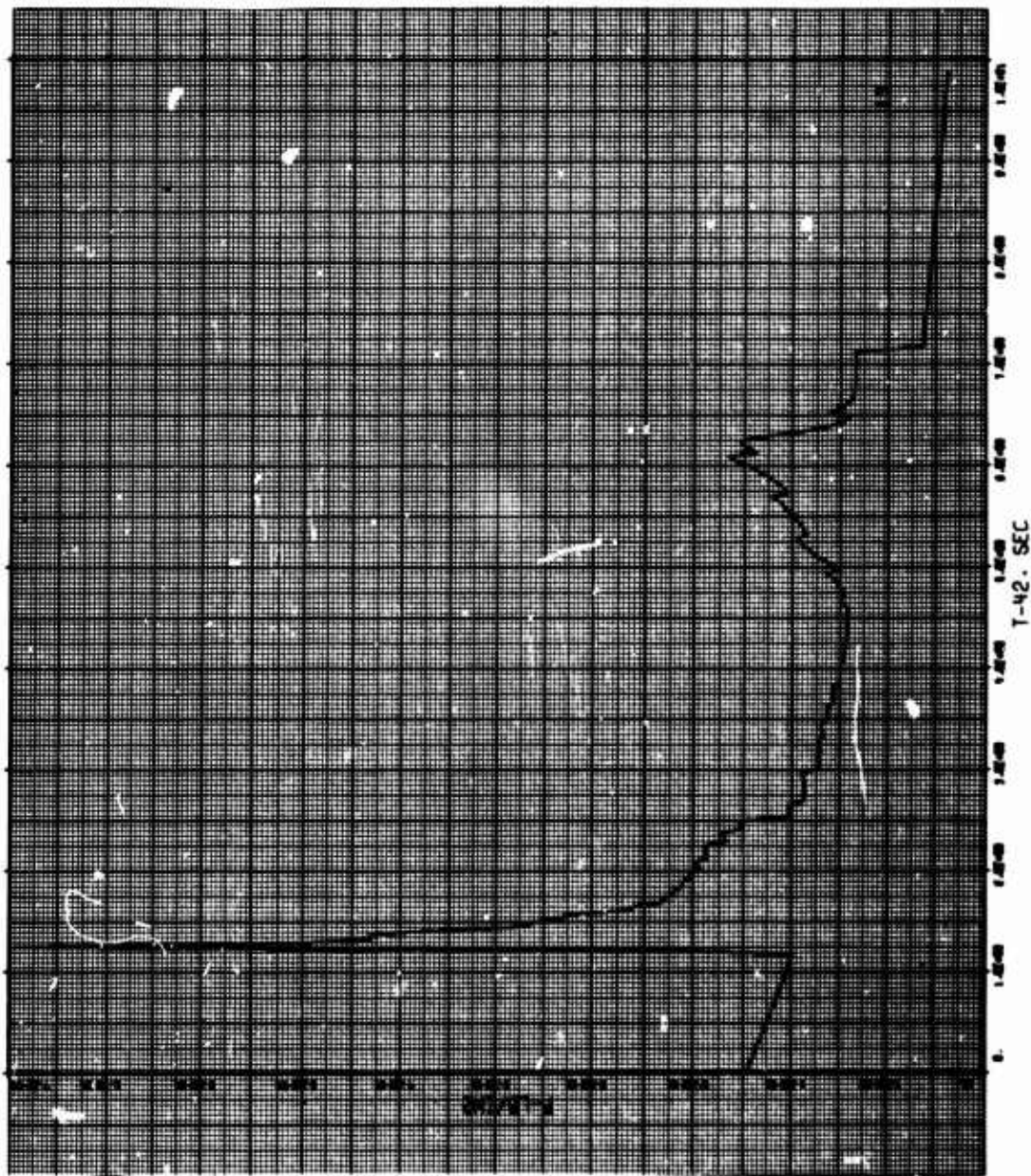


Figure 86. Graph for Miss Distance 2000 Feet

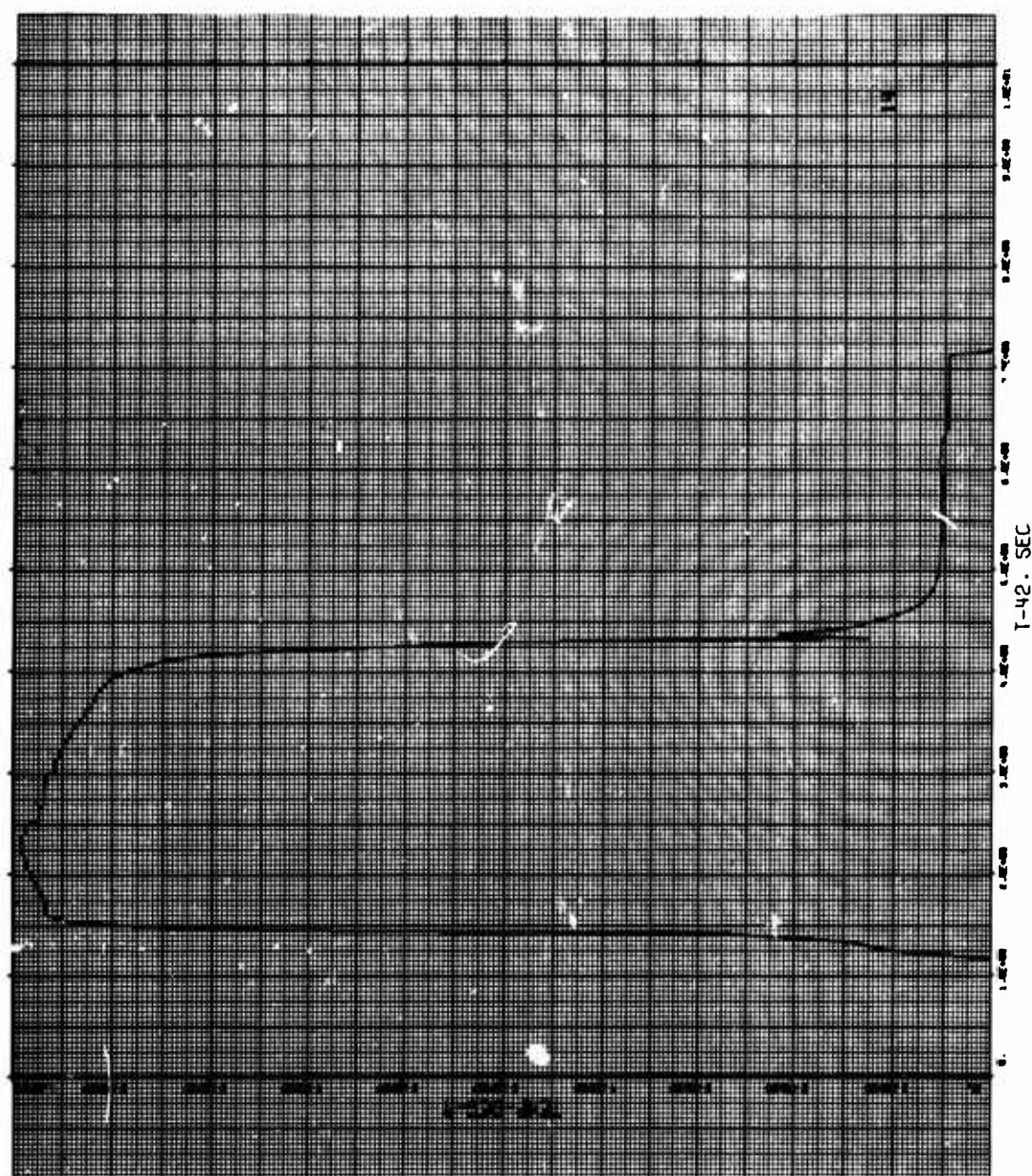


Figure 87. Graph for Miss Distance 2000 Feet

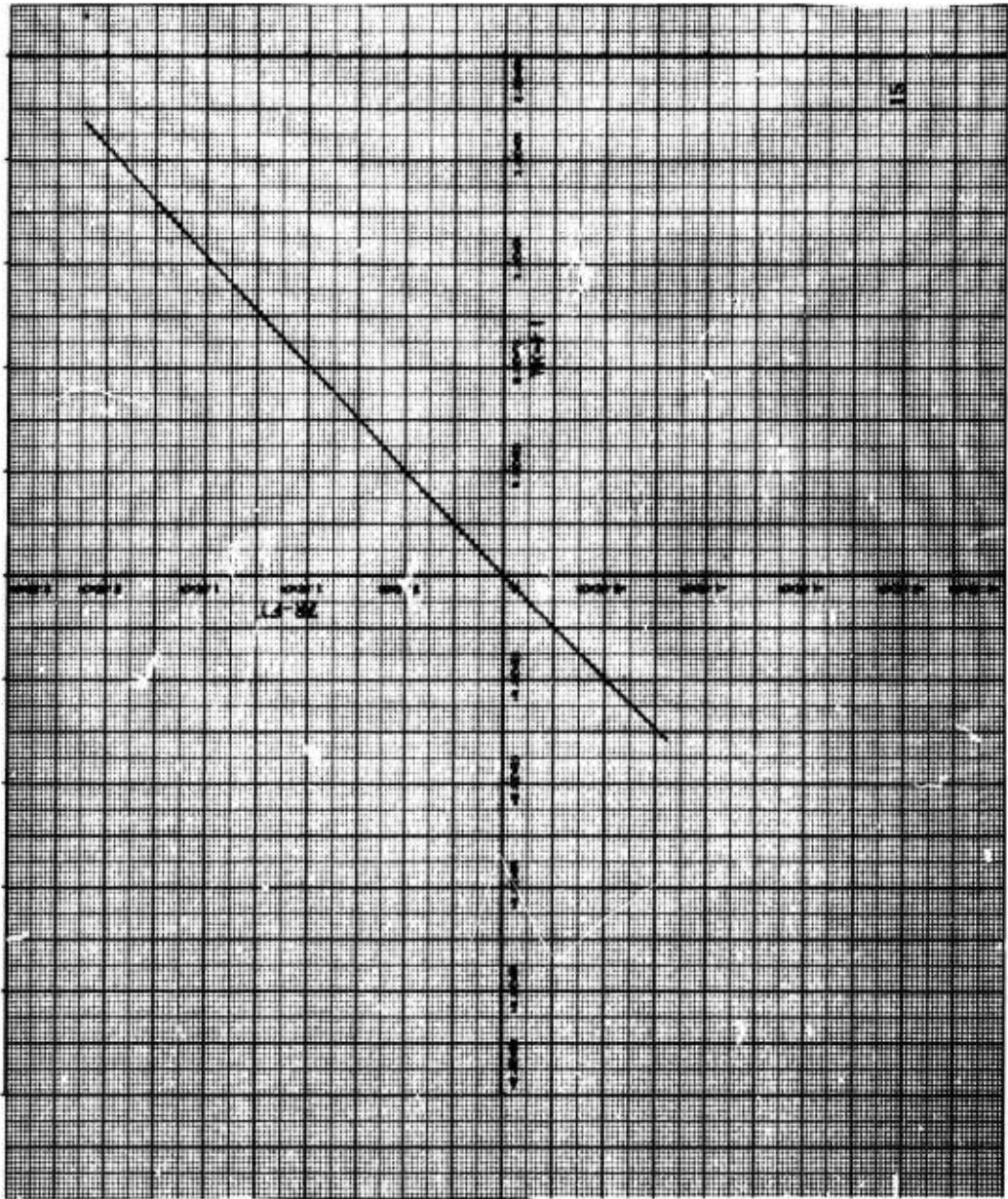


Figure 88. Graph for Miss Distance 2000 Feet

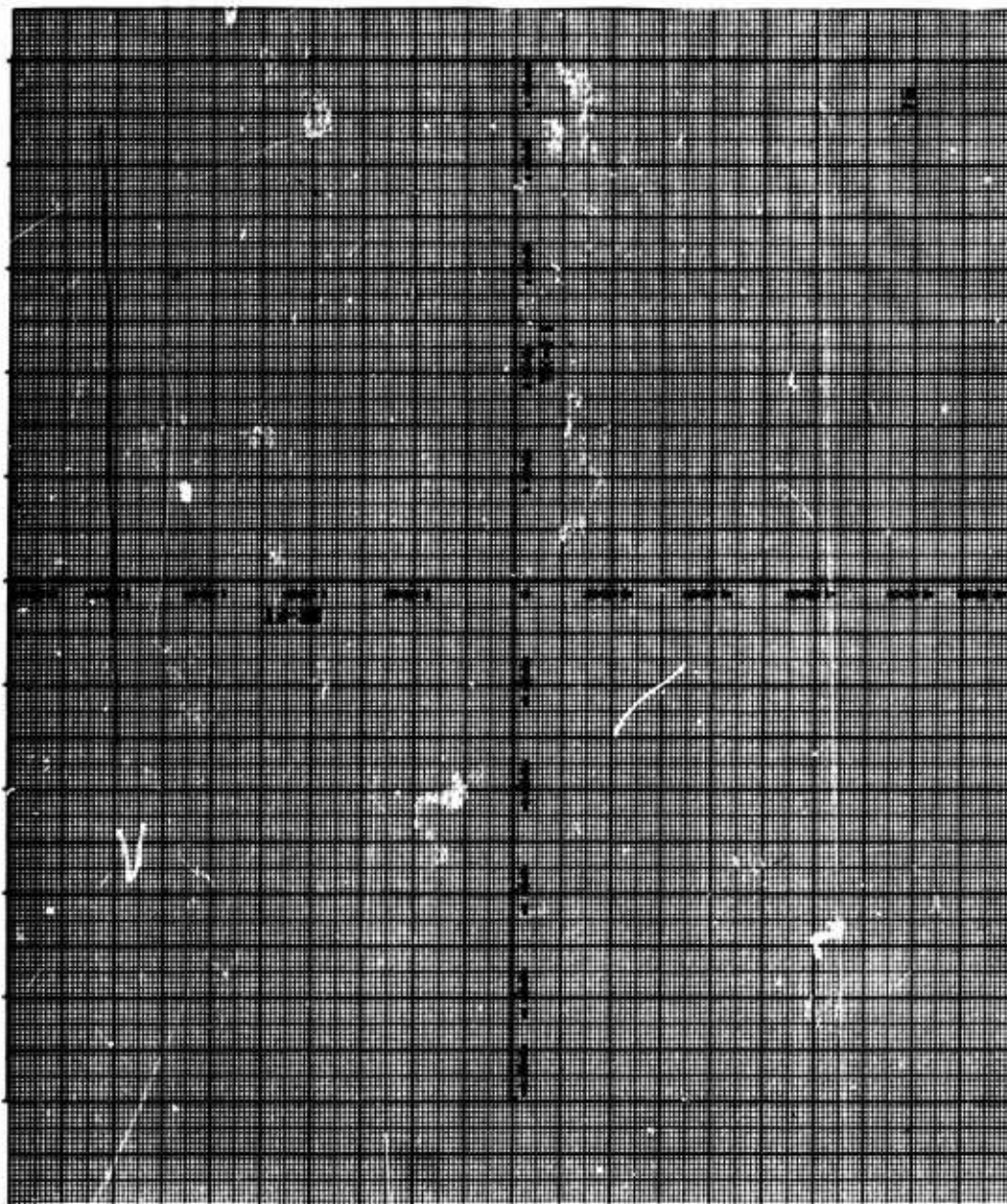


Figure 89. Graph for Miss Distance 2000 Feet

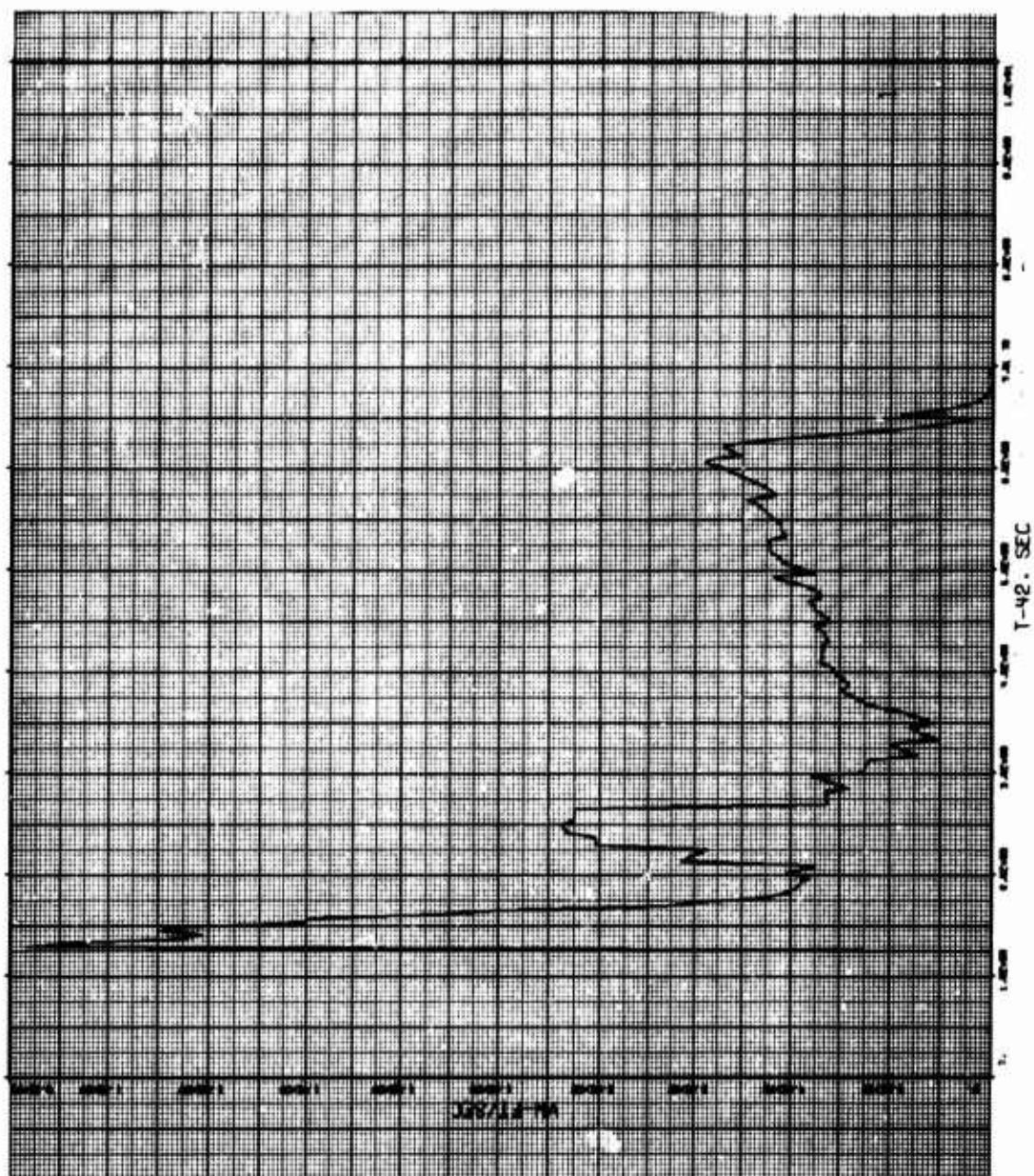


Figure 90. Graph for Miss Distance 3000 Feet

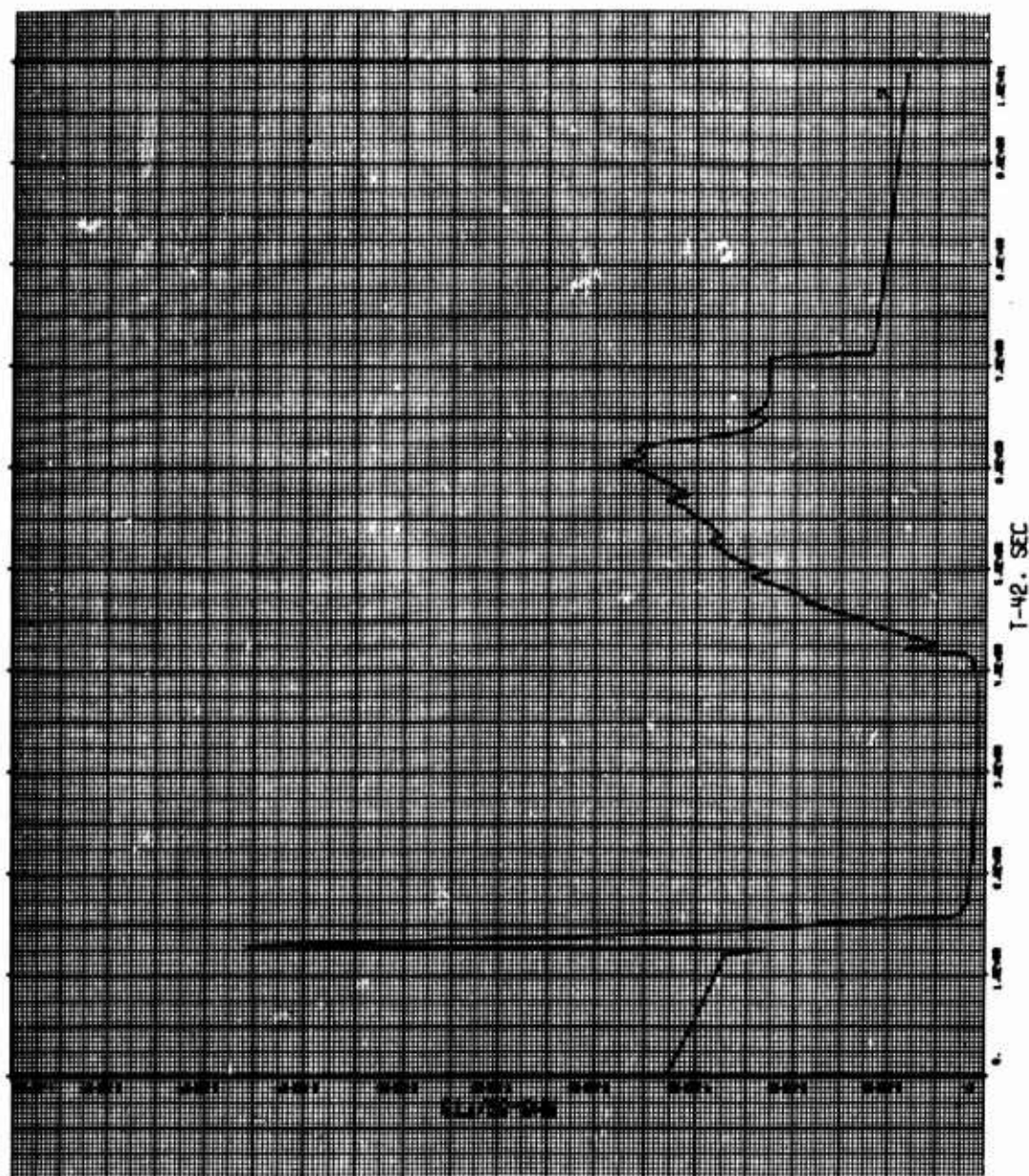


Figure 91. Graph for Miss Distance 3000 Feet

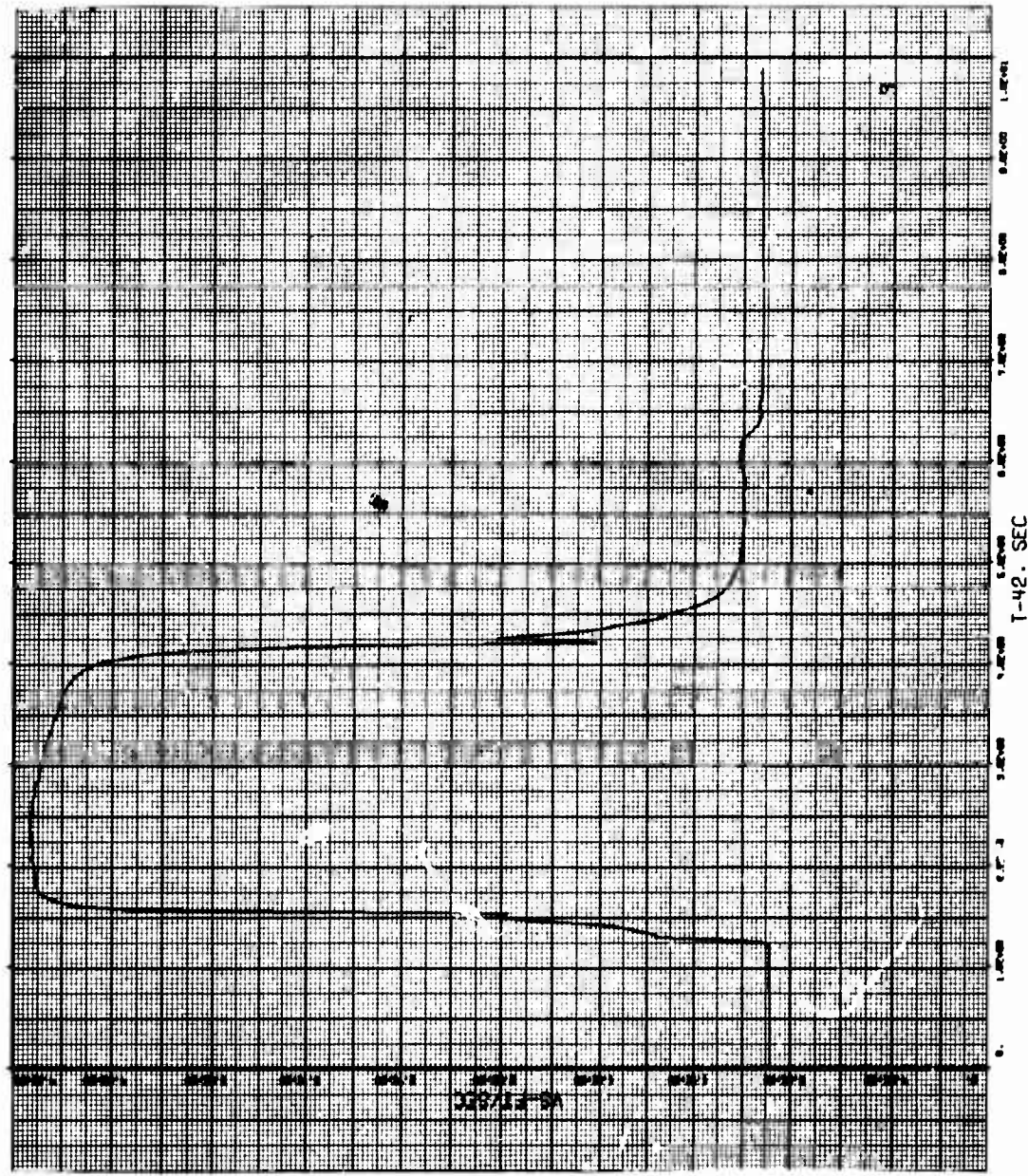


Figure 92. Graph for Miss Distance 3000 Feet

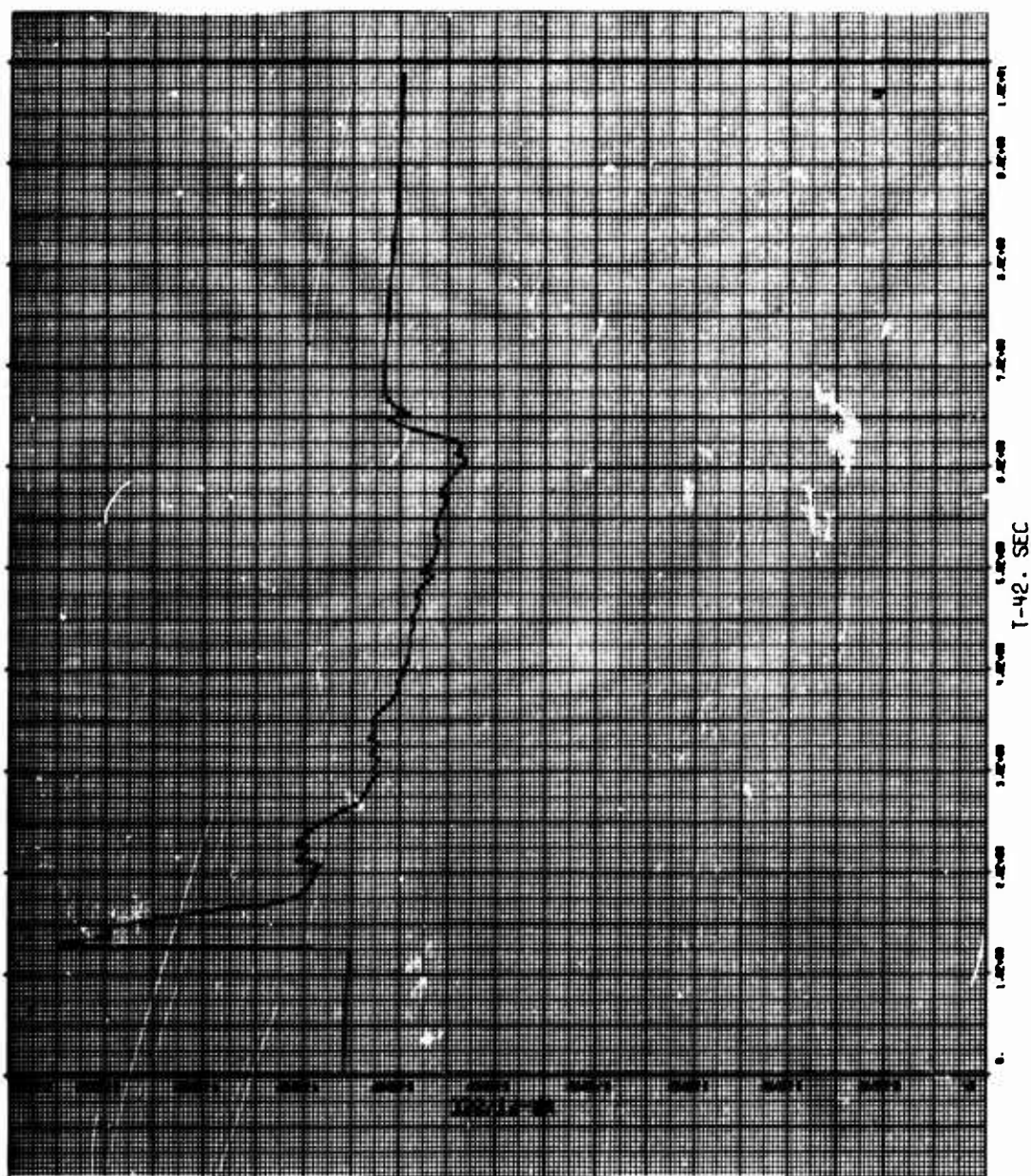


Figure 93. Graph for Miss Distance 3000 Feet

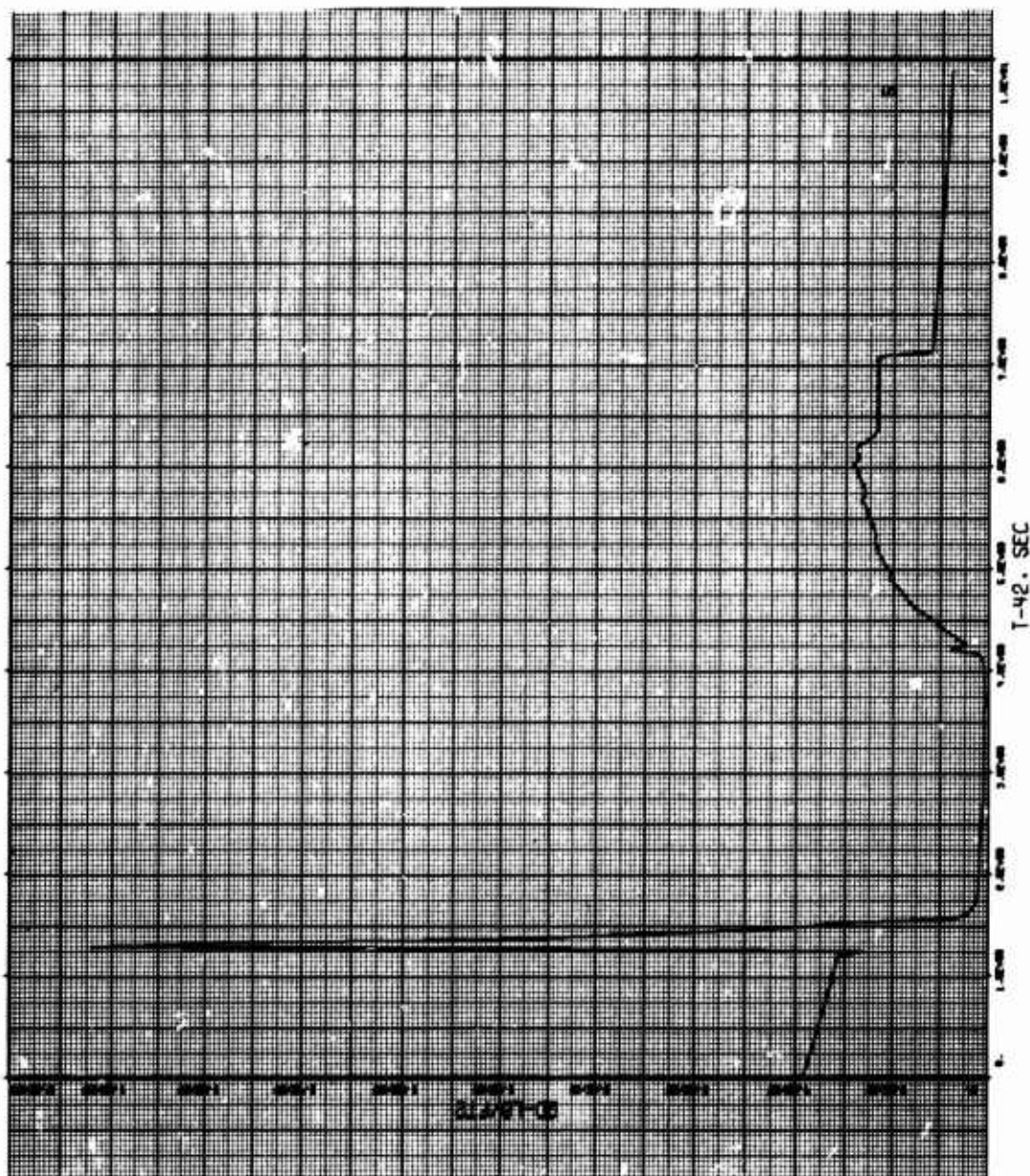


Figure 94. Graph for Miss Distance 3000 Feet

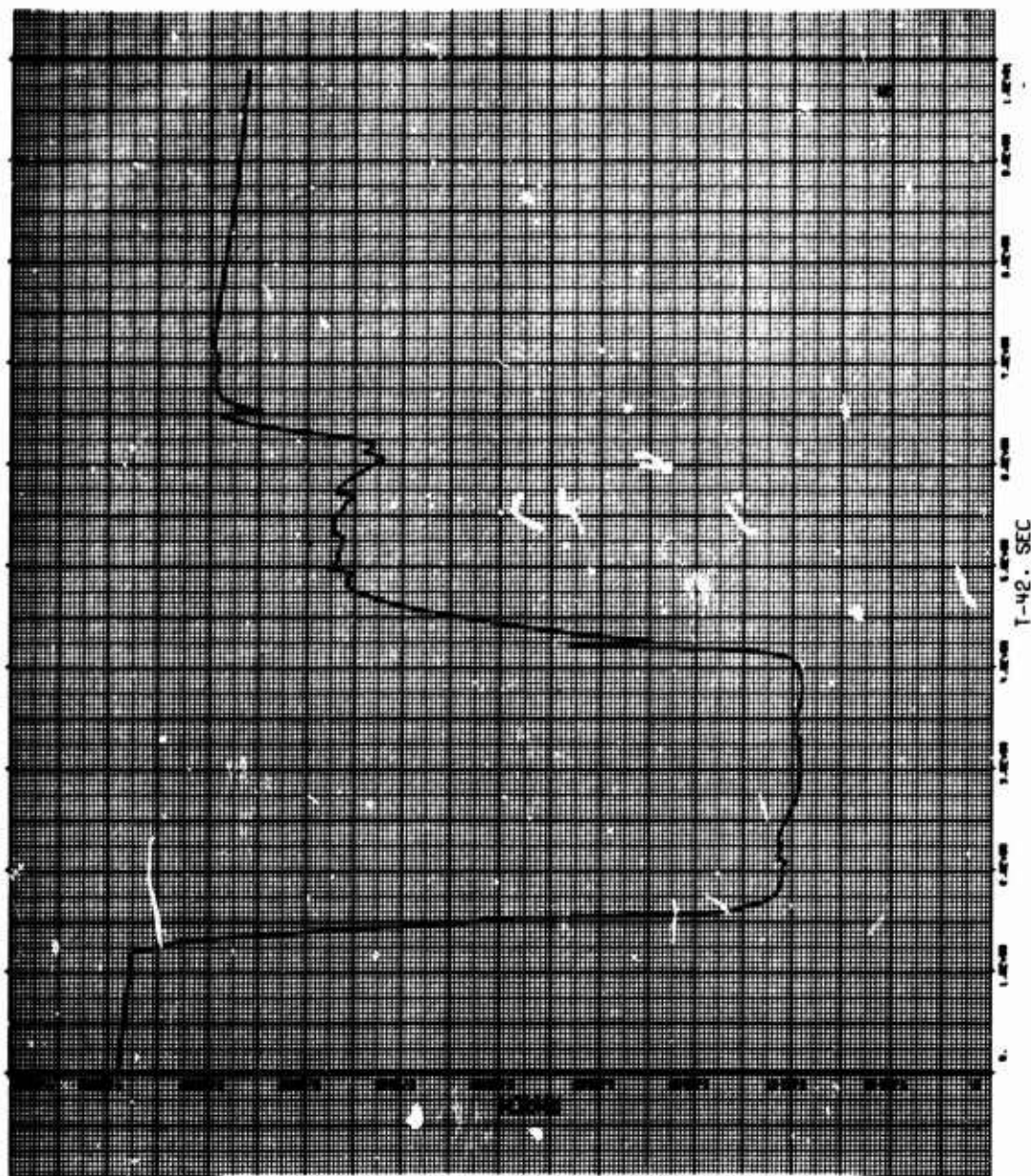


Figure 95. Graph for Miss Distance 3000 Feet

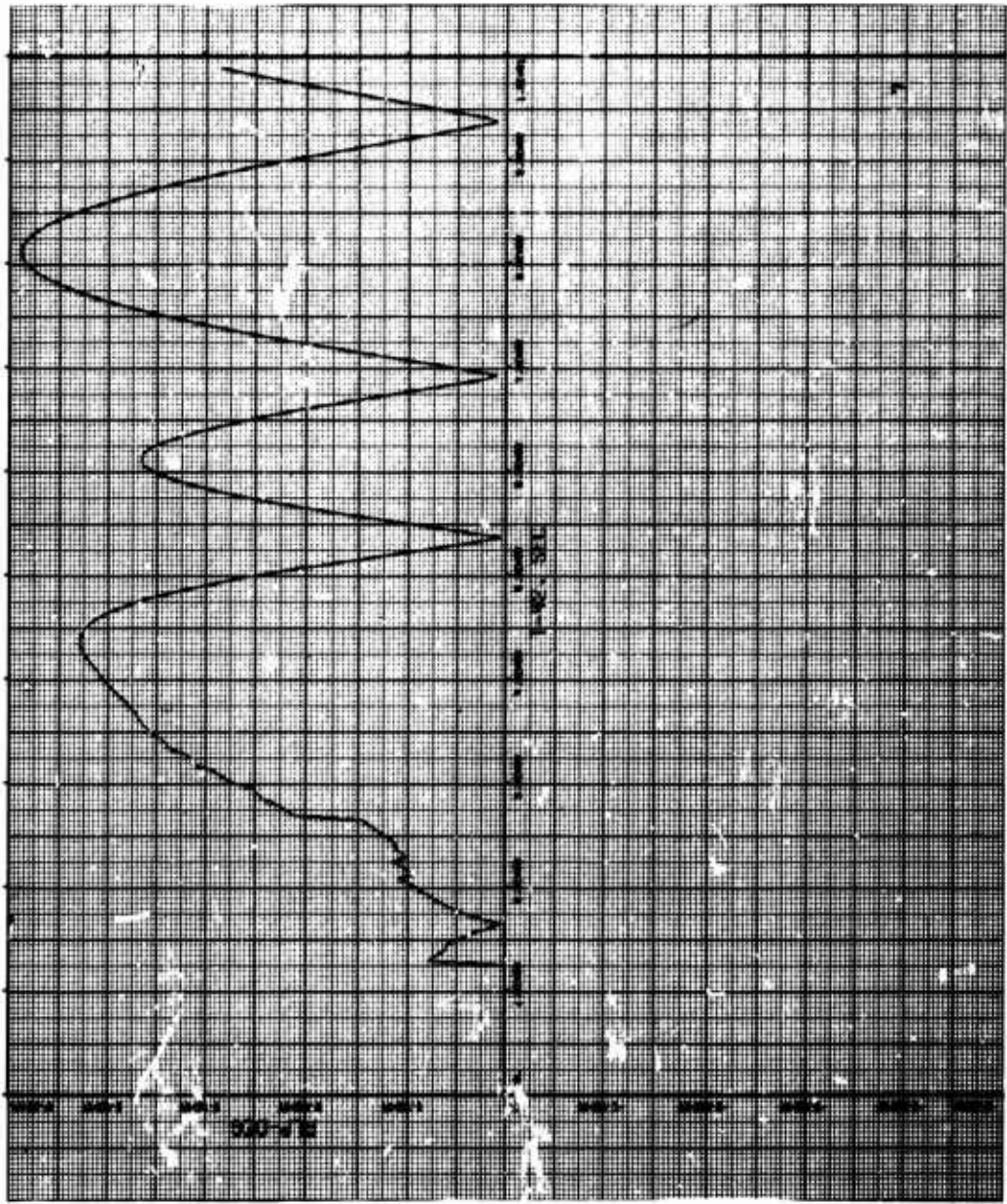


Figure 96. Graph for Miss Distance 3000 Feet

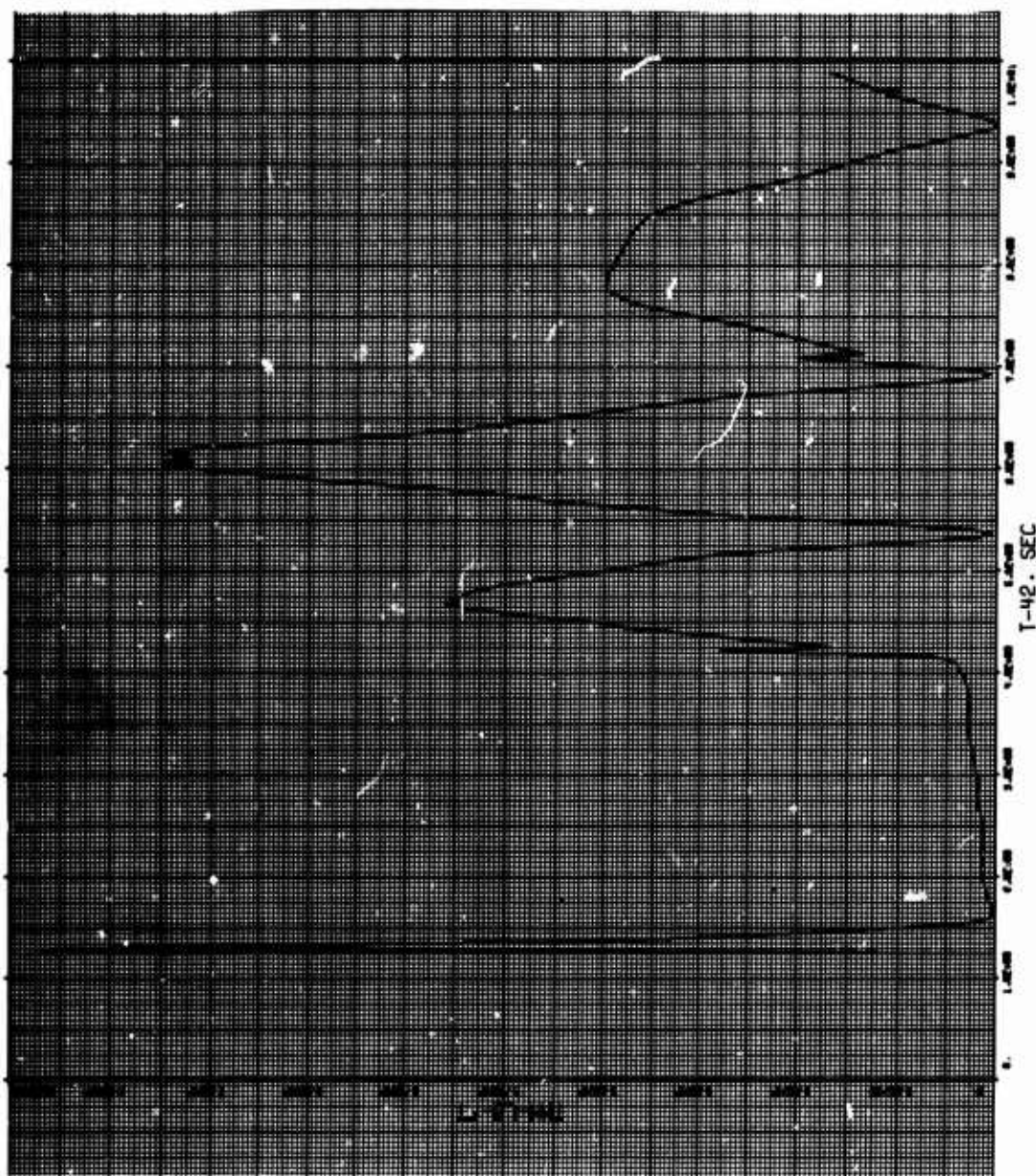


Figure 97. Graph for Miss Distance 3000 Feet

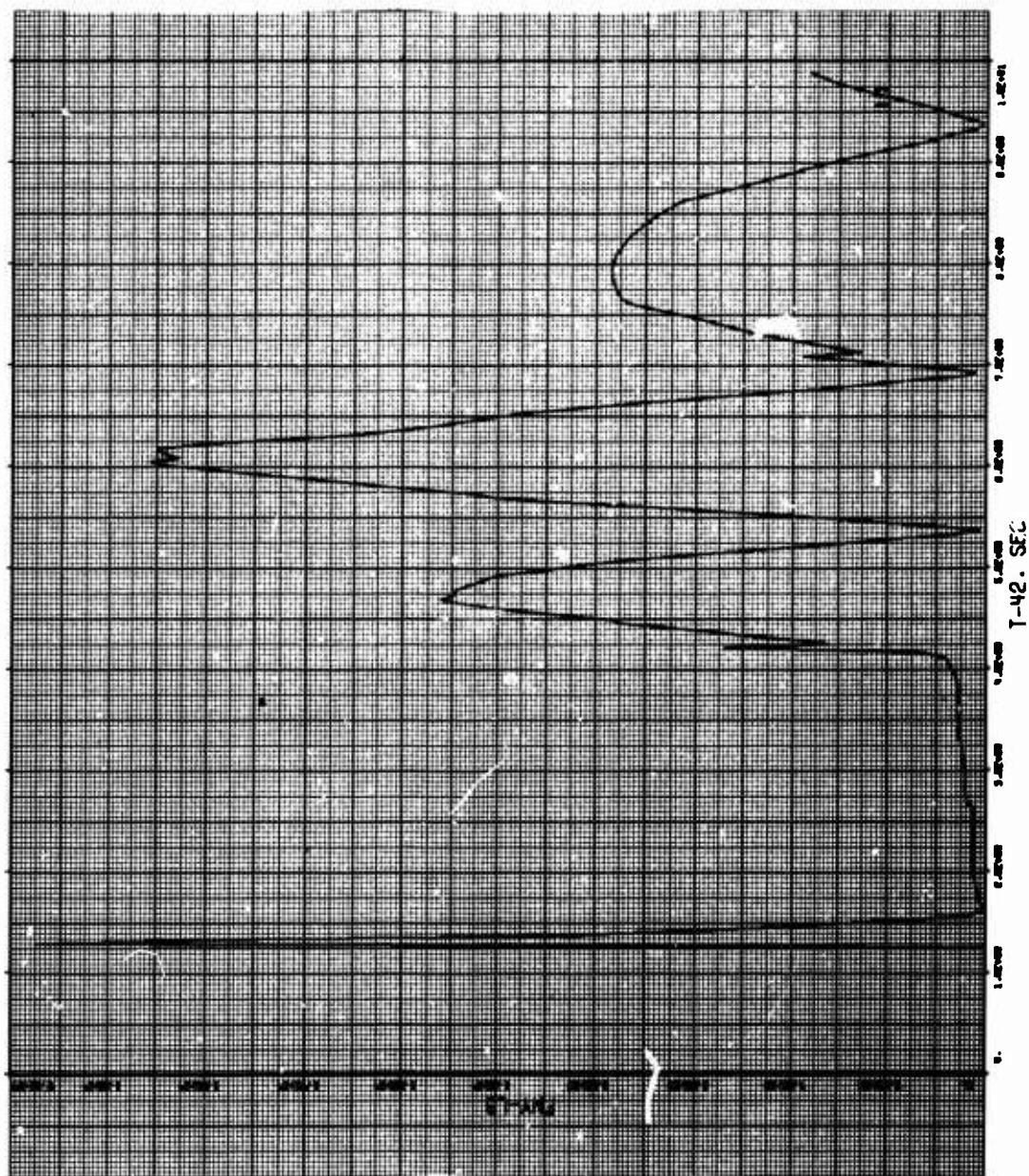


Figure 98. Graph for Miss Distance 3000 Feet

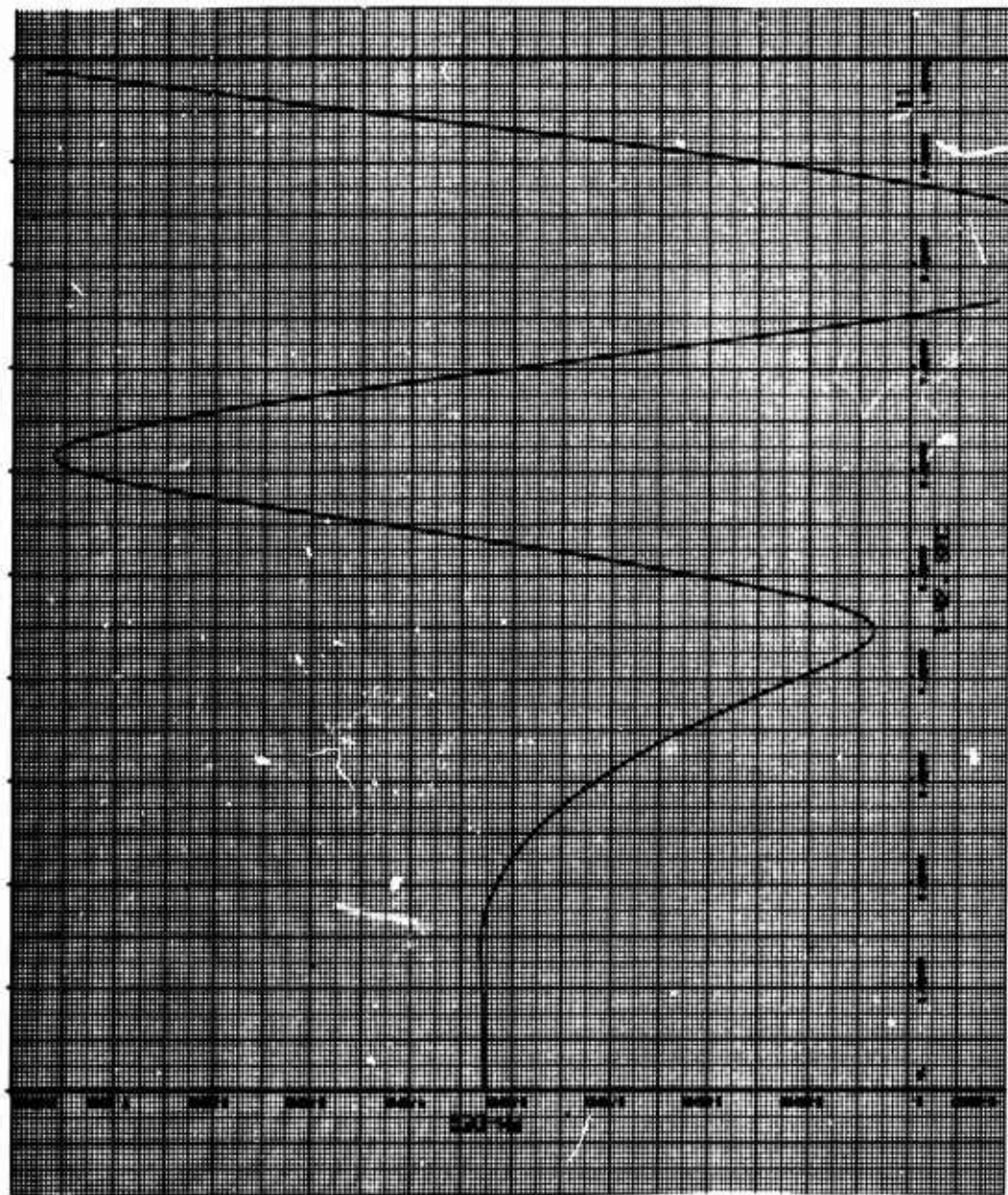


Figure 99. Graph for Miss Distance 3000 Feet

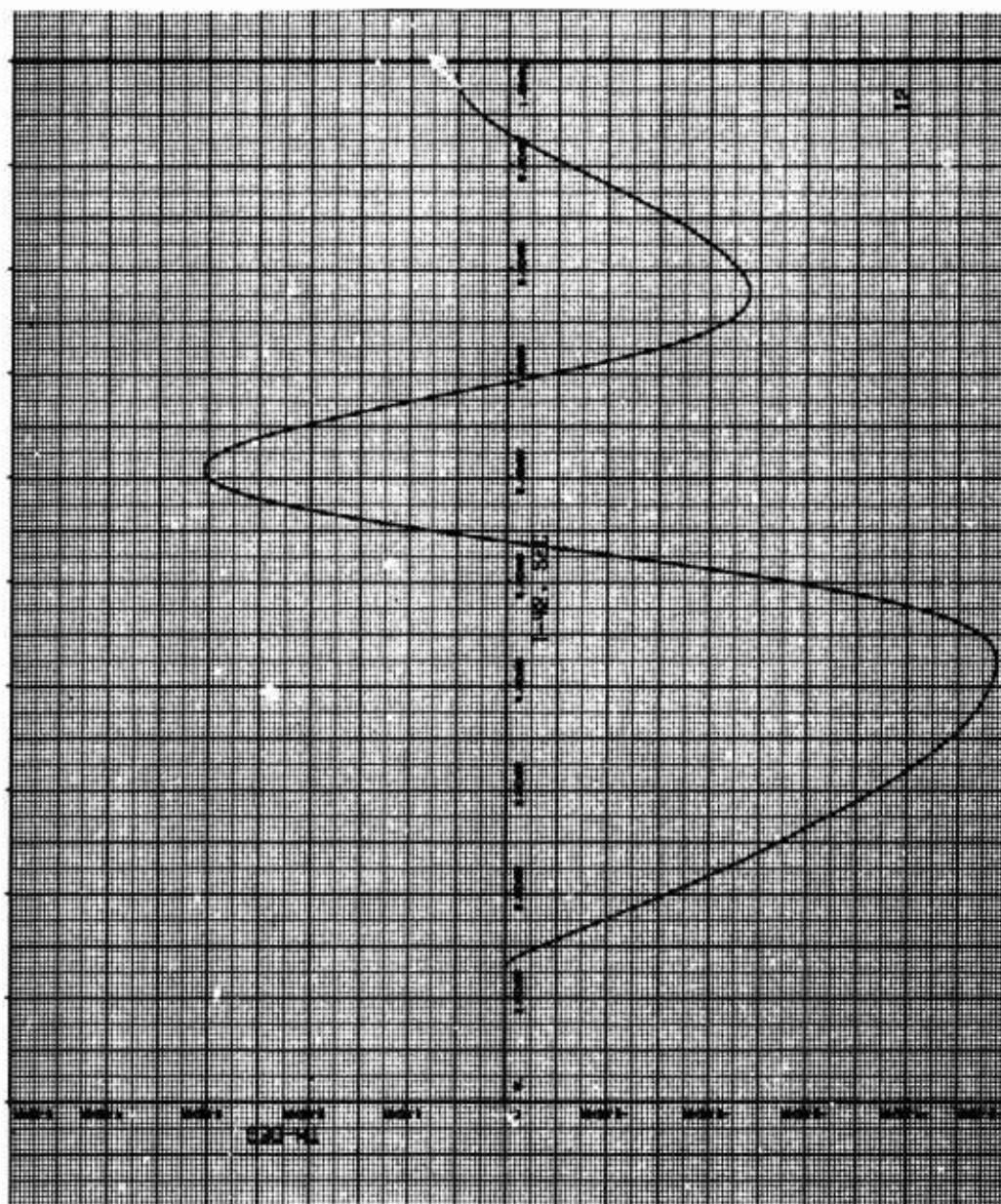


Figure 100. Graph for Miss Distance 3000 Feet

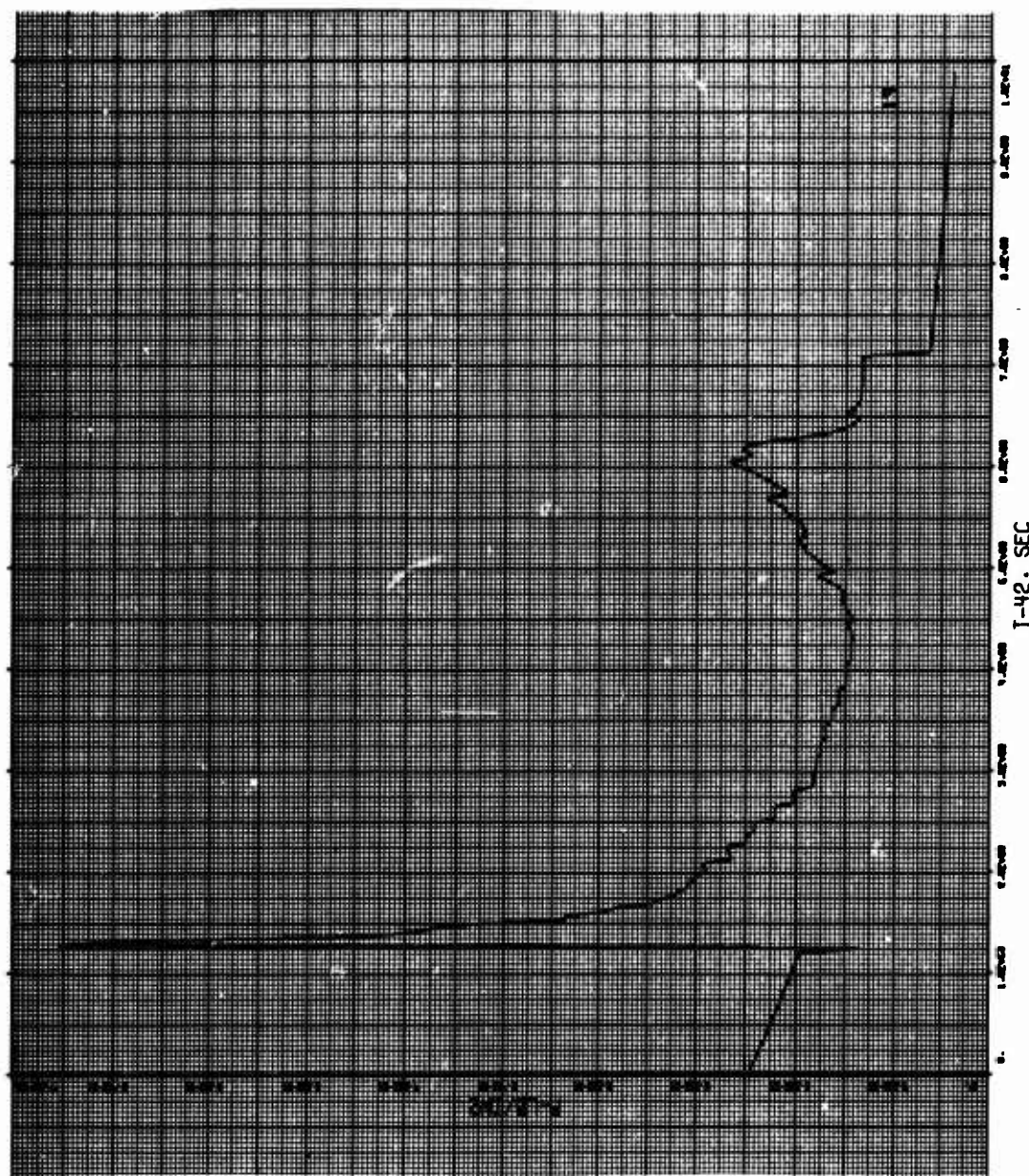


Figure 101. Graph for Miss Distance 3000 Feet

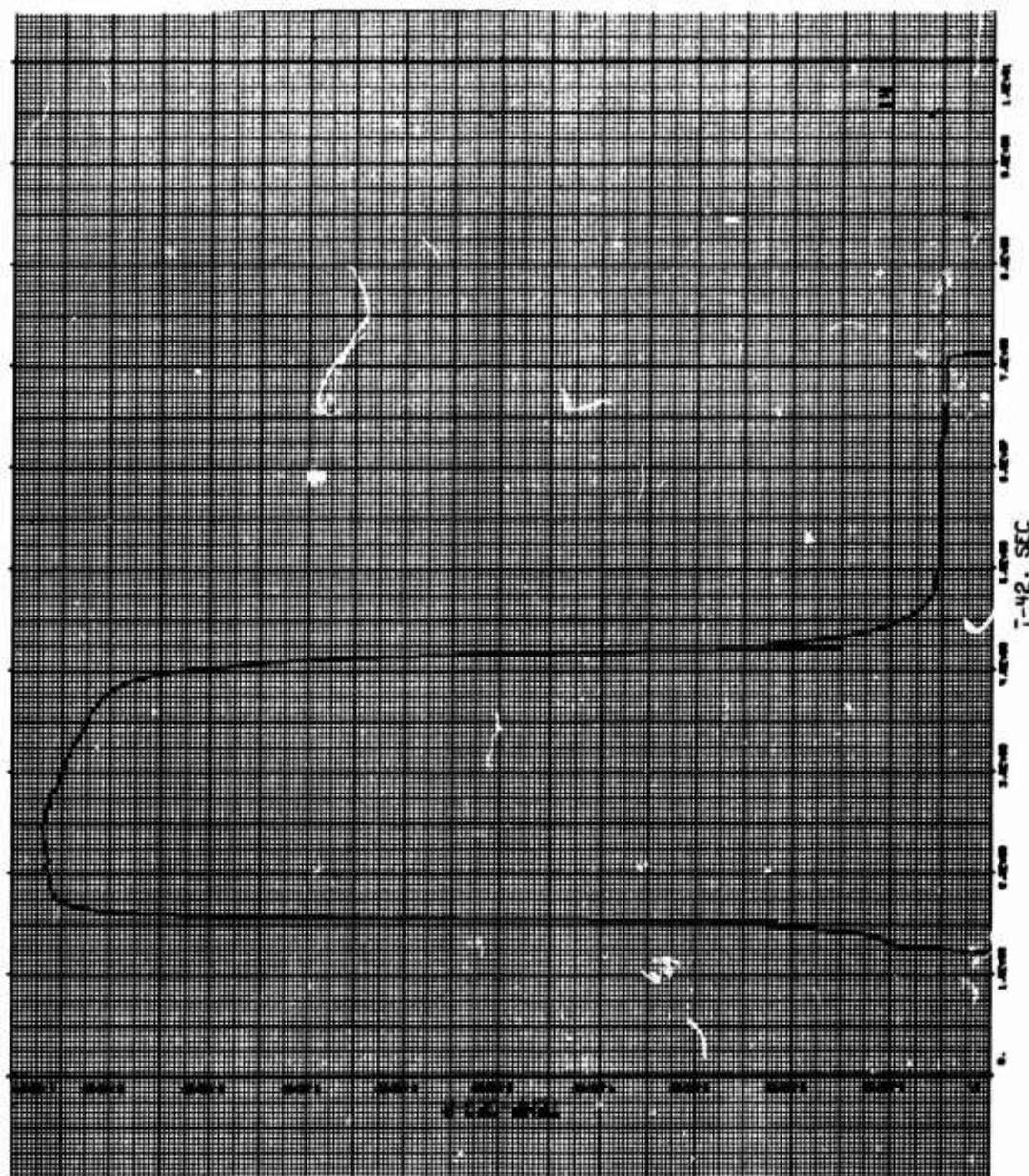


Figure 102. Graph for Miss Distance 3000 Feet

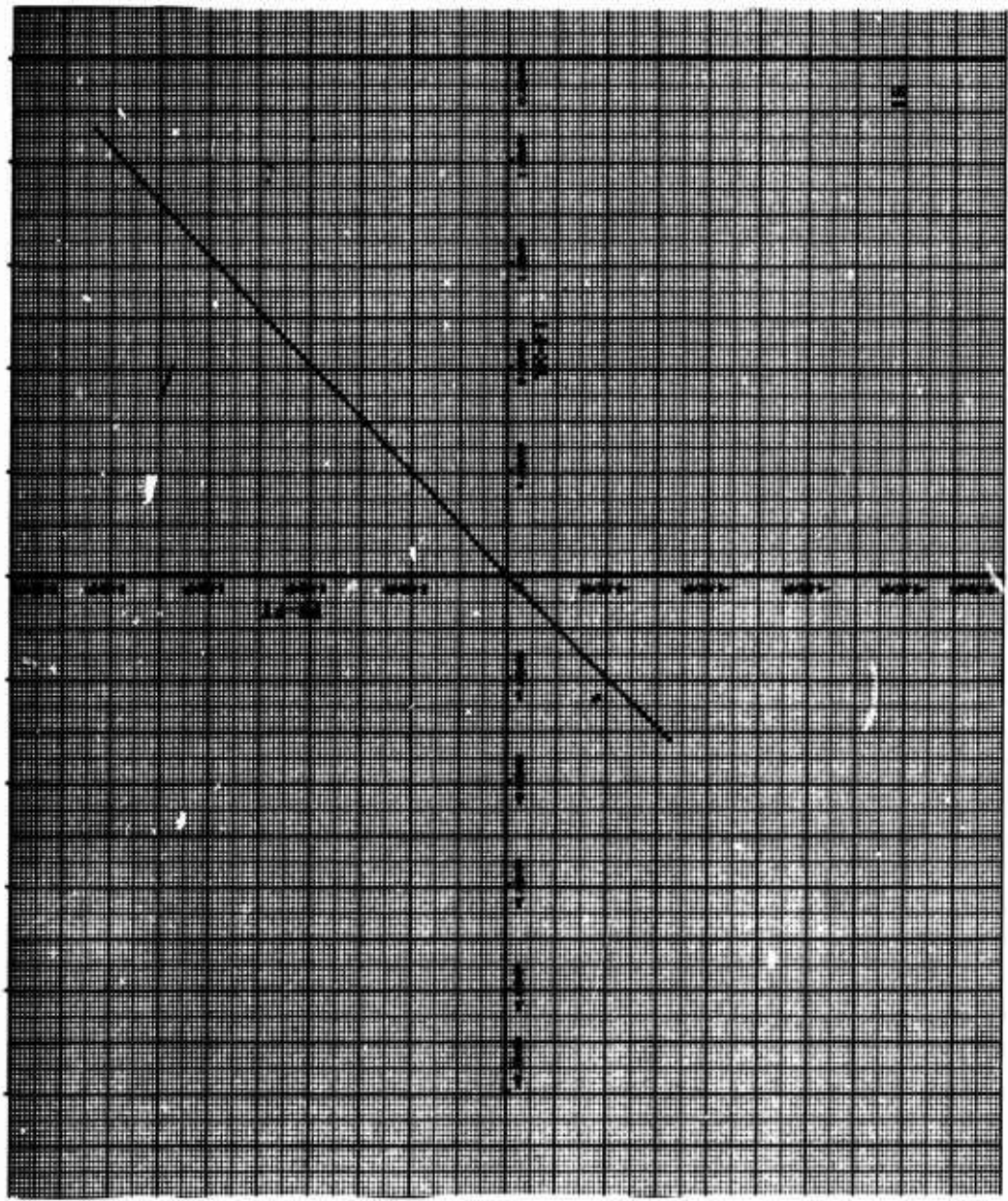


Figure 103. Graph for Miss Distance 3000 Feet

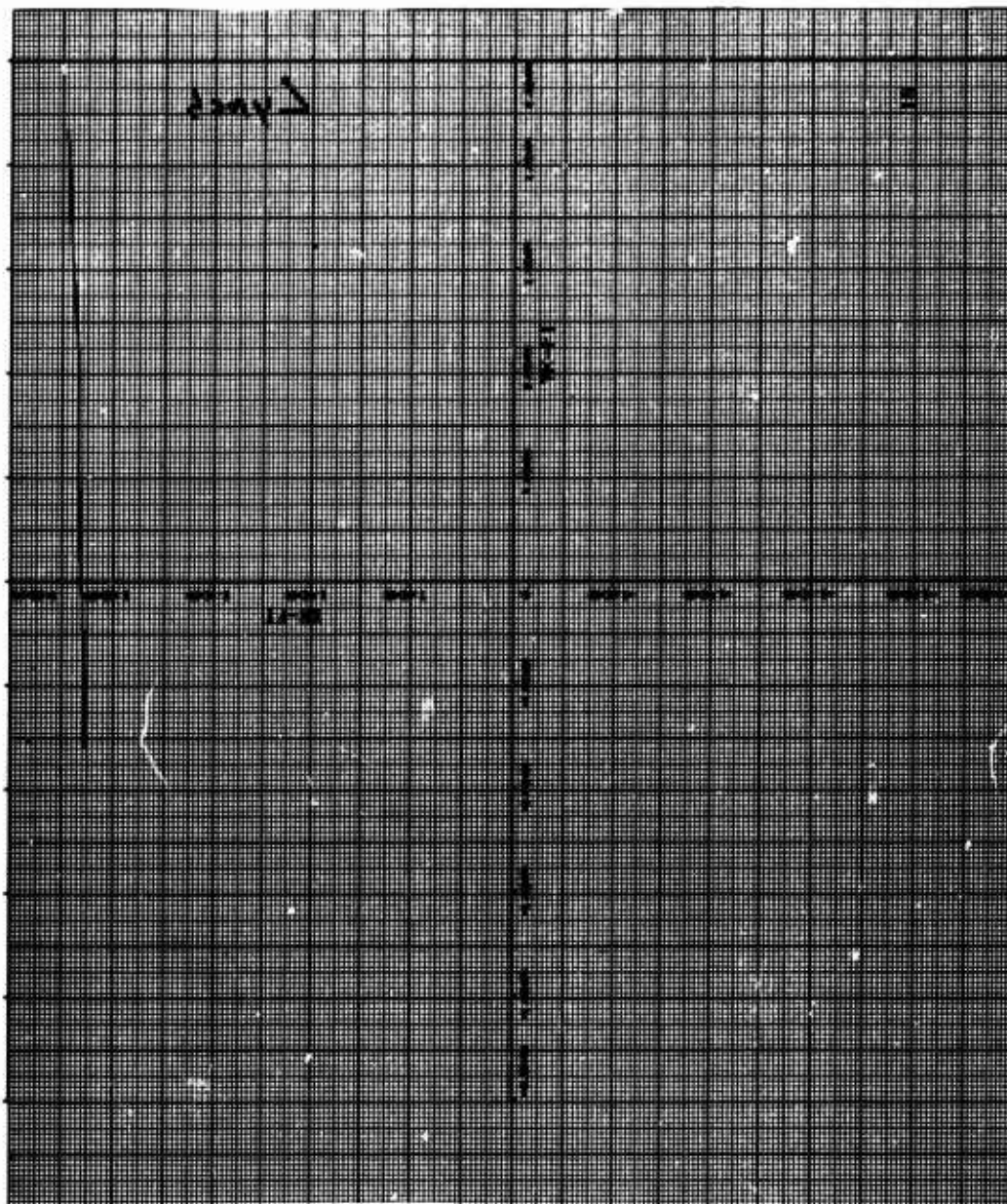


Figure 104. Graph for Miss Distance 3000 Feet

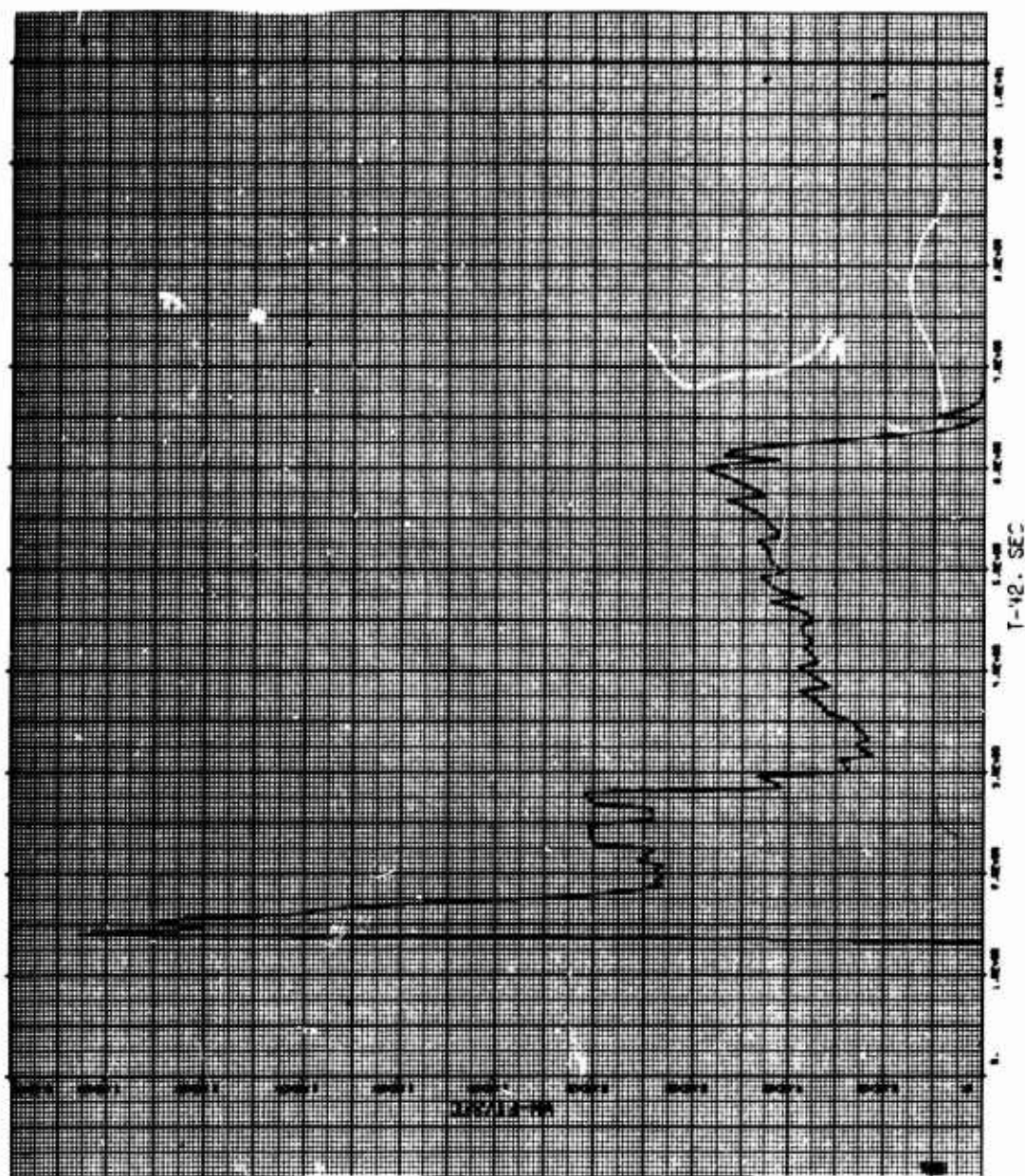


Figure 105. Graph for Miss Distance 4000 Feet

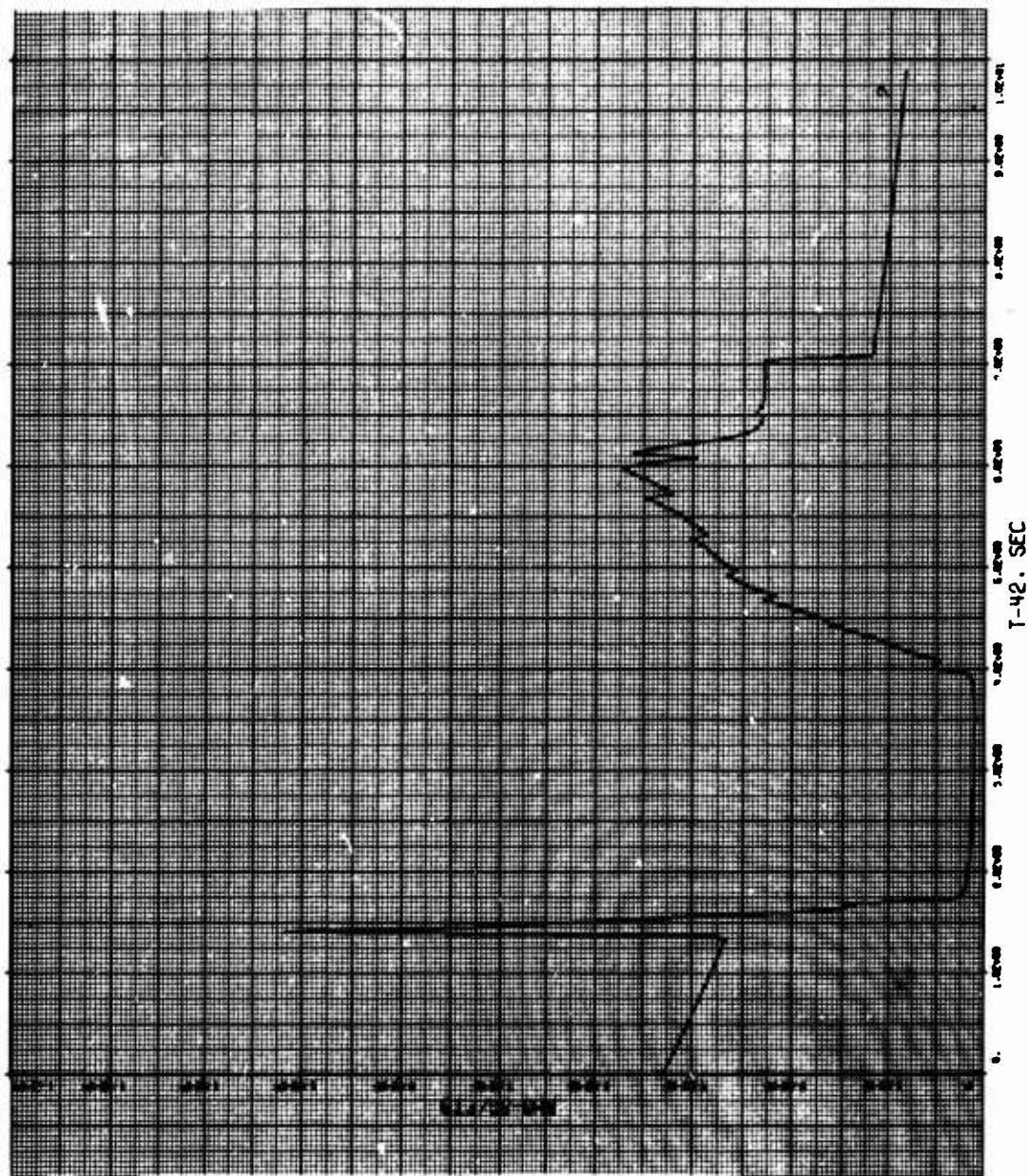


Figure 106. Graph for Miss Distance 4000 Feet

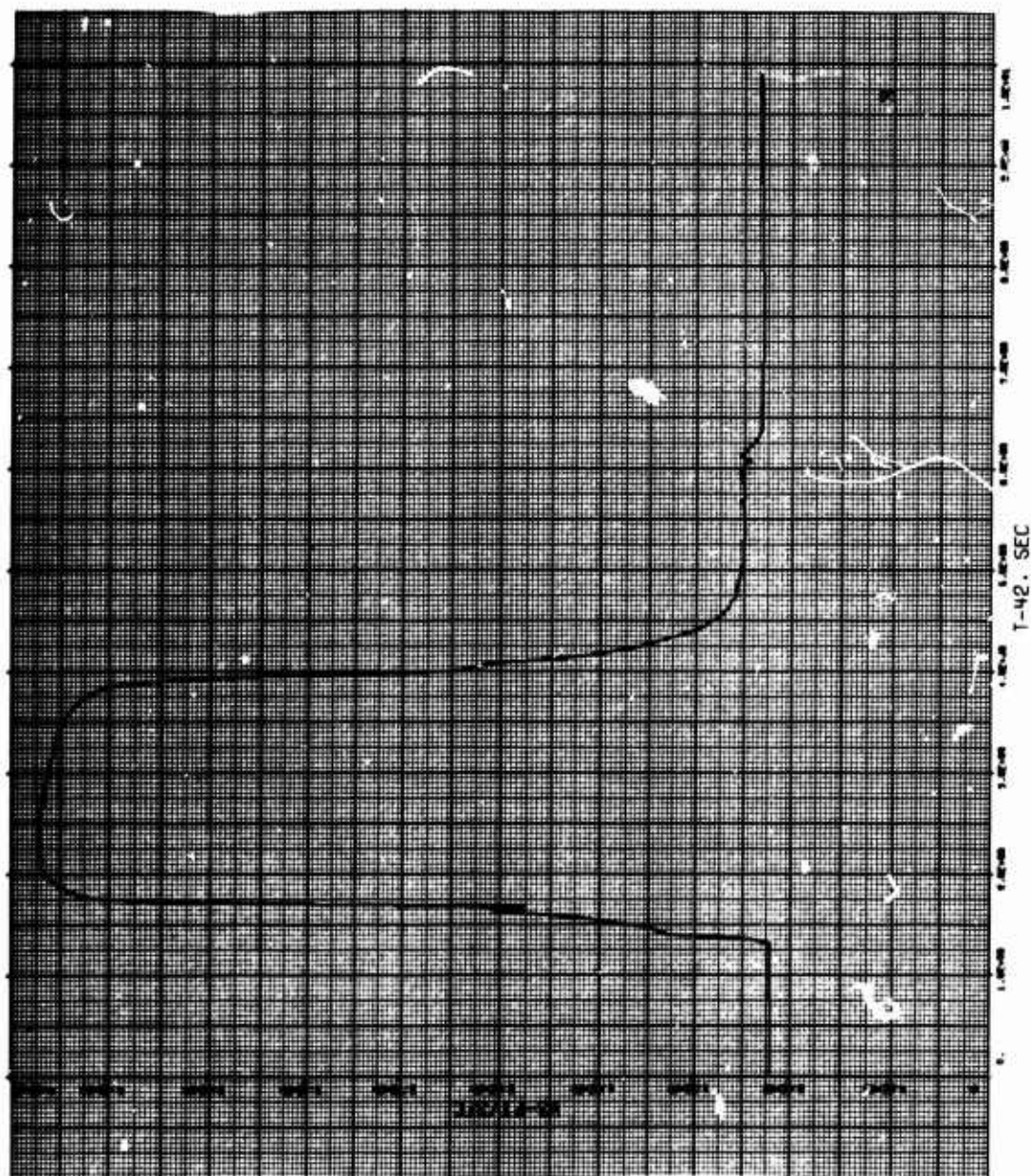


Figure 107. Graph for Miss Distance 4000 Feet

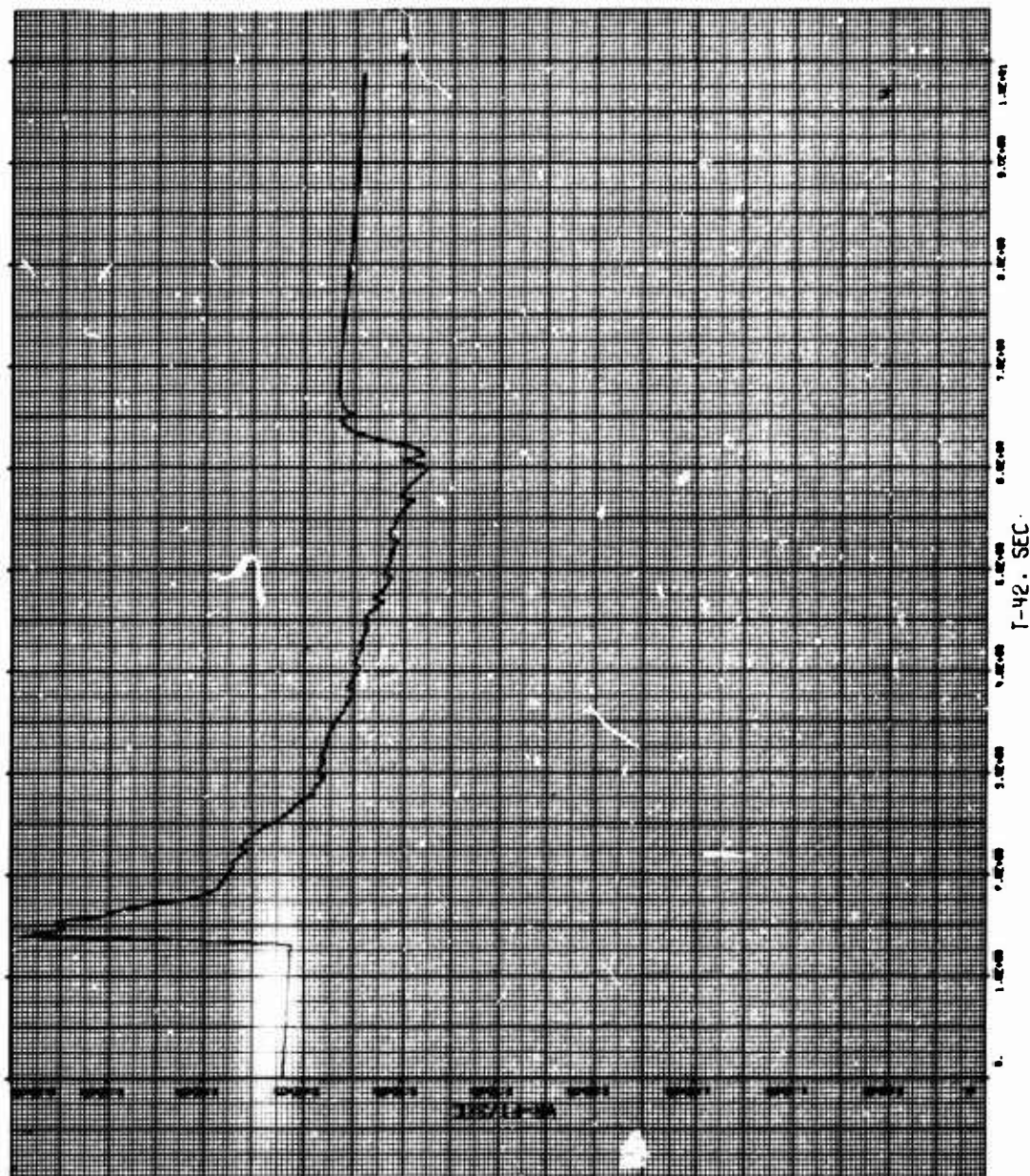


Figure 108. Graph for Miss Distance 4000 Feet

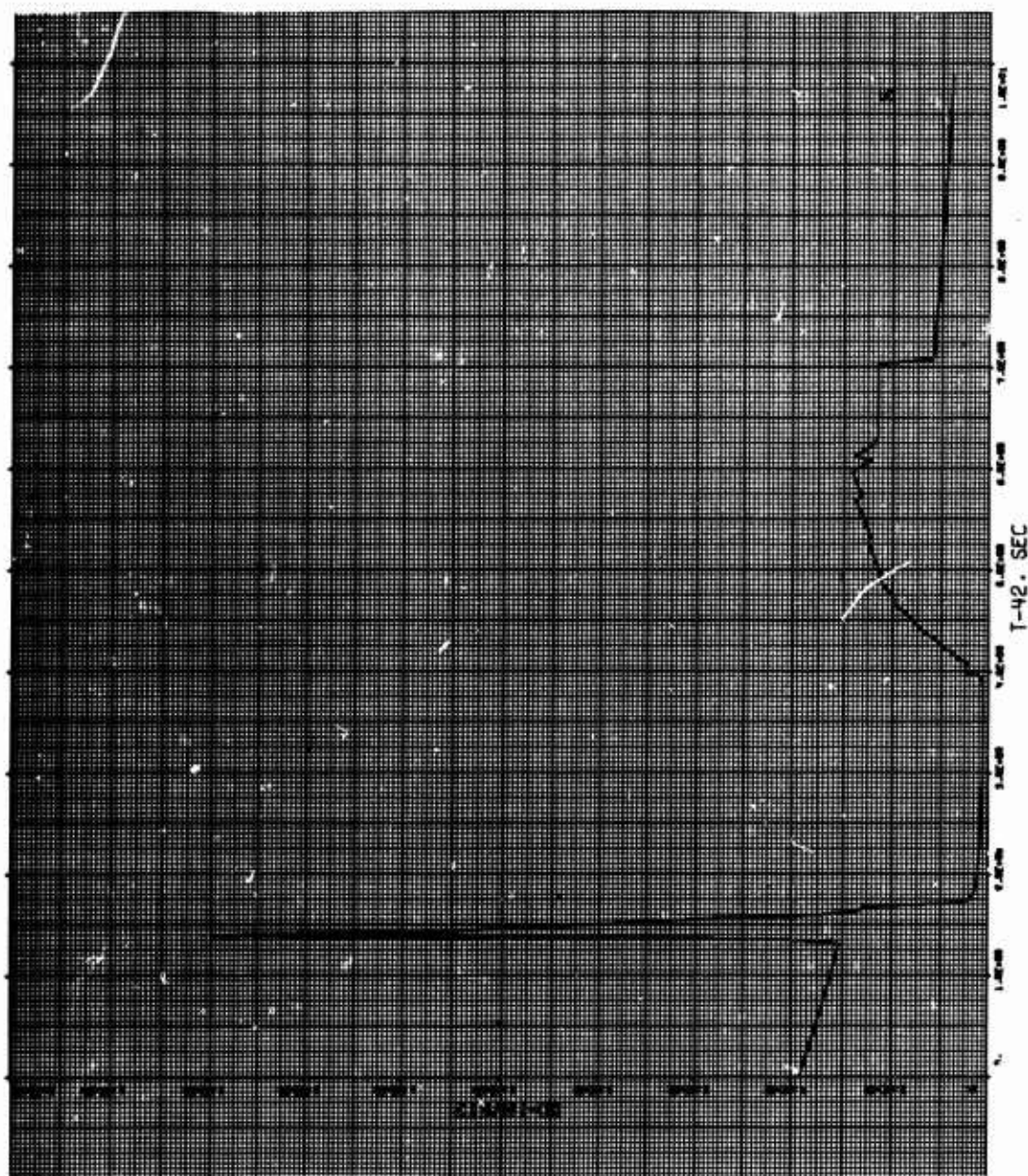


Figure 109. Graph for Miss Distance 4000 Feet

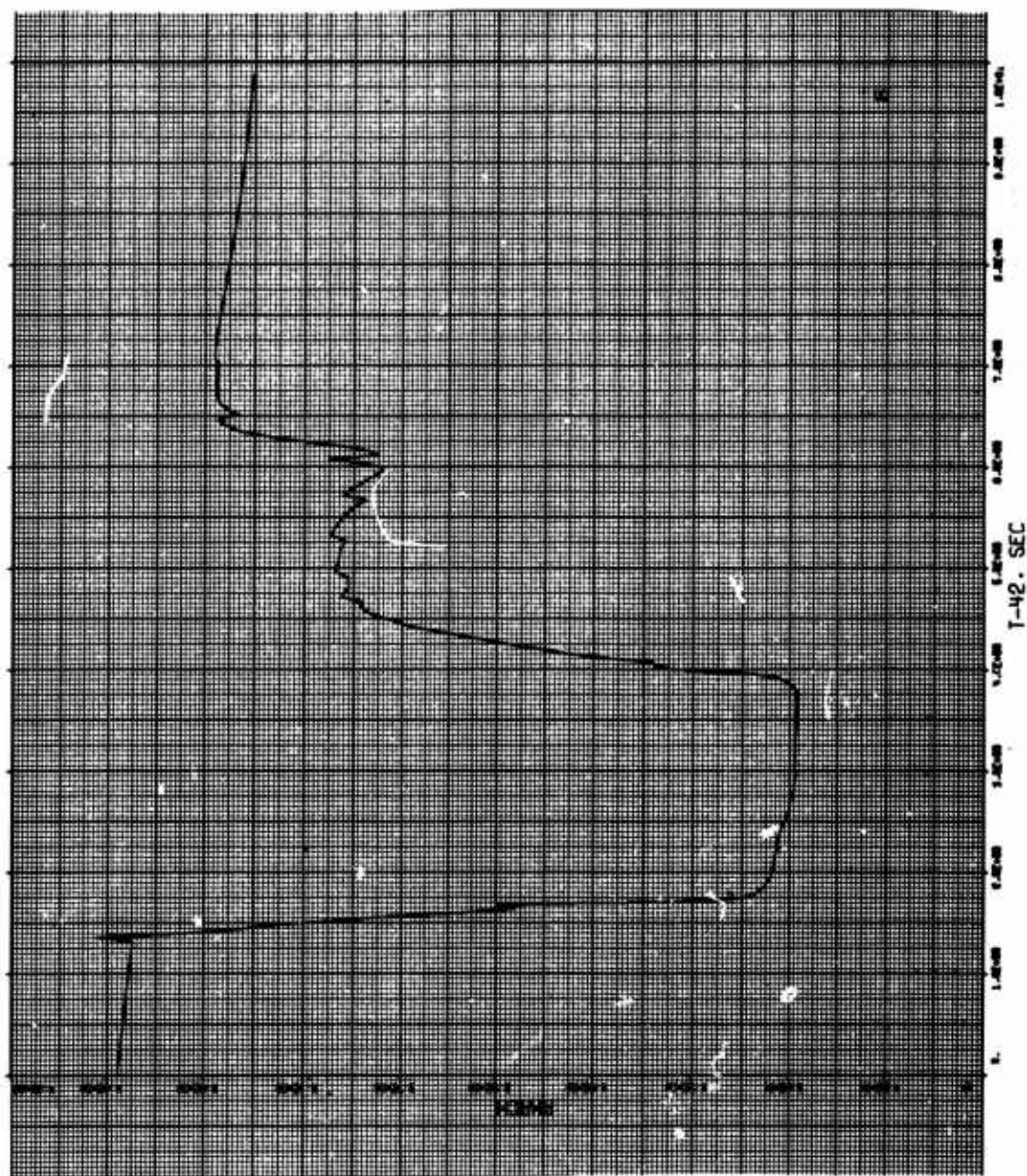


Figure 110. Graph for Miss Distance 4000 Feet

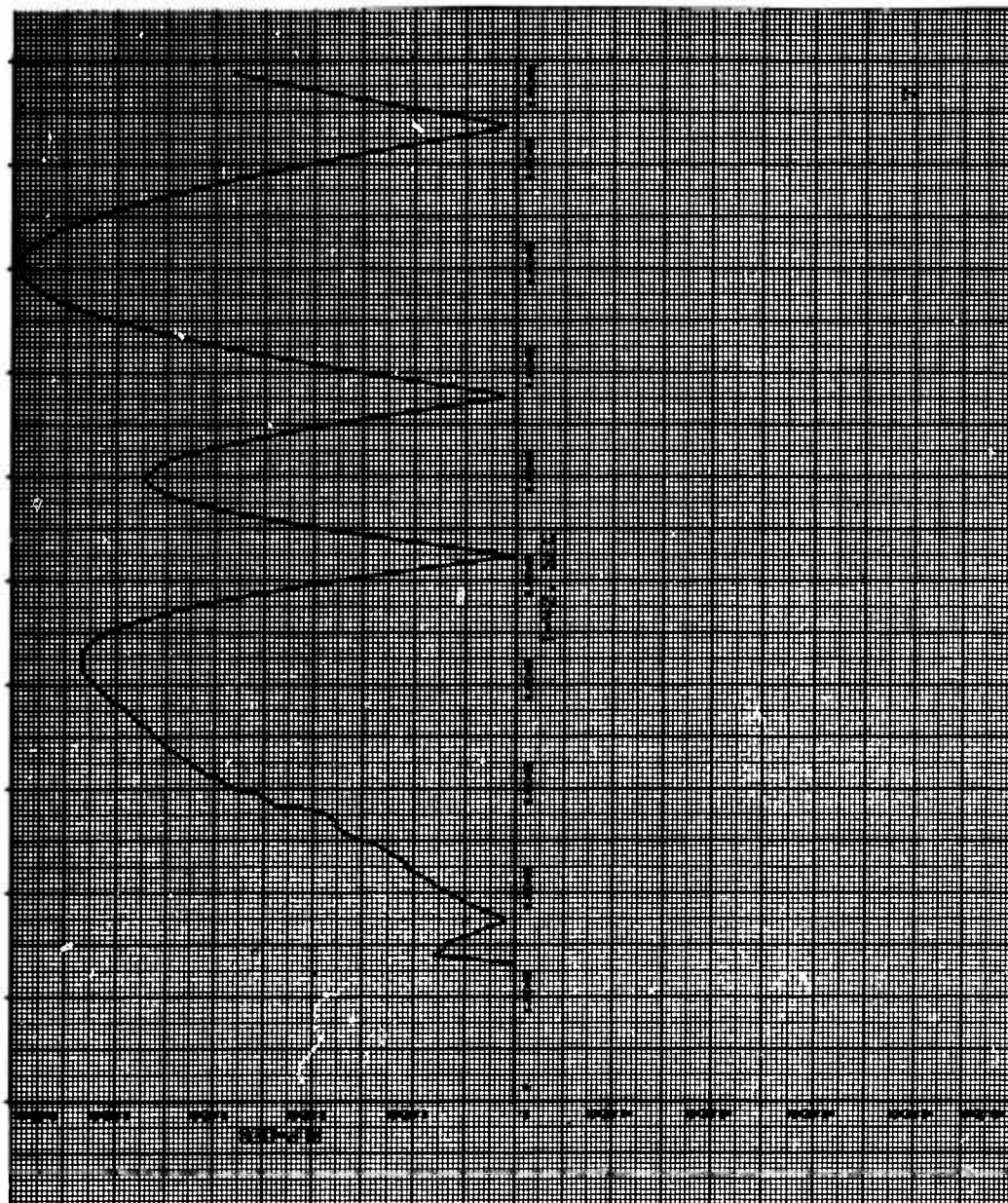


Figure 111. Graph for Miss Distance 4000 Feet

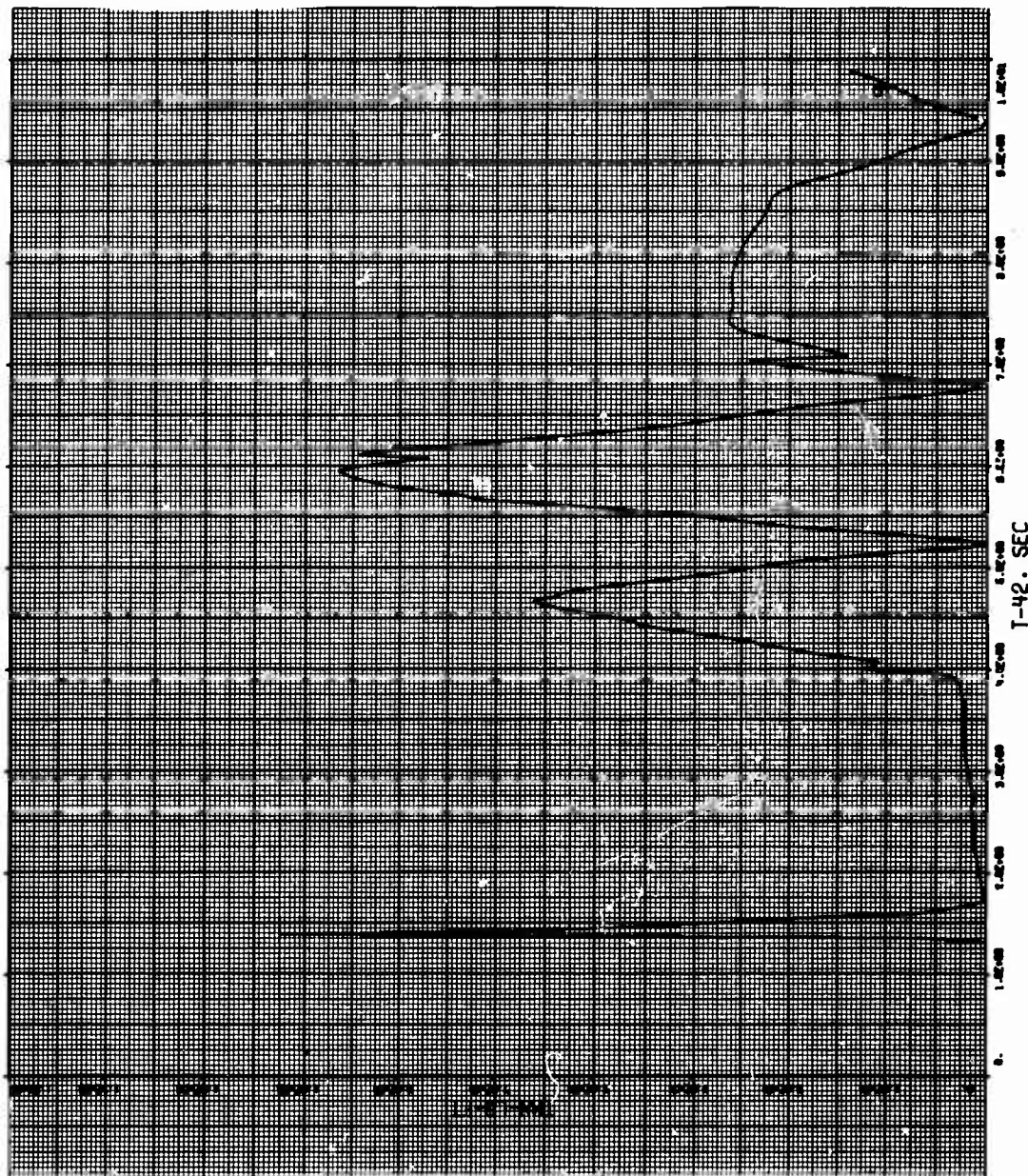


Figure 112. Graph for Miss Distance 4000 Feet

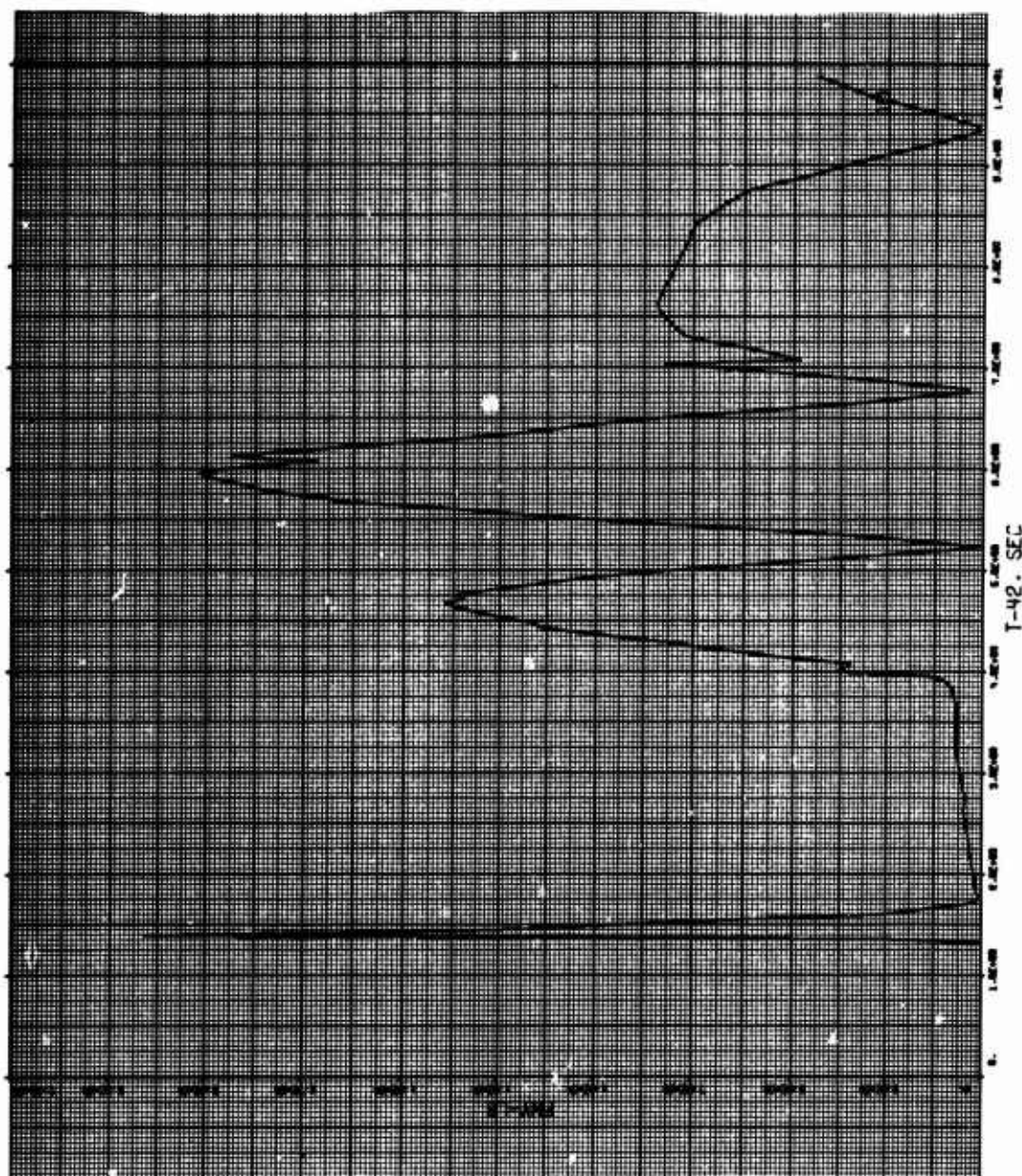


Figure 113. Graph for Miss Distance 4000 Feet

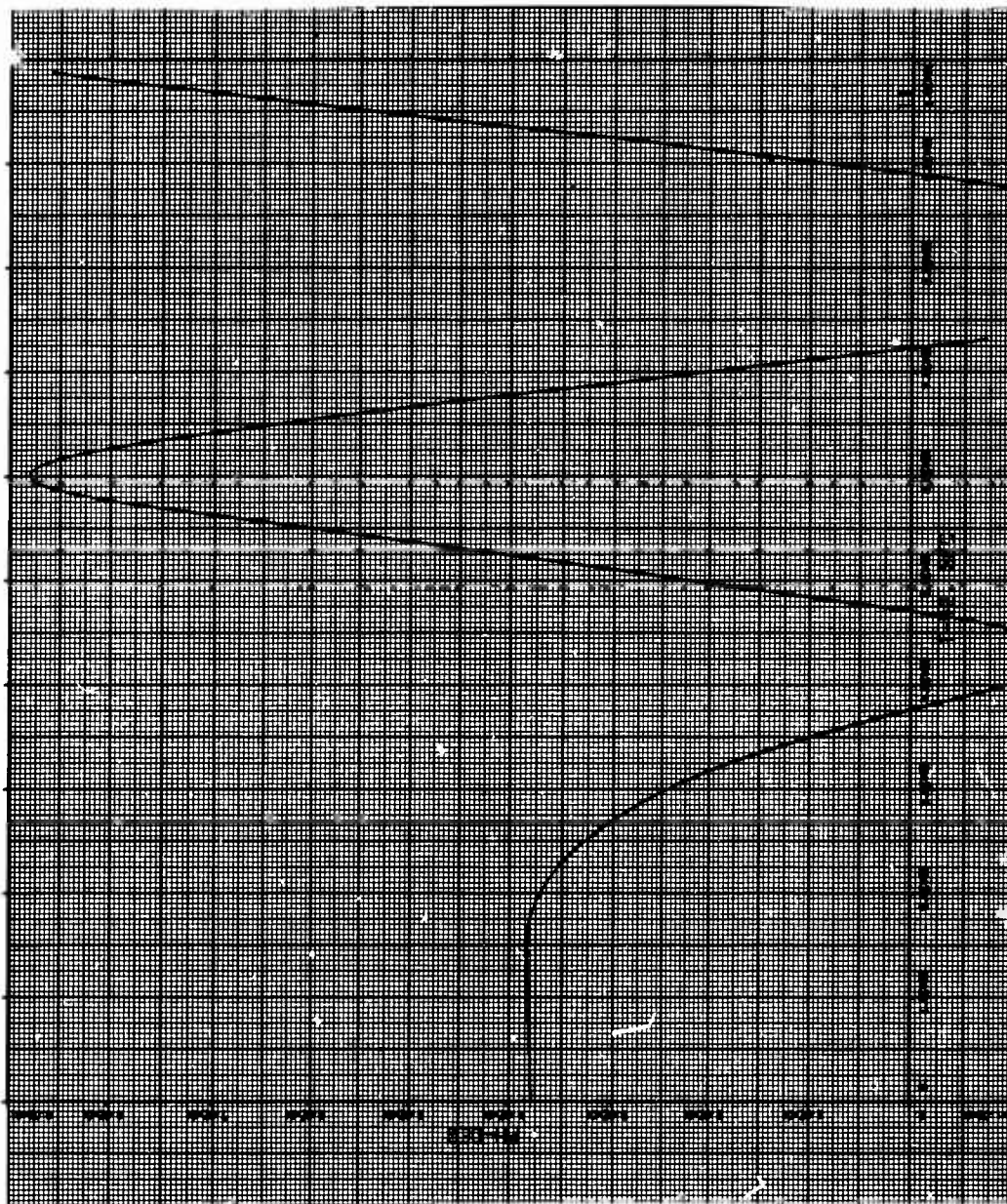


Figure 114. Graph for Miss Distance 4000 Feet

2

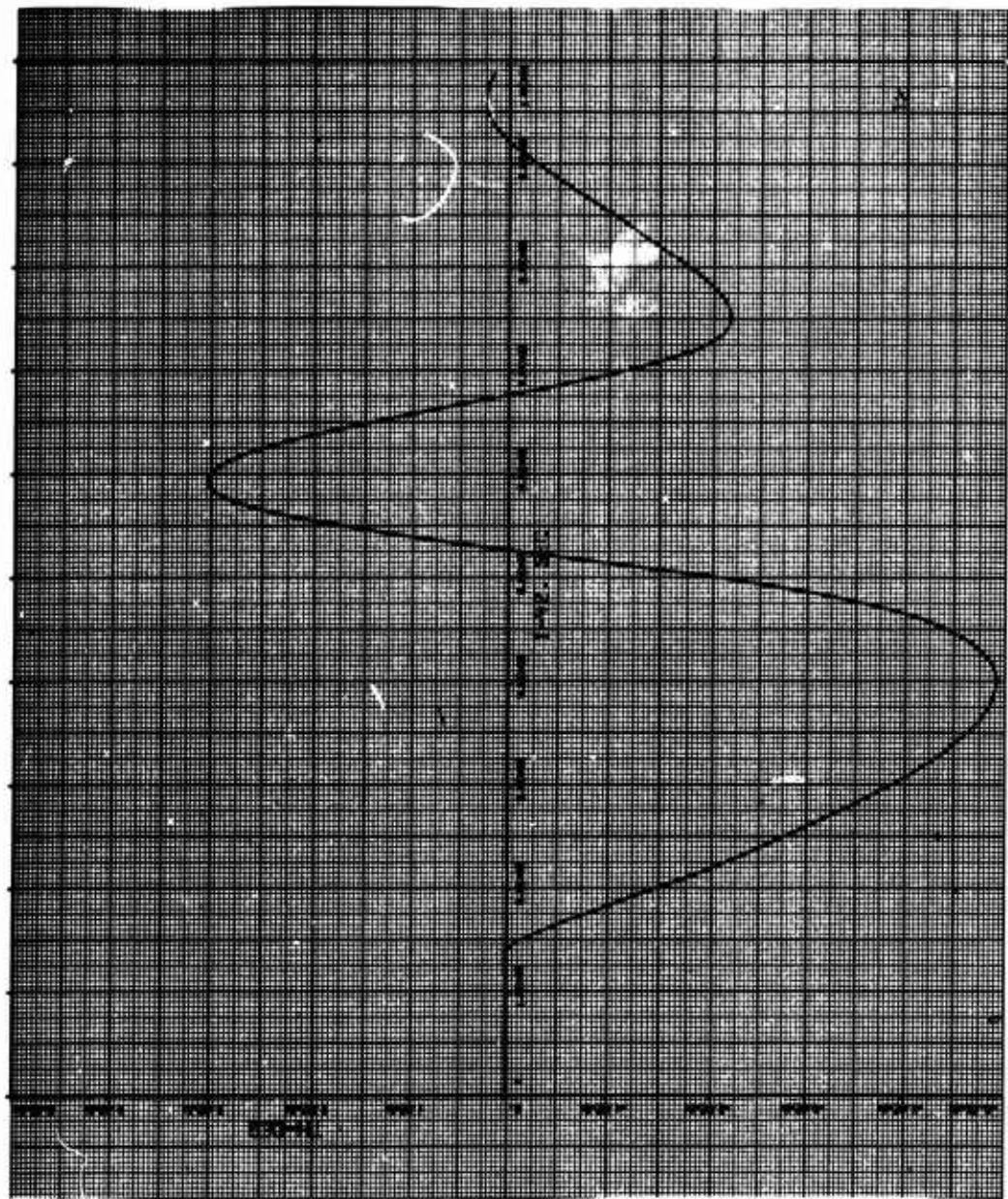


Figure 115. Graph for Miss Distance 4000 Feet

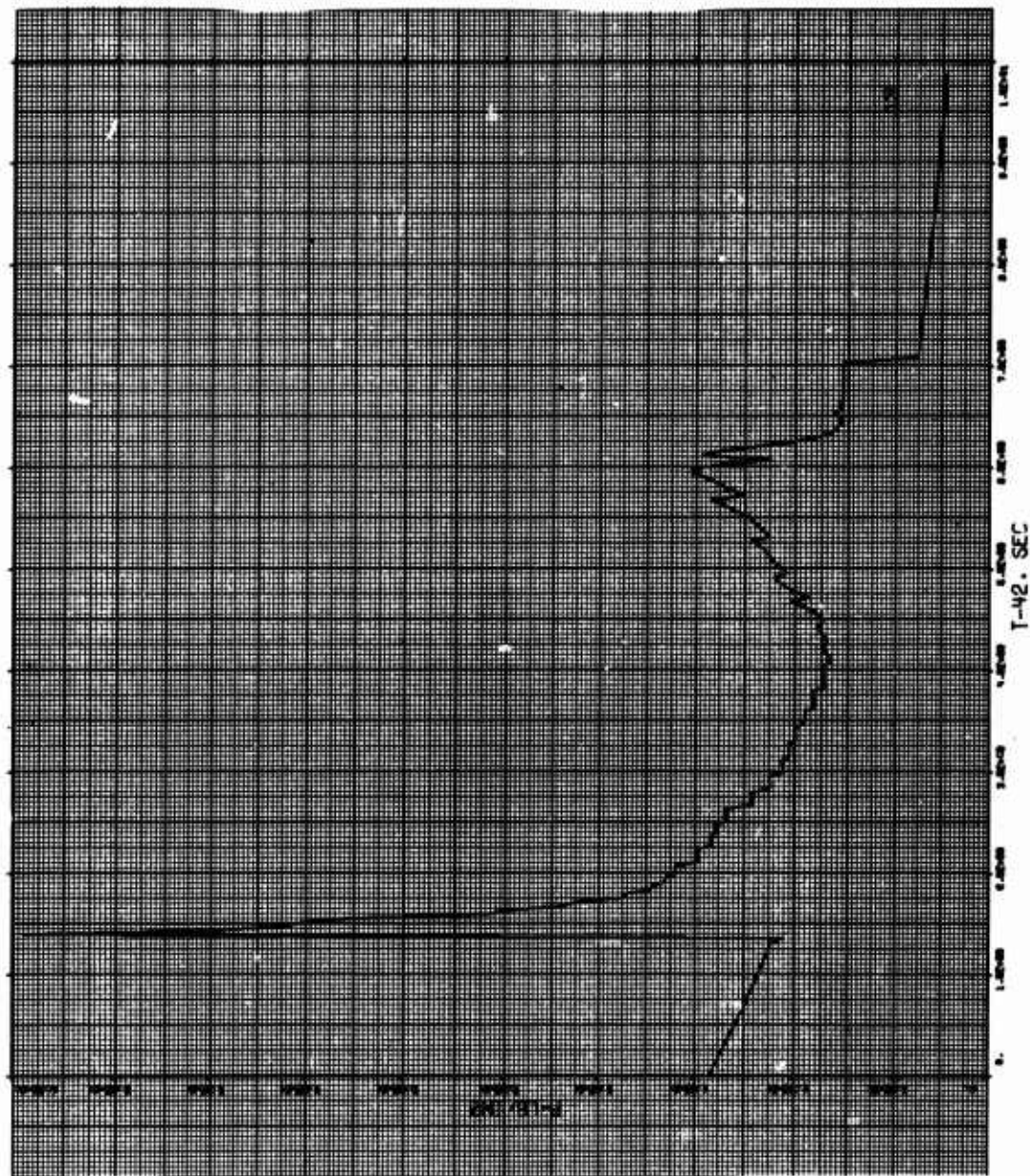


Figure 116. Graph for Miss Distance 4000 Feet

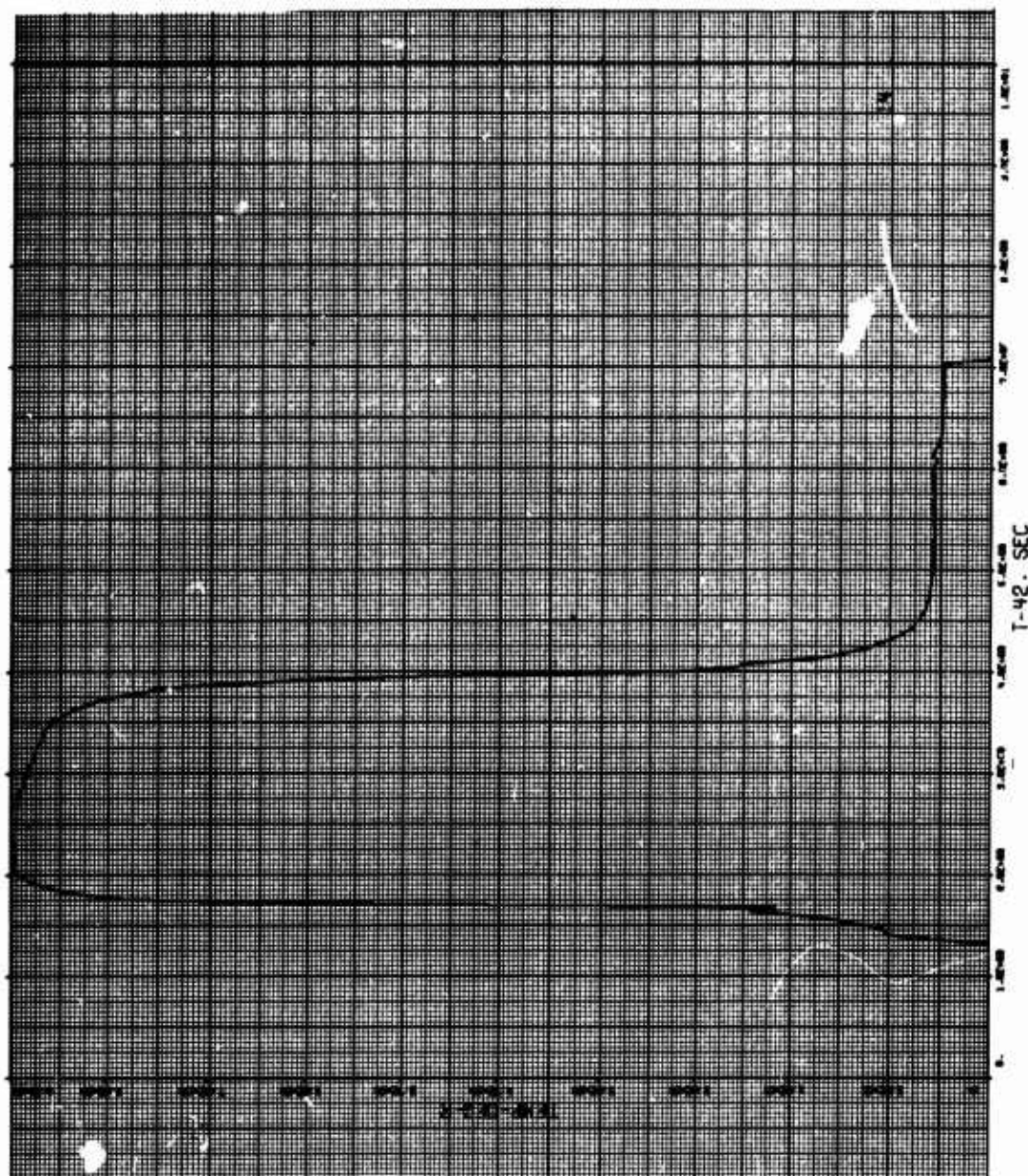


Figure 117. Graph for Miss Distance 4000 Feet

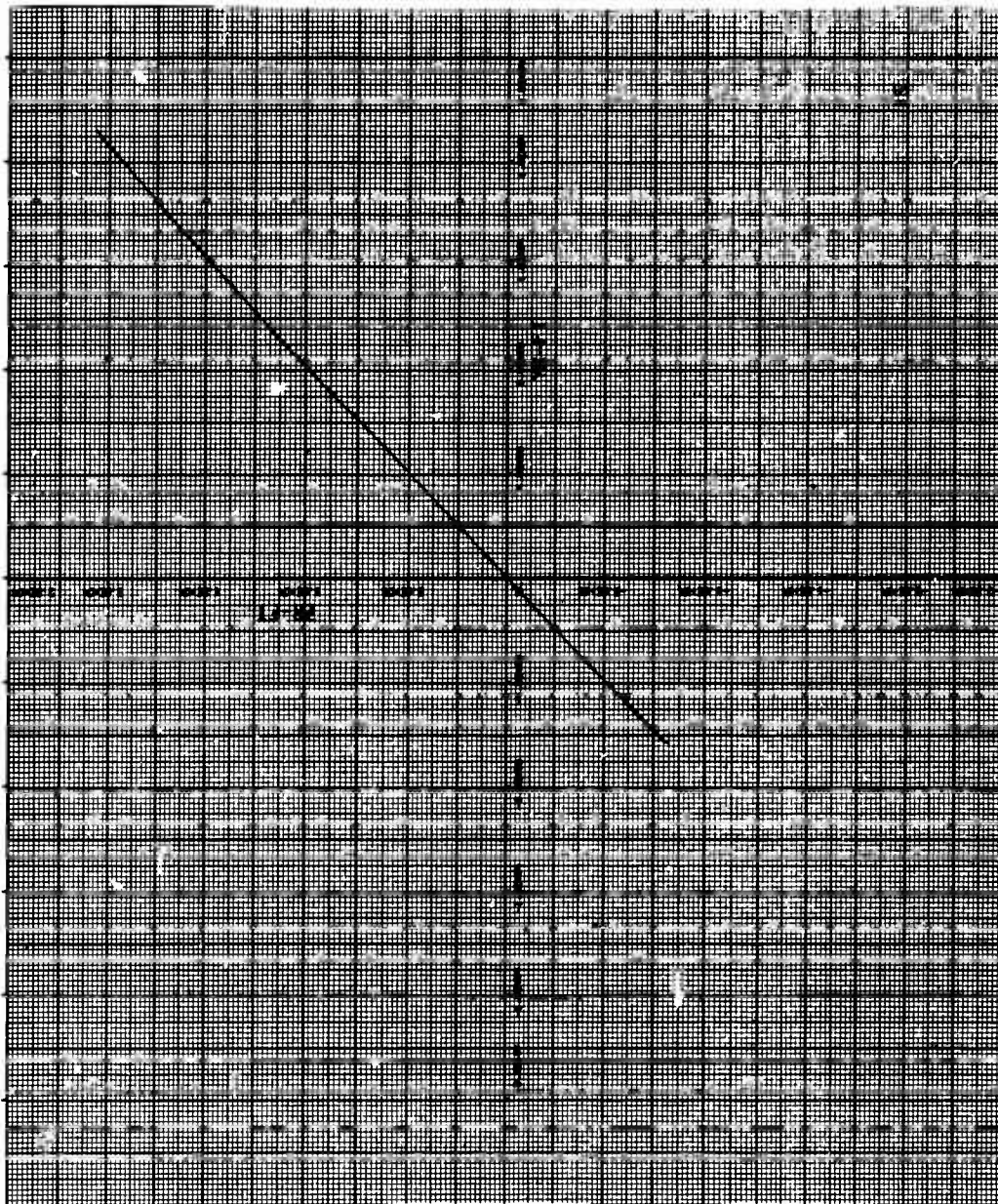


Figure 118. Graph for Miss Distance 4000 Feet

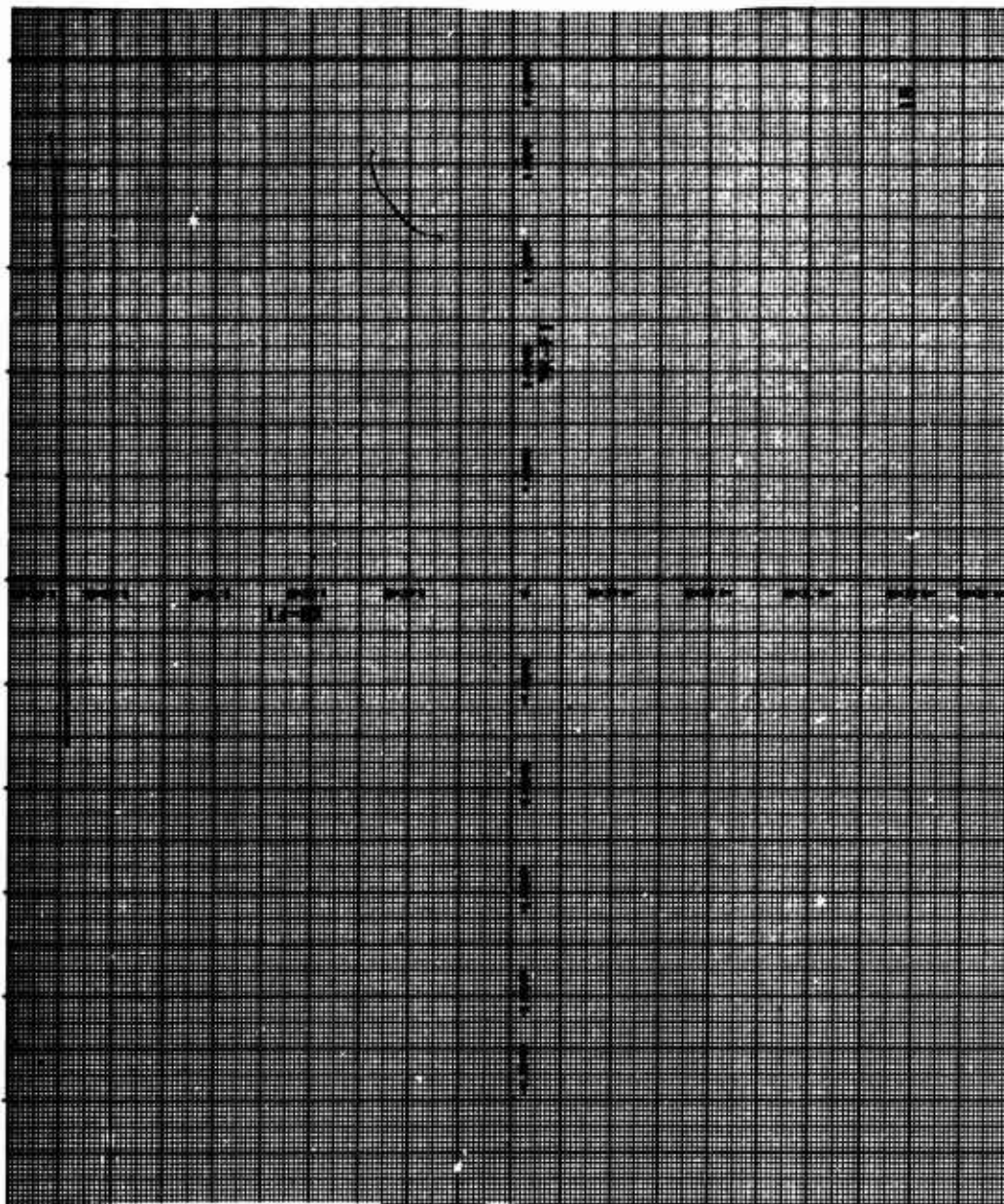


Figure 119. Graph for Miss Distance 4000 Feet

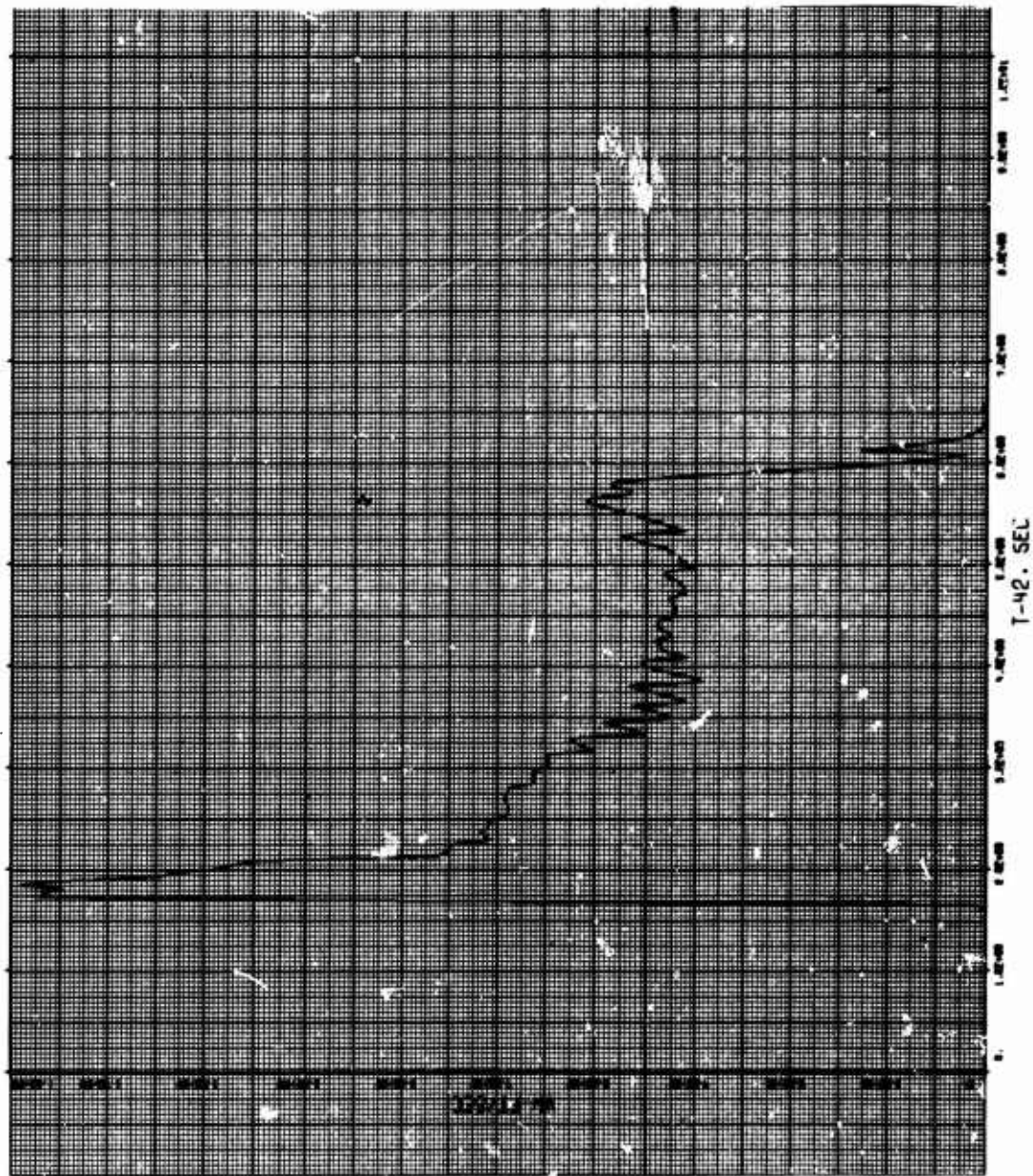


Figure 120. Graph for Miss Distance 6000 Feet.

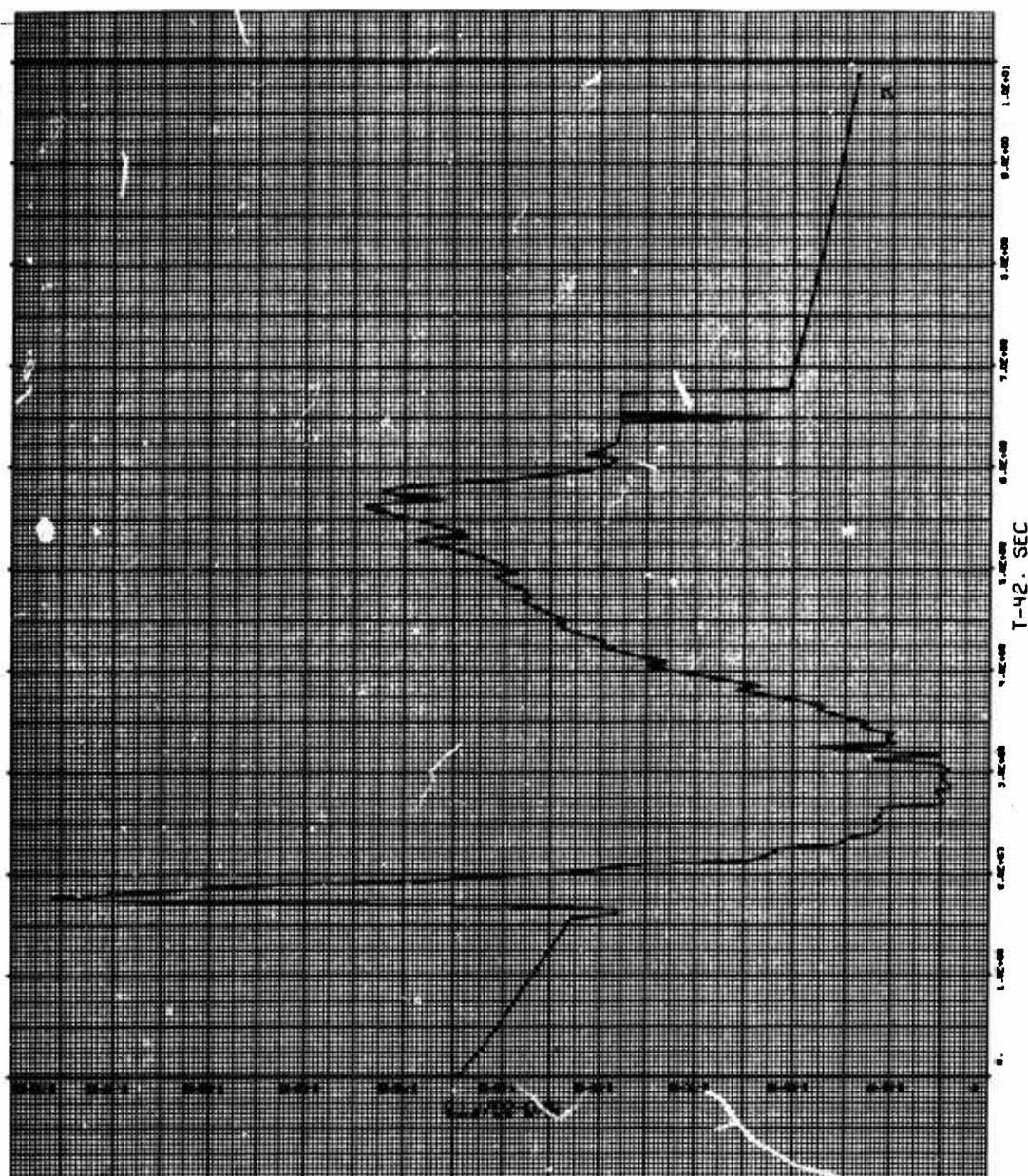


Figure 121. Graph for Miss Distance 6000 Feet

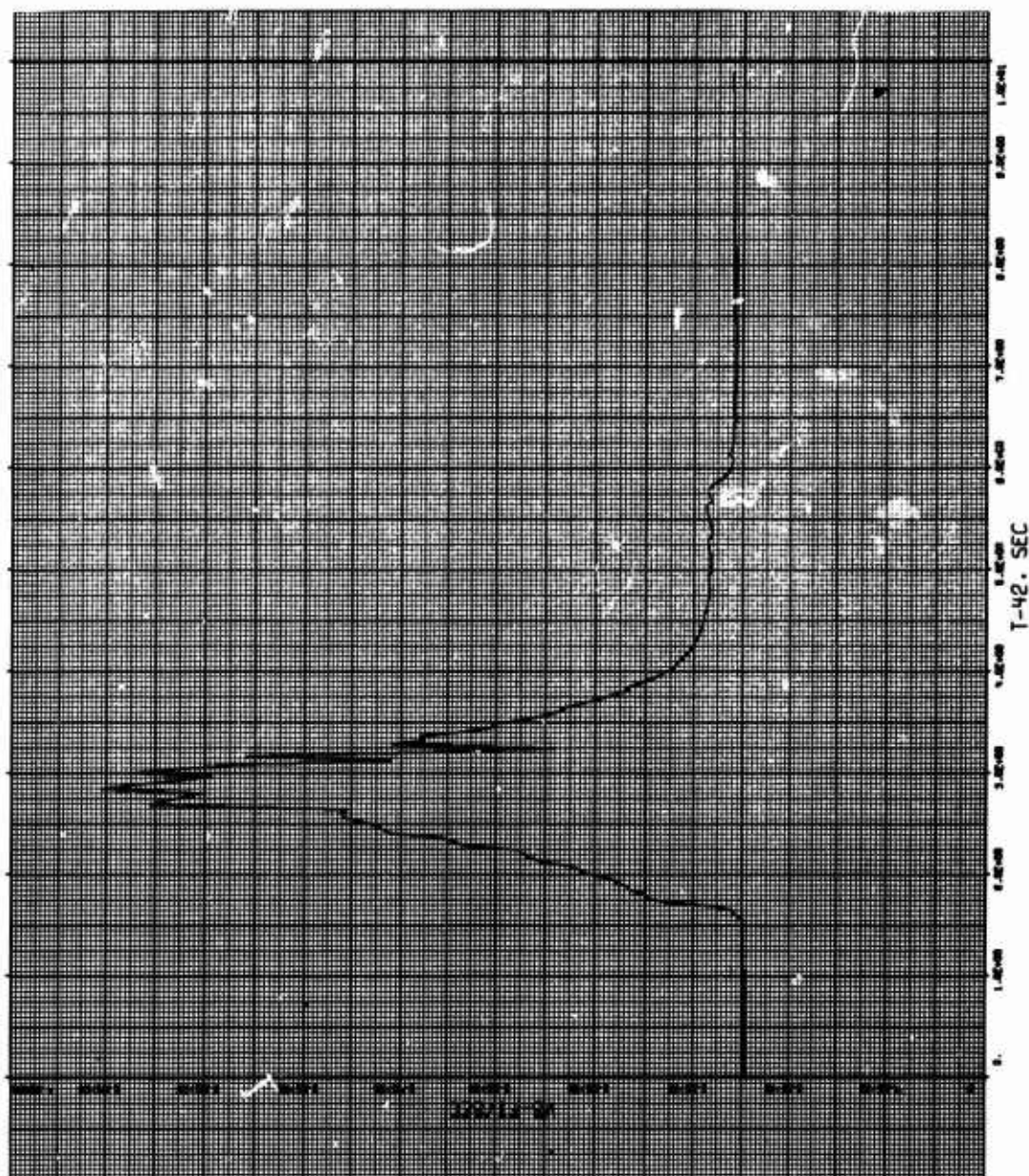


Figure 122. Graph for Miss Distance 6000 Feet

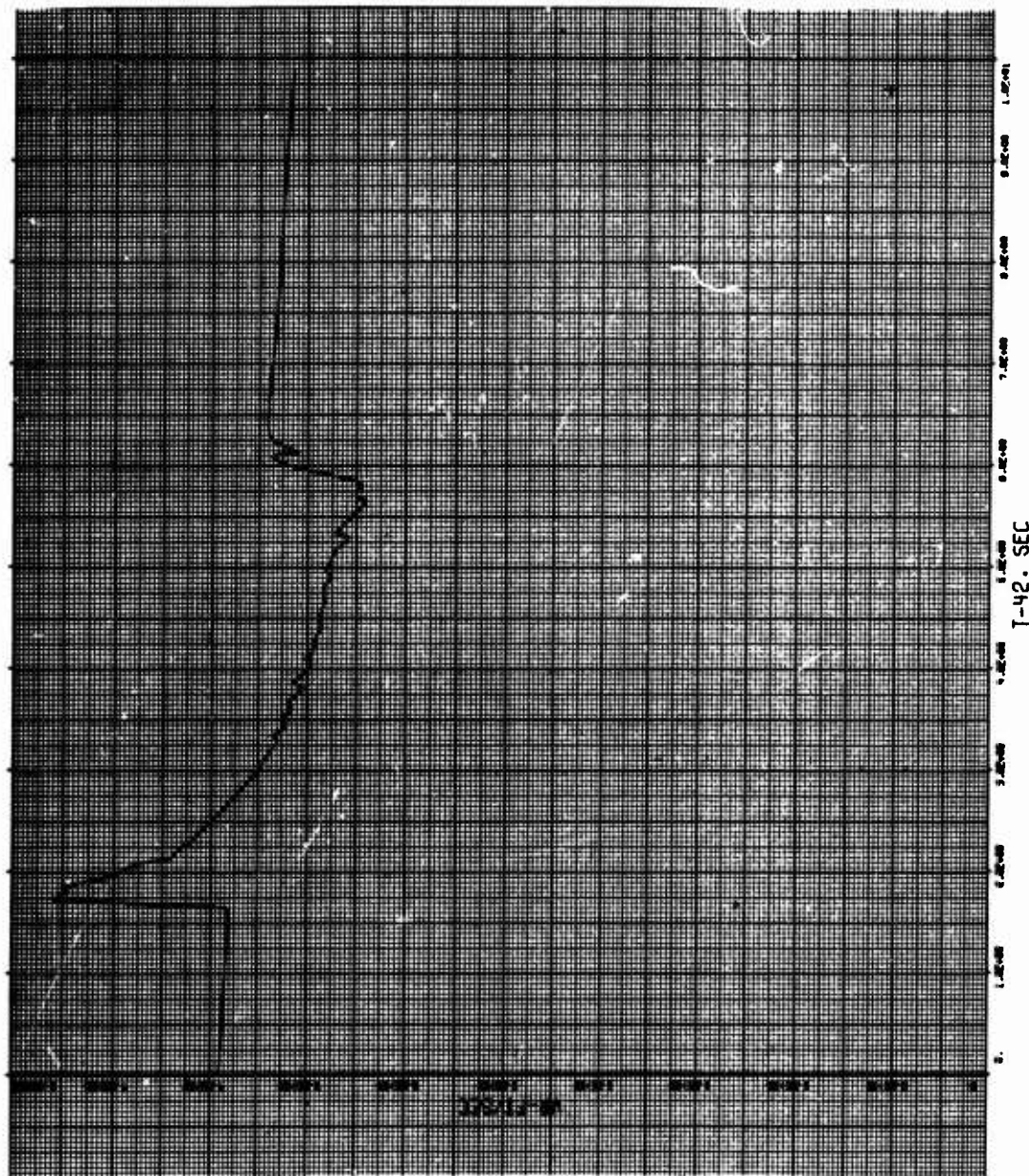


Figure 123. Graph for Miss Distance 6000 Feet

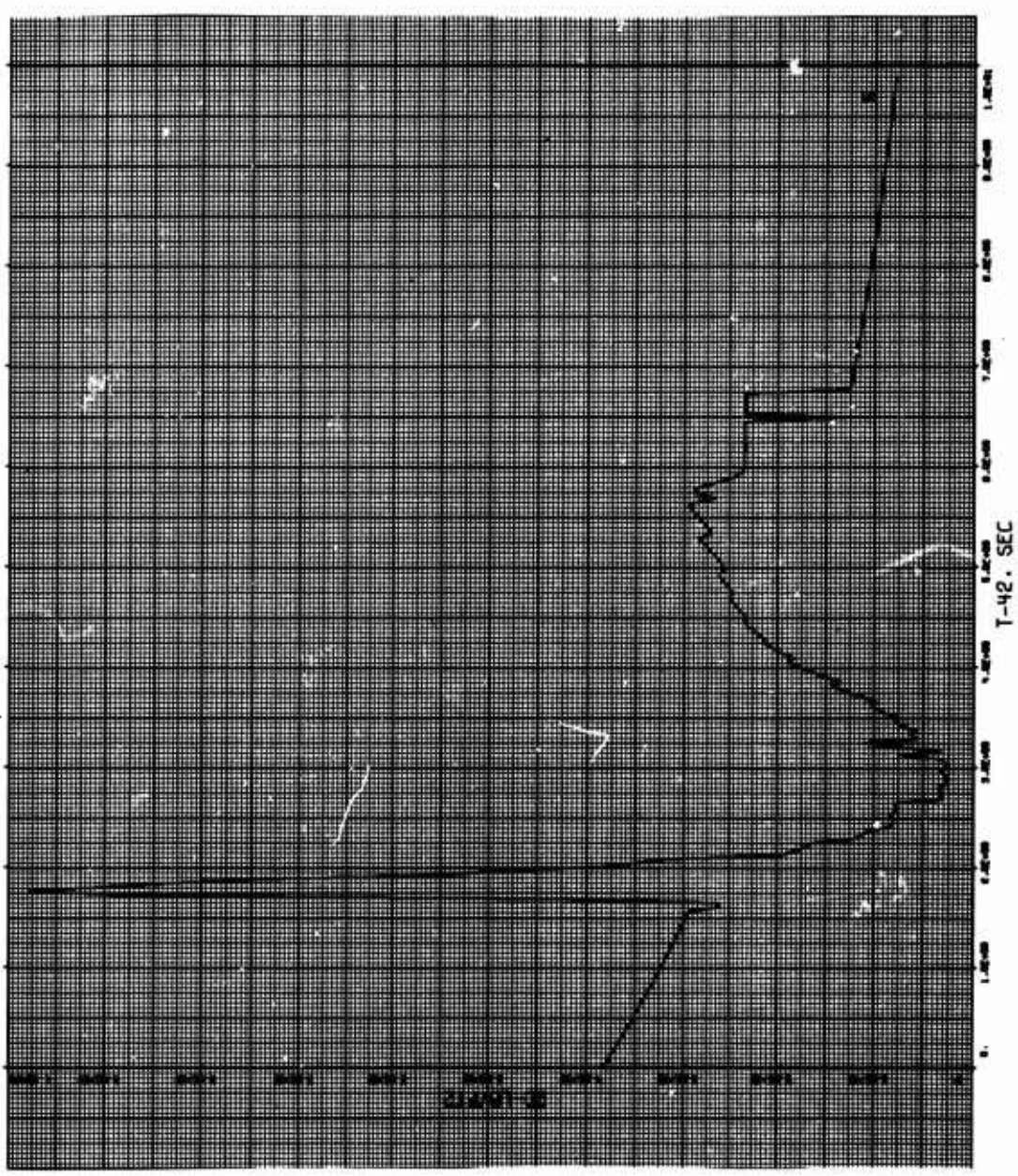


Figure 124. Graph for Miss Distance 6000 Feet

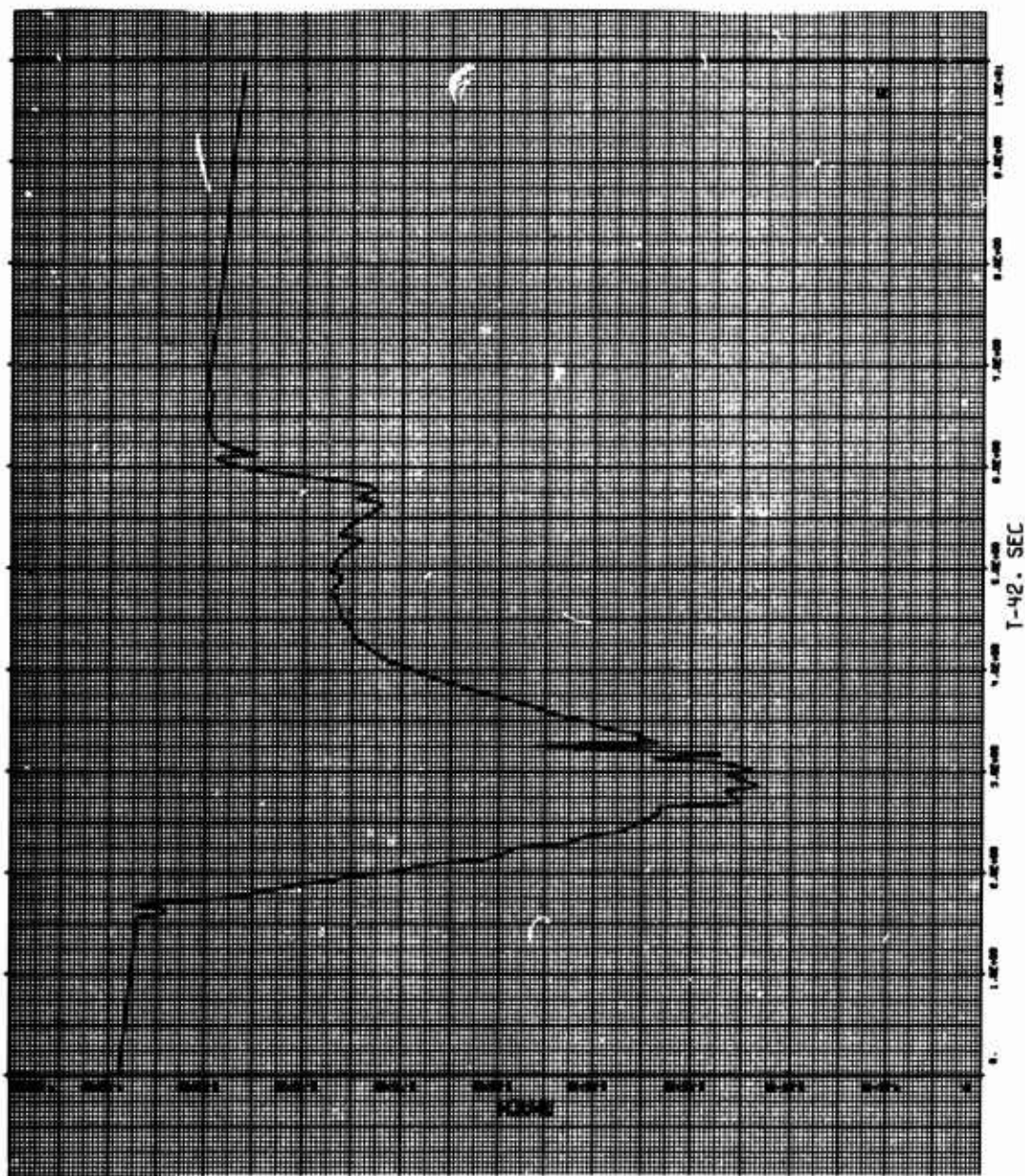


Figure 125. Graph for Miss Distance 6000 Feet

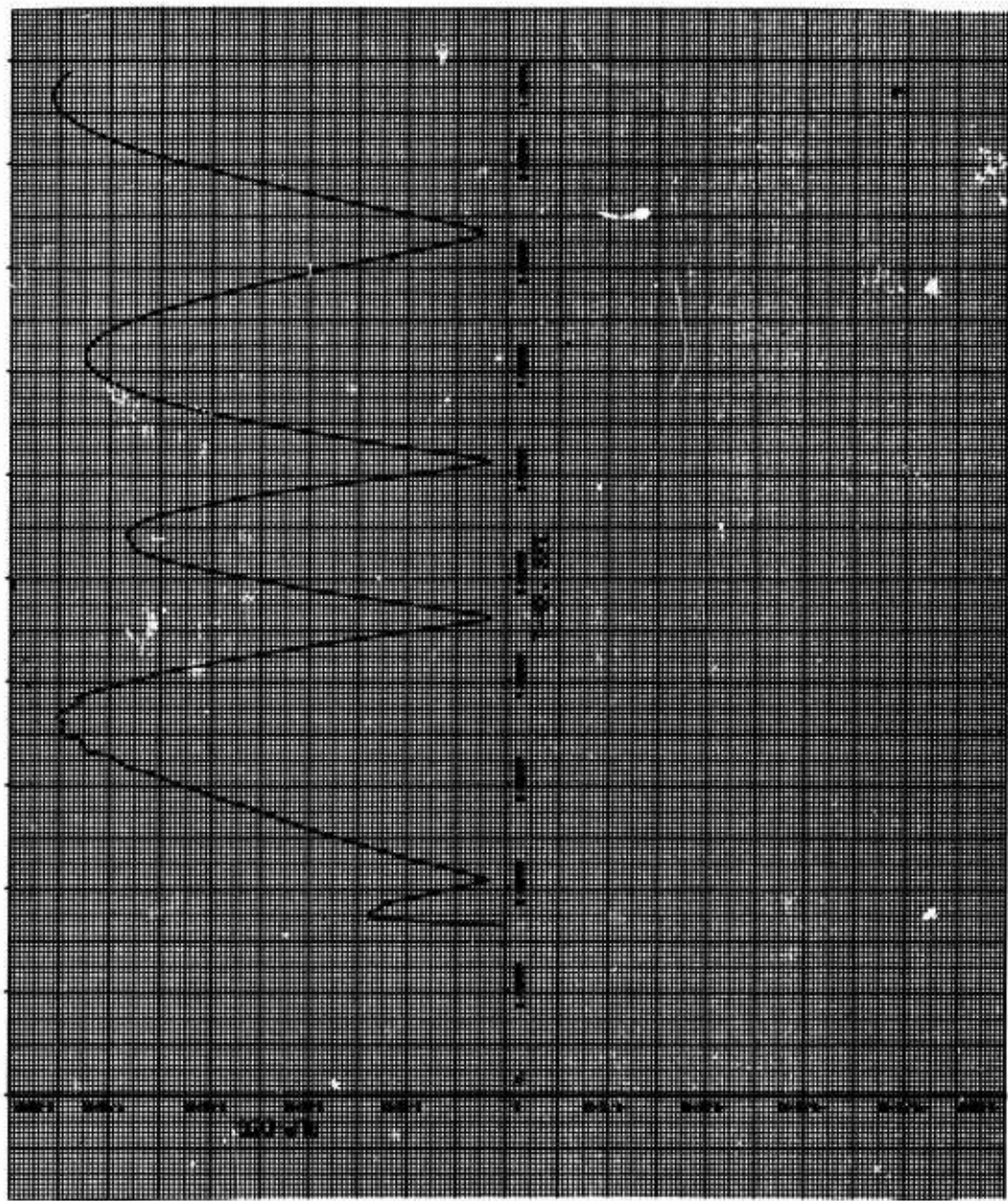


Figure 126. Graph for Miss Distance 6000 Feet

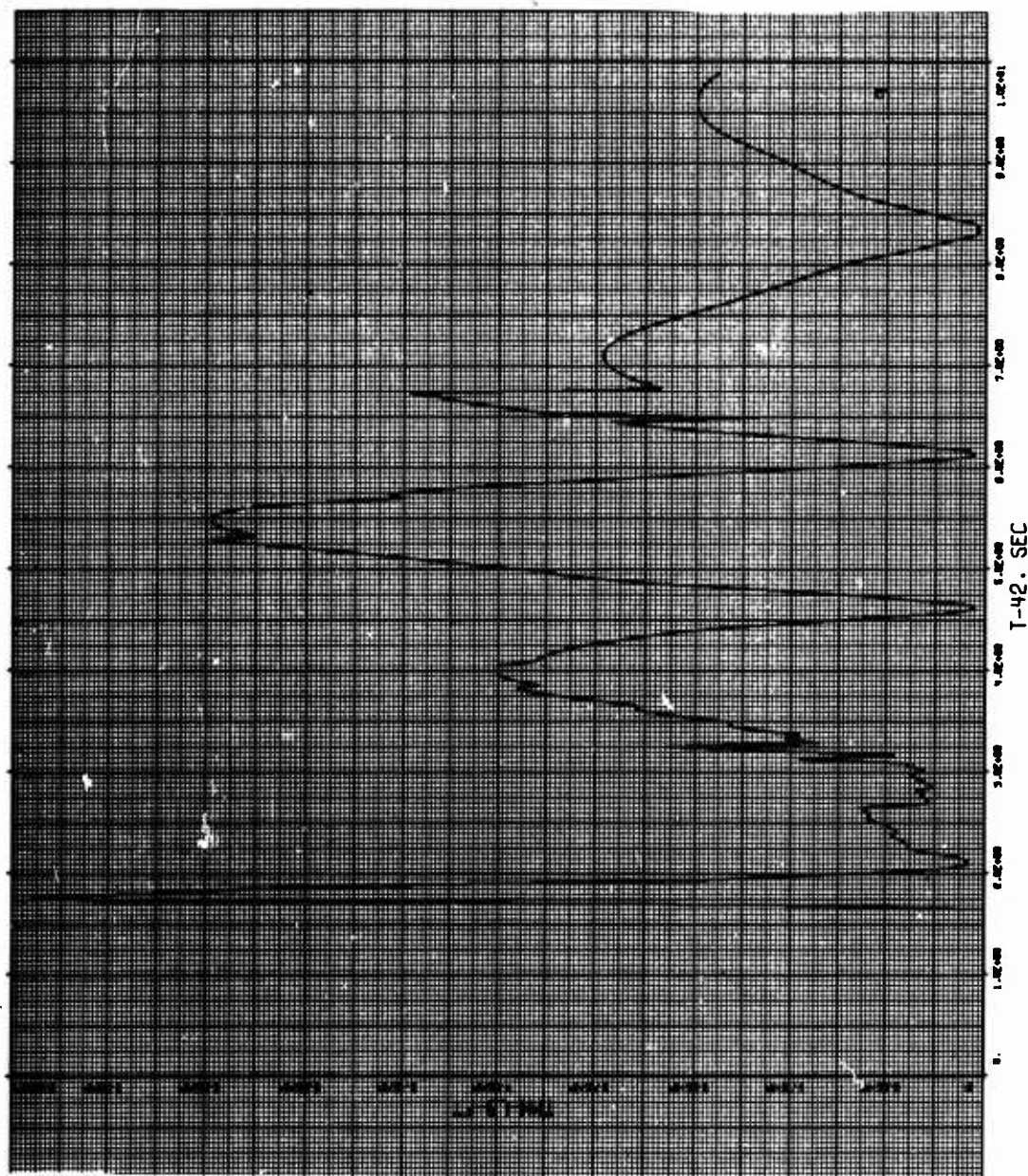


Figure 127. Graph for Miss Distance 6000 Feet

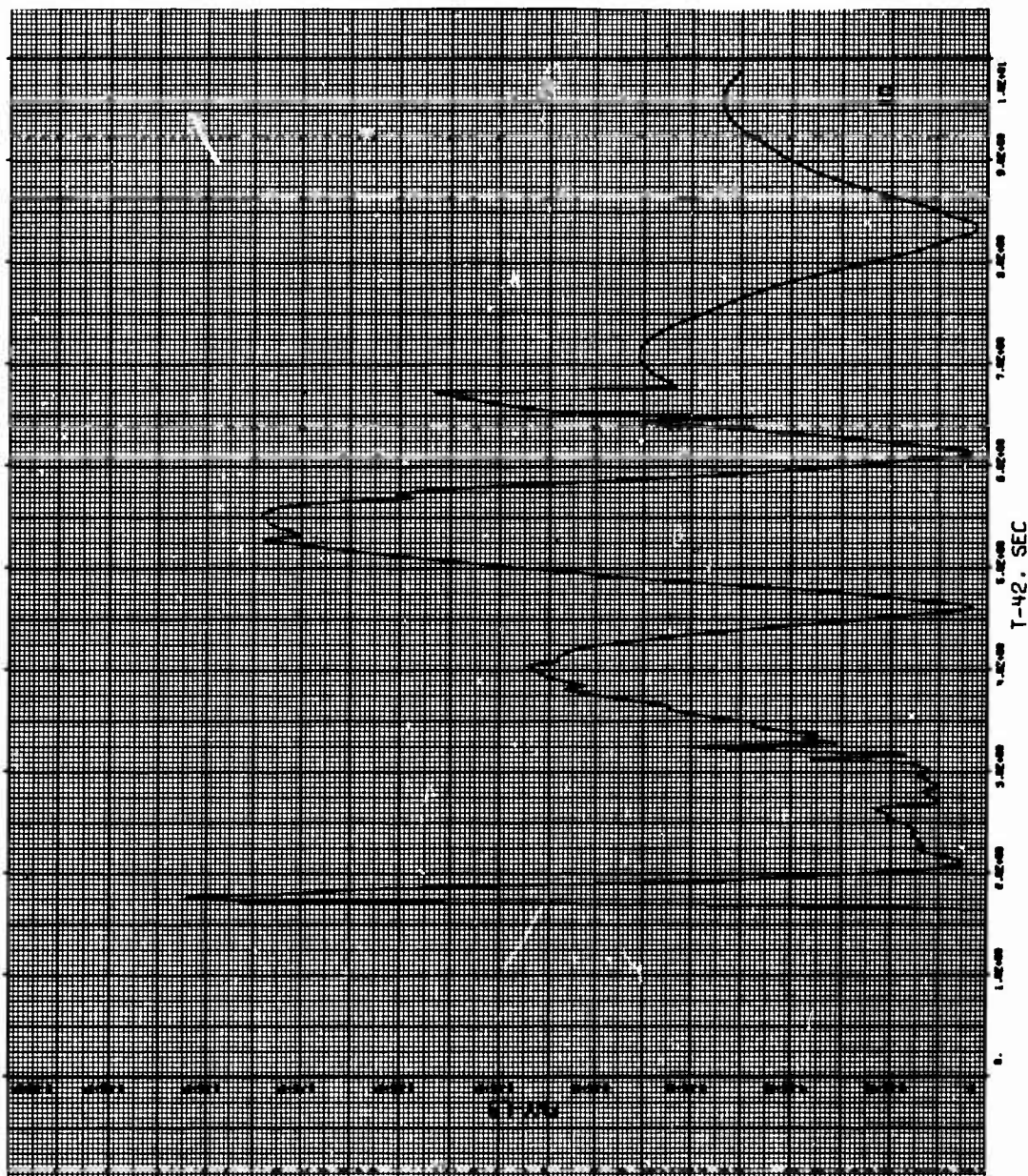


Figure 128. Graph for Miss Distance 6000 Feet

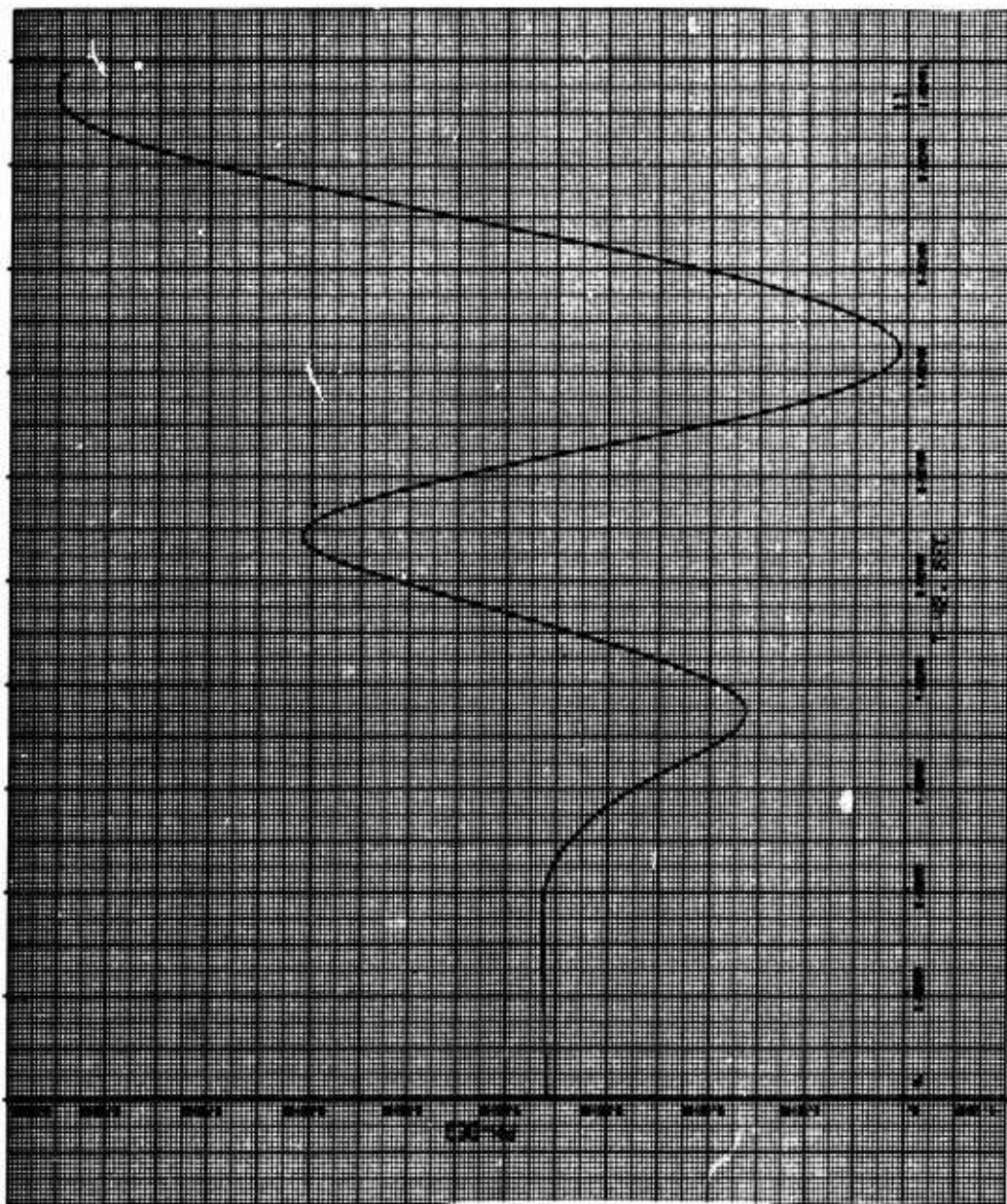


Figure 129. Graph for Miss Distance 6000 Feet

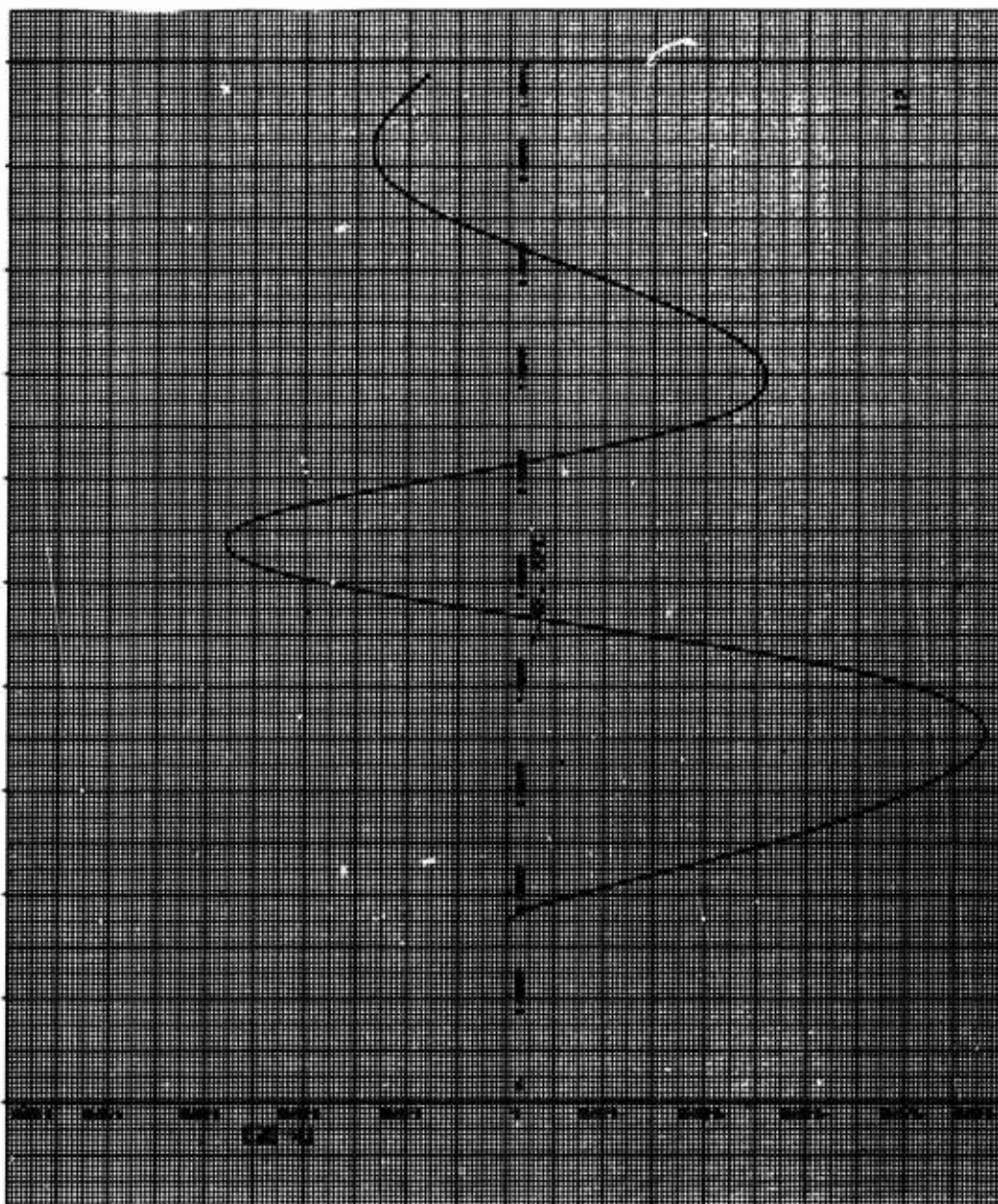


Figure 130. Graph for Miss Distance 6000 Feet

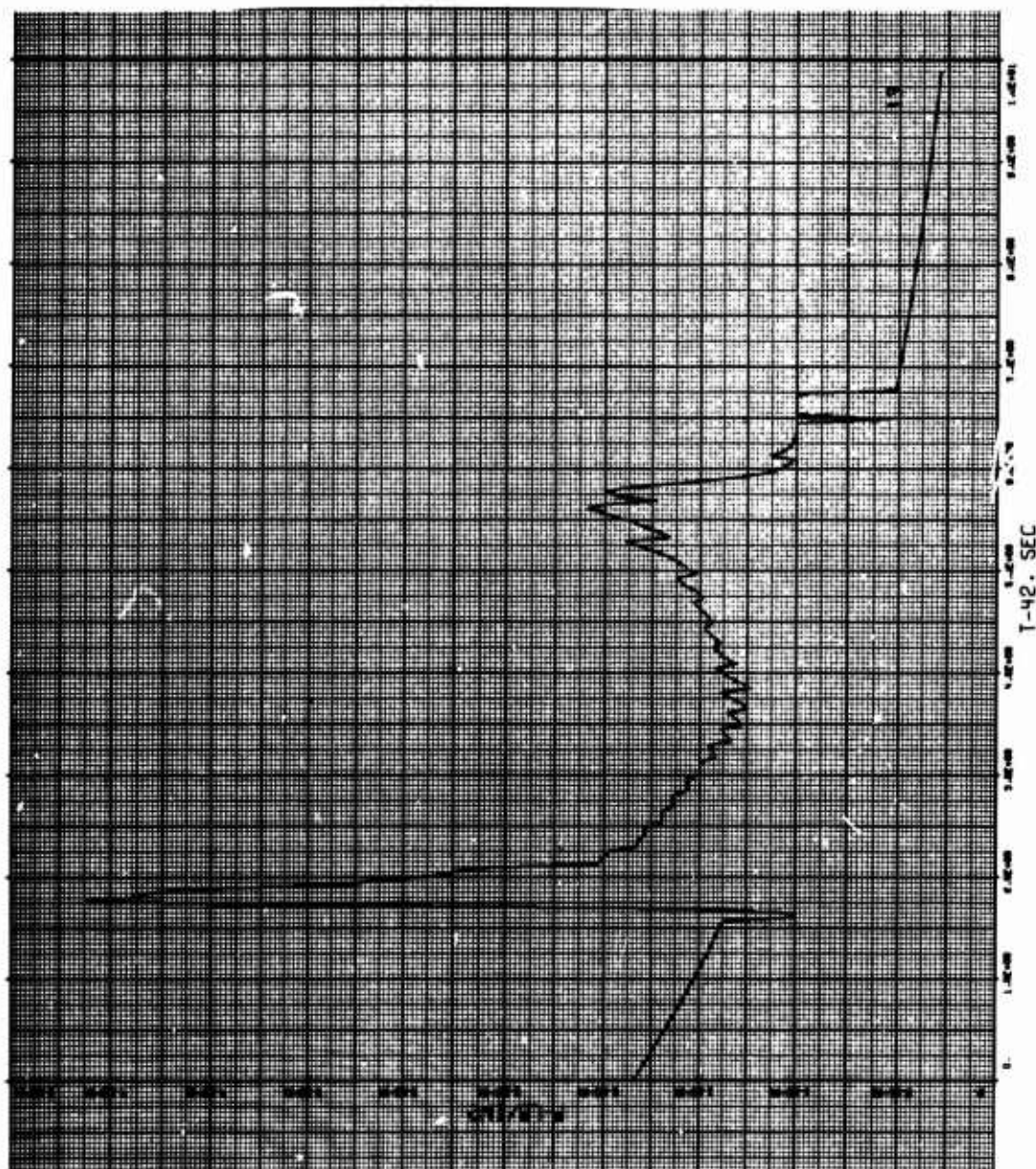


Figure 131. Graph for Miss Distance 6000 Feet

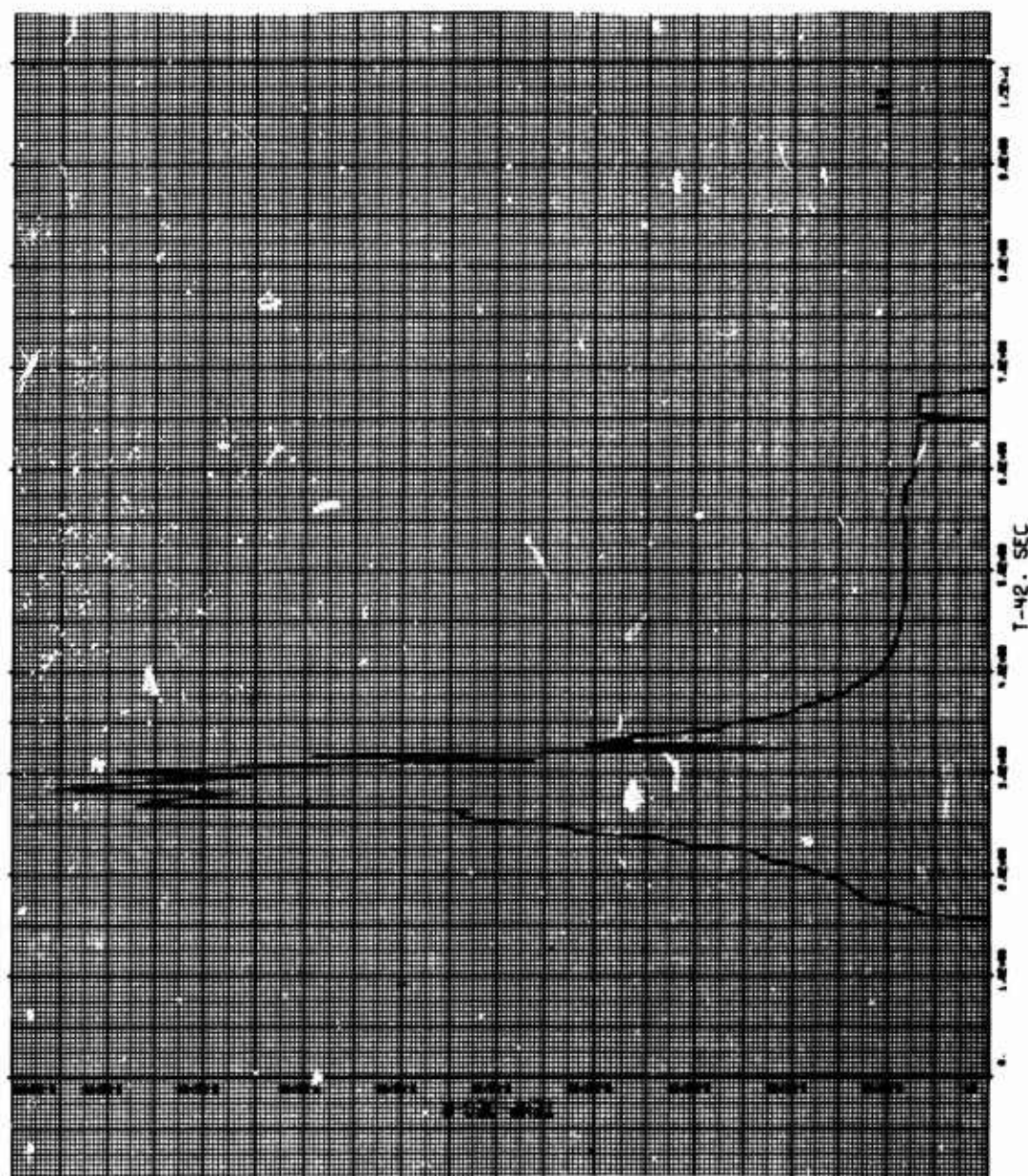


Figure 132. Graph for Miss Distance 6000 Feet

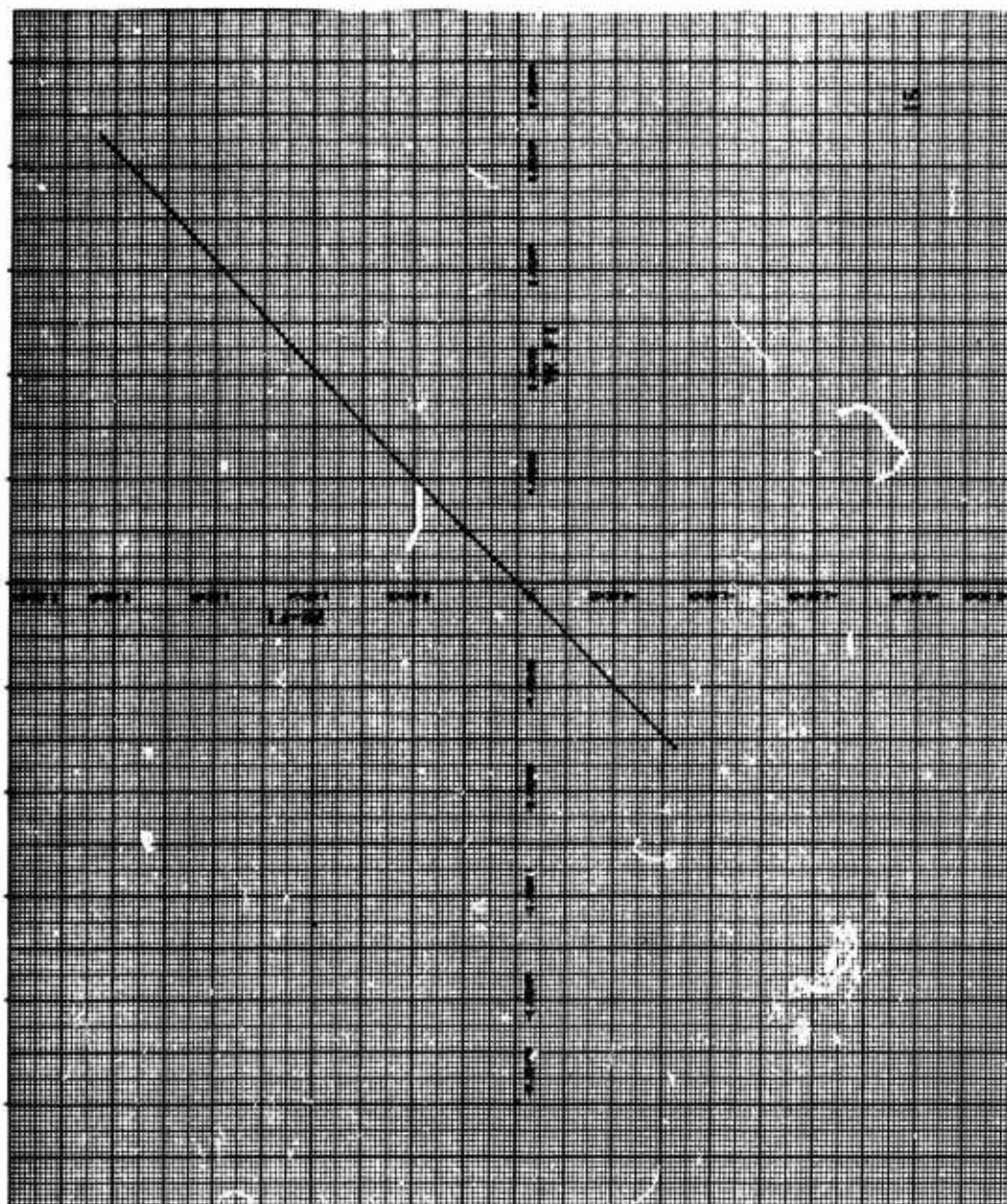


Figure 133. Graph for Miss Distance 6000 Feet

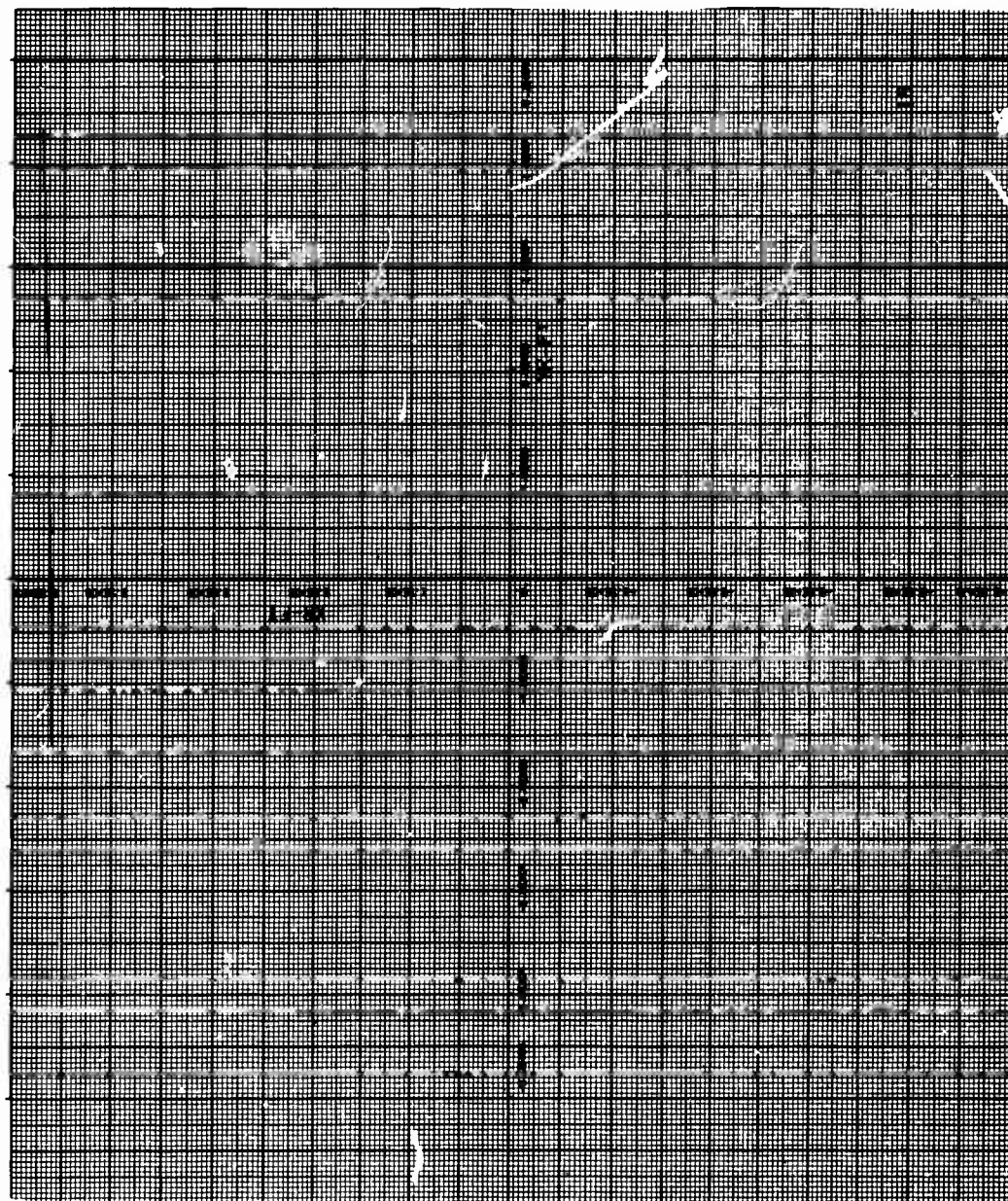


Figure 134. Graph for Miss Distance 6000 Feet

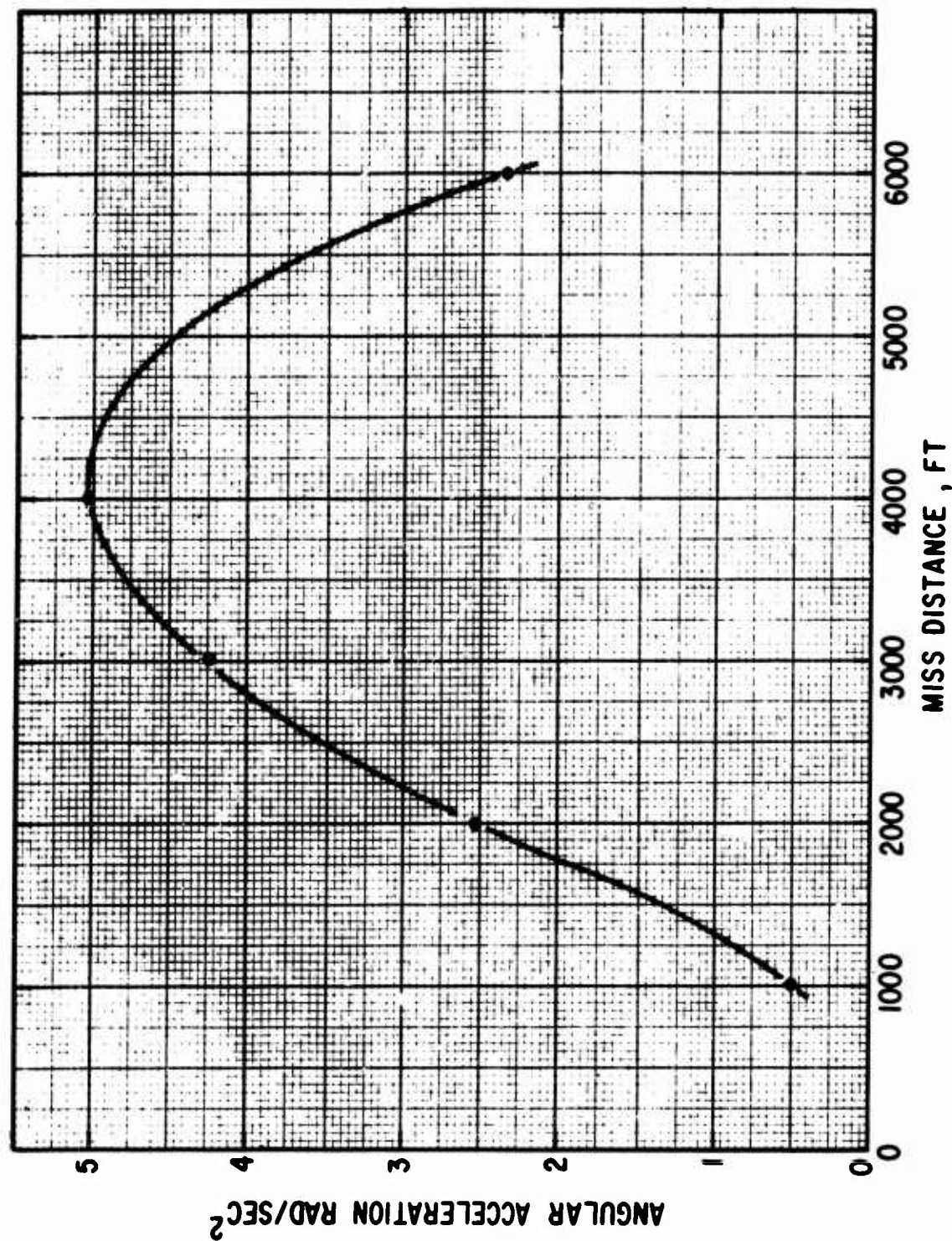


Figure 135. Angular Acceleration at Shock Penetration

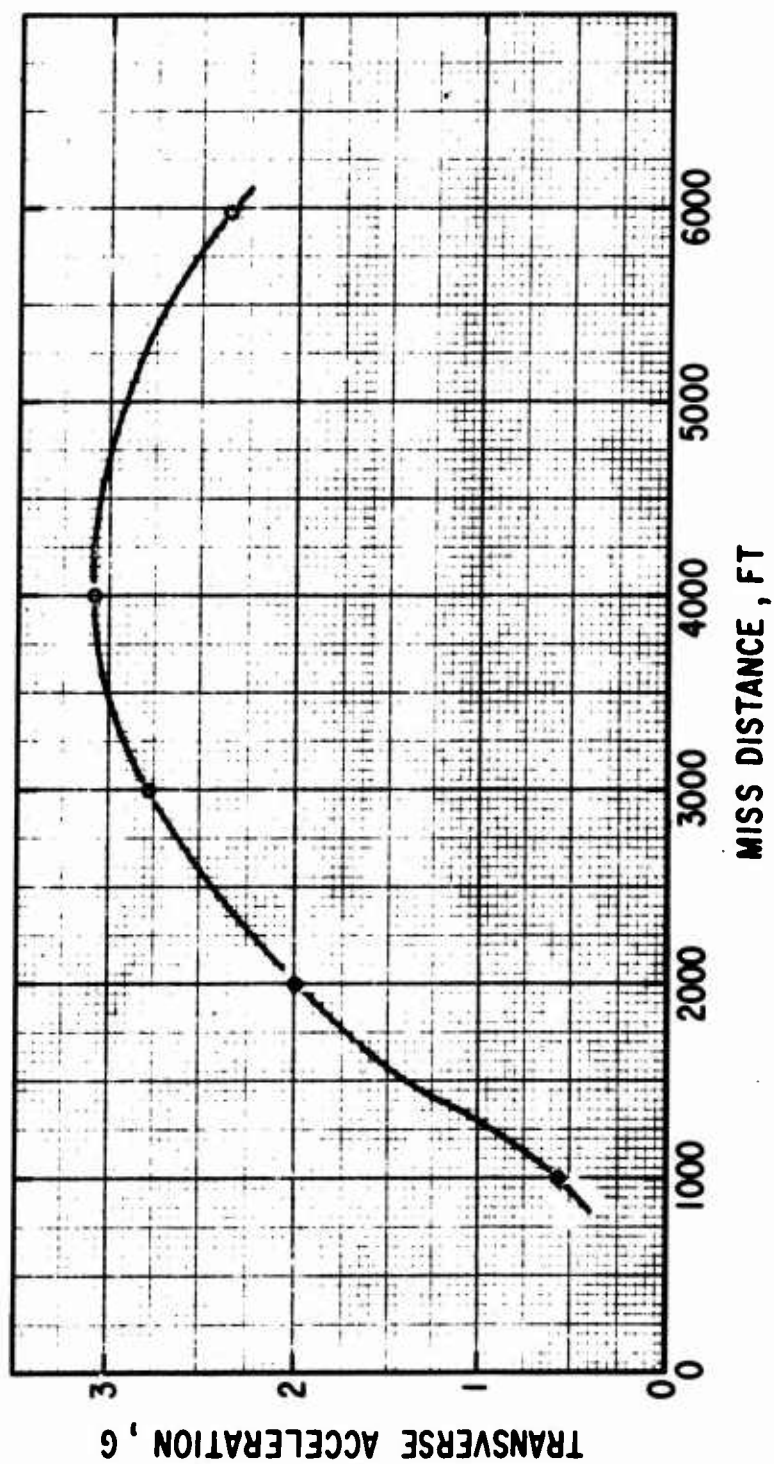


Figure 136. Transverse Acceleration at Shock Penetration

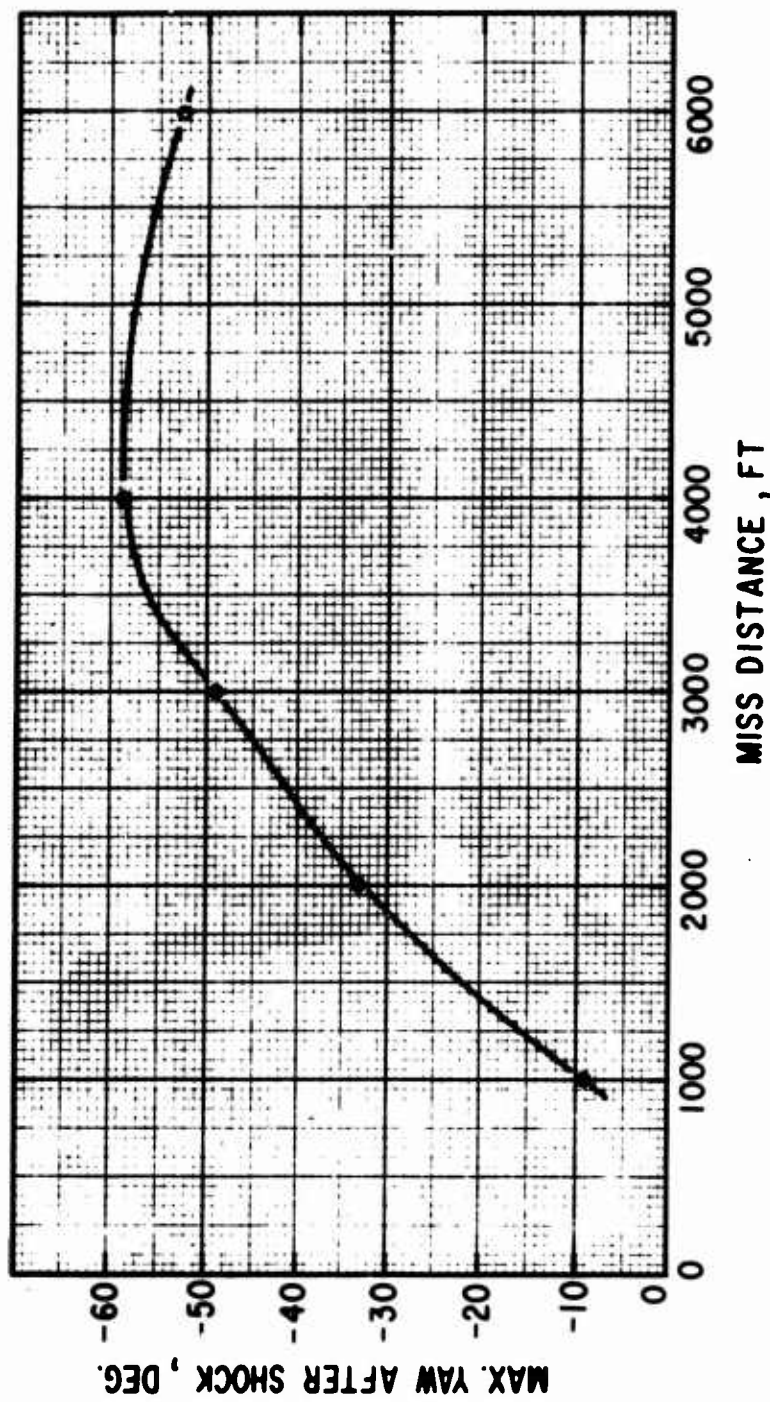


Figure 137. Maximum Yaw Angle After Shock Penetration

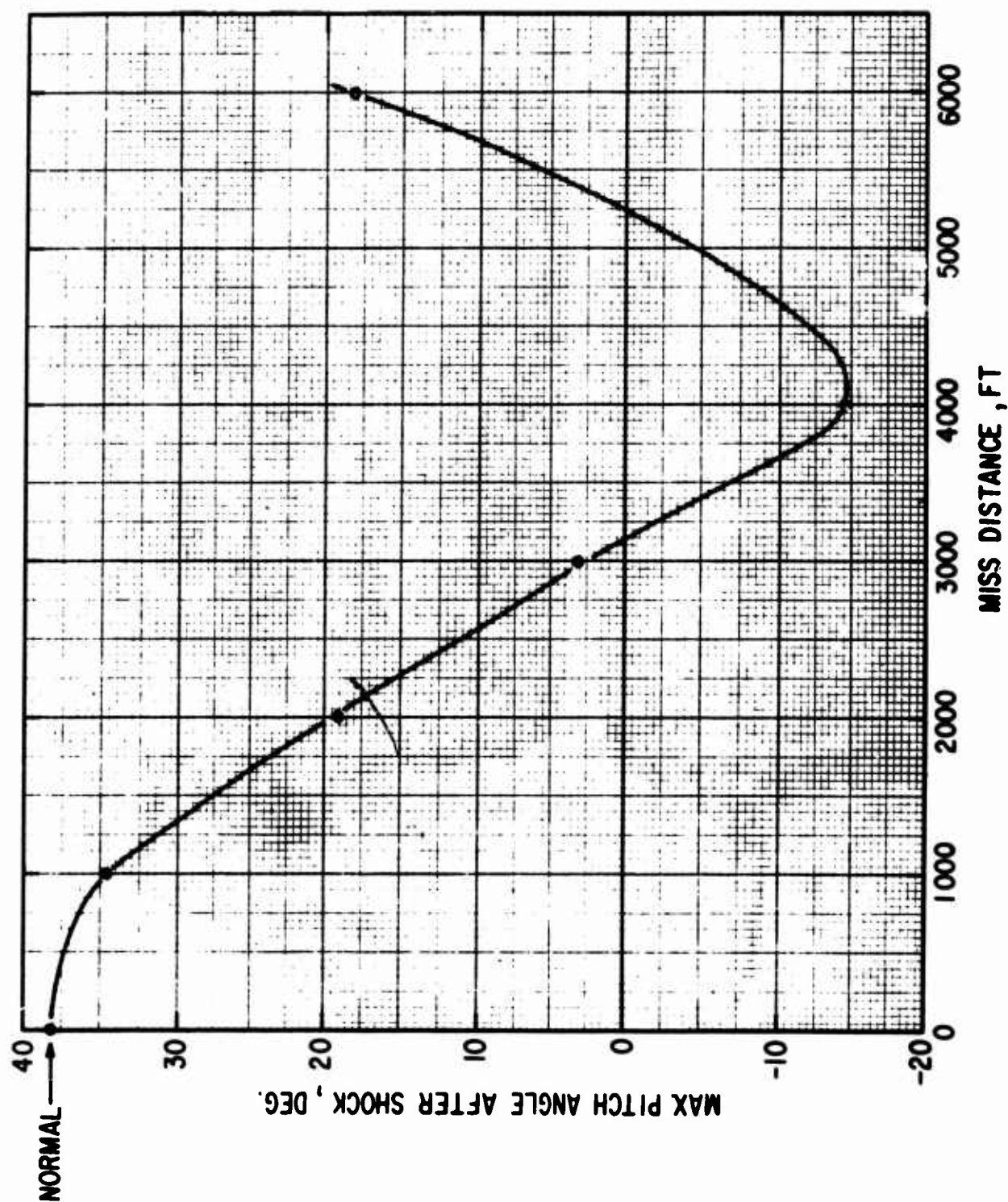


Figure 138. Maximum Pitch Angle After Shock Penetration

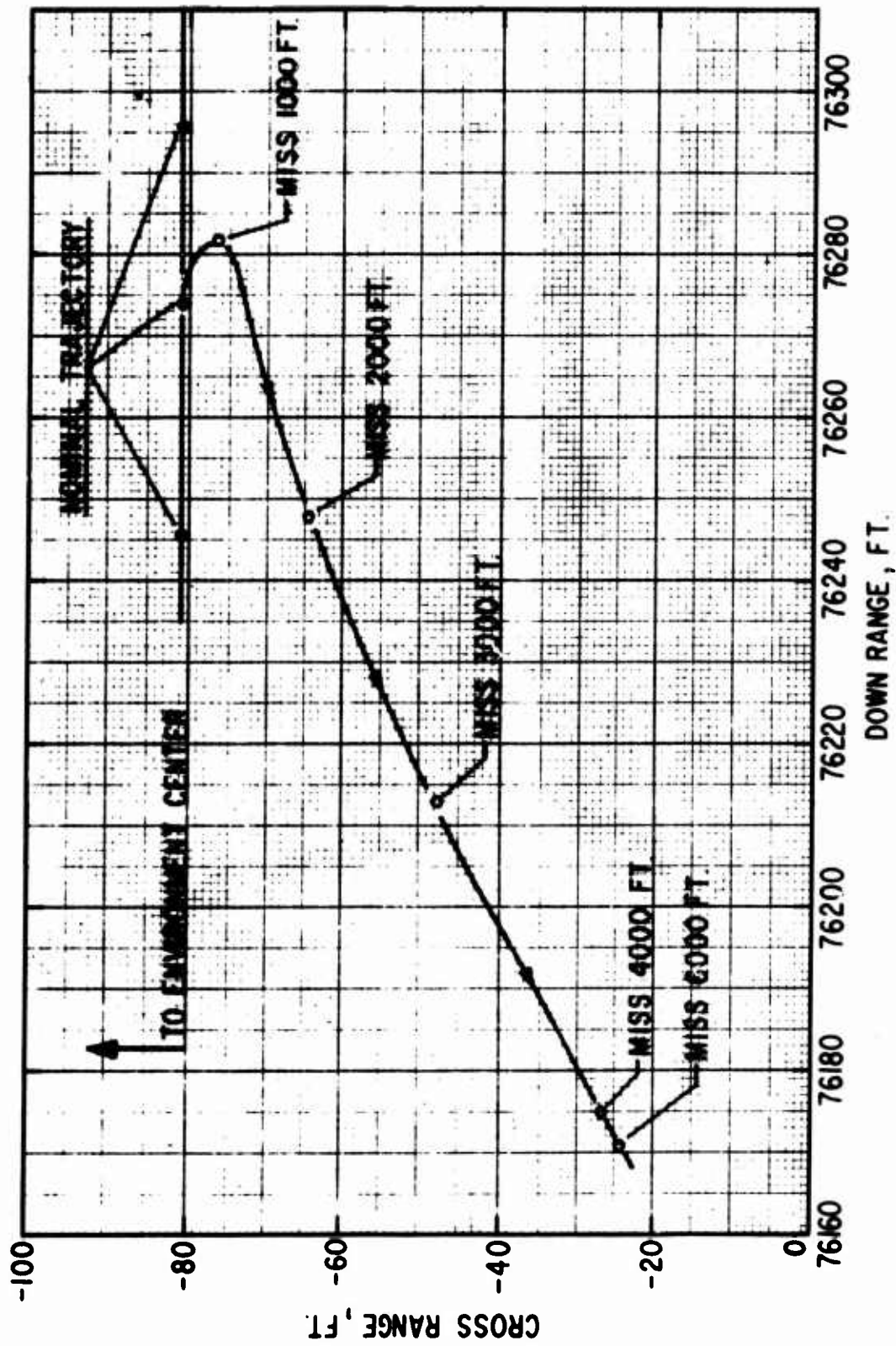


Figure 139. Position Change in Horizontal Plane at 49 Seconds

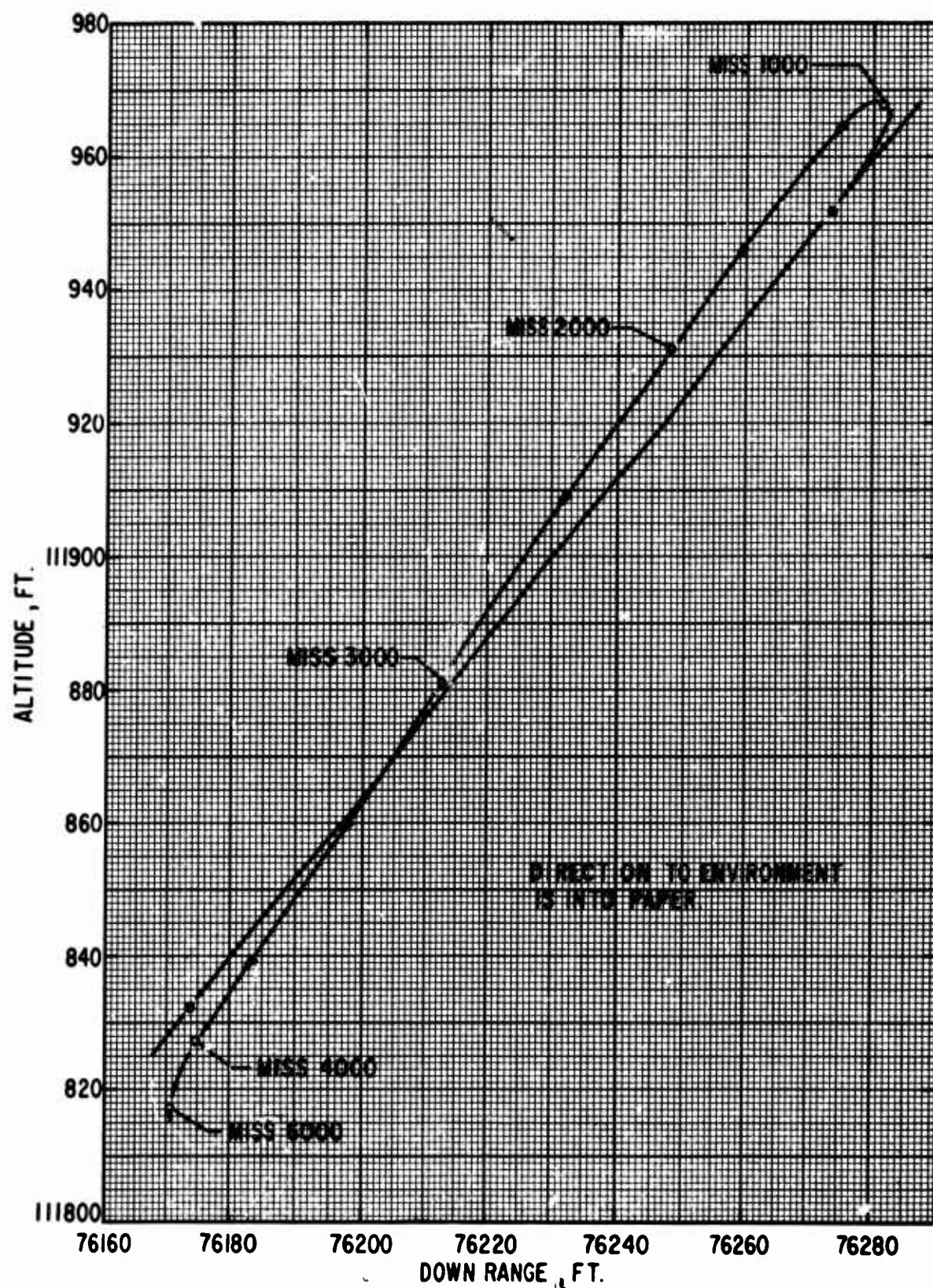


Figure 140. Position Change in Vertical Plane at 49 Seconds

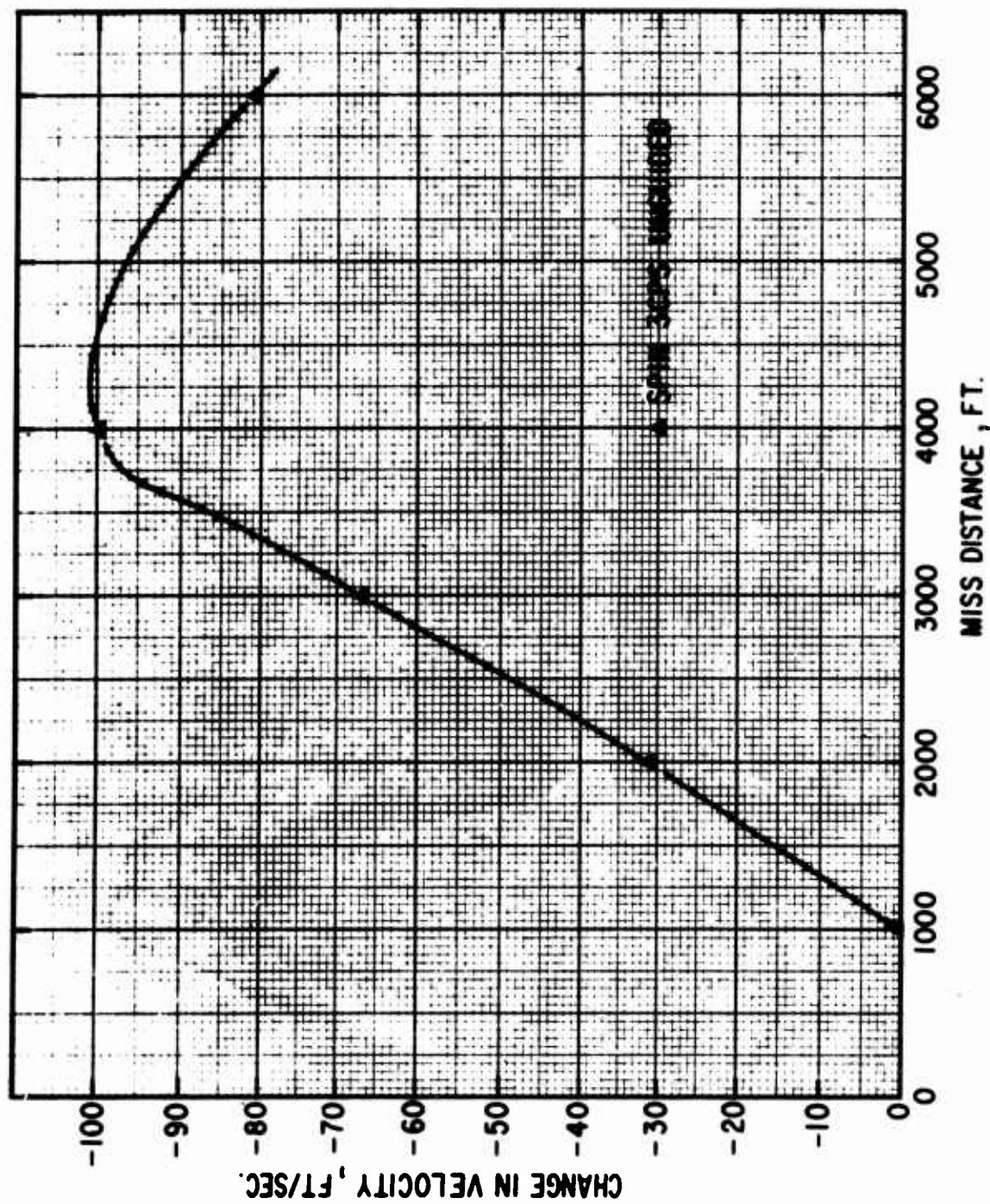


Figure 141. Change in Velocity at 49 Seconds

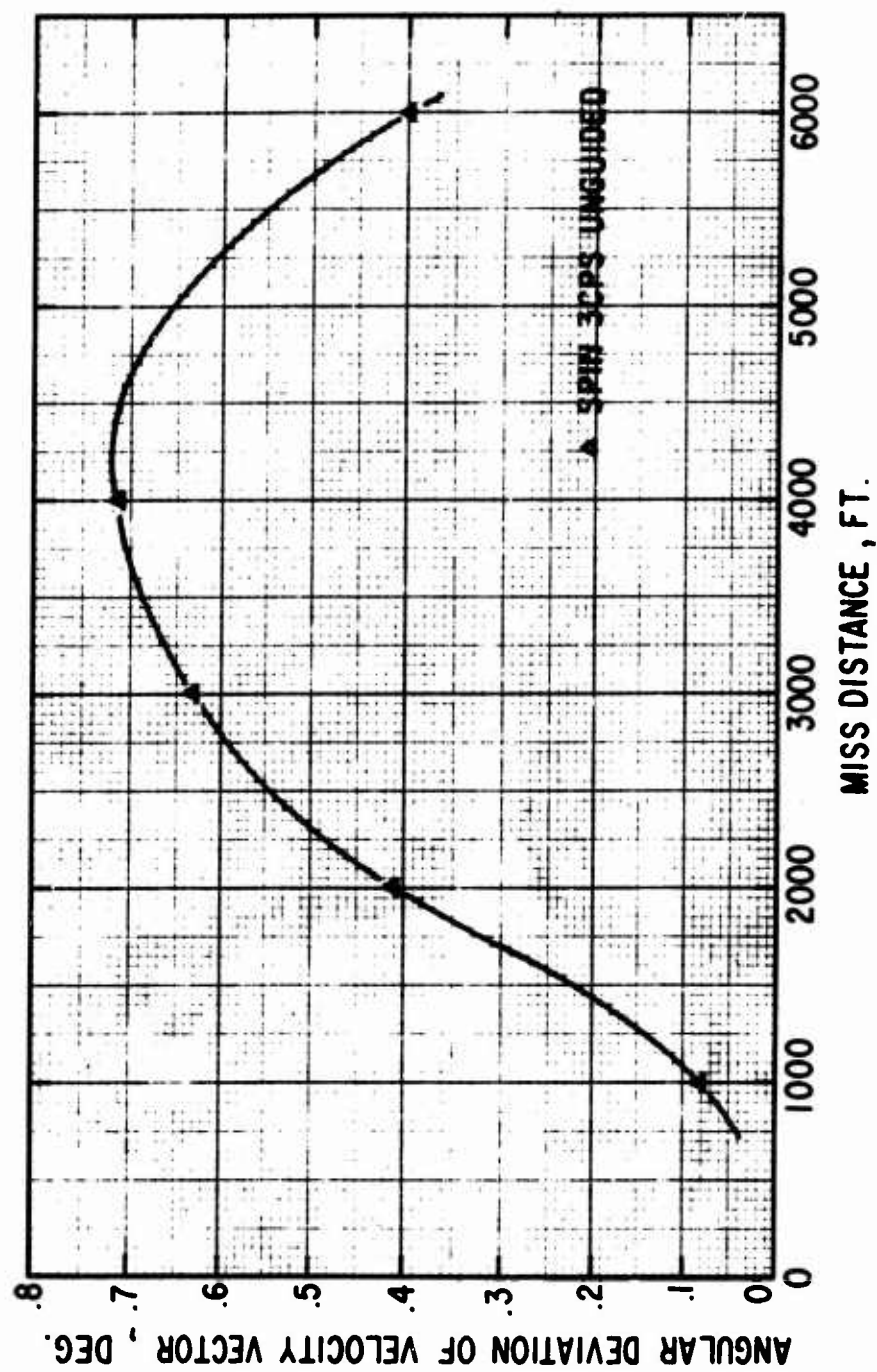


Figure 142. Angular Perturbation of Velocity Vector at 49 Seconds

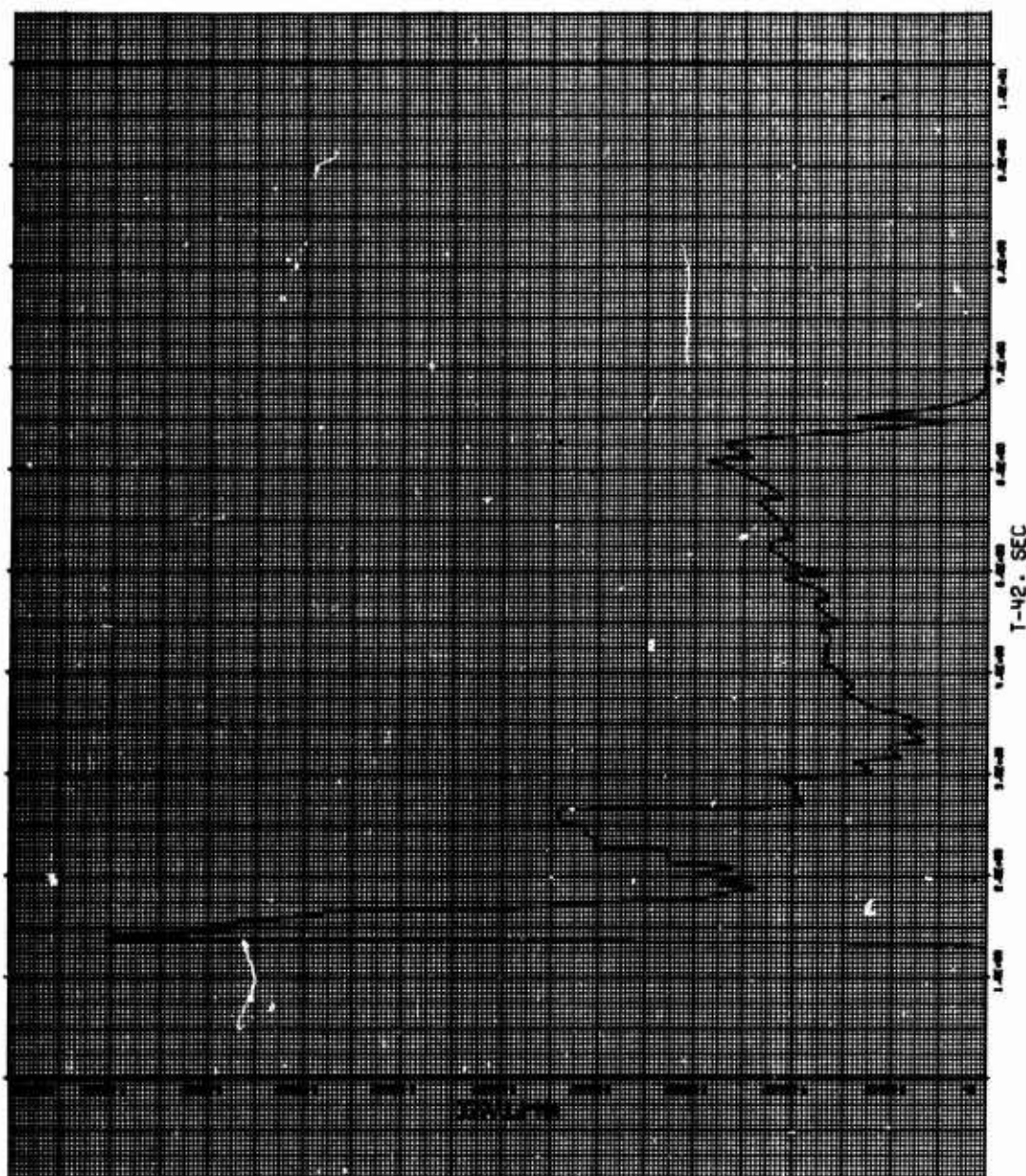


Figure 143. Graph for No Spin

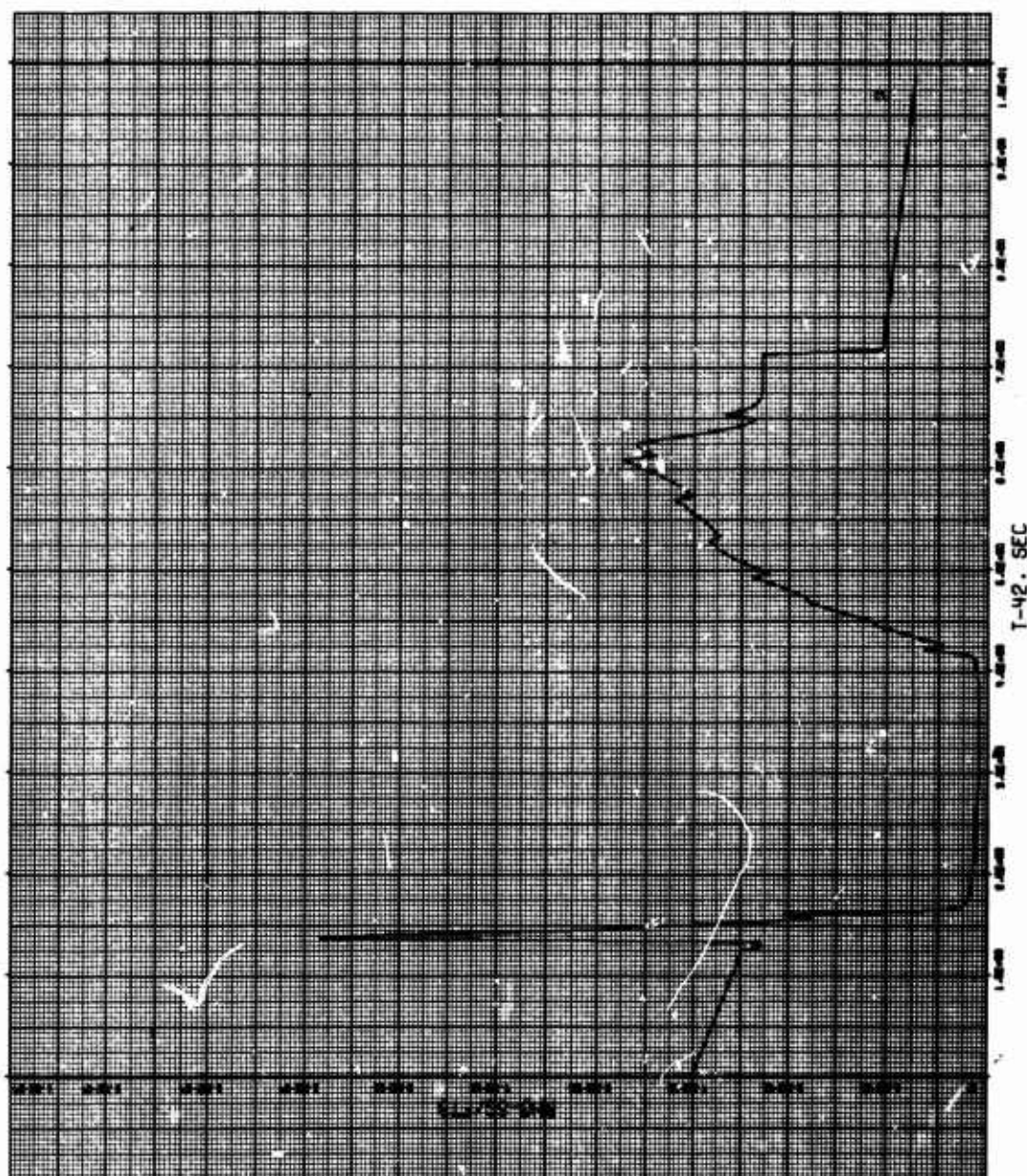


Figure 144. Graph for No Spin

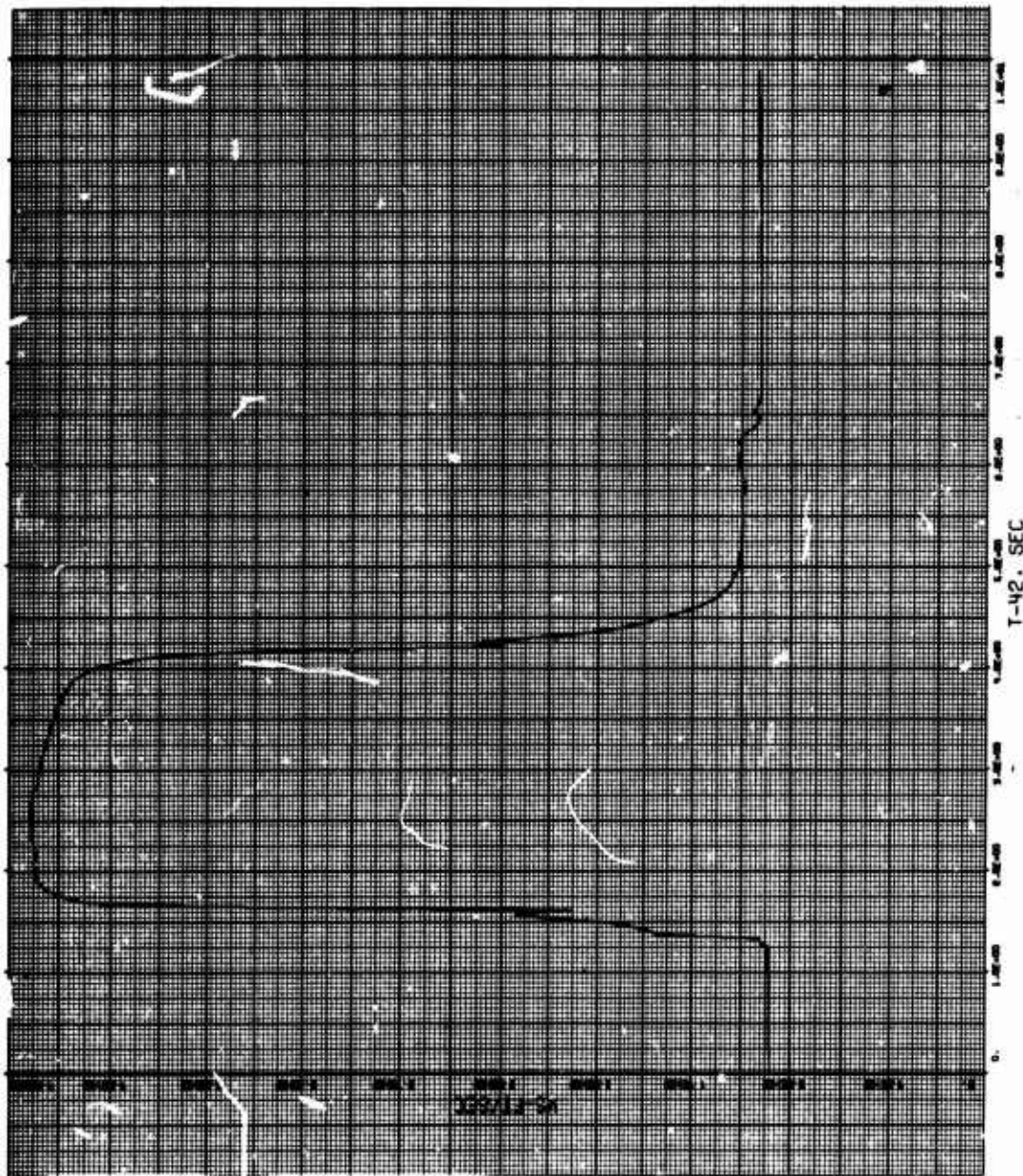


Figure 145. Graph for No Spin

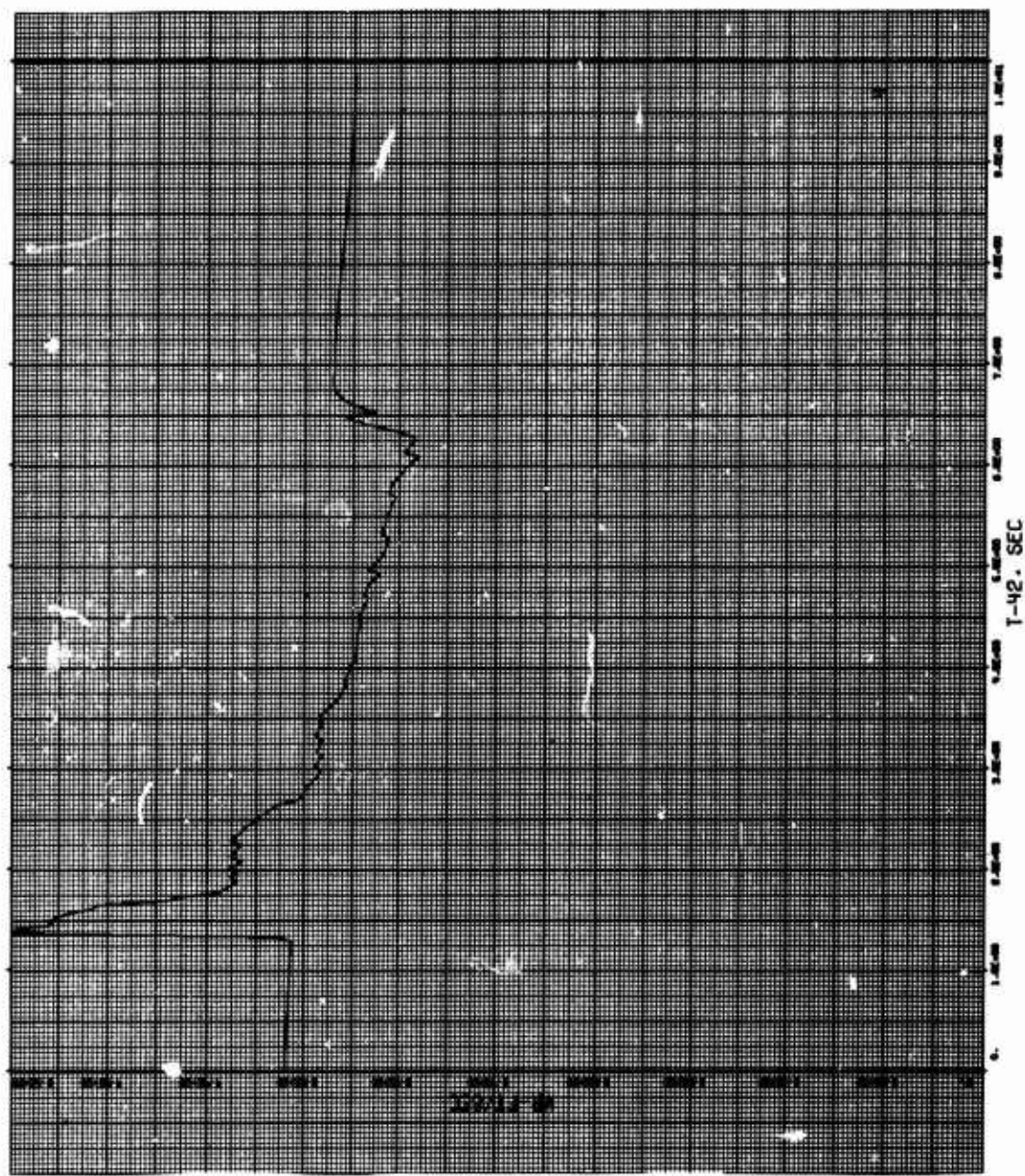


Figure 146. Graph for No Spin

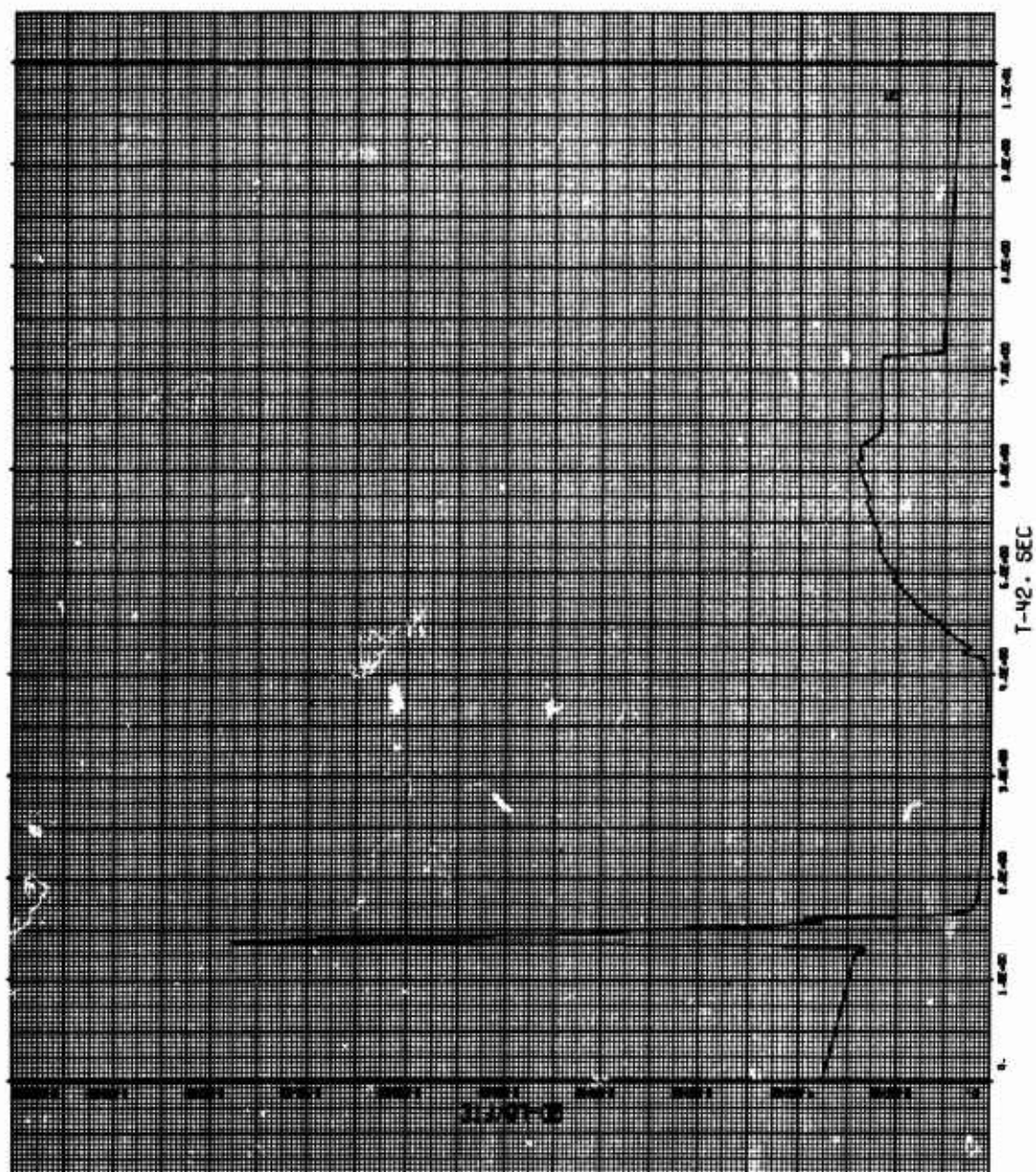


Figure 147. Graph for No Spin

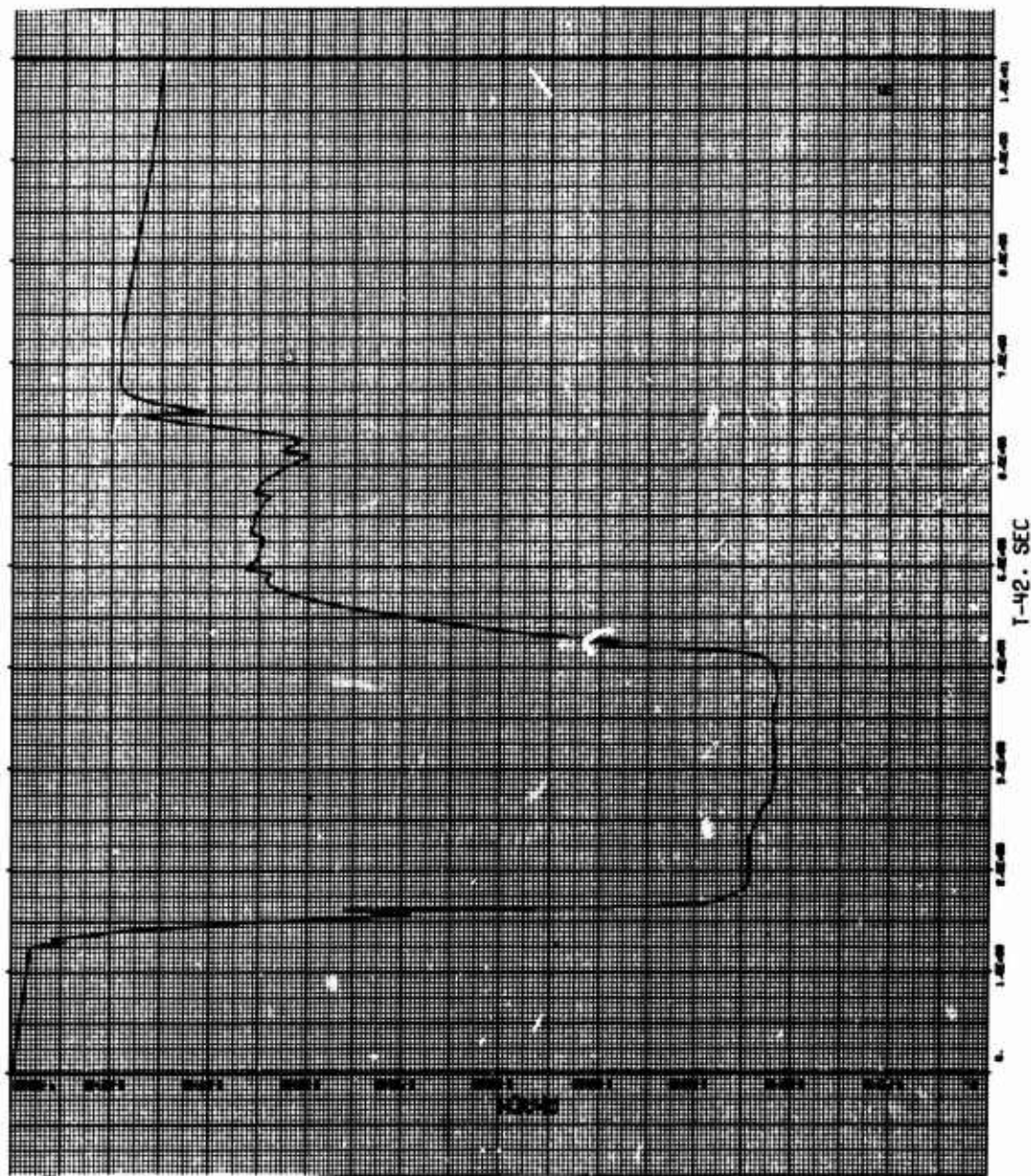


Figure 148. Graph for No Spin

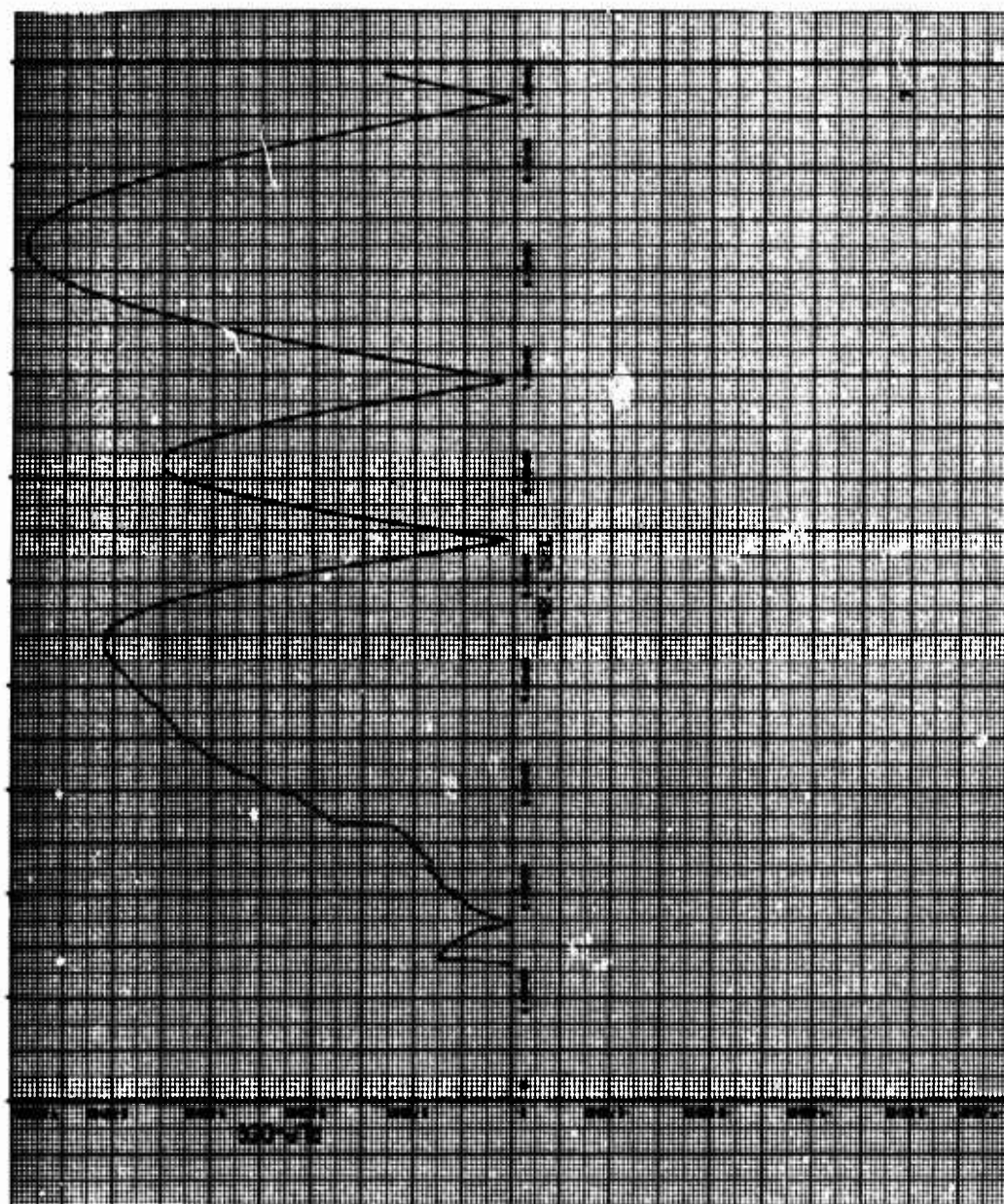


Figure 149. Graph for No Spin

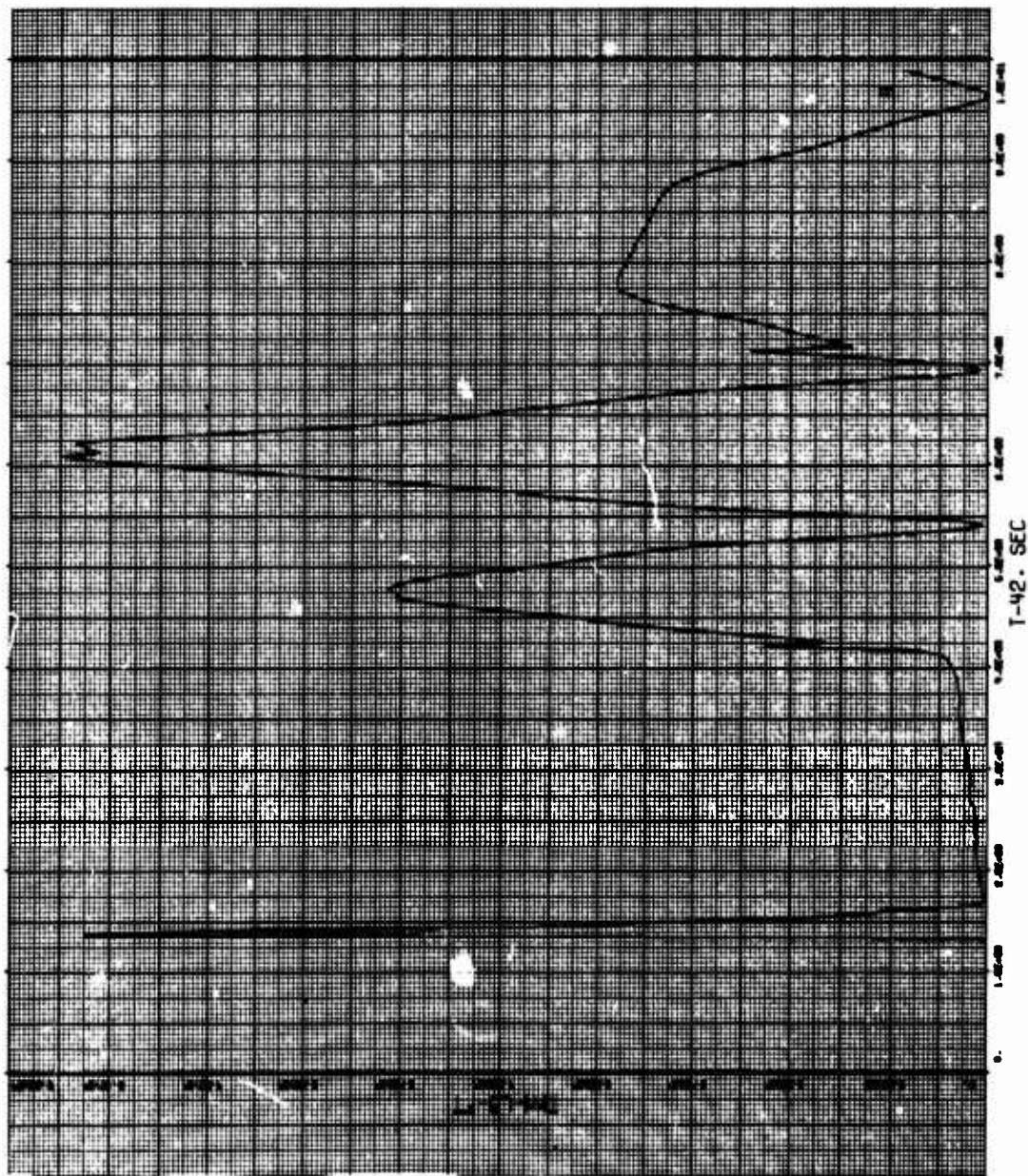


Figure 150. Graph for No Spin

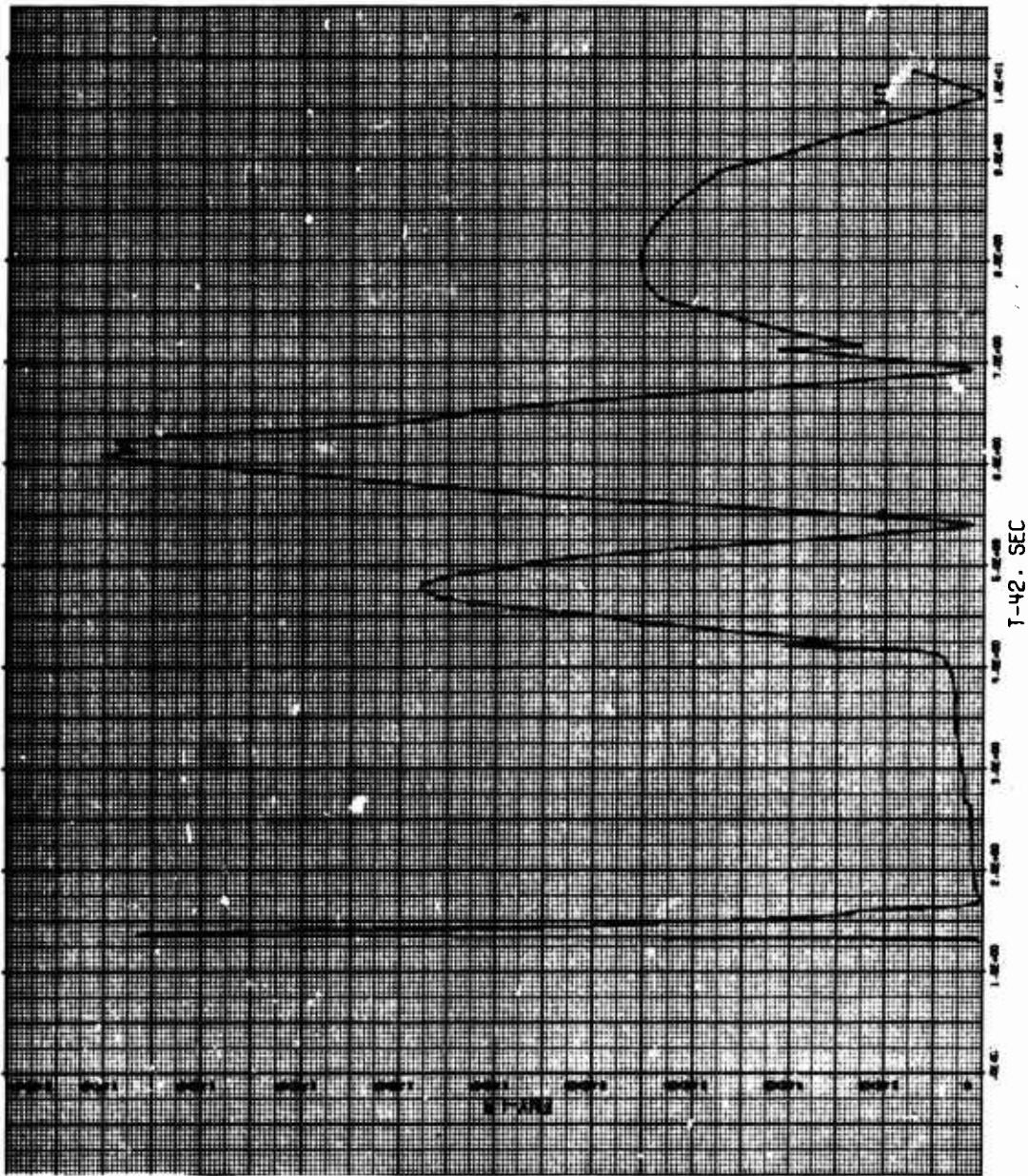


Figure 151. Graph for No Spin

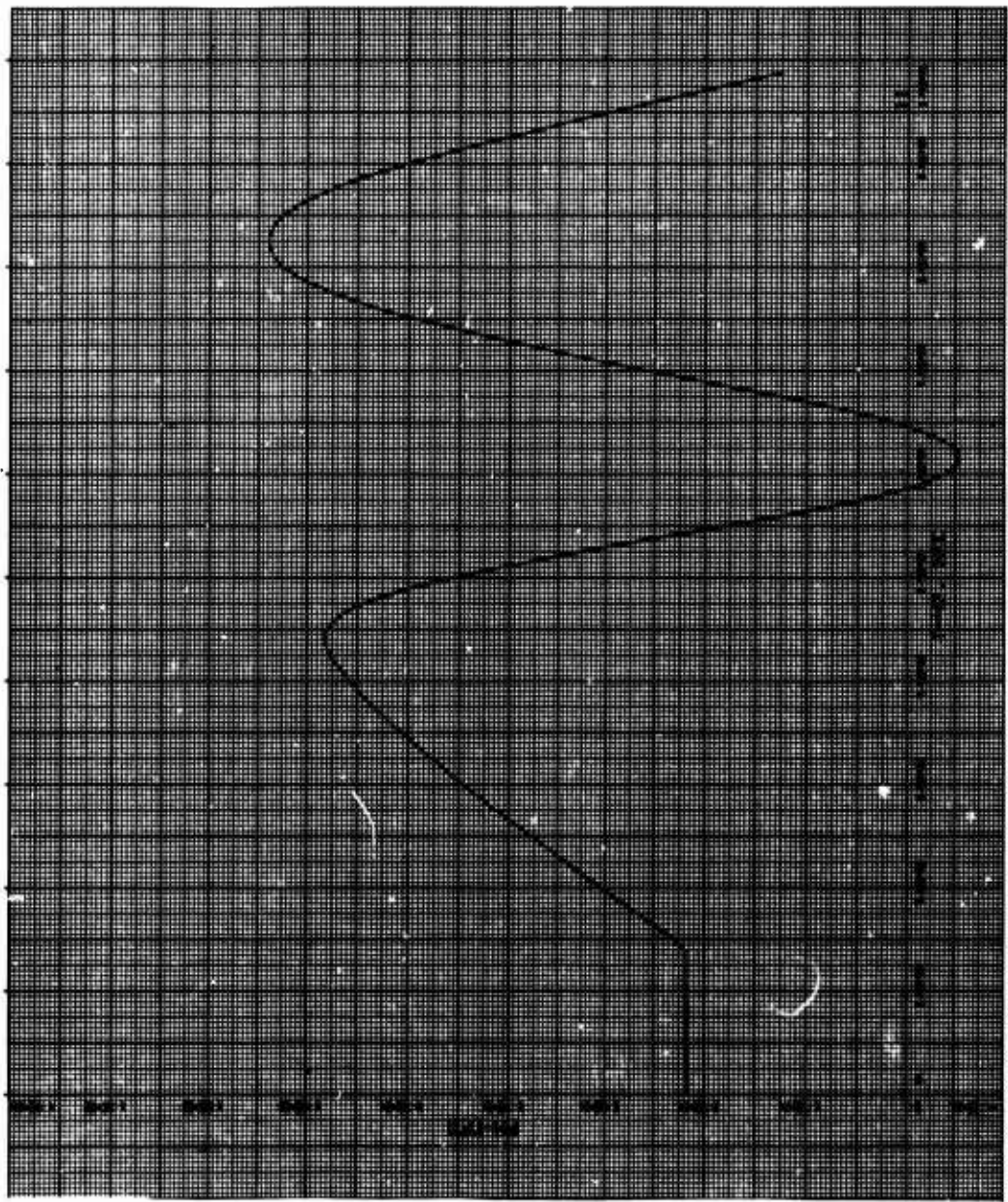


Figure 152. Graph for No Spin

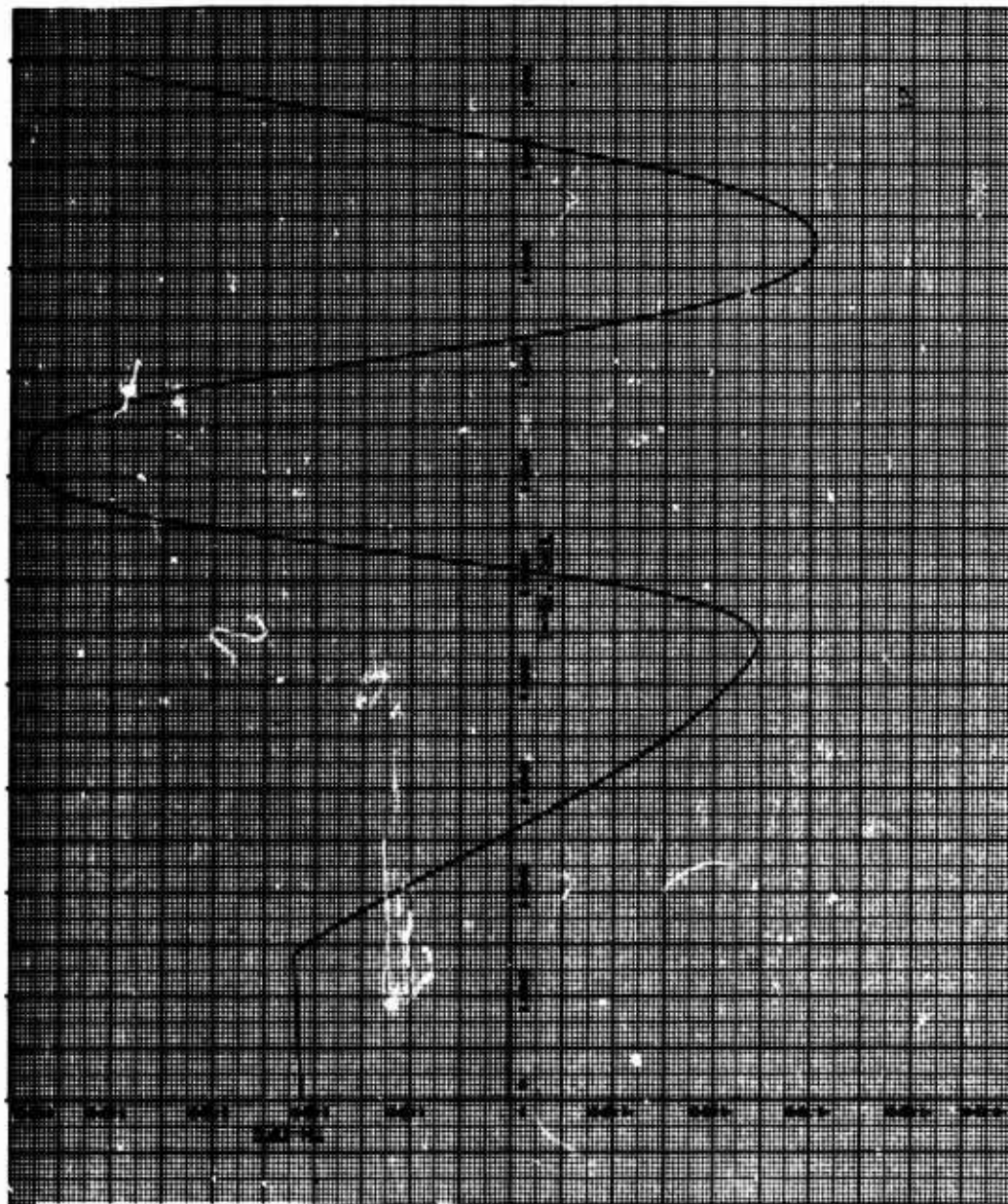


Figure 153. Graph for No Spin

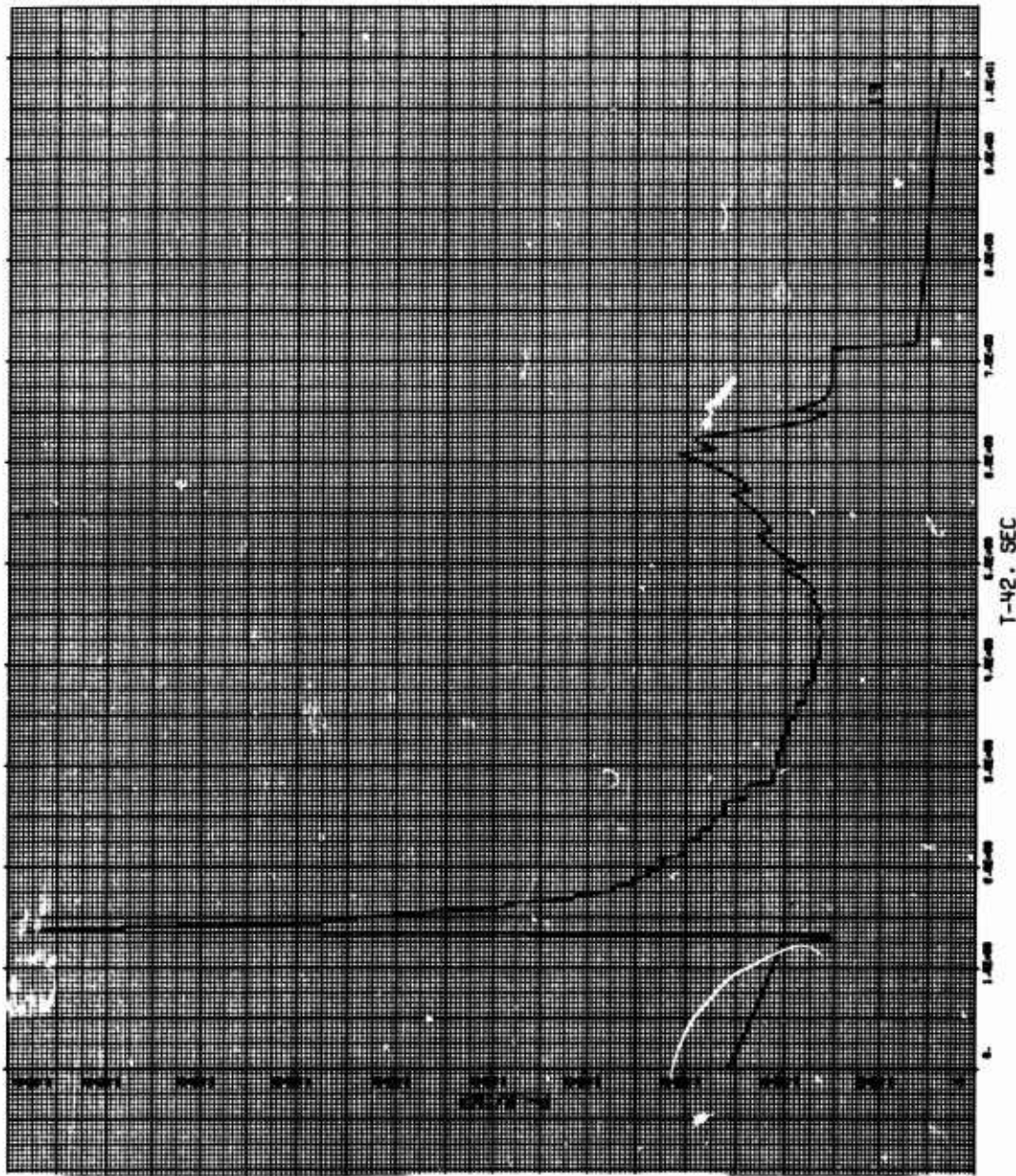


Figure 154. Graph for No Spin

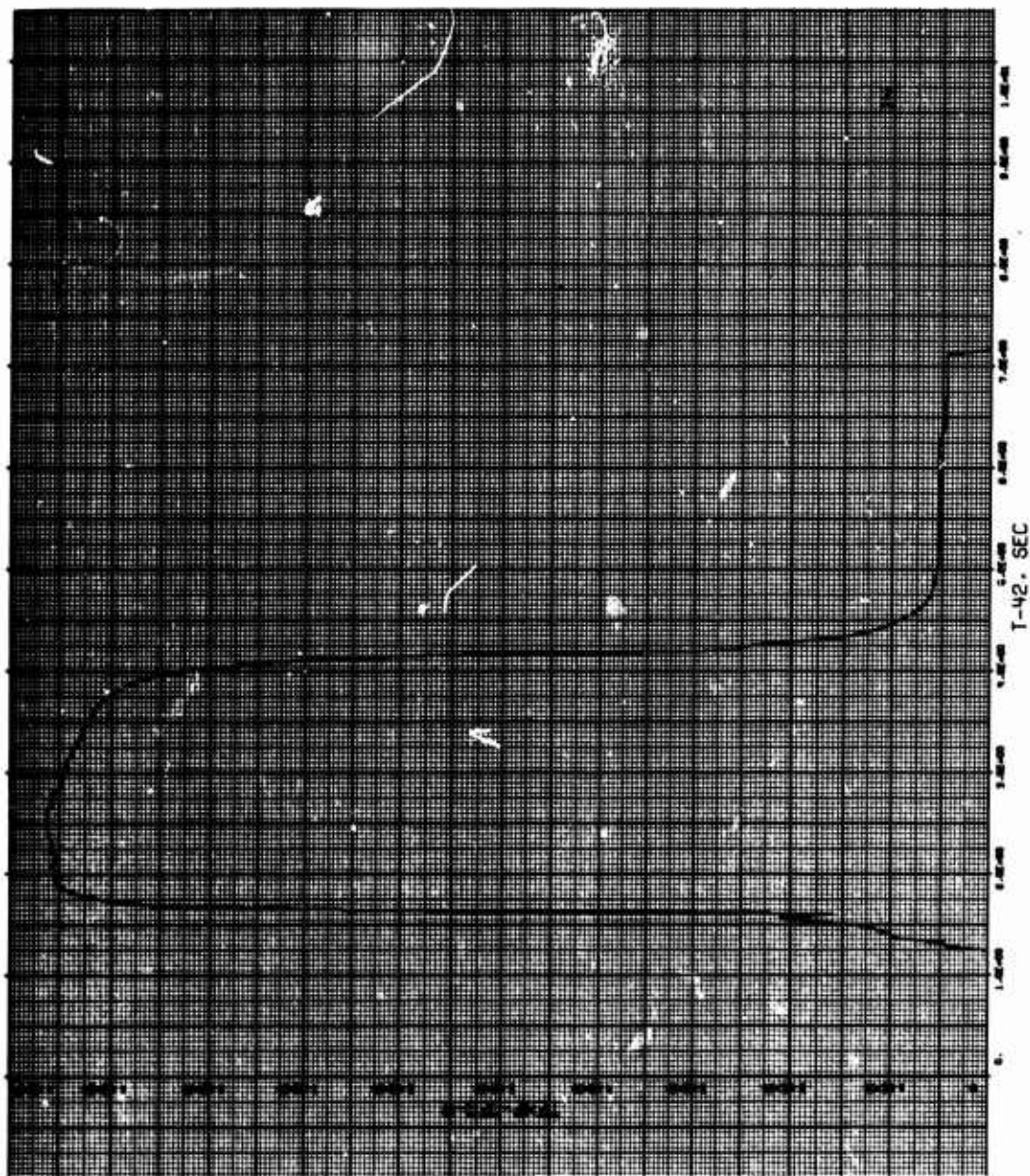


Figure 155. Graph for No Spin

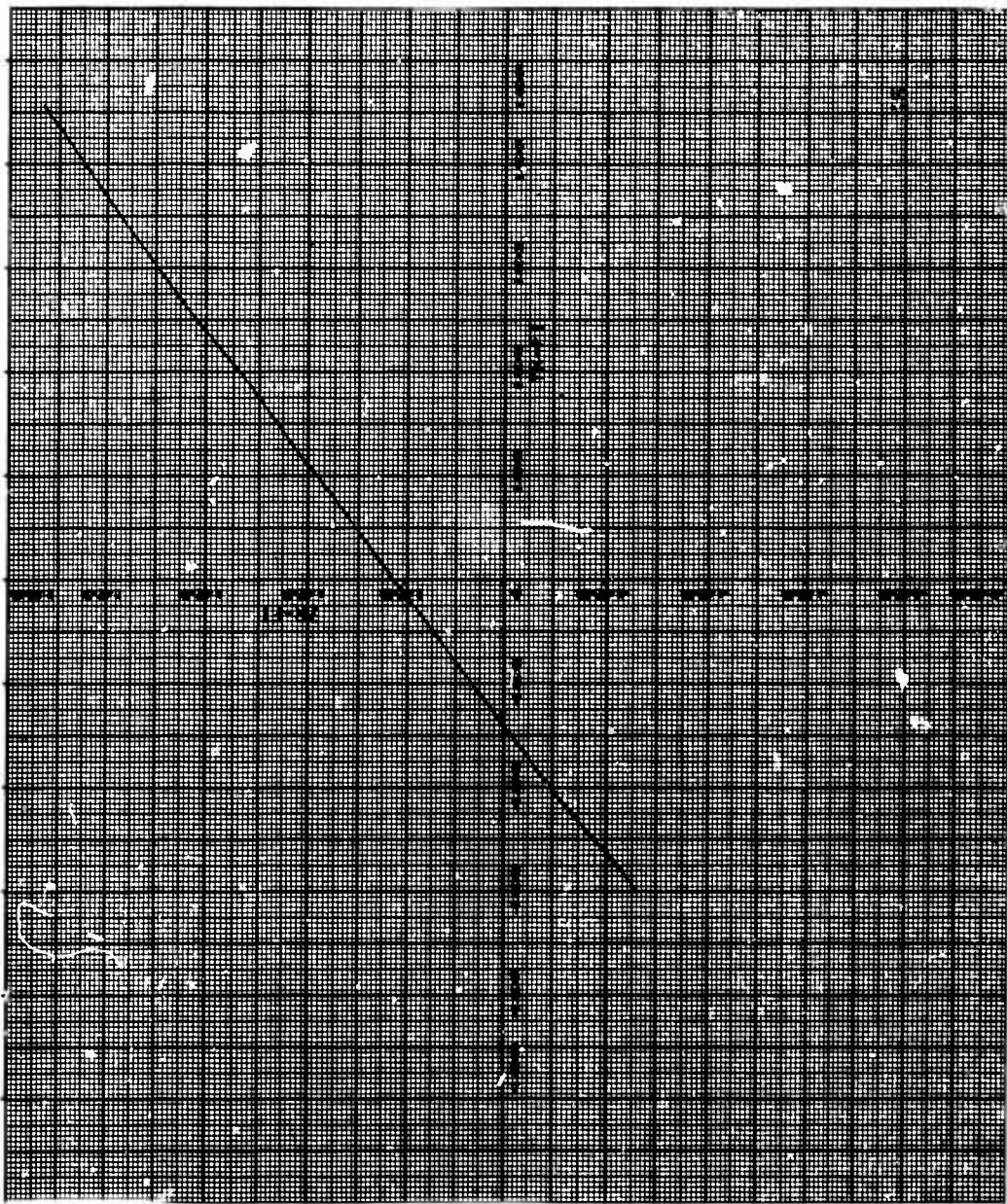


Figure 156. Graph for No Spin

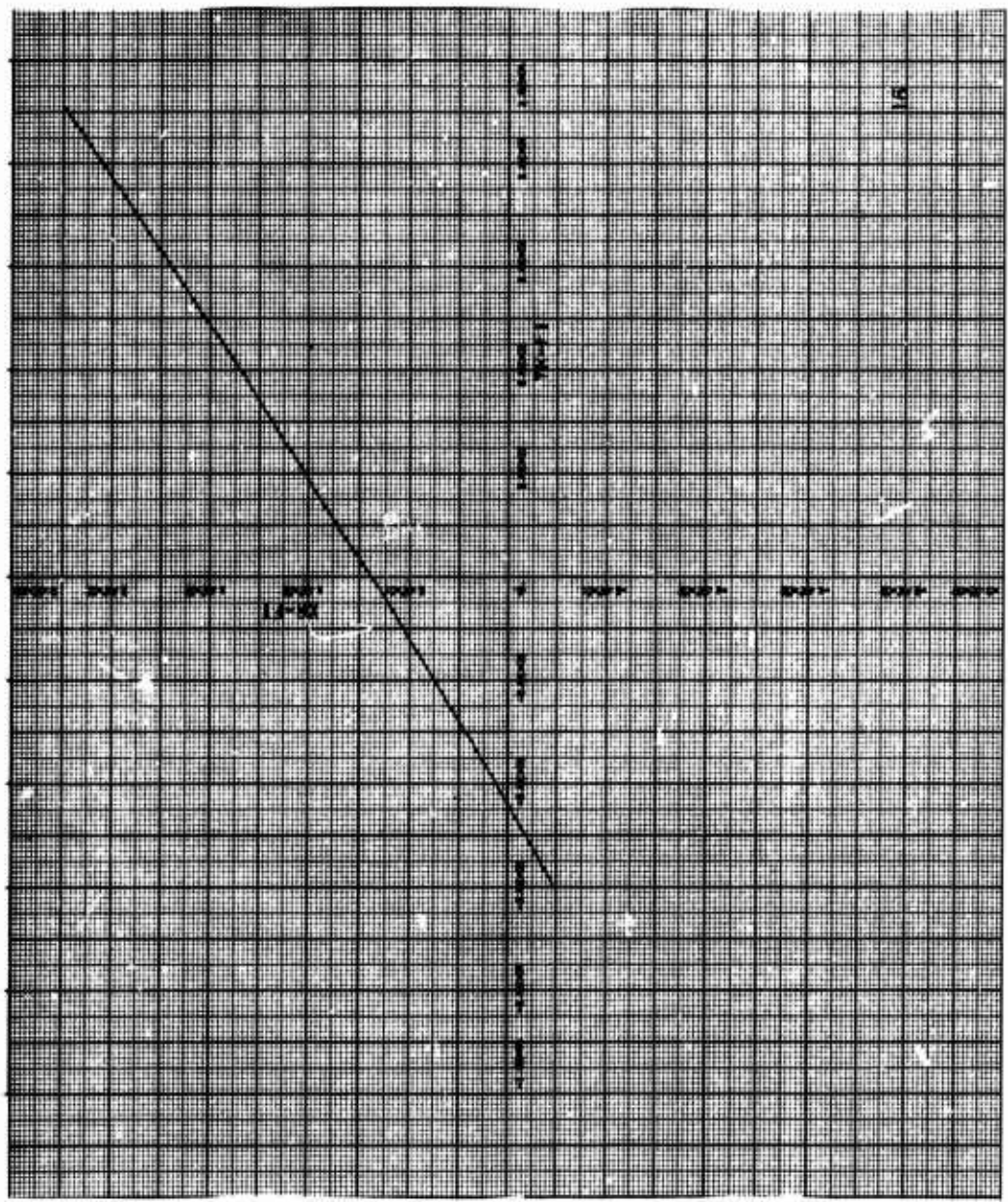


Figure 157. Graph for No Spin

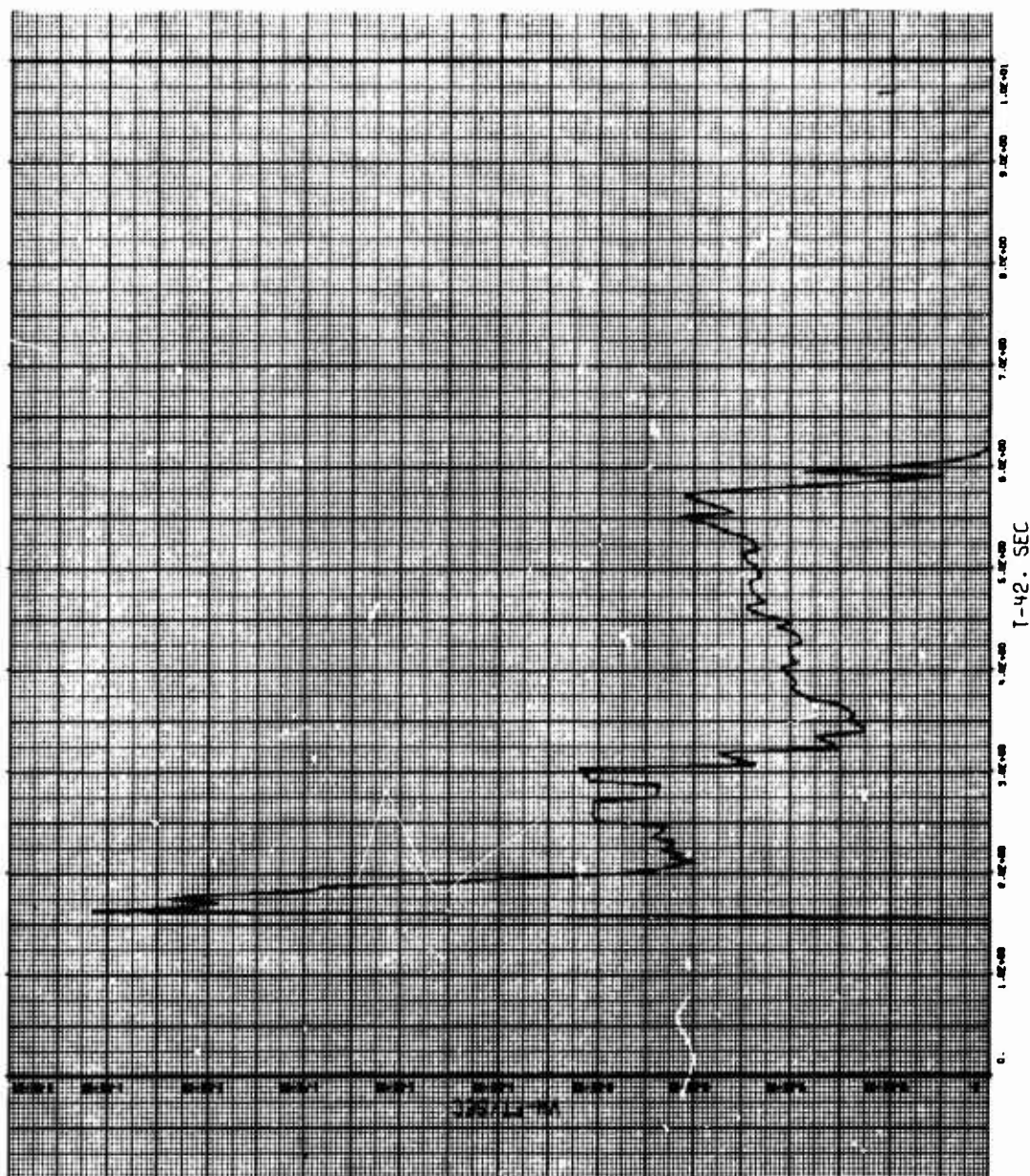


Figure 158. Graph for Guided Vehicle

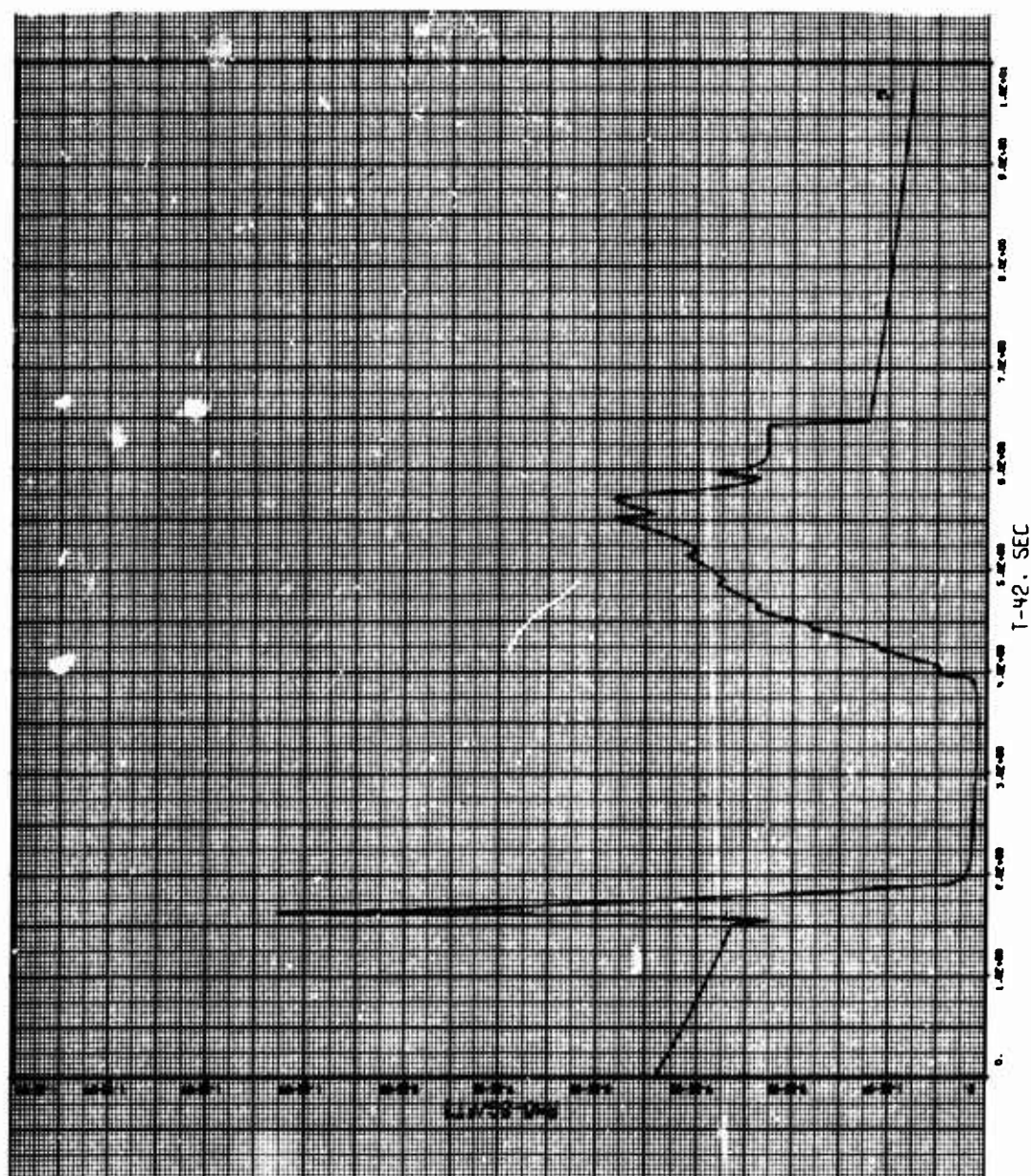


Figure 159. Graph for Guided Vehicle

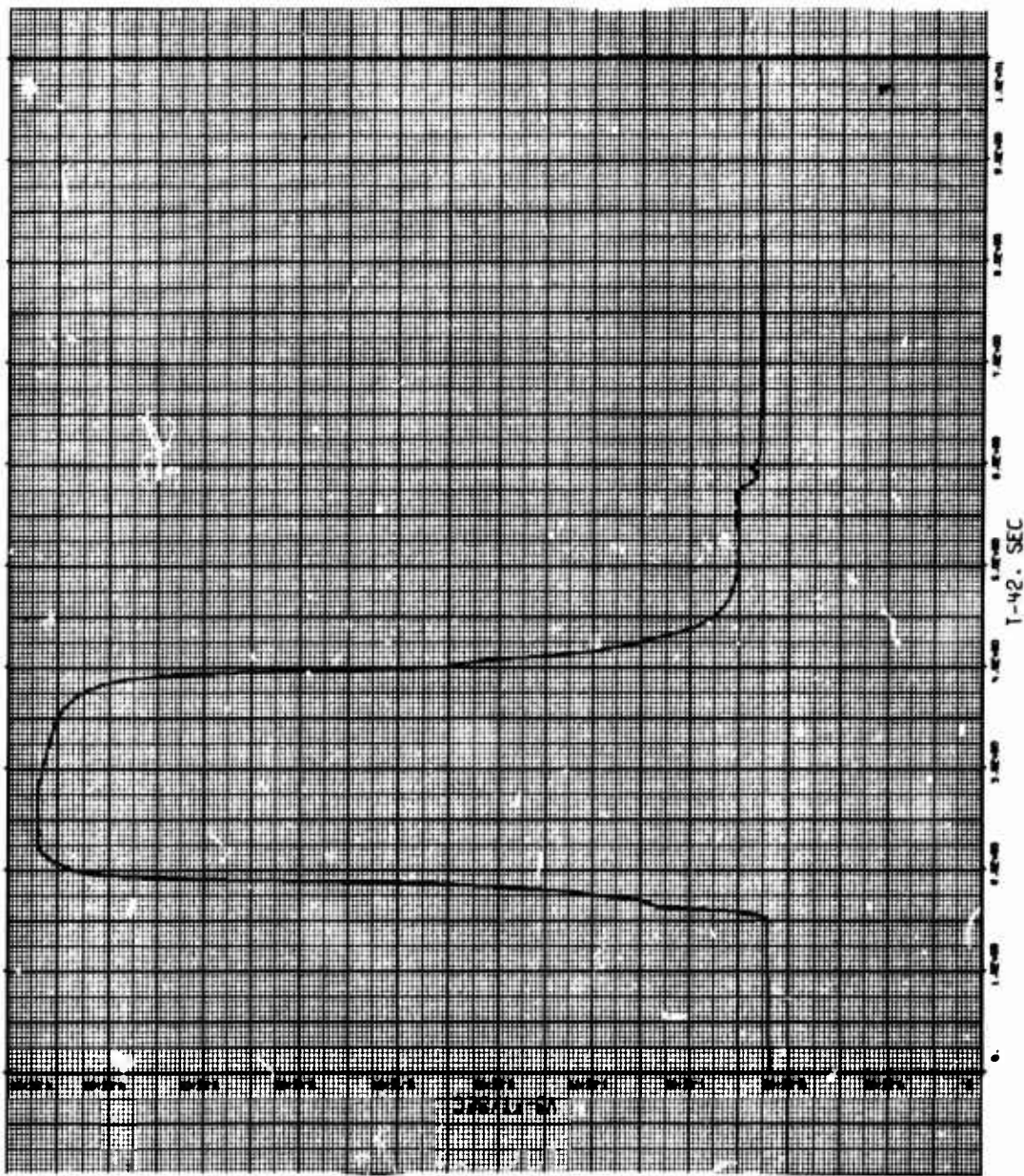


Figure 160. Graph for Guided Vehicle

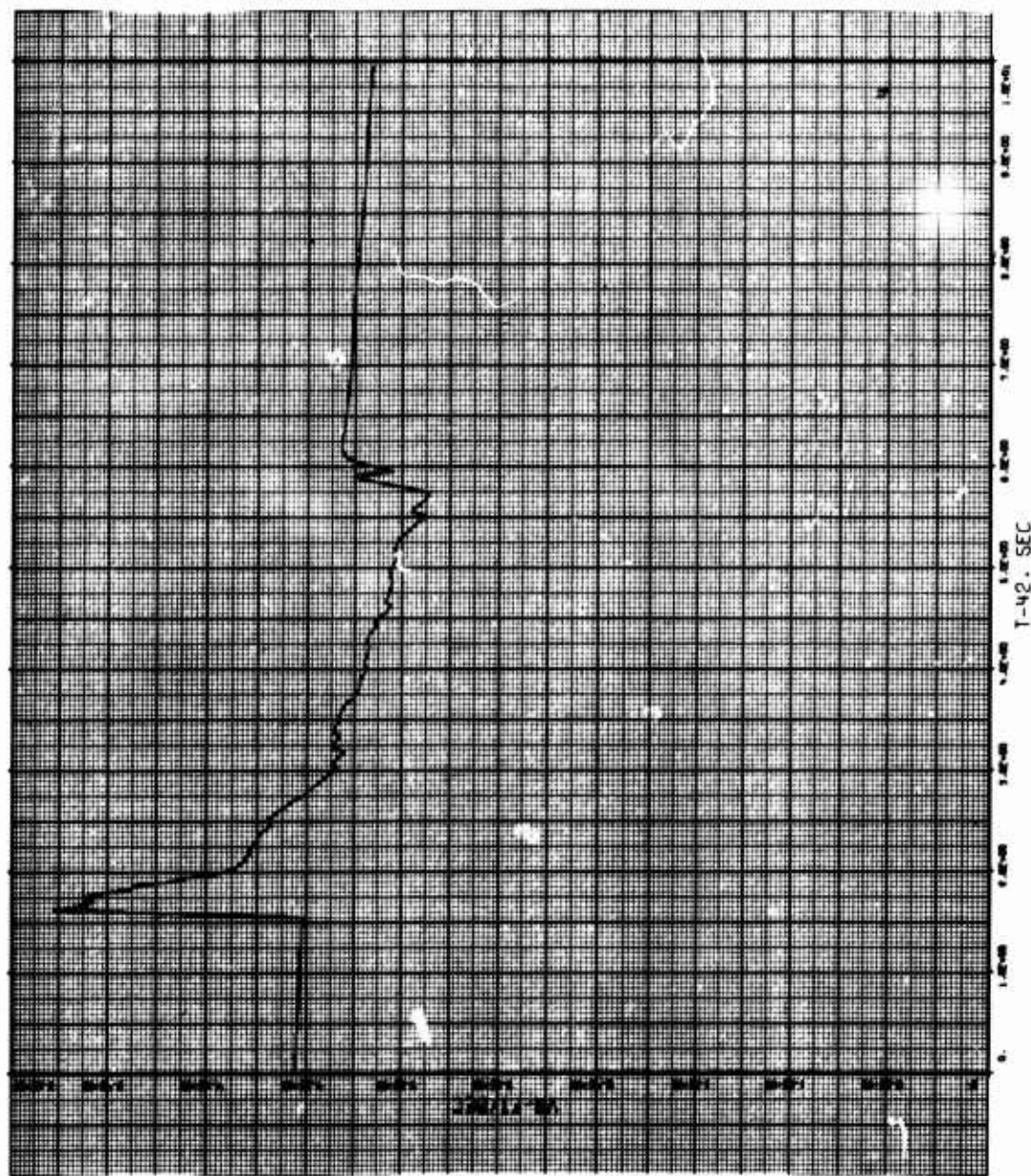


Figure 161. Graph for Guided Vehicle

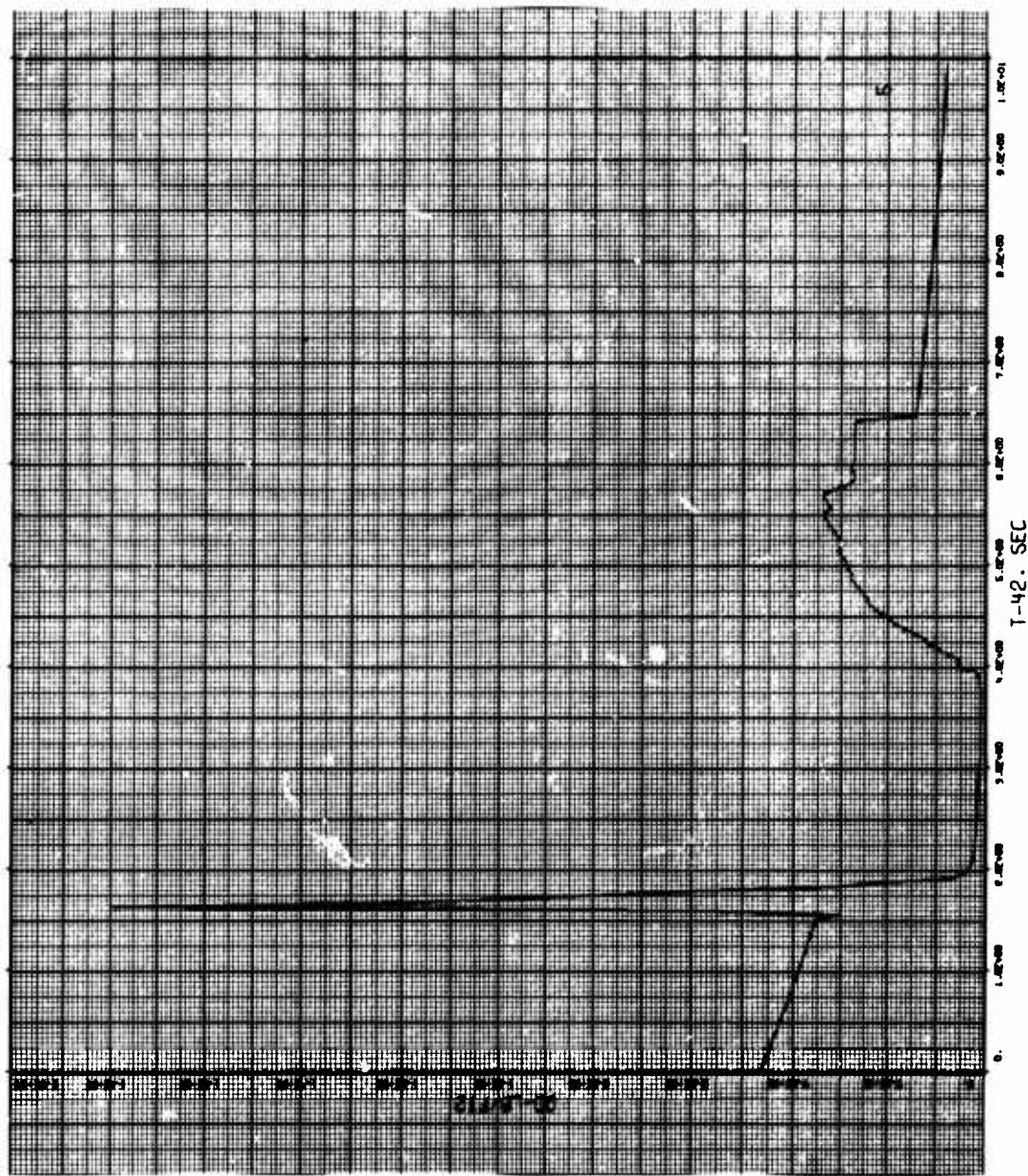


Figure 162. Graph for Guided Vehicle

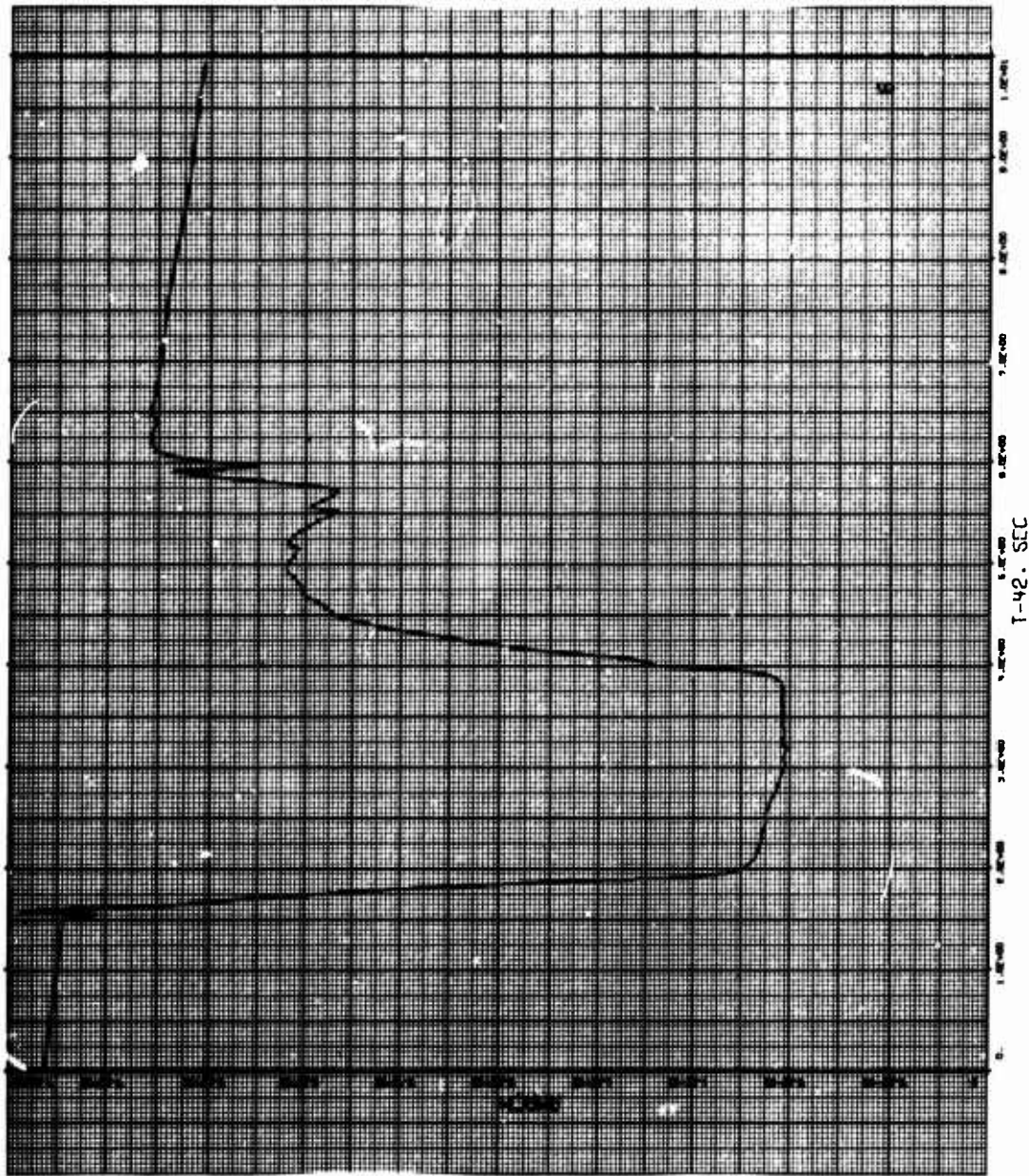


Figure 163. Graph for Guided Vehicle

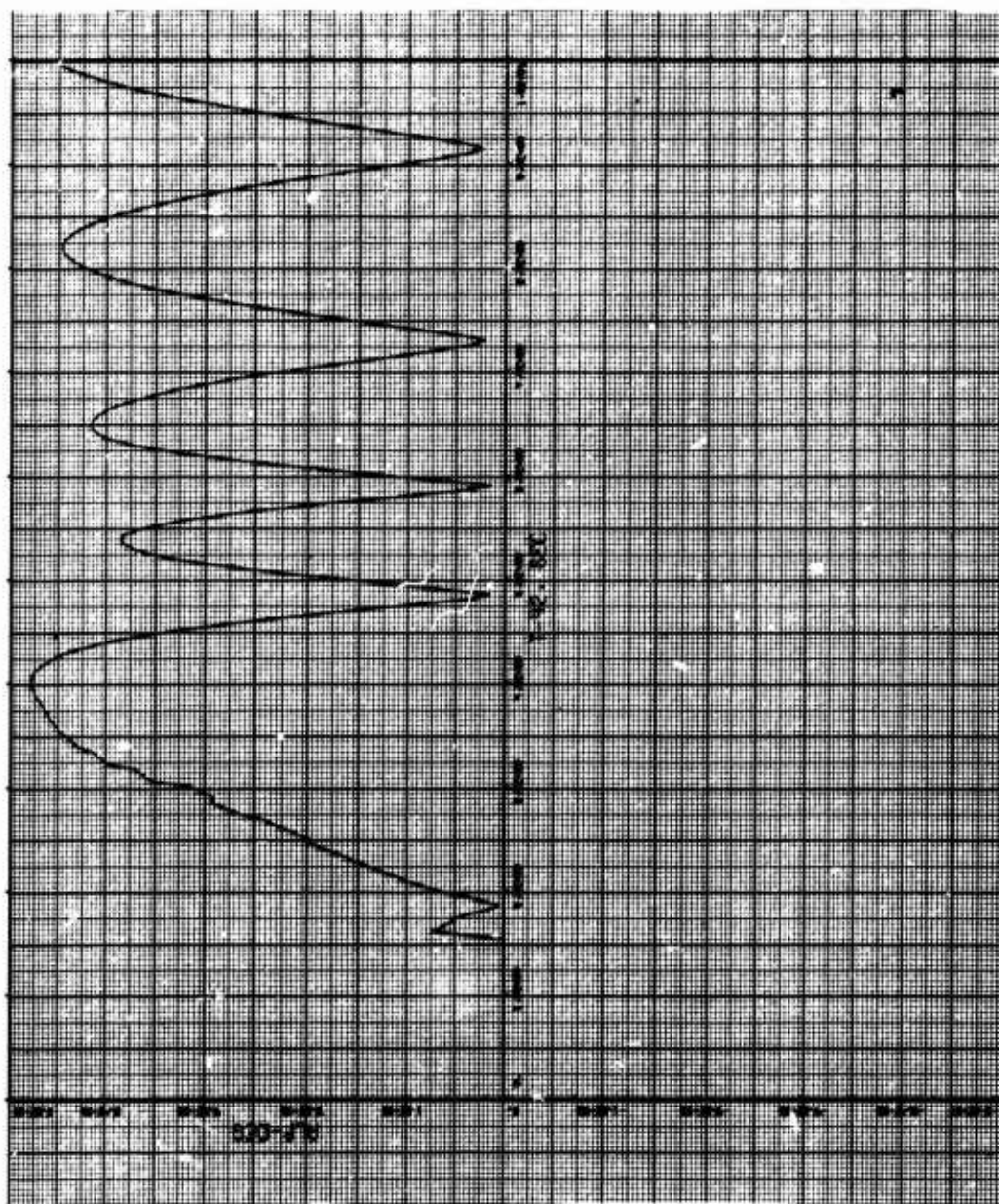


Figure 164. Graph for Guided Vehicle

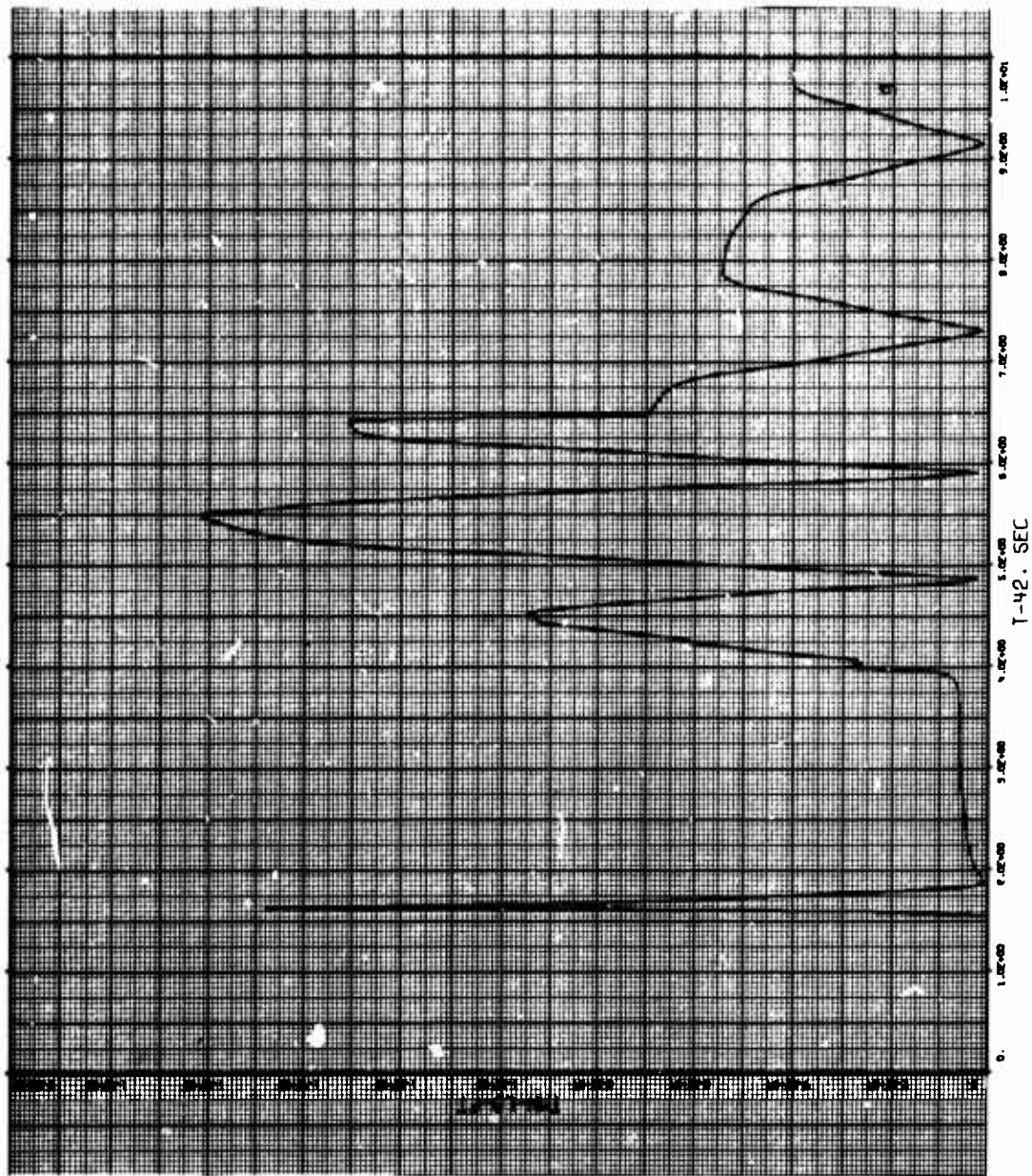


Figure 165. Graph for Guided Vehicle

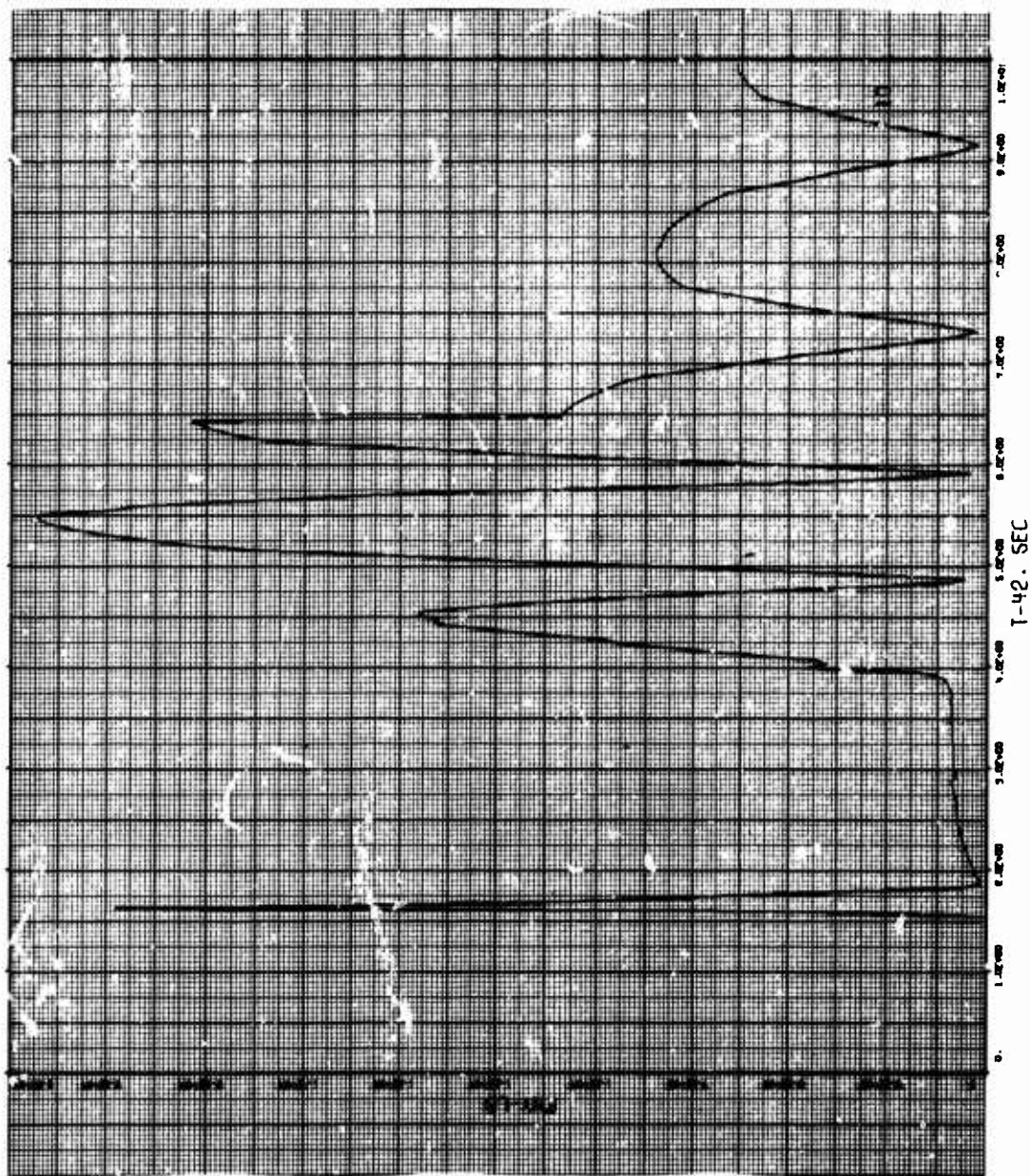


Figure 166. Graph for Guided Vehicle

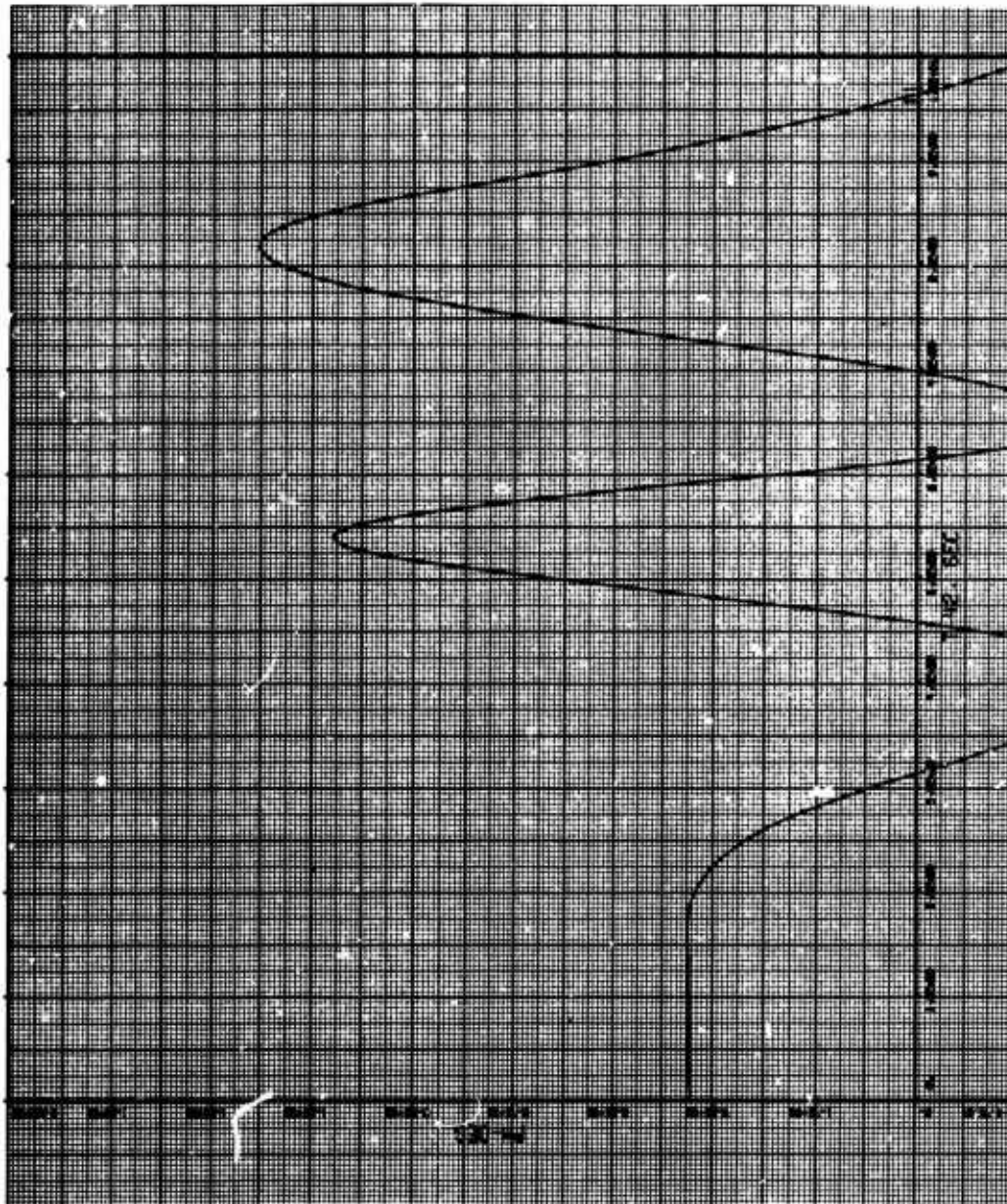


Figure 167. Graph for Guided Vehicle

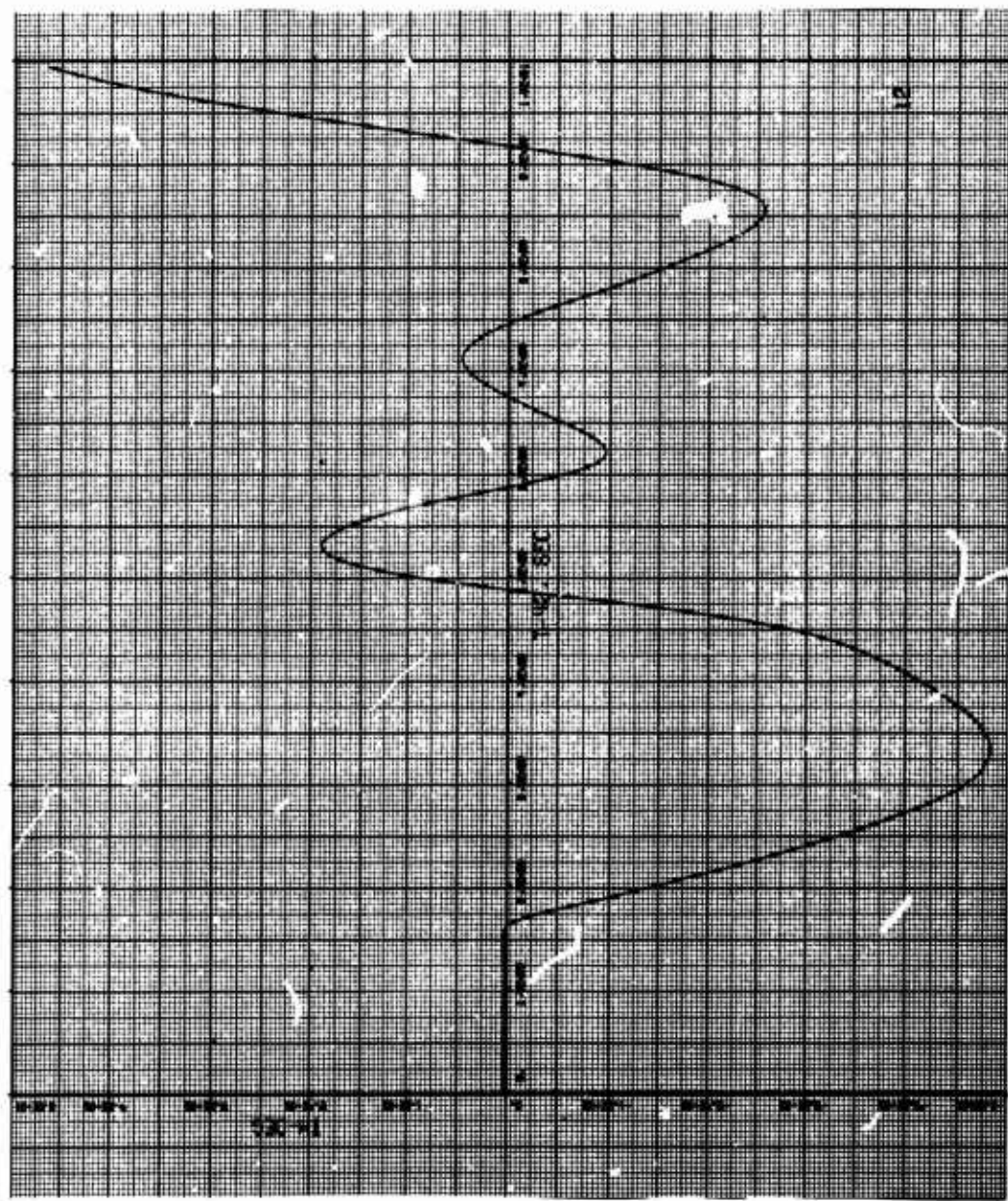


Figure 168. Graph for Guided Vehicle

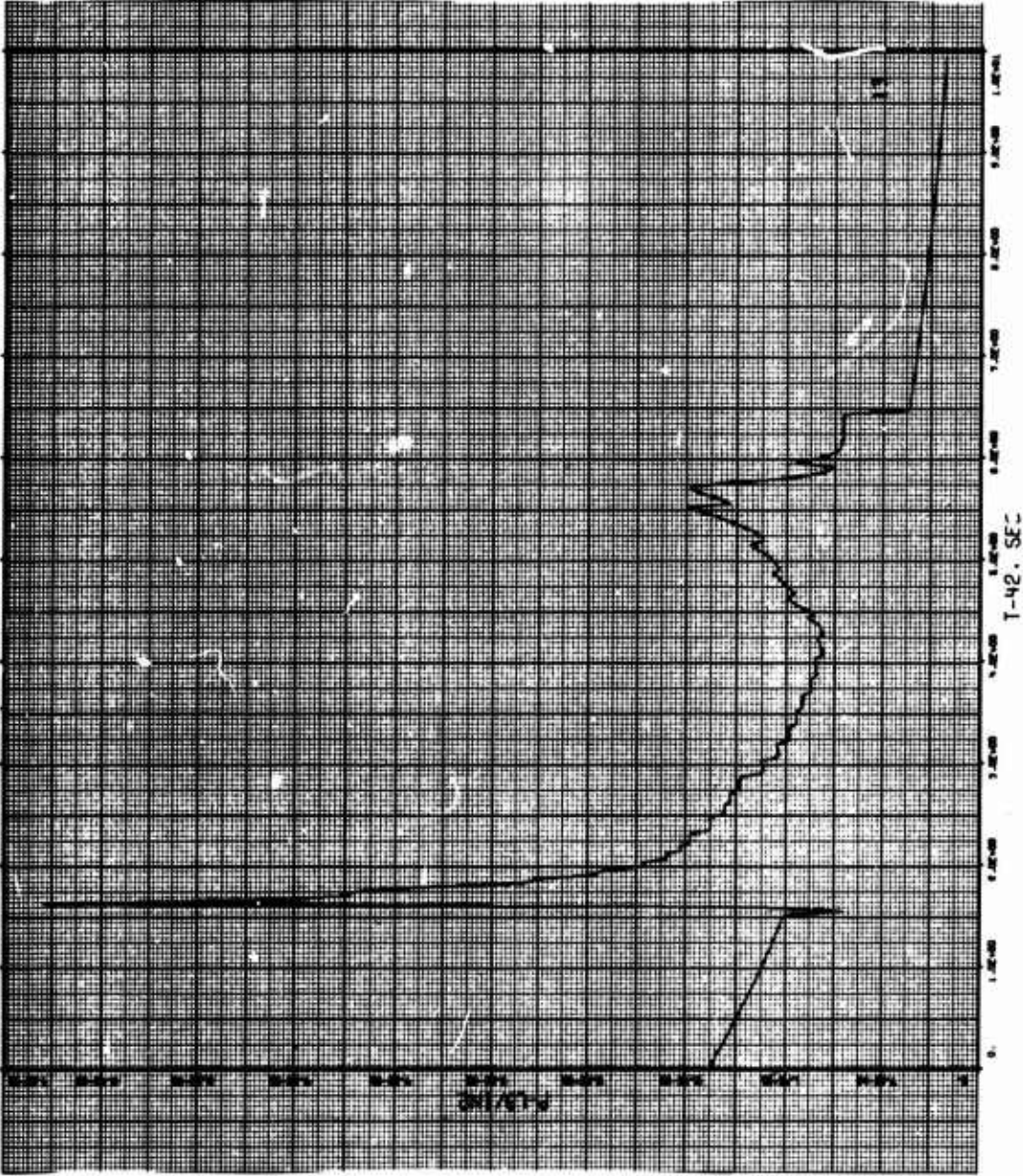


Figure 169. Graph for Guided Vehicle

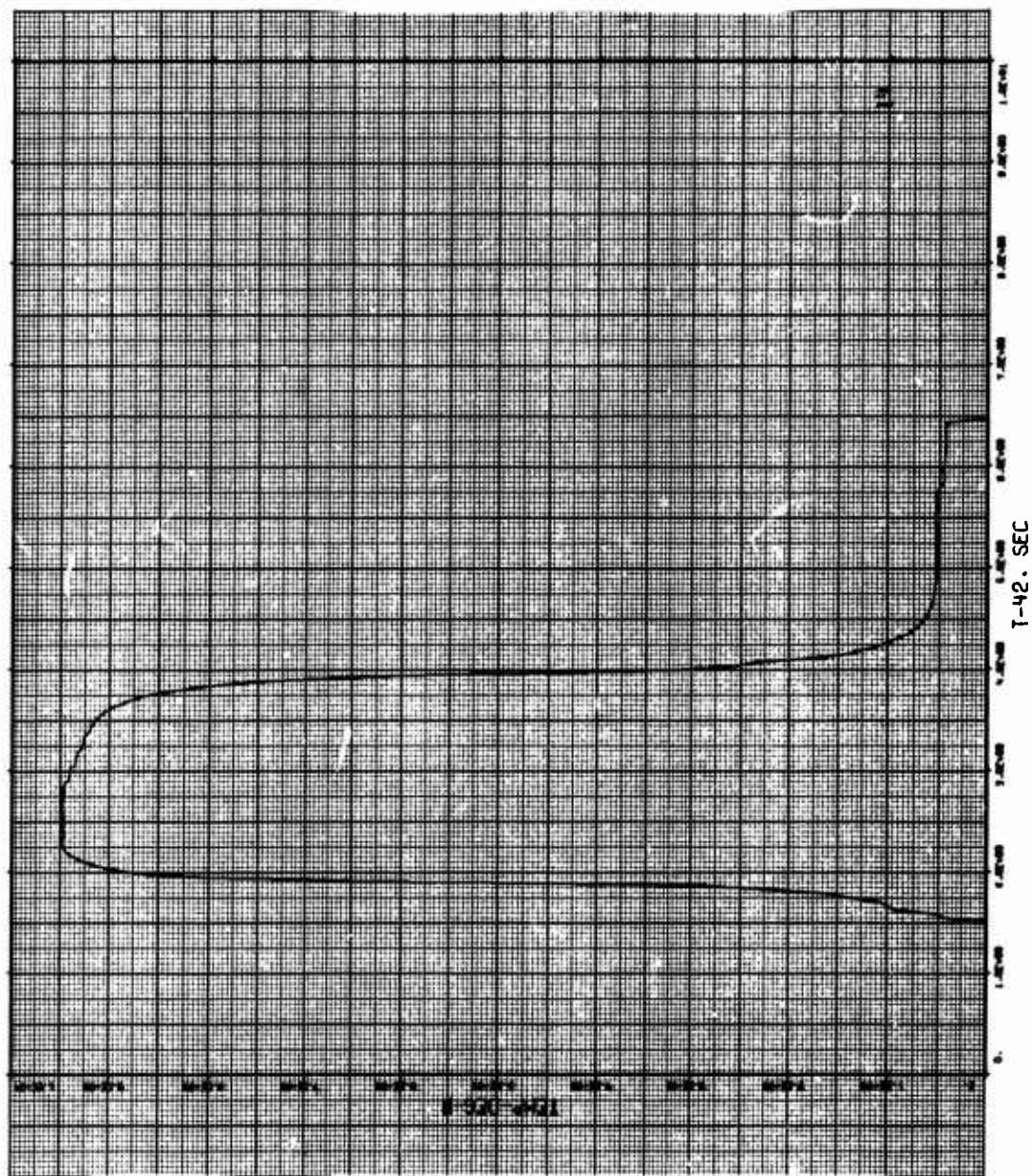


Figure 170. Graph for Guided Vehicle

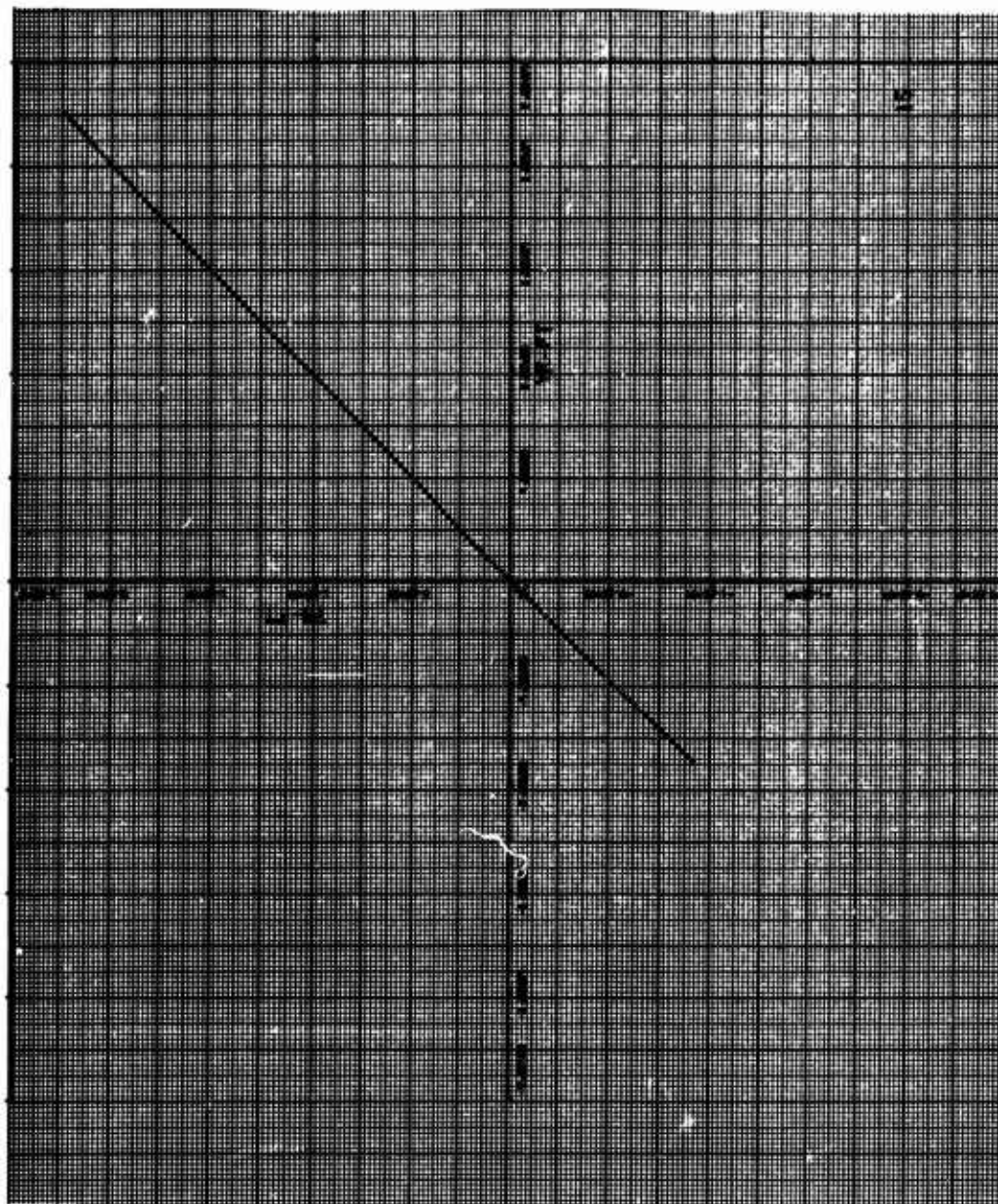


Figure 171. Graph for Guided Vehicle

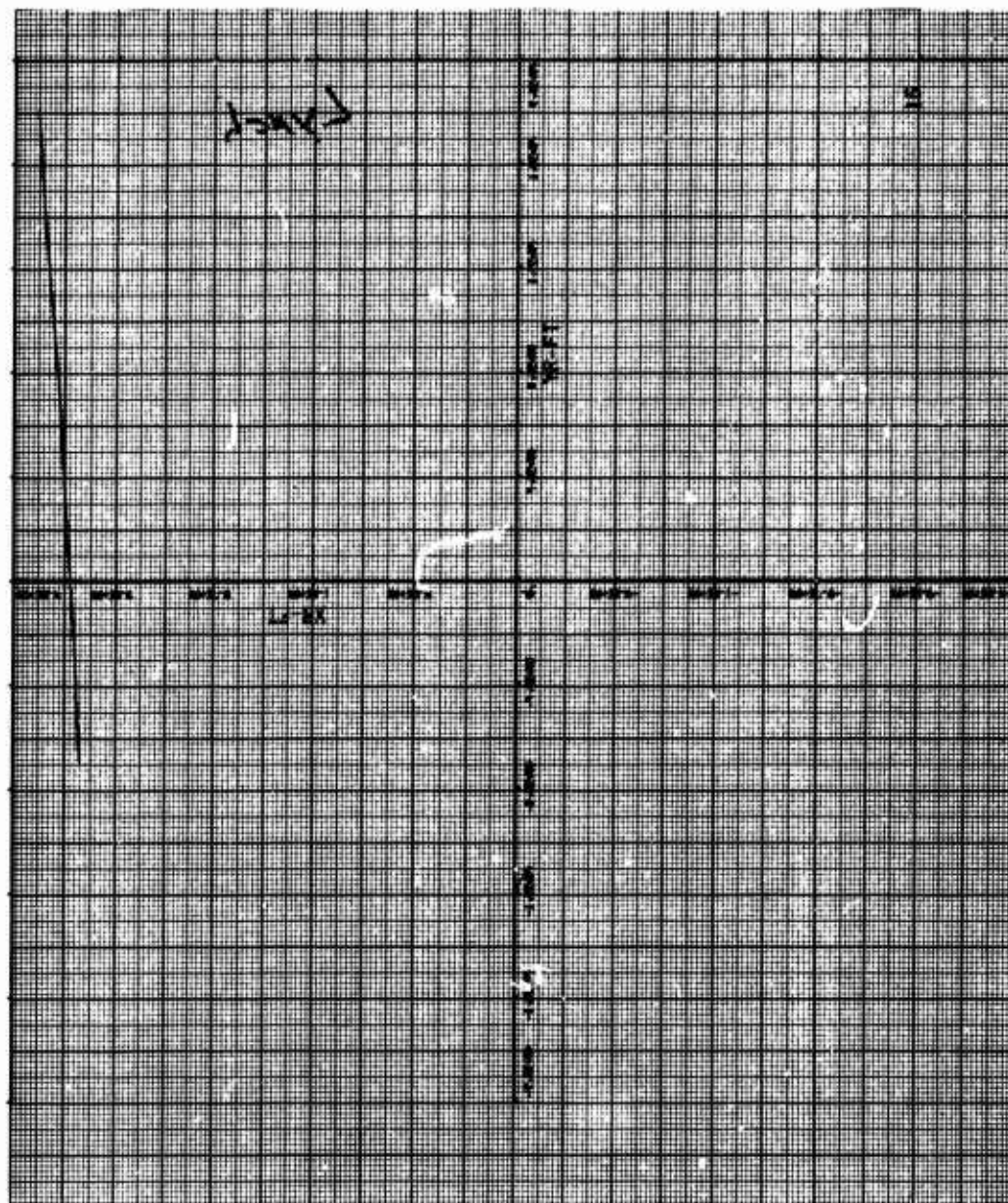


Figure 172. Graph for Guided Vehicle

SECTION VI

CONCLUSIONS

The Blue Goose Six-Degree-of-Freedom Digital Computer Trajectory Calculation (AFWL-TR-66-156) and the SPUTTER computer calculation are accurate simulations of the vehicle dynamics and the explosion environment. The assumptions made in Section II, paragraph 3, concerning the vehicle hydrodynamic interaction with the environment appear to be reasonable for the Blue Goose vehicle (this may not be true for other vehicles). The incorporation of the environment program with vehicle 6-degree program appears to give very good results. The following are the major conclusions:

1. Flight through a nuclear explosion has three characteristic flight regions: penetration of the initial shock characterized by increased angle of attack and high dynamic pressure; flight through the fireball characterized by very low dynamic pressure and essentially vehicle free flight; exit from the environment characterized by high angles of attack and moderate dynamic pressure.
2. The position perturbations given to the vehicle while in the environment (60 feet) are small in comparison to the attitude perturbations (70 degrees). Large angular velocities are imparted to the vehicle as the vehicle penetrates the initial expanding shock. This is immediately followed by flight through the rarefied atmosphere of the fireball where the vehicle experiences essentially free flight and large attitude excursions (70 degrees) occur. As the vehicle leaves the environment, the attitude excursions continue to grow, aided by the loss of dynamic pressure brought on by the exponentially decaying atmospheric density.
3. The worst vehicle perturbations are experienced (for entry at 1 second after detonation) for a trajectory that misses the center of detonation by approximately 4000 feet.
4. The worst dynamic load experienced by the unguided vehicle is an angular acceleration of 5 rad/sec^2 and a transverse acceleration of $2.33g$.
5. The worst velocity vector change for the unguided vehicle is a magnitude decrease of 100 ft/sec and direction change of $.71$ degree.

6. Spin did not significantly aid in maintaining vehicle attitude while in the environment. Spin does aid in keeping the vehicle from tumbling after it leaves the environment.

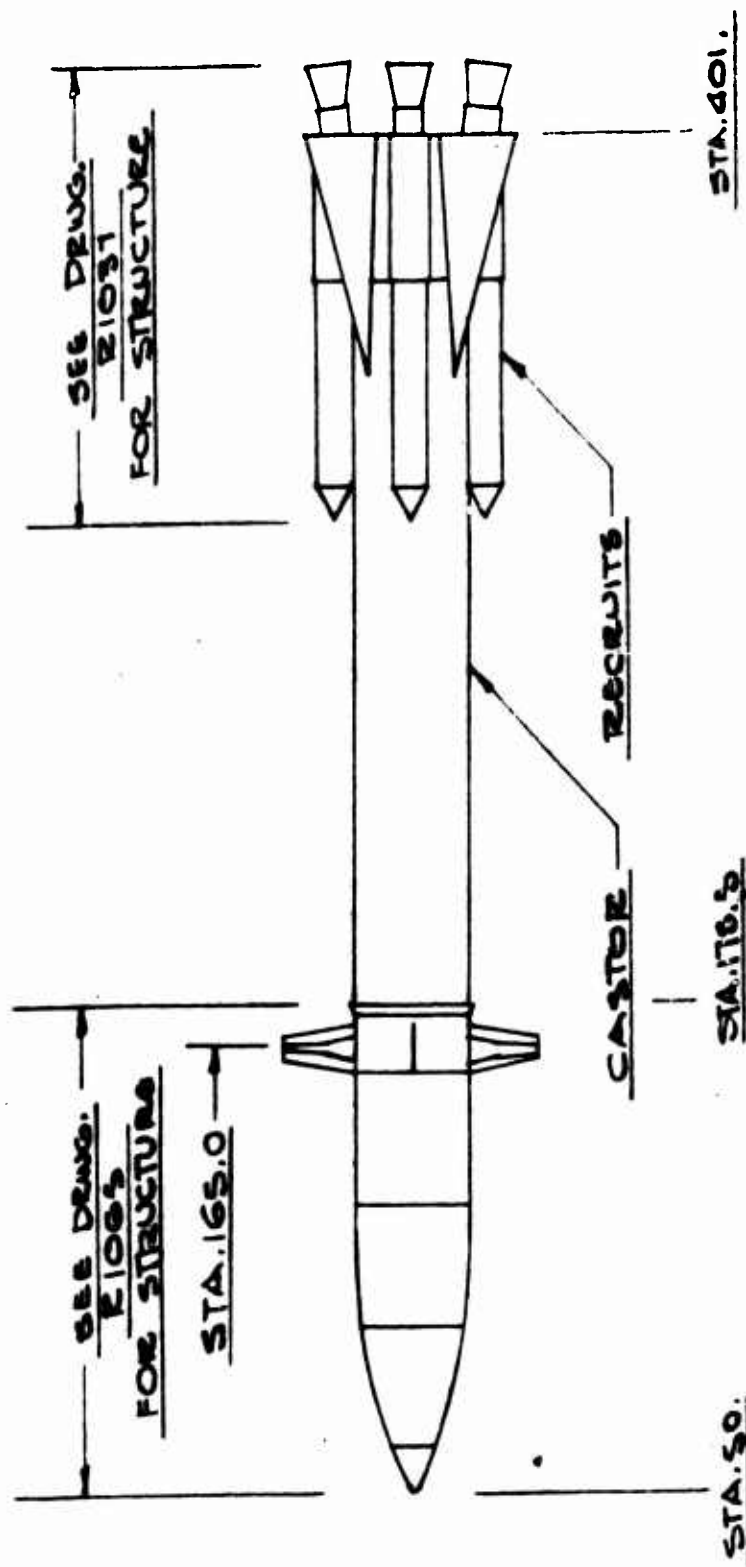
7. The main difference between the unguided and guided vehicles is the higher dynamic loads experienced by the guided vehicle (9 rad/sec^2 and $3.5g$).

(This page intentionally left blank)

APPENDIX I

UNGUIDED BLUE GOOSE VEHICLE

The work reported in this appendix was done by Space Systems, Incorporated, under Air Force Contract AF 29(601)-6311.



VEHICLE ARRANGEMENT

FIG. 1

PREPARED BY	SPACE SYSTEMS, INC.	REPORT NO. 8006-14
CHECKED BY	CITY OF INDUSTRY, CALIFORNIA	PAGE NO. 10
DATE		

2. AERODYNAMICS

2.1 Low Speed Test Description

A one-fifth scale model was fabricated. Alternate sized forward and aft fins were provided to investigate the low speed effect of varying the lifting surfaces. The model was run in the Convair Low Speed Wind Tunnel.

2.2 Transonic Speed Test Description

A one-twenty-fifth scale model was fabricated. As in the low speed model alternate fins were provided. This model was tested in the AEDC PWT 1-foot transonic tunnel.

2.3 High Speed Test Description

The high speed tests, run in the AEDC VFK 12-inch supersonic tunnel (D), employed the same model as was used in the transonic tests.

2.4 Wind Tunnel Test Results

Included as Appendix A, Space Systems, Inc. Report 8006-9, completely reports the results of the wind tunnel testing described above.

2.5 Estimated Aerodynamic Derivatives and Mass Characteristics Employed in Aerodynamic Calculations

All the significant aerodynamic and mass characteristics necessary to calculate a six-degree-of-freedom trajectory are presented in Table 4 and Figures 5 through 15. This information has been determined directly from the Blue Goose wind tunnel test data (Appendix A) and from weight estimates.

PREPARED BY	SPACE SYSTEMS, INC.	REPORT NO. 8006-14
CHECKED BY	CITY OF INDUSTRY, CALIFORNIA	PAGE NO. 11
DATE		

Table 4 presents vehicle time and mass parameters at various events.

Figure 4 shows the positive direction of aerodynamic forces and moments, and the positive orientation of the missile linear velocity.

Figures 5 and 6 give plots of C_{N_α} and C_{m_α} versus Mach number for small pitch angles of attack.

Figures 7 and 8 are plots of C_N and C_m versus angle of attack. This data is applicable for Mach numbers less than .324.

Figure 9 shows C_{A_o} versus Mach number. The data is presented for two values of flight Reynolds numbers that will encompass the significant portion of the missile trajectory effected by axial force

Figure 10 is a plot of C_{A_b} versus Mach number. The total vehicle axial force thrusting and coasting is determined as the sum of C_{A_o} and the applicable portion of C_{A_b} .

Figure 11 gives a plot of $C_{m_{\dot{\theta}}}$ versus Mach number.

Figures 12 and 13 are plots of C_{l_p} and $C_{l_{\dot{\delta}}}$ versus Mach number.

Figure 14 shows weight and center of gravity position versus time.

Figure 15 presents transverse and roll moment of inertia data versus time.

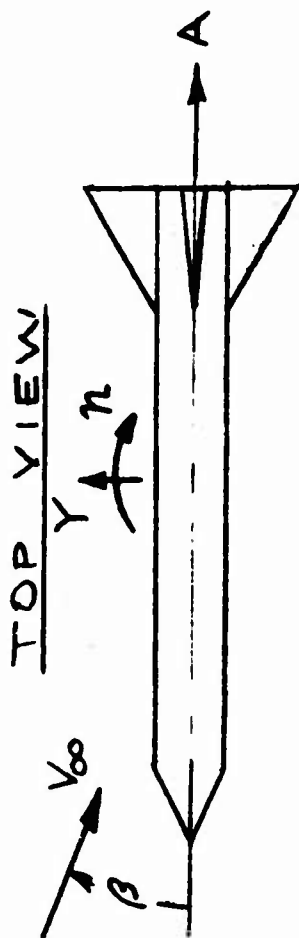
All symbolic nomenclature throughout this report is in accordance with Table 5.

TABLE 4
EVENT TIME HISTORY AND ASSOCIATED VEHICLE PARAMETERS

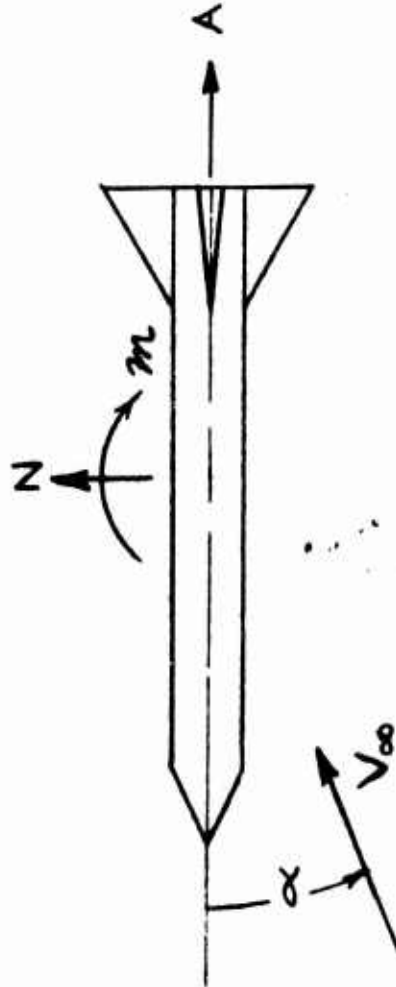
Event	t	W	X c.g.	I _T Traverse Moment of Inertia Slug-Ft ²	I _X Roll Moment of Inertia ² Slug-Ft ²
Ignition signal to launcher spin rockets	0	15,505.	250.9	31,566.4	651.80
Ignition signal to Castor (45° travel)	.31				
Ignition signal to 4 Recruits (.16 inch travel)	.44				
Vehicle leaves launcher (3-inch pins)	.48	15,435.5	250.8	31,566.43	651.80
Recruit burnout	2.92	13,832.2	242.2	28,337.0	540.1
Castor burnout	41.25	7,009.2	215.9	21,543.9	339.57

PREPARED BY	SPACE SYSTEMS, INC.	REPORT NO. 8006-14
CHECKED BY	CITY OF INDUSTRY, CALIFORNIA	PAGE NO 13
DATE		FIGURE 4

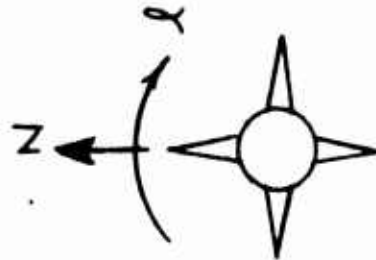
NOTE: POSITIVE DIRECTION
'SHOWN



SIDE VIEW



END VIEW



BODY-AXIS SYSTEM

PREPARED BY	SPACE SYSTEMS, INC.	REPORT NO. 8006-14
CHECKED BY	CITY OF INDUSTRY, CALIFORNIA	PAGE NO. 14
DATE		

TABLE 5

AERODYNAMIC SYMBOLS

N	-	Normal force, pounds
m	-	Pitching moment, foot-pounds
A	-	Axial force, pounds
ℓ	-	Rolling moment, foot-pounds
P	-	Rolling velocity, radians per second
q	-	Pitching velocity, radians per second
V	-	Total linear velocity, feet per second
δ	-	Fin cant angle, degrees
α	-	Pitch angle of attack, degrees
q	-	Free stream dynamic pressure, pounds per square foot
S_{ref}	-	Reference area, square feet
d_{ref}	-	Reference length, feet
C_N	-	Normal force coefficient
$C_{N\alpha}$	-	Rate of change of normal force coefficient with pitch angle of attack, per degree
C_m	-	Pitching moment coefficient
$C_{m\alpha}$	-	Rate of change of pitching moment coefficient with pitch angle of attack, per degree
β	-	Yaw angle of attack, degrees
r	-	Yawing velocity, radians per second

PREPARED BY	SPACE SYSTEMS, INC.	REPORT NO. 8006-14
CHECKED BY	CITY OF INDUSTRY, CALIFORNIA	PAGE NO. 15
DATE		

- $C_{m\dot{q}}$ - Rate of change of pitching moment coefficient with pitching velocity, per radian
 C_{A_0} - Axial force coefficient at zero angle of attack without base axial force coefficient
 C_{A_b} - Base axial force coefficient
 $C_{l\dot{p}}$ - Rate of change of rolling moment coefficient with rolling velocity, per radian
 $C_{l\delta}$ - Rate of change of rolling moment coefficient with fin cant angle, per degree
 Y - Side force, pounds
 n - Yawing moment, foot-pounds
 W - Weight, pounds
 X_{cg} - Center of gravity location, inches from station O
 I_T - Transverse moment of inertia, slug-ft²
 $I_X I_Y I_Z$ - Roll, pitch, and yaw moments of inertia, slug-ft²

PREPARED BY	SPACE SYSTEMS, INC.	REPORT NO. 8006-14
CHECKED BY	CITY OF INDUSTRY, CALIFORNIA	PAGE NO. 16
DATE		

The characteristics produced by yaw angles and yaw angular velocities are equal in magnitude to the pitch data due to missile symmetry.

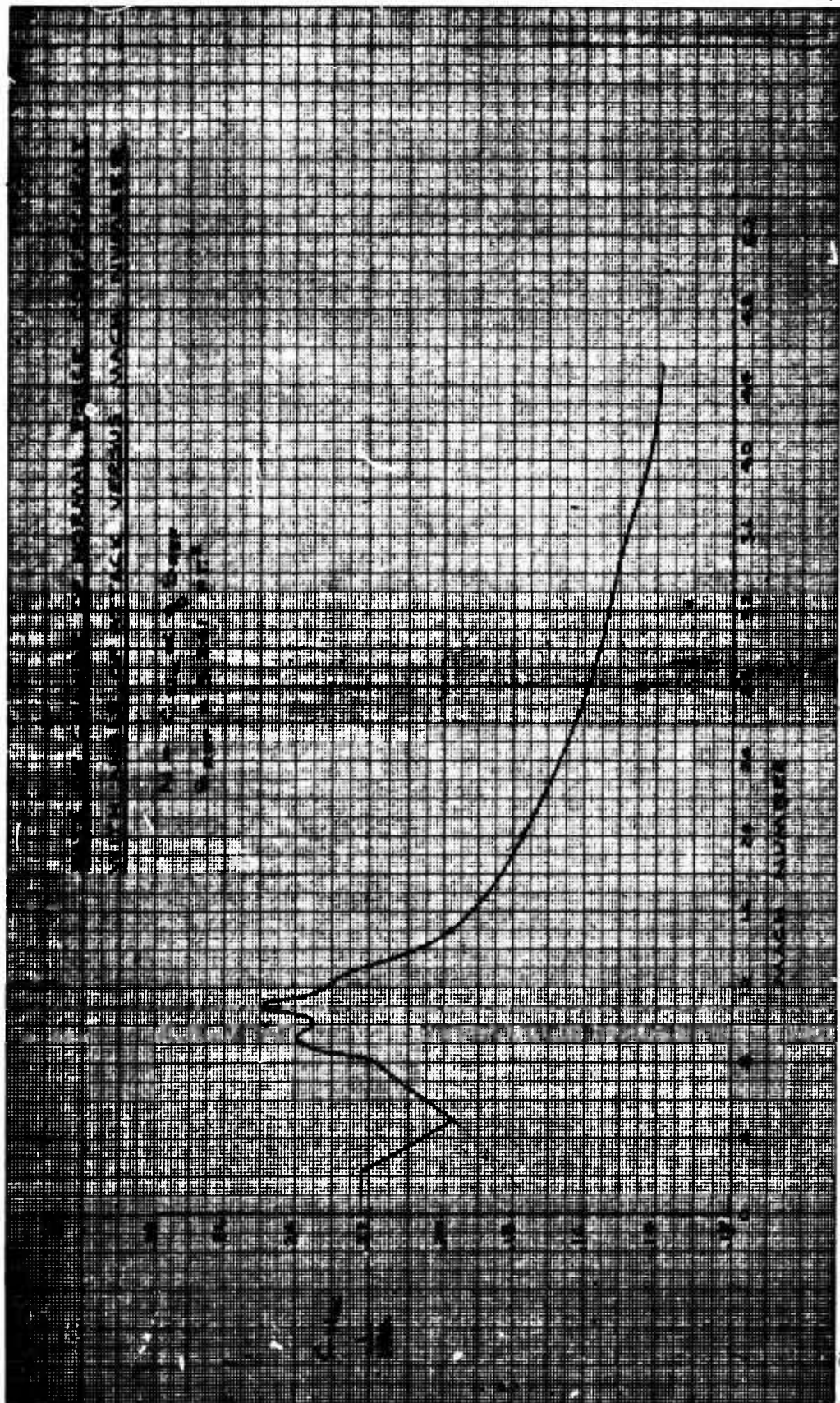
Hence,

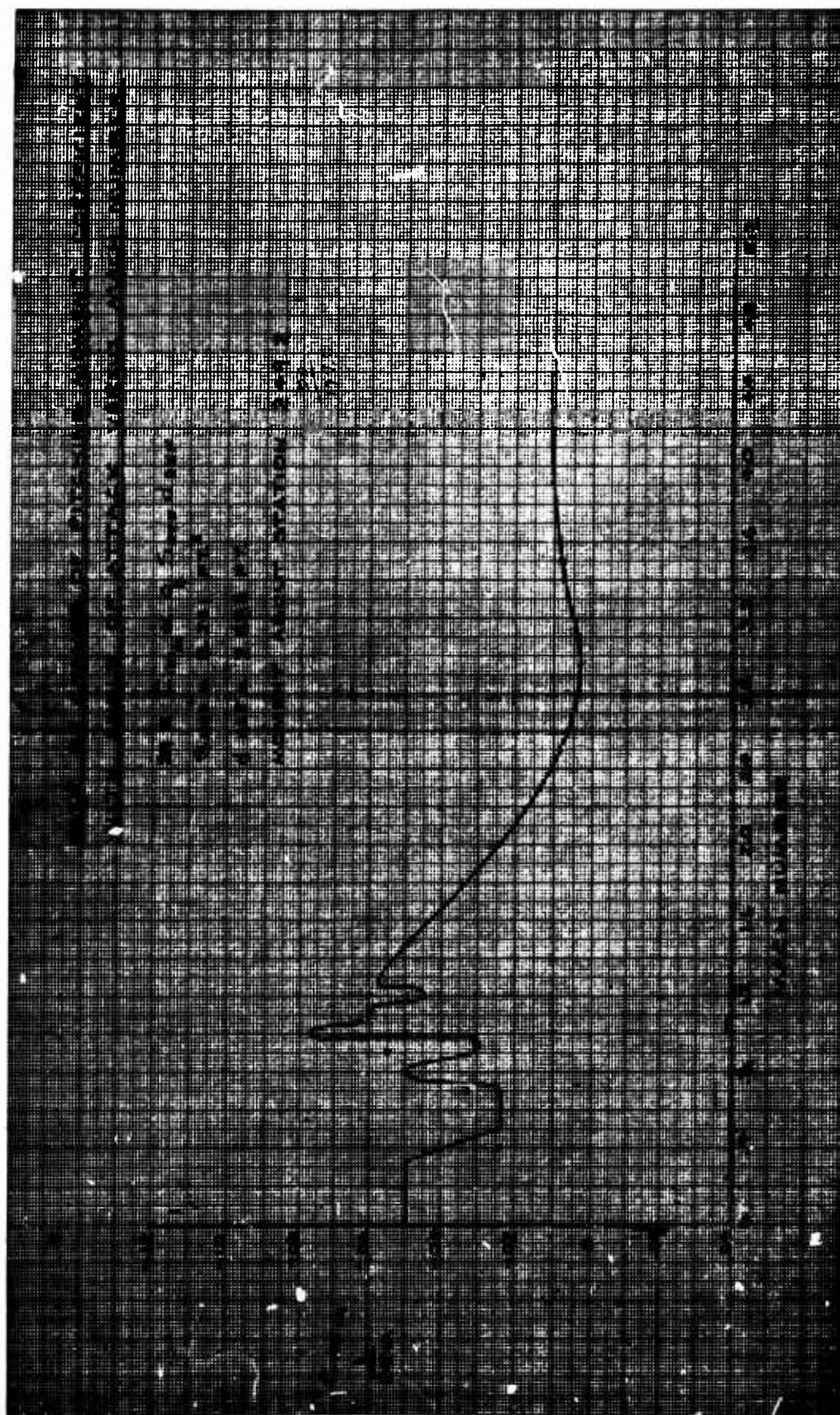
$$C_{Y\beta} = -C_{N\alpha}$$

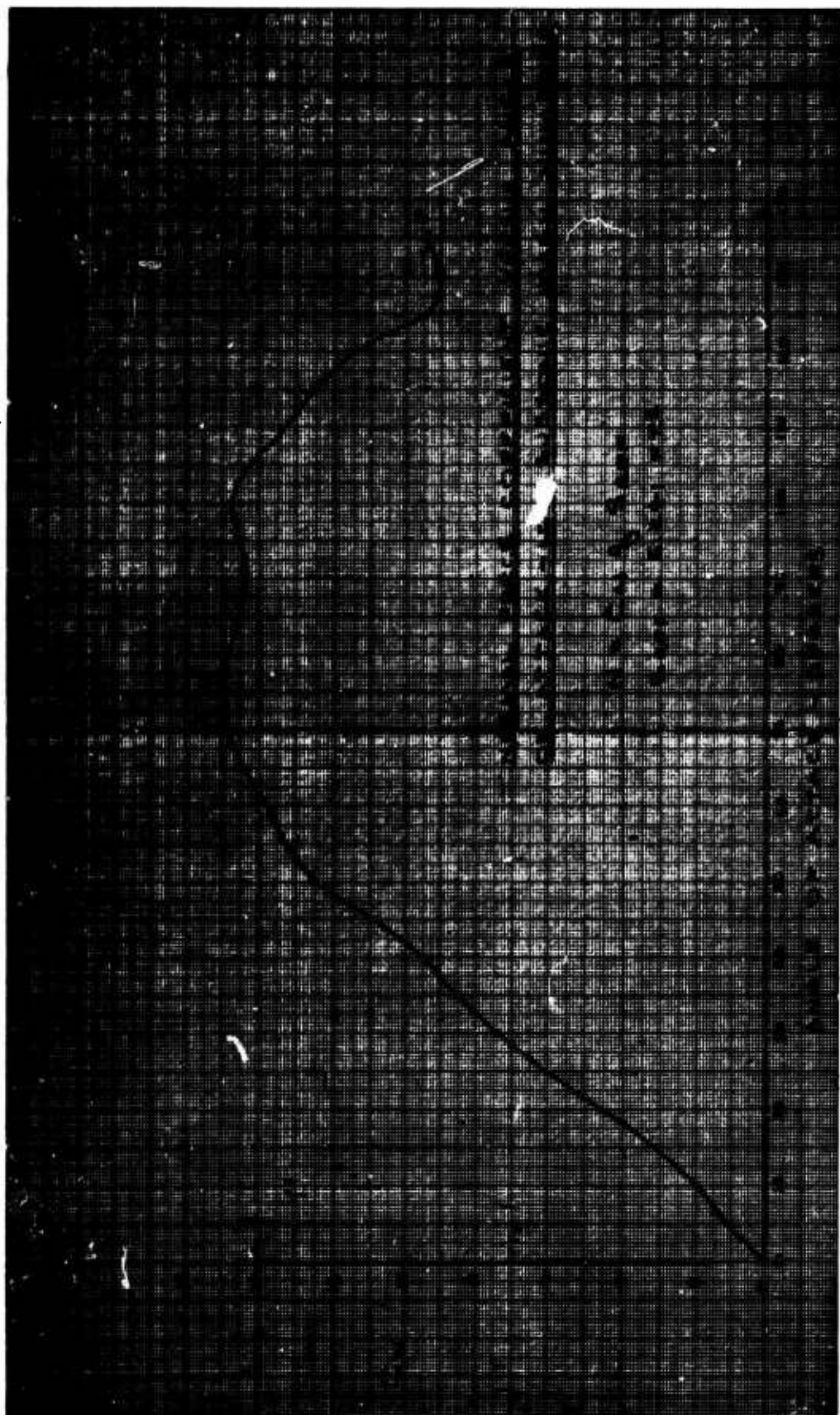
$$C_{n\beta} = -C_{m\alpha}$$

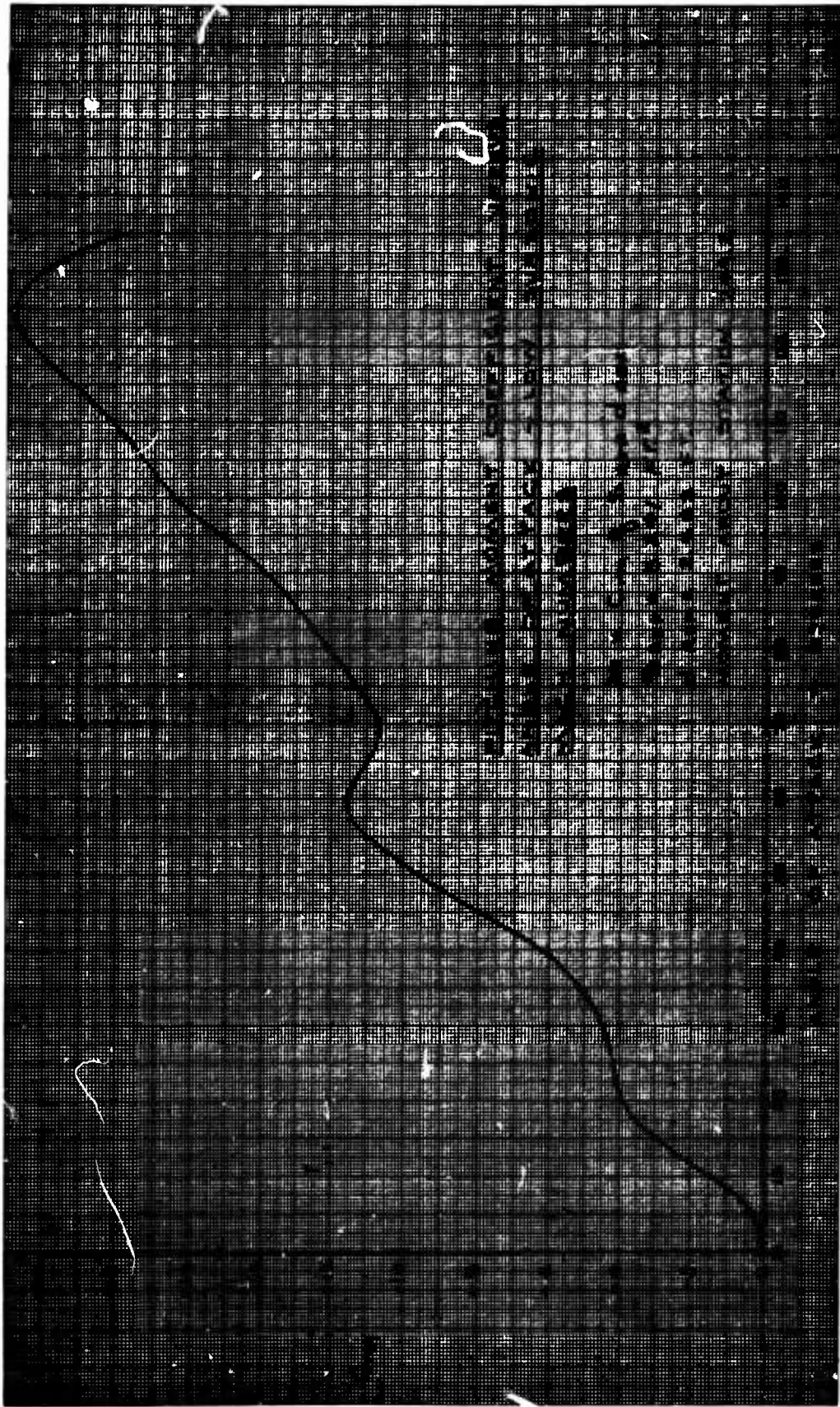
$$C_{nr} = C_{mq}$$

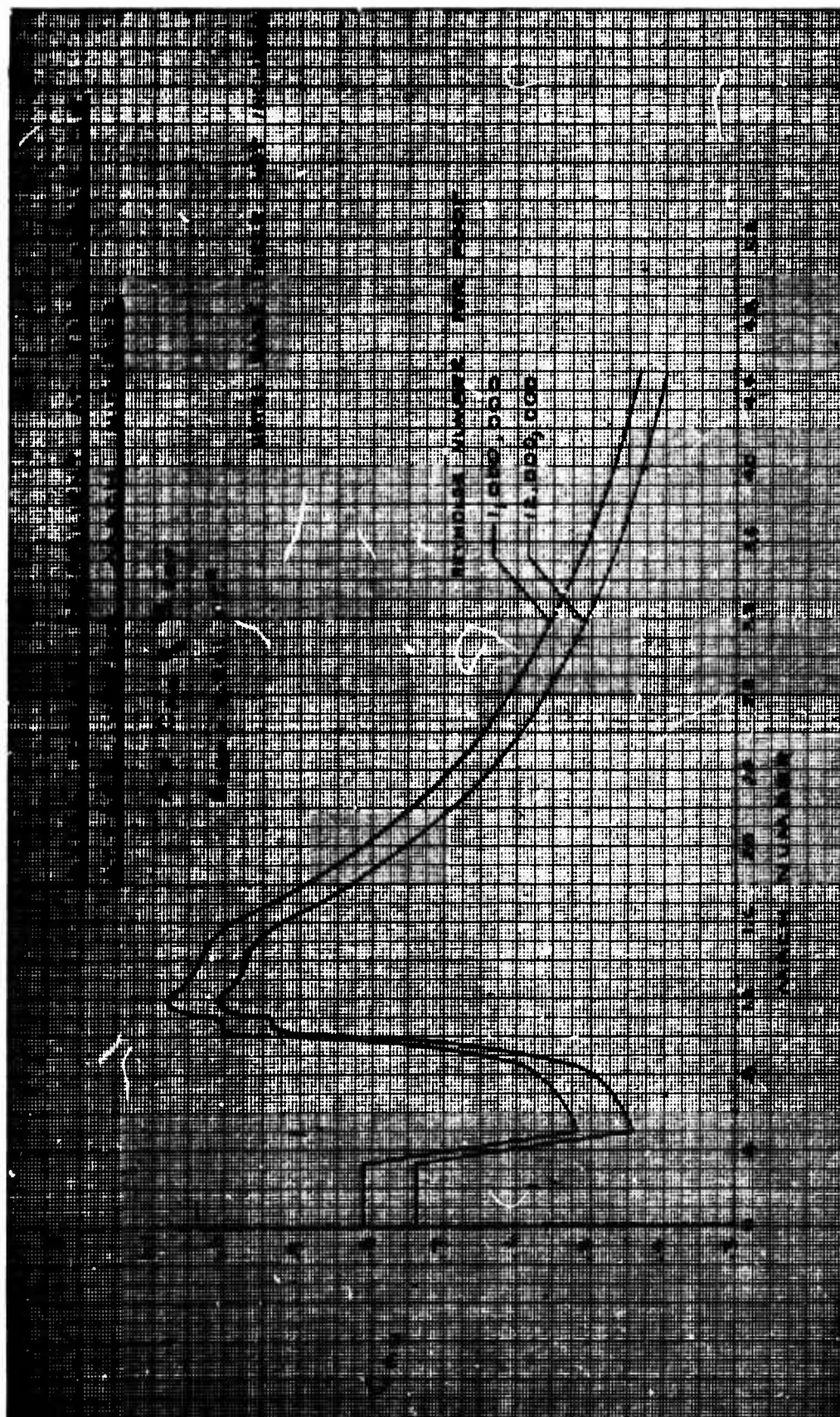
$$I_T = I_Y = I_Z$$

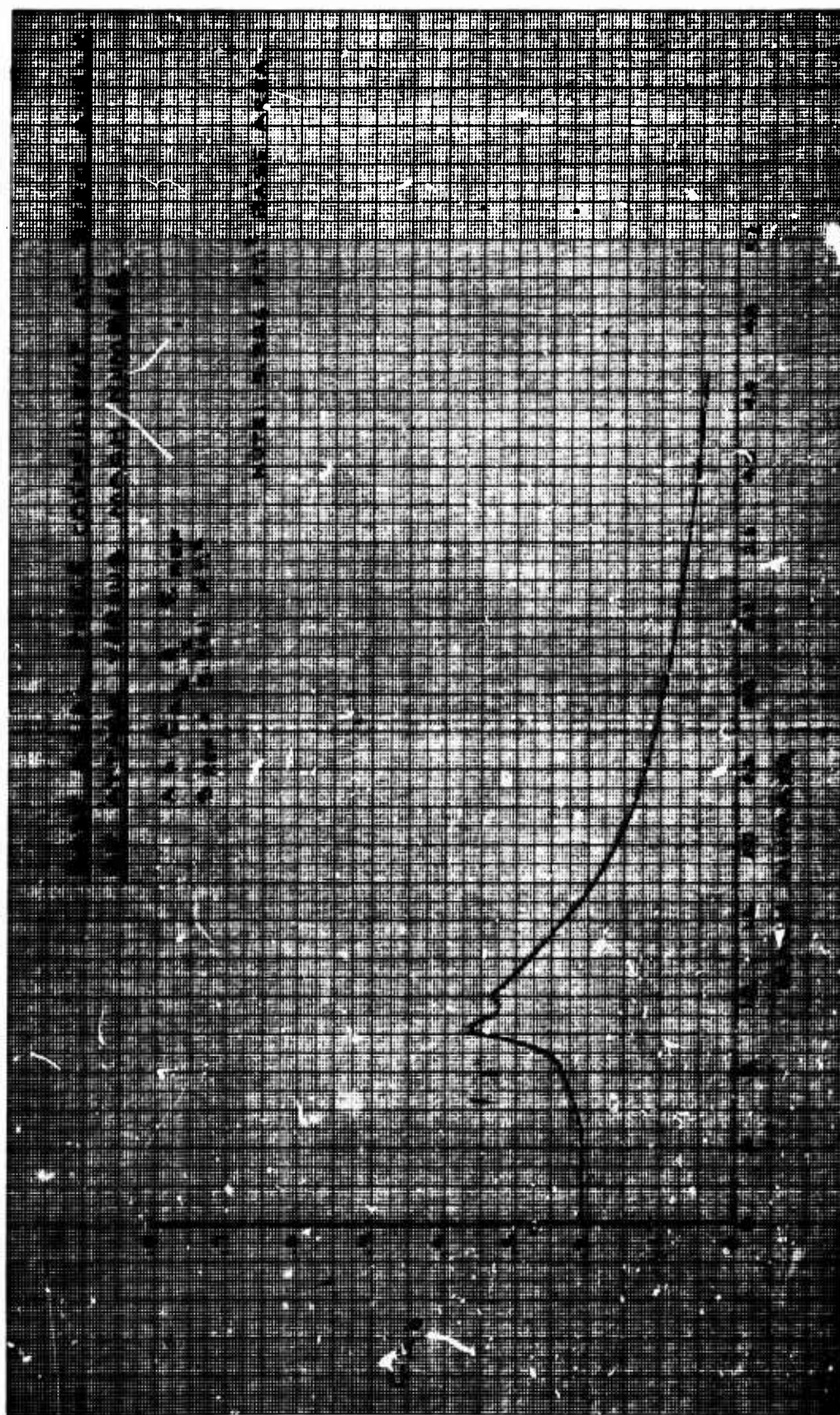


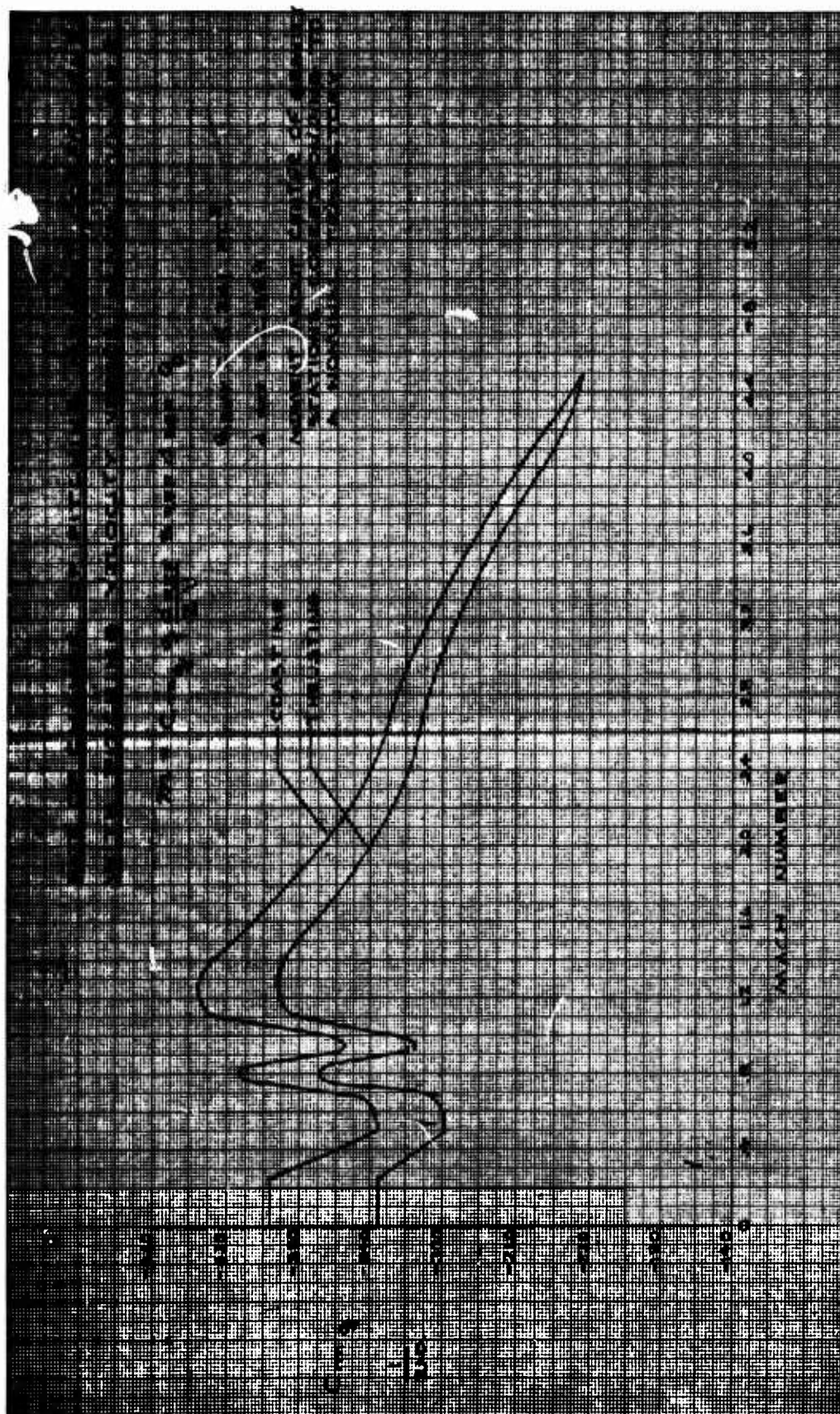


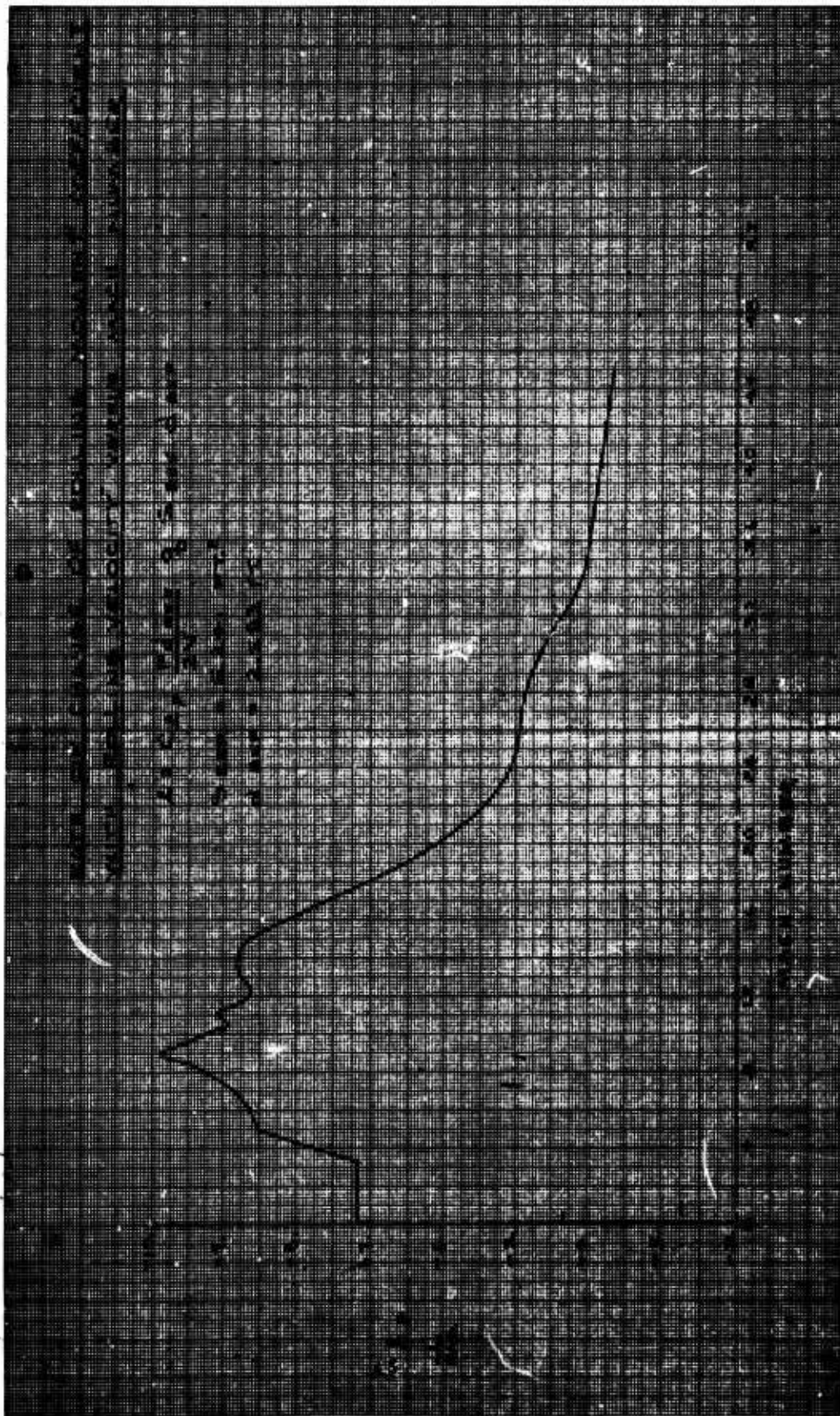


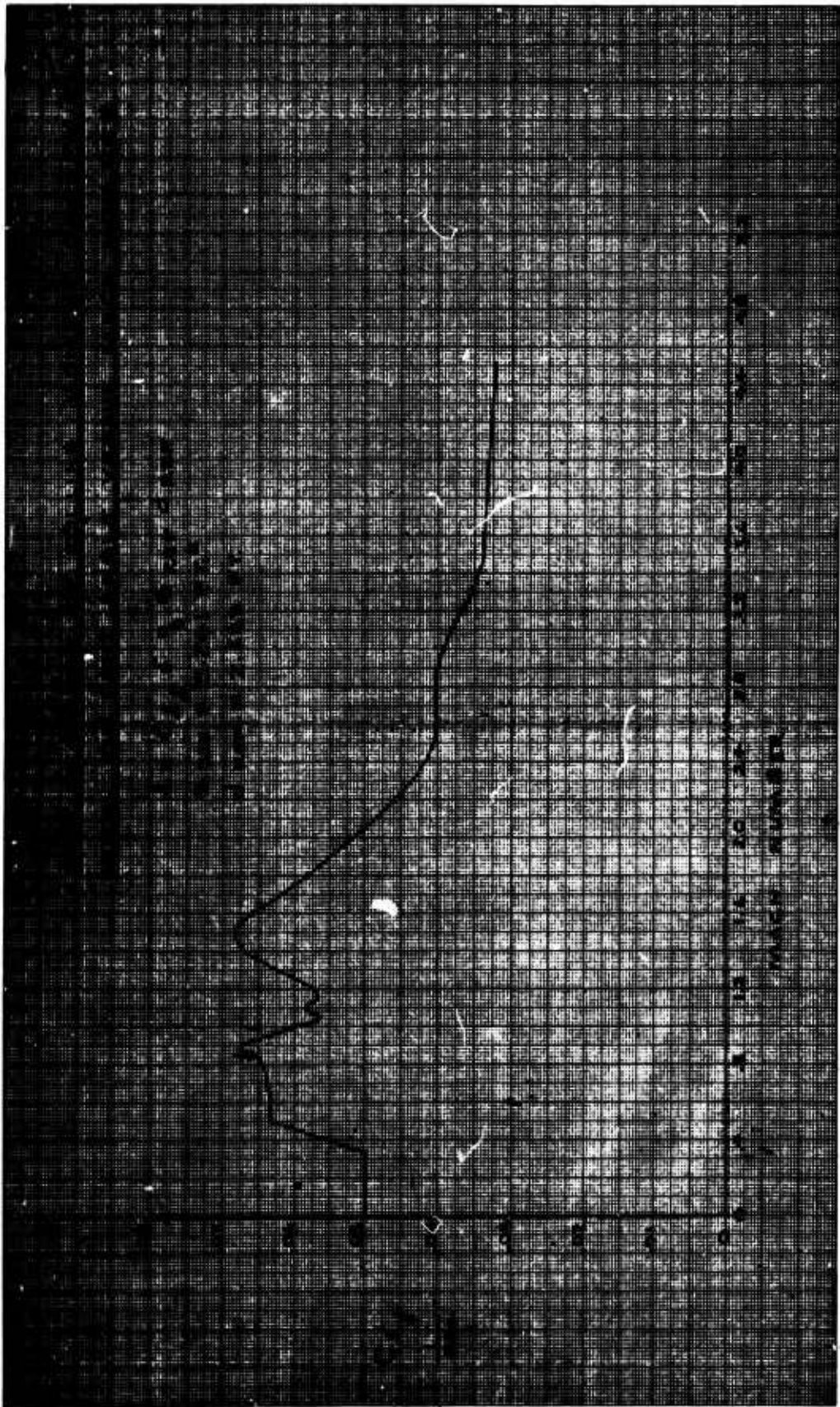












APPENDIX II
GUIDED BLUE GOOSE VEHICLE

This work is extracted from AFWL-TR-67-93.

SECTION II

BLUE GOOSE VEHICLE

1. Vehicle Modification

The original Blue Goose vehicle was slightly modified for the guided vehicle. The original unguided vehicle had a Thiokol Castor XM33-E8 for the main booster and four Thiokol Recruit XM19-E1 for auxiliary boosters. The sole purpose of the auxiliary boosters on the unguided vehicle was for high acceleration at lift-off to decrease wind effect. The Recruits remained with the vehicle so as not to add to vehicle dispersion through ejecting the spent motors. As it turned out, the added velocity gained at lift-off through the use of the boosters was negated in later flight by the added structural weight, and increased drag incurred by not ejecting the spent motors. Since the Recruits added nothing to the payload carrying capability of the vehicle, they were left off the guided vehicle version at a considerable cost savings. Even though the guided vehicle is more wind sensitive at lift-off, the guidance system is well capable of overcoming the aerodynamic wind forces.

2. Vehicle Configuration and Physical Properties

The guided Blue Goose configuration is shown in figure 1. The length of the vehicle is 351 inches, and the basic diameter is 31 inches. The aft fins are 5 feet square, and the forward fins are 1 foot square. The basic physical properties are shown in table I.

Table I

GUIDED BLUE GOOSE PROPERTIES

Event	Weight (lb)	C.G. (from nose, in.)	Transverse Moment of Inertia (slug-ft ²)	Roll Moment of Inertia (slug-ft ²)
Castor B.O.	6205	145.6	16627	263
Castor Propellant	7427	219		
Launch	13632	185.6	25620	473

Normal force coefficient slope, $C_{N\alpha}$, and pitching moment coefficient slope, $C_{M\alpha}$, are shown in figures 2 and 3. Thrusting drag coefficient, C_{DO} , is shown in figure 4. All aerodynamic data are smoothed wind tunnel data.

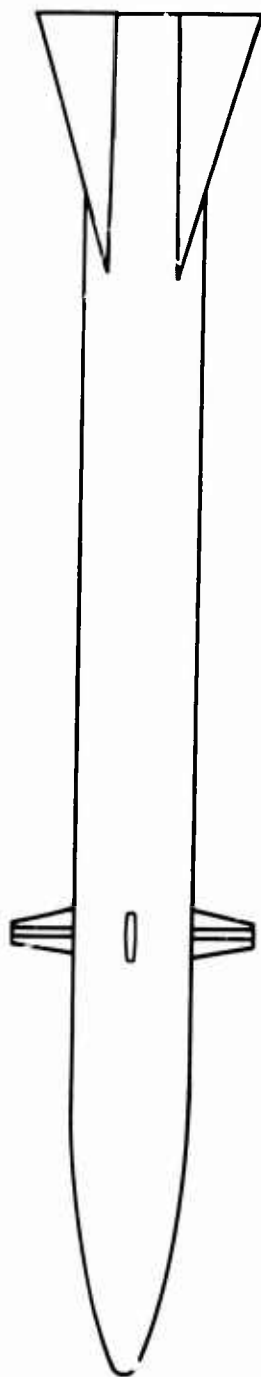
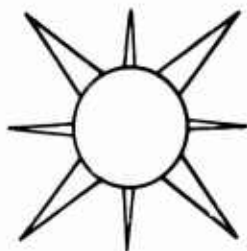


Figure 1. Guided Blue Goose Vehicle.

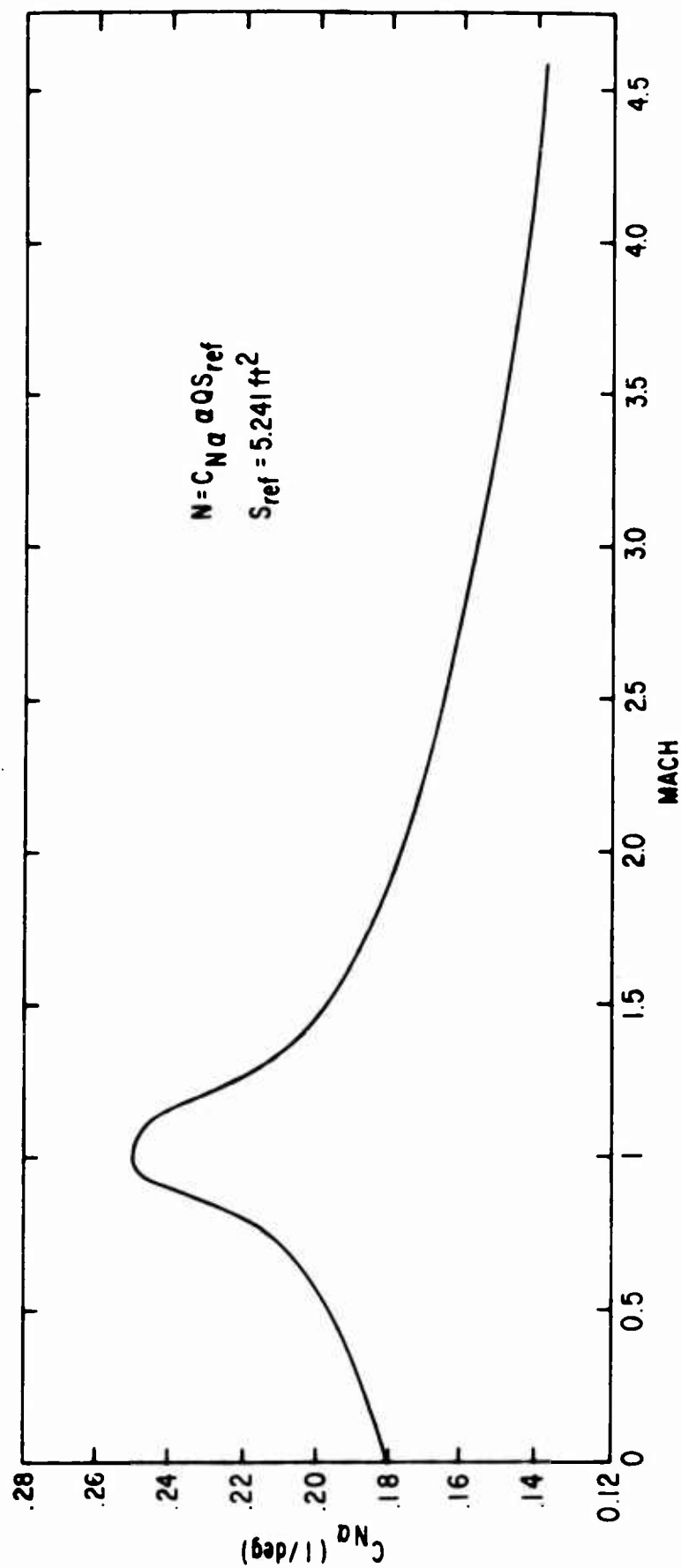


Figure 2. Normal Force Coefficient Slope vs. Mach.

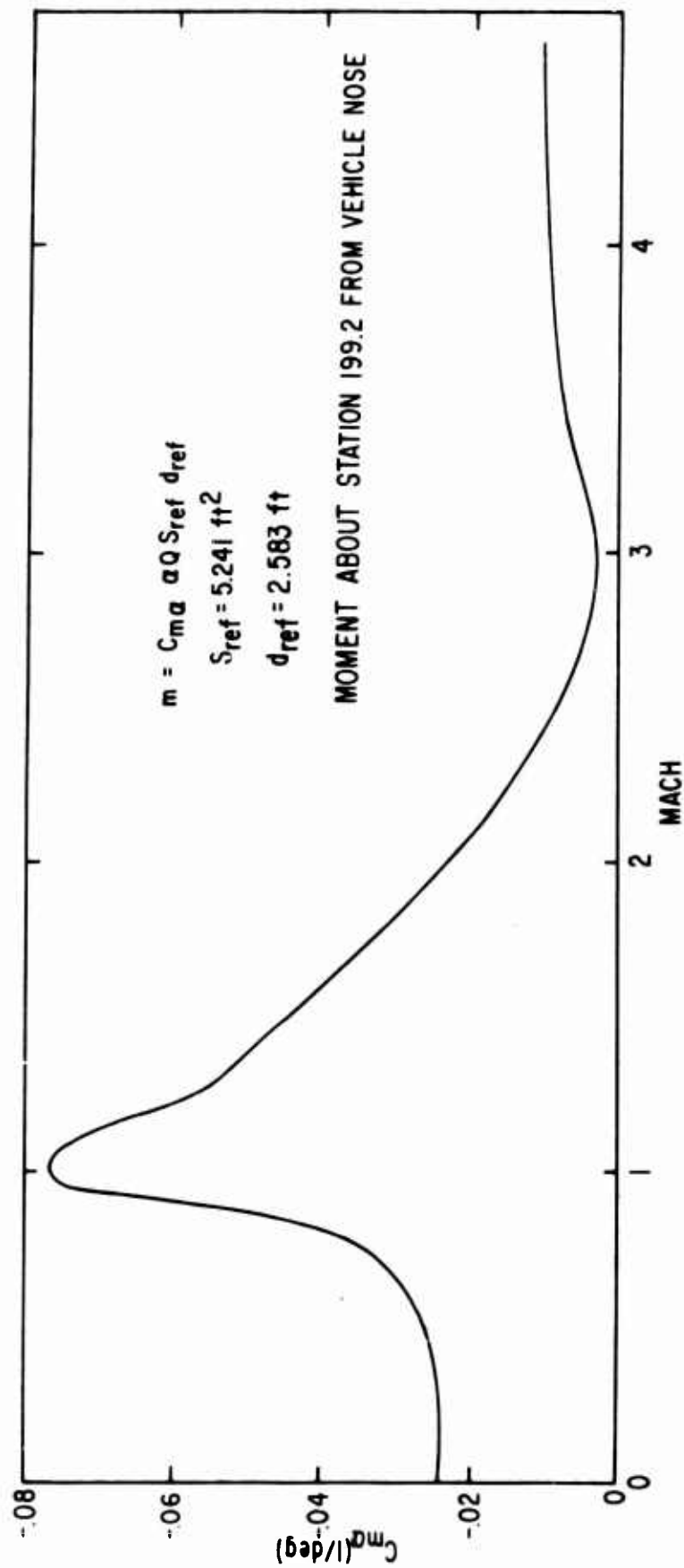


Figure 3. Pitching Moment Coefficient Slope vs. Mach.

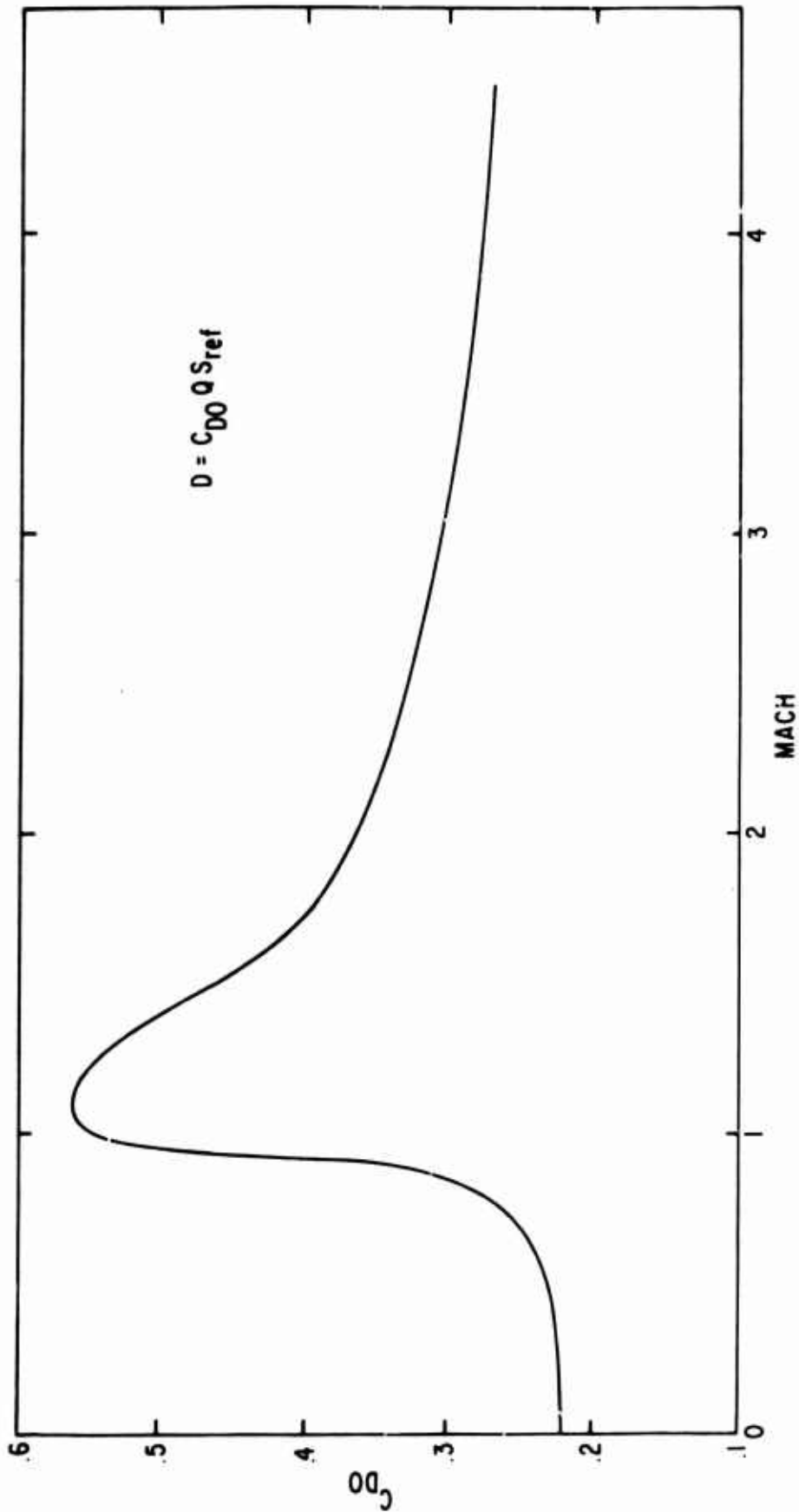


Figure 4. Thrusting Drag Coefficient vs. Mach.

3. Vehicle Nominal Performance

The desired nominal trajectory for the vehicle is the non-perturbated ballistic trajectory. This trajectory was calculated with the Blue Goose Six-Degree-of-Freedom Digital Computer Trajectory Calculation*. The six-degree calculation uses an oblate, spheroidal, rotating earth model and has the capability to calculate trajectory dispersions for the major perturbed parameters (i.e., wind, launch angles, tip-off, thrust misalignment, drag, thrust, etc.). Nominal trajectory performance is shown in figures 2 through 10.

*"Blue Goose Six-Degree-of-Freedom Digital Computer Trajectory Calculation," AFWL-TR-66-156, March 1967.

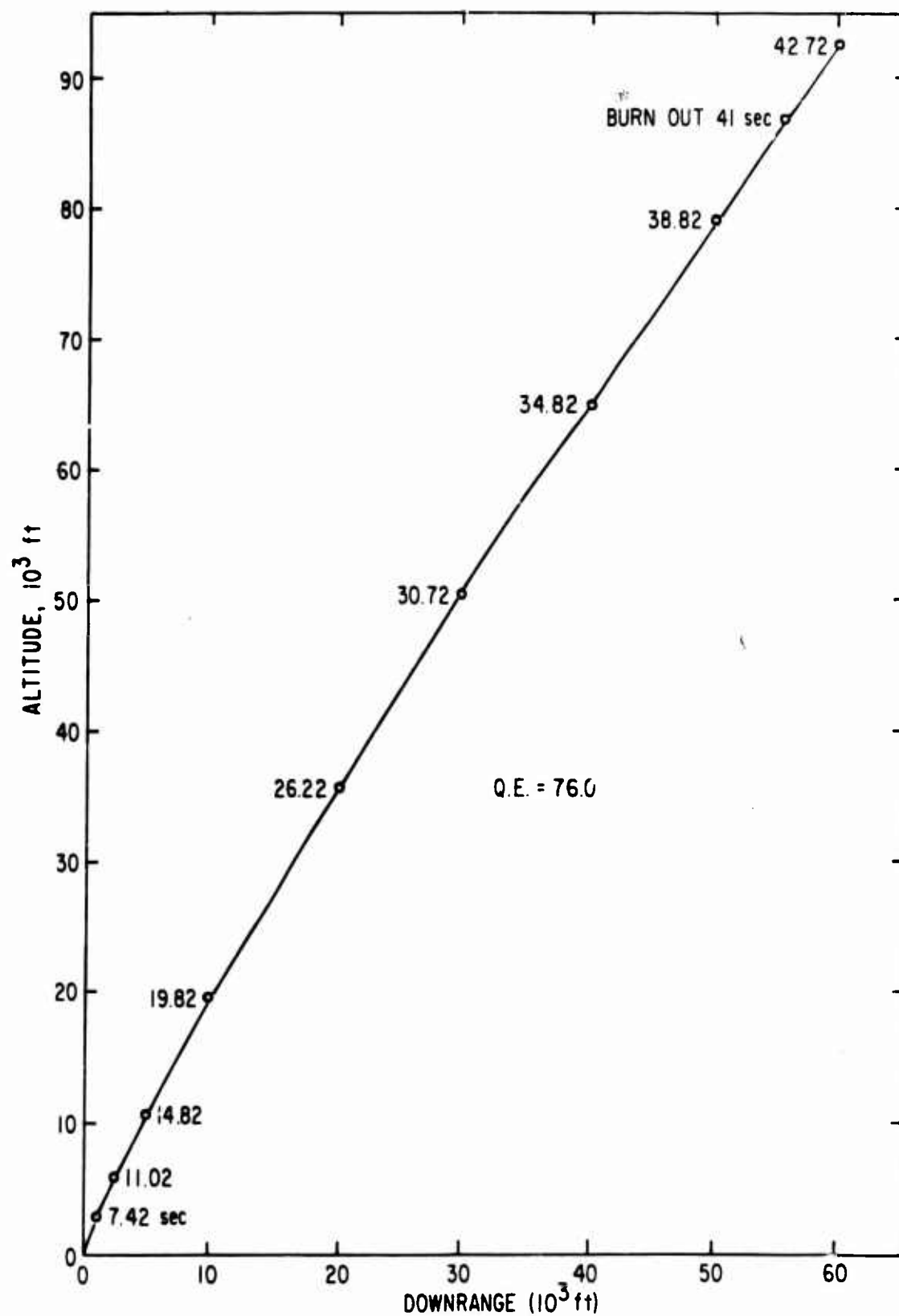


Figure 5. Nominal Powered Trajectory.

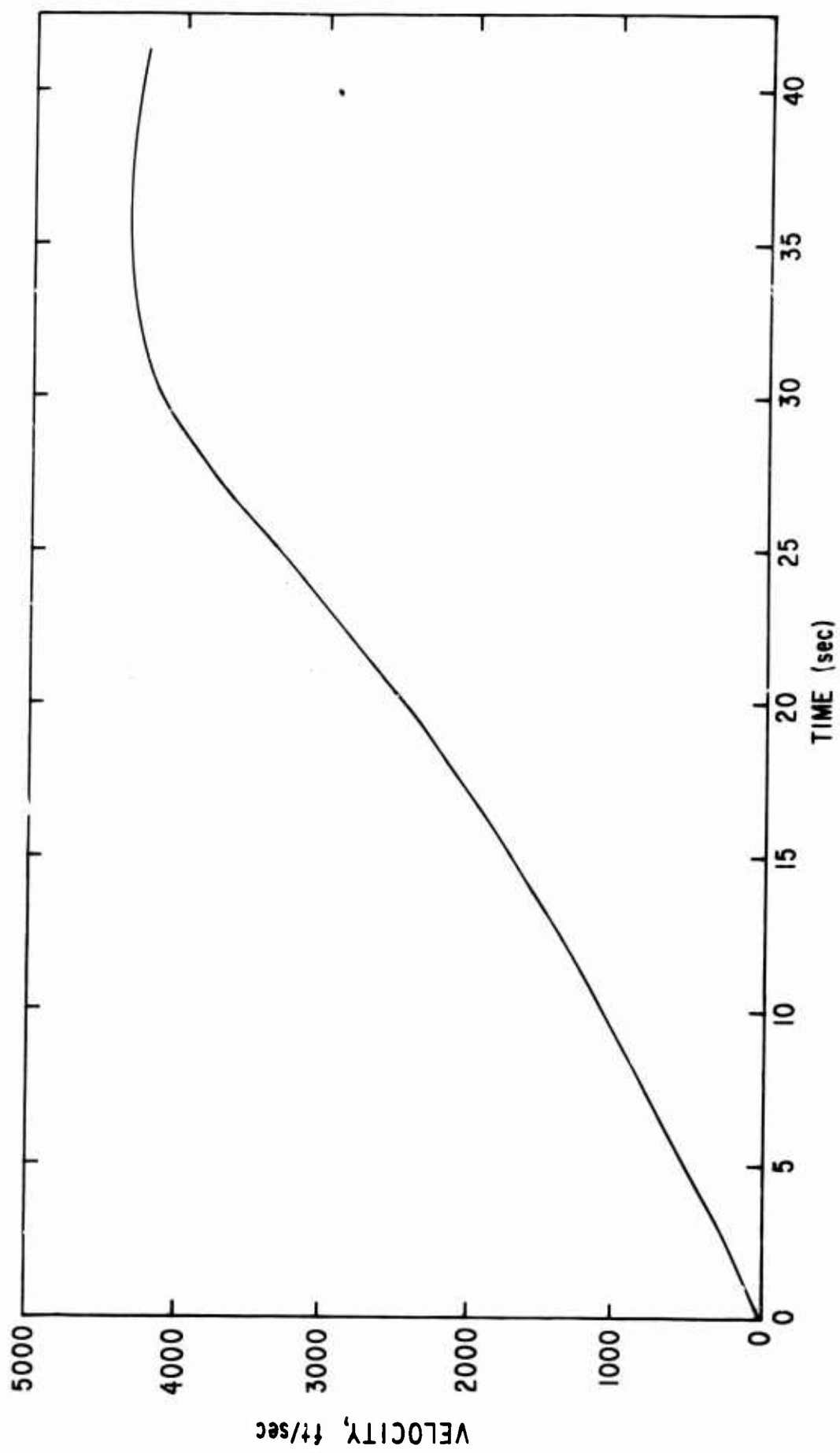


Figure 6. Velocity vs. Time.

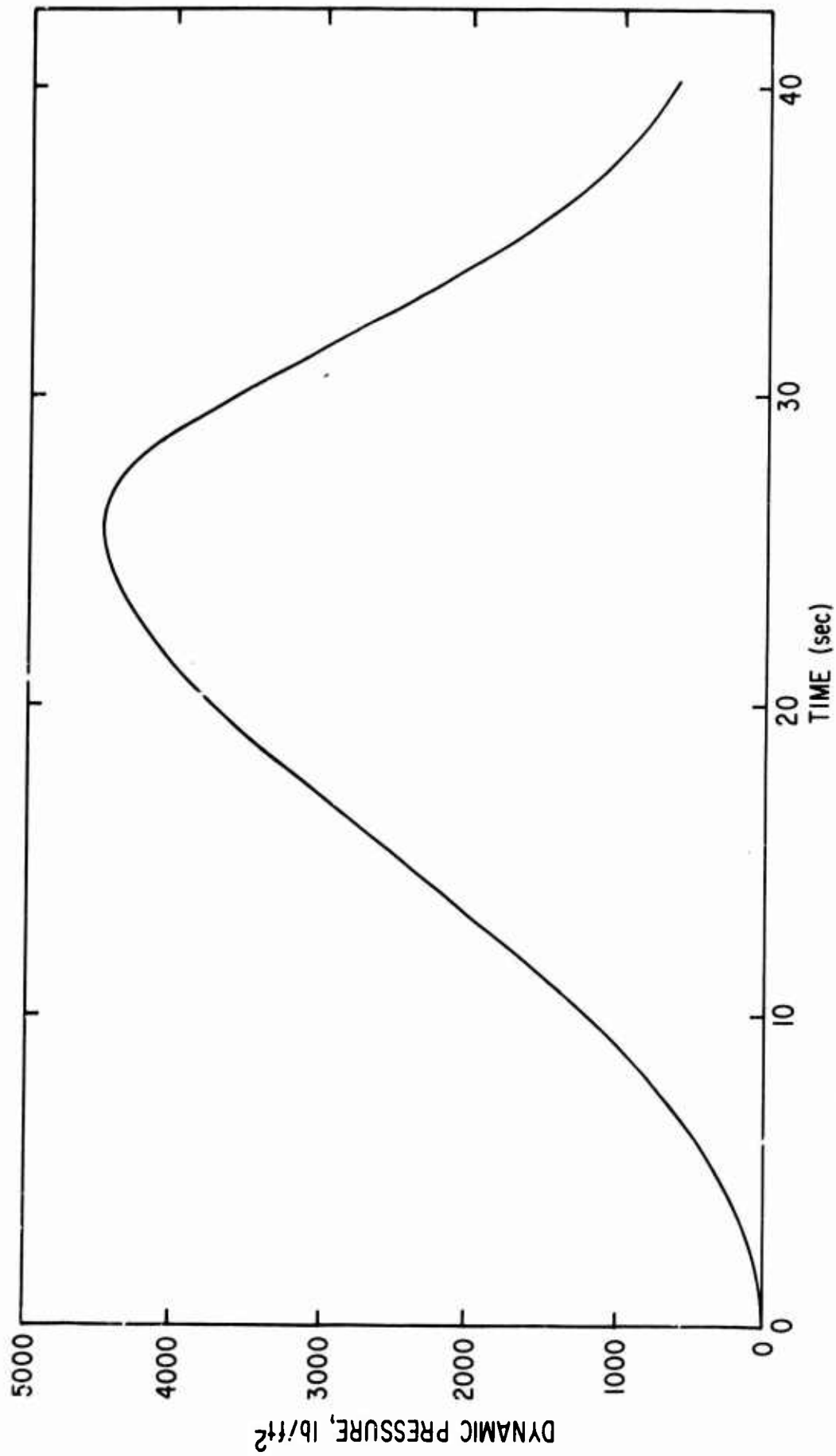


Figure 7. Dynamic Pressure vs. Time.

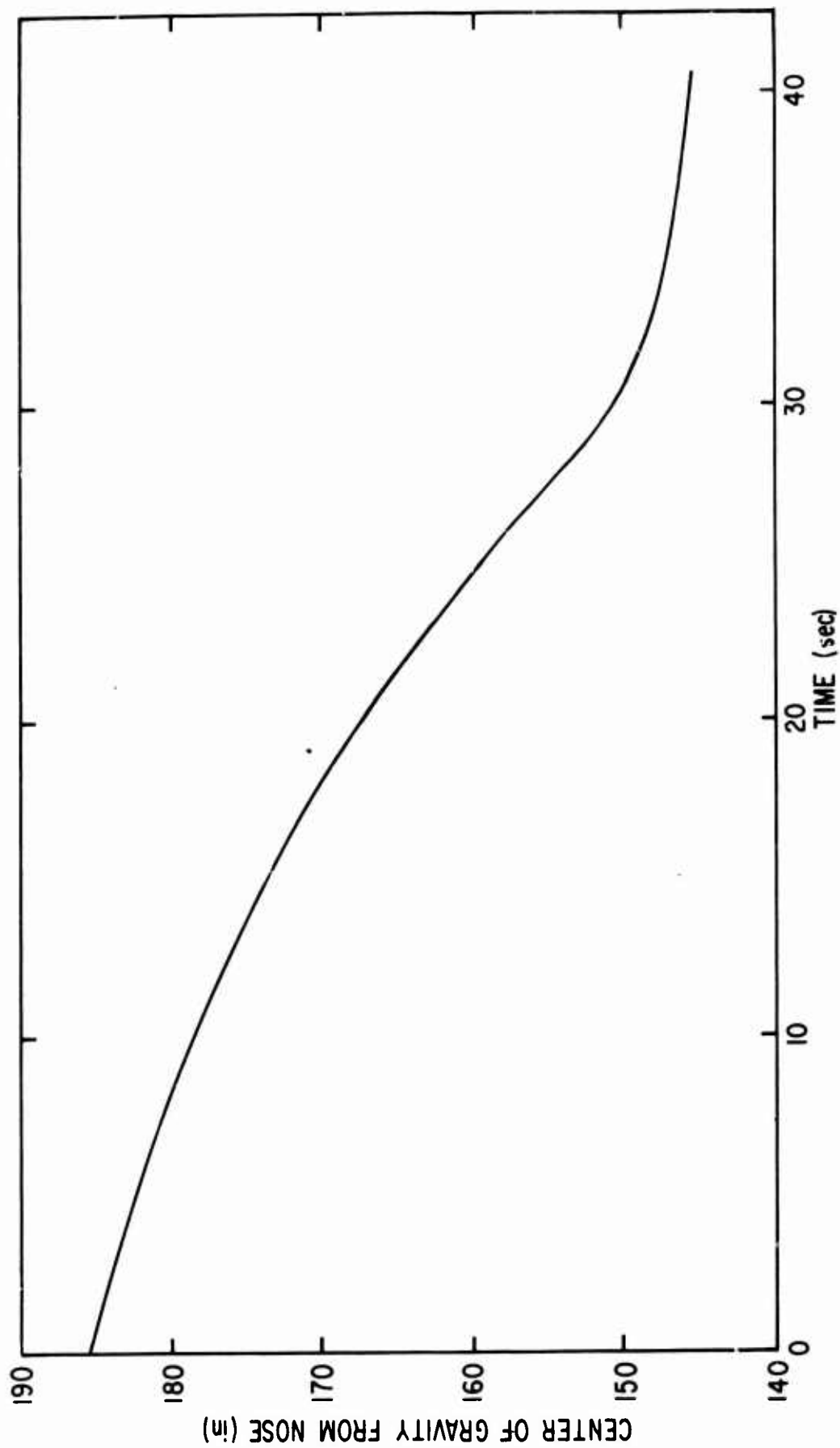


Figure 8. Center of Gravity vs. Time.

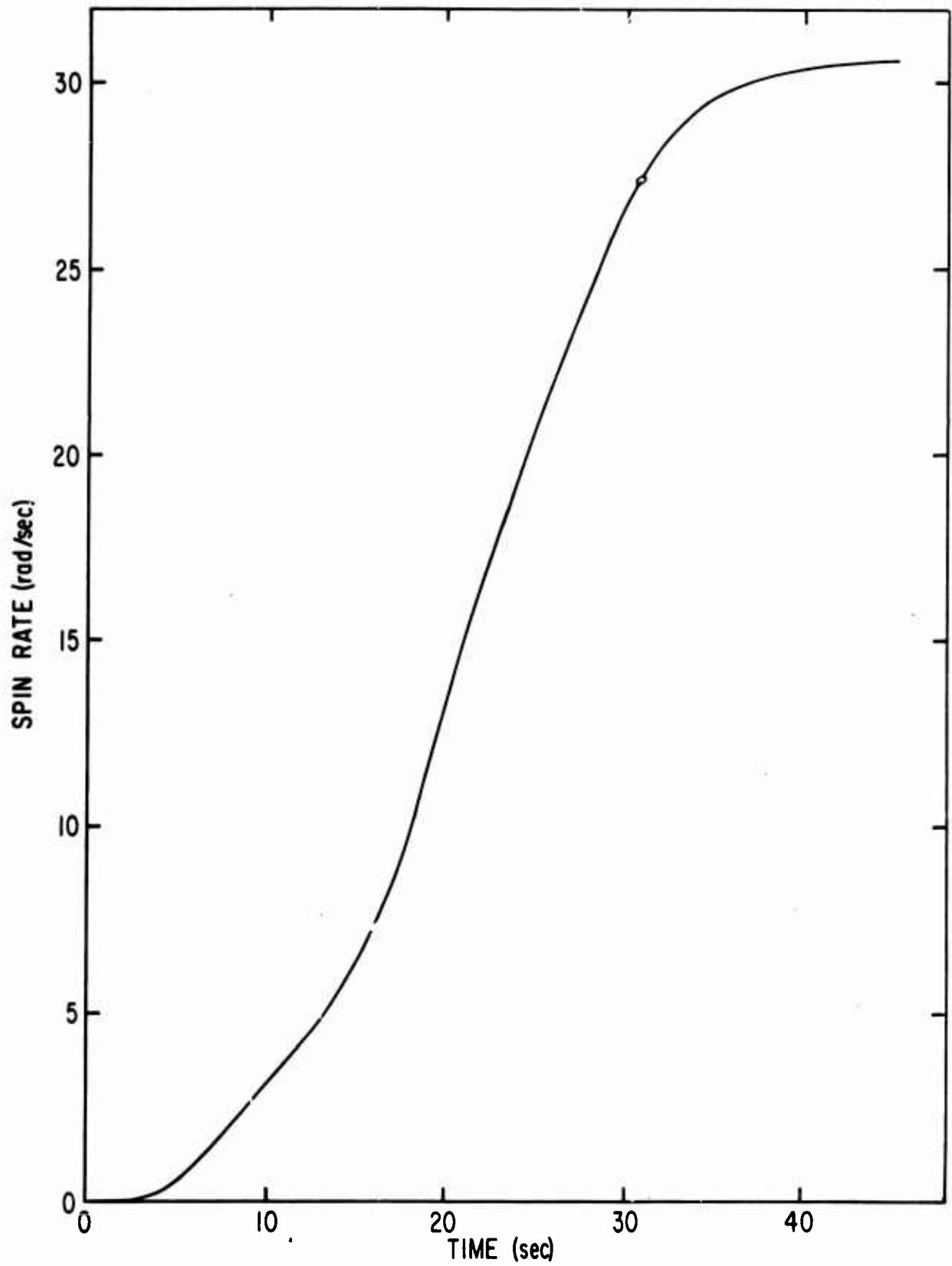


Figure 9. Spin Rate vs. Time.

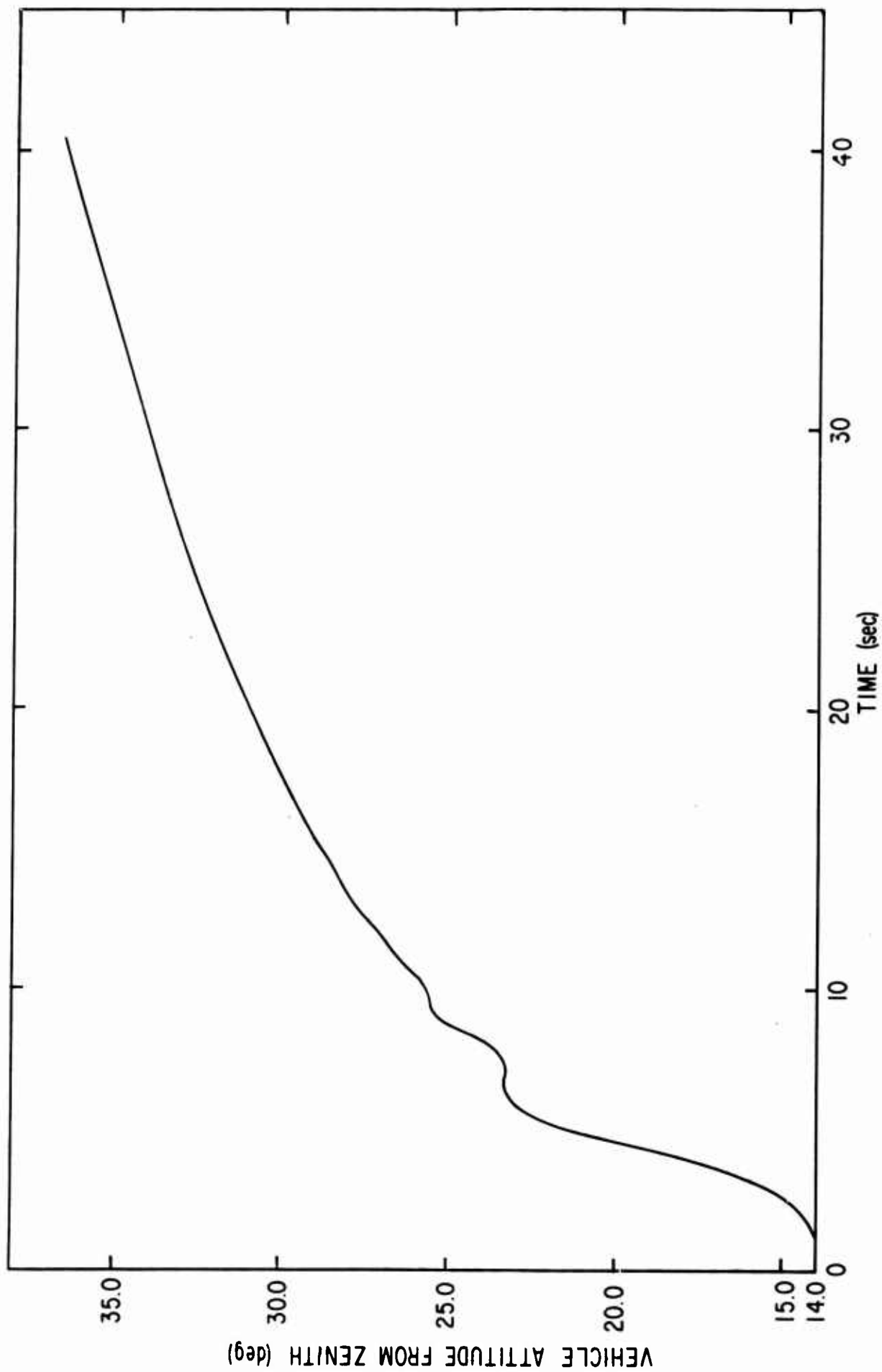


Figure 10. Vehicle Attitude vs. Time.

DISTRIBUTION

No. cys

HEADQUARTERS USAF

1 Hq USAF (AFTAC), Wash, DC 20330

MAJOR AIR COMMANDS

1 AUL(SE)-67-464, Maxwell AFB, Ala 36112

2 USAFIT-L, Bldg 640, Wright-Patterson AFB, Ohio 45433

AFSC ORGANIZATIONS

1 AFSC STLO, R&T Div, AFUPO, Los Angeles, Calif 90045

1 AF Avionics Lab, Wright-Patterson AFB, Ohio 45433

1 AF Flight Dynamics Lab, Wright-Patterson AFB, Ohio 45433

1 ASD (ASAPR), Wright-Patterson AFB, Ohio 45433

1 AEDC, Arnold AFS, Tenn 37289

1 SAMSO (SMQ), AFUPO, Los Angeles, Calif 90045

1 ESD (ESTI), L. G. Hanscom Fld, Bedford, Mass 01730

1 APGC (PGBPS-12), Eglin AFB, Fla 32542

KIRTLAND AFB ORGANIZATIONS

1 AFSWC (SWEH), Kirtland AFB, NM 87117

AFWL, Kirtland AFB, NM 87117

12 (WLIL)

20 (WLRT)

OTHER AIR FORCE AGENCIES

1 AFCRL, L. G. Hanscom Fld, Bedford, Mass 01731

ARMY ACTIVITIES

1 Comdg Off, Ballistic Rsch Lab (AMXBR-TB, J. Meszaros), Aberdeen Proving Ground, Md 21005

NAVY ACTIVITIES

1 Comdg Off, NRL, Wash, DC 20390

1 Comdr, NOL (Code 730), White Oak, Silver Spring, Md 20910

DISTRIBUTION (cont'd)

No. cys

OTHER DOD ACTIVITIES

1	Dir, DASA (Tech Lib), Wash, DC 20305
1	Comdr, Fld Comd, DASA (FCAG3), Sandia Base, NM 87115
1	Dir, ARPA, DOD, Pentagon, Wash, DC 20301
1	Ofc, Dir Def Rsch and Engr (J. E. Jackson, Ofc Atomic Programs), Rm 3E1071, Pentagon, Wash, DC 20330
20	DDC (TIAAS), Cameron Sta, Alexandria, Va 22314

AEC ACTIVITIES

1	Sandia Corp (Info Dist Div), Box 5800, Sandia Base, NM 87117
1	UCLRL (Tech Info Div), Berkeley, Calif 94720
1	Dir, LASL (Report Librarian), P. O. Box 1663, Los Alamos, NM 87554

OTHER

1	Aerospace Corp (Acquis Gp), P. O. Box 95085, Los Angeles, Calif 90045
1	Applied Physics Lab, Johns Hopkins Univ, 8621 Georgia Ave, Silver Spring, Md 20910
1	Convair, Div General Dynamics Corp, P. O. Box 1950, San Diego, Calif 92112
1	Gulf Gen Atomic Inc (Lib), P. O. Box 608, San Diego, Calif 92112
1	General Dynamics/ Fort Worth Div, P.O. Box 371, Fort Worth, Tex 76101
1	Gen Elec Co-MSD, Rm M9120 (F. A. Lucy), P.O. Box 8555, Philadelphia, Pa 19101
1	Inst for Def Anlys, Rm 2B257, Pentagon, Wash, DC 20330 THRU: ARPA
1	Lockheed Missiles and Space Co, Div Lockheed Acft Corp (Dr. D. Moffatt), 1111 Lockheed Way, Sunnyvale, Calif 94086
1	MIT, Div Indust Coop, 77 Massachusetts Ave, Cambridge, Mass 02739
1	NASA Sci & Tech Info Fclty (Doc Svcs Dept), P.O. Box 33, College Park, Md 20740
1	Official Record Copy (Capt Lynch, WLRT)

(This page intentionally left blank)

UNCLASSIFIED
Security Classification

DOCUMENT CONTROL DATA - R & D		
(Security classification of title, body of abstract and indexing annotation must be entered when the overall report is classified)		
1. ORIGINATING ACTIVITY (Corporate author)		2a. REPORT SECURITY CLASSIFICATION
Air Force Weapons Laboratory (WLRT) Kirtland Air Force Base, New Mexico 87117		UNCLASSIFIED
		2b. GROUP
3. REPORT TITLE		
FLIGHT DYNAMICS OF THE BLUE GOOSE VEHICLE TRAVERSING A HIGH ALTITUDE NUCLEAR EXPLOSION		
4. DESCRIPTIVE NOTES (Type of report and inclusive dates)		
January 1967 to November 1967		
5. AUTHOR(S) (First name, middle initial, last name)		
Urban H. D. Lynch, Capt, USAF		
6. REPORT DATE	7a. TOTAL NO. OF PAGES	7b. NO. OF REFS
January 1968	248	
8a. CONTRACT OR GRANT NO.	9a. ORIGINATOR'S REPORT NUMBER(S)	
b. PROJECT NO. 5710	AFWL-TR-67-134	
c. Subtask 7.505T	9b. OTHER REPORT NO(S) (Any other numbers that may be assigned this report)	
d.		
10. DISTRIBUTION STATEMENT This document is subject to special export controls and each transmittal to foreign governments or foreign nationals may be made only with prior approval of AFWL (WLRT), Kirtland AFB, NMex 87117. Distribution is limited because of the technology discussed in the report.		
11. SUPPLEMENTARY NOTES		12. SPONSORING MILITARY ACTIVITY
		AFWL (WLRT) Kirtland AFB, NMex 87117
13. ABSTRACT (Distribution Statement No. 2)		
<p>This report investigates the flight dynamics of the Blue Goose vehicle traversing a high altitude nuclear explosion. The problem is analyzed for a detonation of 200 kilotons at an altitude of 30 kilometers. The vehicle is launched such that it intercepts the fireball edge at approximately 1 second after detonation. Calculation of vehicle trajectory is done by incorporating the output of a detailed one-dimensional hydrodynamic calculation of the explosion environment, with a six-degree-of-freedom computer program for the vehicle. The report analyzes the attitude and position time histories of the vehicle, time history of environment as seen by the vehicle, vehicle dynamic loads, trajectory dispersion, and worst flight path through the environment.</p>		

DD FORM 1473
1 NOV 65

UNCLASSIFIED
Security Classification

~~UNCLASSIFIED~~
Security Classification

Vehicle flight
Nuclear explosion
Hydrodynamic interaction

AFSC-HOLLOMAN AFB, NMEX

UNCLASSIFIED
Security Classification